

CLÁUDIA SOFIA FERREIRA RAPOSO DE MAGALHÃES

**ESTABLISHMENT OF FARMED FISH WELFARE BIOMARKERS;
A MULTIOMICS APPROACH**



2023

CLÁUDIA SOFIA FERREIRA RAPOSO DE MAGALHÃES

**ESTABLISHMENT OF FARMED FISH WELFARE BIOMARKERS; A
MULTIOMICS APPROACH**

Doutoramento em Ciências do Mar, da Terra e do Ambiente
Ramo de Ciências Biológicas

Trabalho efetuado sob a orientação de:

Professor Doutor Pedro Miguel Rodrigues

Professor auxiliar da Universidade do Algarve e Investigador do Centro de Ciências
do Mar (CCMAR)

Doutor Marco Cerqueira

Investigador do Centro de Ciências do Mar (CCMAR)



2023

Declaração de autoria de trabalho

ESTABLISHMENT OF FARMED FISH WELFARE BIOMARKERS; A MULTOMICIS APPROACH

Declaro ser a autora deste trabalho, que é original e inédito. Autores e trabalhos consultados estão devidamente citados no texto e constam da listagem de referências incluída.

(Cláudia Raposo de Magalhães)

© Cláudia Sofia Ferreira Raposo de Magalhães, 2023

A Universidade do Algarve reserva para si o direito, em conformidade com o disposto no Código do Direito de Autor e dos Direitos Conexos, de arquivar, reproduzir e publicar a obra, independentemente do meio utilizado, bem como de a divulgar através de repositórios científicos e de admitir a sua cópia e distribuição para fins meramente educacionais ou de investigação e não comerciais, conquanto seja dado o devido crédito ao autor e editor respetivos.

“The important thing is not to stop questioning.”

– Albert Einstein

ACKNOWLEDGMENTS

This four-year journey allowed me to work and collaborate with great scientists and great people, to whom I am deeply thankful.

First, and foremost, I would like to express my sincere gratitude to my supervisors:

Prof. Dr. Pedro Rodrigues, who first trusted me back in 2015 and with whom I've been working since. I thank him for his endless guidance, for always being present, for supporting my ideas, for all the work abroad, courses and conferences that he gave me the opportunity to participate in, for the laughs, for the friendship. His trust and support have allowed me to significantly improve my scientific skills and to grow as a researcher, and for all that you will always have my deepest gratitude.

And Dr. Marco Cerqueira, for his mentoring, for his invaluable passion for fish welfare and for transmitting that to me, for being so supportive and motivational, for always being available to discuss new ideas, for all the opportunities, for the tireless help he dedicated to my experimental trials, papers, and thesis, for the knowledge shared during long phone calls, for the good moments, for the friendship.

A special thanks goes to my colleague and friend Denise Schrama, who will always be my unofficial supervisor, who taught me proteomics and innumerable other lab techniques and how to be an independent researcher, who is always available to help, who has unlimited patience, and who has the best organizational skills I know. Thank you also for the great moments together all around the world.

My deepest acknowledgements extend to Dr. Ana Paula Farinha, for her scientific input, for explaining me so much so eloquently, for her invaluable advice, for her critical thinking and for stimulating mine, for always being available to share thoughts, for the kind and motivational words, for the long conversations, for the friendship.

I thank all the other researchers that I had the opportunity to collaborate with and to work with in the labs I visited, whose contributions were crucial to this thesis:

Dr. Annette Kuehn and Dominique Revets, from the Luxembourg Institute of Health (LIH), Luxembourg; Dr. Surintorn Boonanuntanasarn, Dr. Chatsirin Nakharuthai, Khanakorn Phonsiri and Araya Janprai, from the Suranaree University of Technology, Thailand; Dr. Gavin Blackburn and Dr. Phillip Whitfield, from the Glasgow Polyomics, University of Glasgow, United Kingdom; Dr. Kenneth Sandoval and Dr. Grace McCormack, from the Ryan Institute & School of Natural Sciences, University of Galway, Ireland, and Dr. Ferenc Kagan, from the University of Bergen, Norway.

As getting through a PhD requires more than scientific support I would also like to thank:

All my colleagues and friends from Aquagroup, especially Rita Teodósio, Rita Colen and Sara Ferreira, for their help in the lab and fish sampling, but mainly for the coffee

and lunch breaks, and all the good times; and the Ramalhete team for their help with the fish trials. A special thanks to Rachel, MJ and Cabano from my “Aquagroup-sub30” group (which eventually became “Aquagroup-sub35”), for the friendship developed outside the lab, for the board game nights, for the summer vacations, for the laughs and for all the good moments we shared.

My non-biological sister Irina, who has always been there since the first day of university, and Tiago, for our Fariceira visits, for all the adventures, for the sincerest friendship I could ask for, for everything.

My dearest friend Ritinha, for being so present, for all the frequent visits to Faro, for all the cherished moments, for being you.

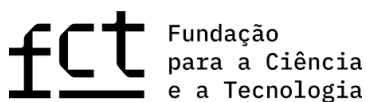
Aos meus três avós, que não ficaram cá para ver o final desta viagem académica que tanto ambicionaram para mim, por sempre acreditarem, e por tudo o que me deram.

Aos meus Pais, os meus pilares de resiliência e perseverança, pela educação que me deram, pela liberdade que me deram, por apoiarem as minhas escolhas, por me ensinarem a não desistir, pelo percurso académico e por todas as oportunidades que me proporcionaram sem hesitar e sem duvidar de mim, pelo orgulho que transbordam. Muito do que sou hoje, devo-o a vocês!

And finally, to my husband Tomás, for your unconditional love and support, for sharing the last 12 years of your life with me, for teaching me so much, for your patience and calmness in the good and in the bad moments, for your tremendous encouragement, for being the most kind, respectful and humble person I know, for doing everything whilst I wrote this thesis, and for everything else that I do not have enough words to describe it.

FUNDING

Cláudia Raposo de Magalhães was supported by the Portuguese Foundation for Science and Technology (FCT) through the PhD scholarship SFRH/BD/138884/2018, financed by national funds from MCTES, via FCT, and co-funded by the European Union (EU) through the European Social Fund, by an EURASTiP exchange grant, funded by the project “Promoting Multi-Stakeholder Contributions to International Cooperation on Sustainable Solutions for Aquaculture Development in South-East Asia” (ID: 728030) within the EU Horizon 2020 program “H2020-EU.3.2.3 - Unlocking the potential of aquatic living resources”, and by the EU Horizon 2020 research and innovation program under grant agreement No 730984, ASSEMBLE Plus project. This work was integrated into the project WELFISH (Ref^a 16-02-05-FMP-12) financed by Mar2020, in the framework of Portugal2020, and received Portuguese national funds from FCT through projects UIDB/04326/2020, UIDP/04326/2020, and LA/P/0101/2020, and from the operational programs CRESC Algarve 2020 and COMPETE 2020 through projects EMBRC.PT ALG-01-0145-FEDER-022121 and BIODATA.PT ALG-01-0145-FEDER-022231.



DISSEMINATION

The results generated during this PhD originated the following publications and communications:

Publications in indexed peer-reviewed journals:

1. Raposo de Magalhães, C.S.F., Cerqueira, M.A.C., Schrama, D., Moreira, M.J.V., Boonanuntanasarn, S., Rodrigues, P.M.L., 2020. A Proteomics and other Omics approach in the context of farmed fish welfare and biomarker discovery. *Reviews in Aquaculture* 12, 122-144. **doi: 10.1111/raq.12308**
2. Raposo de Magalhães, C., Schrama, D., Farinha, A.P., Revets, D., Kuehn, A., Planchon, S., Rodrigues, P.M., Cerqueira, M., 2020. Protein changes as robust signatures of fish chronic stress: a proteomics approach to fish welfare research. *BMC Genomics* 21, 309. **doi: 10.1186/s12864-020-6728-4**
3. de Magalhães, C.R., Carrilho, R., Schrama, D., Cerqueira, M., Rosa da Costa, A.M., Rodrigues, P.M., 2020. Mid-infrared spectroscopic screening of metabolic alterations in stress-exposed gilthead seabream (*Sparus aurata*). *Scientific Reports* 10, 16343. **doi: 10.1038/s41598-020-73338-z**
4. Raposo de Magalhães, C., Schrama, D., Nakharuthai, C., Boonanuntanasarn, S., Revets, D., Planchon, S., Kuehn, A., Cerqueira, M., Carrilho, R., Farinha, A.P., Rodrigues, P.M., 2021. Metabolic plasticity of gilthead seabream under different stressors: analysis of the stress responsive hepatic proteome and gene expression. *Frontiers in Marine Science* 8, 676189. **doi: 10.3389/fmars.2021.676189**
5. Raposo de Magalhães, C., Farinha, A.P., Blackburn, G., Whitfield, P.D., Carrilho, R., Schrama, D., Cerqueira, M., Rodrigues, P.M., 2022. Gilthead seabream liver integrative proteomics and metabolomics analysis reveals regulation by different pro-survival pathways in the metabolic adaptation to stress. *International Journal of Molecular Sciences*, 23(23), 15395. **doi: 10.3390/ijms232315395**
6. Raposo de Magalhães, C., Farinha, A.P., Carrilho, R., Schrama, D., Cerqueira, M., Rodrigues, P.M., 2023. A new window into fish welfare: a proteomic discovery study of stress biomarkers in the skin mucus of gilthead seabream

(*Sparus aurata*). Journal of Proteomics, In Press, **doi: 10.1016/j.jprot.2023.104904**

7. Raposo de Magalhães, C., Sandoval, K., Kagan, F., McCormack, G., Schrama, D., Carrilho, R., Farinha, A.P., Rodrigues, P.M., Cerqueira, M. 2023. Underlining the hepatic transcriptional changes behind *Sparus aurata* responses to different aquaculture challenges: an RNA-seq study. BMC Genomics, **Submitted**

Article in magazine journal:

1. Raposo de Magalhães, C., Rodrigues, P. M., 2021. New ways to assess stress in fish are urgently needed in aquaculture. Research Outreach.

Oral communications in conferences:

1. Raposo de Magalhães, C., Farinha, A.P., Carrilho, R., Schrama, D., Cerqueira, M., Rodrigues, P.M., 2019. Identification of welfare biomarkers in farmed gilthead sea bream: integrating multi-omics data. LACQUA 2019 - Latin American & Caribbean aquaculture, San José, Costa Rica.
2. Raposo de Magalhães, C., Farinha, A.P., Carrilho, R., Schrama, D., Cerqueira, M., Rodrigues, P.M., 2021. Comparative Analysis of the stress responsive hepatic proteome and gene expression: identification of stress biomarkers. Aquaculture Europe 2020, online.
3. Raposo de Magalhães, C., Farinha, A.P., Carrilho, R., Schrama, D., Cerqueira, M., Rodrigues, P.M., 2021. In search of stress biomarkers: label-free shotgun proteomics analysis of gilthead seabream hepatic and skin mucus proteome. Aquaculture Europe 2021, Funchal, Madeira, Portugal.
4. Raposo de Magalhães, C., Farinha, A.P., Carrilho, R., Schrama, D., Cerqueira, M., Rodrigues, P.M., 2022. The promisor role of skin mucus to screen for fish stress biomarkers: a proteomics approach. Aquaculture America 2022, San Diego, USA.
5. Raposo de Magalhães, C., Farinha, A.P., Carrilho, R., Schrama, D., Cerqueira, M., Rodrigues, P.M., 2022. Proteomic profiling of farmed gilthead seabream skin mucus stress response: a biomarker discovery study. ProteoVilamoura 2022, Vilamoura, Portugal.

6. Raposo de Magalhães, C., Farinha, A.P., Carrilho, R., Schrama, D., Cerqueira, M., Rodrigues, P.M., 2022. Integrative proteomics and metabolomics profiling of farmed gilthead seabream hepatic stress response. 14th International Congress on the Biology of Fish, Montpellier, France.

Poster presentations in conferences:

1. Magalhães, C., Cerqueira, M., Schrama, D., Farinha, A. P., Kuehn, A., Revets, D., Boonanuntanasarn, S., Nakharuthai, C., Rodrigues, P. M., 2019. Establishment of farmed fish welfare biomarkers; a multi-omics approach. XIII Annual Congress of the European Proteomics Association: From Genes via Proteins and their Interactions to Functions, Berlin, Germany.
2. Magalhães, C., Cerqueira, M., Schrama, D., Farinha, A. P., Kuehn, A., Revets, D., Boonanuntanasarn, S., Nakharuthai, C., Rodrigues, P. M., 2019. Using an integrated multi-omics approach to validate more robust welfare biomarkers in gilthead seabream. Multiomics to Mechanisms - Challenges in Data Integration, Heidelberg, Germany.

Awards:

1. Best student presentation, entitled “The promisor role of skin mucus to screen for fish stress biomarkers: a proteomics approach” at Aquaculture America 2022, San Diego, USA

SUMMARY

The sustainability of the aquaculture industry hinges on its ability to operate in harmony with the environment. To achieve this, it is essential to prioritize the welfare of farmed fish minimizing the stress levels associated with aquaculture practices. In this context, it is imperative to conduct a comprehensive study of fish physiological stress. The stress response in fish is initiated by an elaborate endocrine machinery that culminates in an overall metabolic reprogramming induced by the action of glucocorticoids. It can either increase fitness or induce further changes at the whole animal level and impair welfare. This process is orchestrated through a multilayered cellular program, and thus a multiomics approach can provide a holistic overview of the molecular stress response. Knowledge of the key regulators behind the adaptation mechanisms could provide valuable markers of stress to complement the existing measures. *Sparus aurata*, one of the most important species in Mediterranean aquaculture, was used in this study. Adult fish were subjected to three challenges: overcrowding, net handling, and hypoxia. The plasma proteome was assessed to verify the effect of the different challenges on the fish immune system and to measure the levels of typical stress indicators, i.e., cortisol, glucose, and lactate. A multiomics approach was employed to characterize the hepatic stress response, as the liver is the central organ in mounting the stress response. Lastly, skin mucus was used to identify stress biomarkers as it is easily collectable, and a mucosal tissue known to respond to stress. This work demonstrated that *Sparus aurata* can adapt better to high stocking densities than to net handling or hypoxia. The latter two challenges induced stress in hepatocytes and promoted several prosurvival pathways, e.g., autophagy, unfolded protein response, and DNA replication stress. Furthermore, a set of 28 candidate biomarkers was identified in the skin mucus, which could be further validated as lab-based welfare indicators. This research provides scientific knowledge that can be used to develop species-specific welfare assessment protocols, promote farmed fish safety, and enhance positive societal outcomes while promoting aquaculture sustainability.

Keywords: Aquaculture; Gilthead seabream; Metabolomics; Proteomics; Stress; Transcriptomics

RESUMO

A produção de pescado de aquacultura tem vindo a registar um aumento significativo nas últimas décadas, devido a uma procura crescente para consumo humano, aliada a uma forte diminuição dos stocks de peixe nos oceanos a nível mundial. A aquacultura é atualmente o setor da produção alimentar que regista um crescimento mais acelerado, tendo alcançado em 2020 um valor recorde de 87.5 milhões de toneladas, equivalente a aproximadamente 50% da produção de pescado e de outros produtos derivados do mar, a nível global. No mesmo ano, em Portugal, registou-se uma produção de 17 mil toneladas de peixe de aquacultura, representando um crescimento de 18.6% face ao ano anterior, sendo a dourada (*Sparus aurata*) uma das três espécies com maior produção.

A aquacultura desempenha assim um papel crucial no cumprimento das metas propostas pelas Nações Unidas para um desenvolvimento sustentável (*SDG goals*) no âmbito da Agenda 2030. No entanto, a crescente intensificação na produção neste setor gera também enormes desafios a nível da sustentabilidade ambiental, económica e social. Atualmente, o bem-estar animal é reconhecido como sendo um fator preponderante para uma produção mais sustentável, assim como para a maior aceitação e valorização do produto ao nível do consumidor. Por outro lado, a preocupação com o bem-estar animal e a execução de medidas visando a sua implementação, tem vindo a ser adoptada nas políticas públicas num número crescente de países. O comprometimento das condições de bem-estar animal traduzem-se normalmente numa maior suscetibilidade a agentes patogéneos e aumento das doenças associadas, para além de um menor crescimento, resultando em perdas económicas significativas para o setor aquícola. A evidência científica de senciência, dor e sofrimento nos peixes desencadeou também um aumento significativo no número de estudos com abordagem ao stress e iniciativas em prol do bem-estar animal em peixes de aquacultura.

As condições de cultivo adversas e determinados procedimentos de rotina, como sejam o manuseamento e/ou o transporte, podem desencadear stress nos animais. O stress não é necessariamente prejudicial, estando mesmo demonstrado por diversos estudos que a exposição aguda a situações de stress pode ser benéfica, na medida em que promove uma maior resiliência nos animais. No entanto, a longo-prazo, este pode afetar o crescimento, a imunidade, o comportamento, e o bem-estar,

podendo mesmo levar à morte nos casos mais extremos. Os peixes têm mecanismos neuroendócrinos específicos para lidar com o desequilíbrio fisiológico através de uma panóplia de adaptações metabólicas, num processo globalmente designado de “resposta ao stress”. Este mecanismo é iniciado pela ativação do eixo hipotálamo-pituitária-interrenal (HPI) que induz a produção e libertação de cortisol para a corrente sanguínea, a hormona responsável por ativar posteriormente diversas vias metabólicas em diferentes órgãos, promovendo a adaptação ao stress. O fígado é o órgão central na integração da resposta ao stress, sendo responsável pela biossíntese e distribuição de substratos energéticos, tais como a glucose e o lactato, essenciais ao próprio fígado, músculo e cérebro.

Numa exploração aquícola, por forma a avaliar o bem-estar dos peixes, são mais frequentemente utilizados os denominados “indicadores de bem-estar operacionais”, que englobam parâmetros tais como o comportamento, a agressividade, a existência de lesões externas e o nível de oxigénio. Outros indicadores de stress e.g., fisiológicos, estão associados a níveis elevados de cortisol e glucose, para além dos indicadores hematológicos, que incluem níveis elevados de eritrócitos e de hematócrito. Estes parâmetros são, no entanto, utilizados com menor frequência, dado que implicam a colheita de amostras por pessoal especializado e envio de amostras para análise em laboratório. Estes indicadores são designados de “indicadores de bem-estar laboratoriais” e, contrariamente aos anteriores, tendem a ser mais eficazes na prevenção atempada de consequências graves derivadas da exposição prolongada ao stress, evitando assim perdas económicas. Contudo, a fiabilidade do cortisol como indicador de stress tem sido posta em causa, nomeadamente em situações de stress crónico. De facto, os níveis de cortisol regressam a valores basais passadas algumas horas após a exposição ao stress. Por outro lado, a existência de diversos fenótipos comportamentais nos peixes, traduzidos em diferentes formas de lidar com o stress (i.e., *coping styles*) faz com que a resposta ao cortisol possa ser afetada por outros aspectos não diretamente relacionados com o stress, como sejam os ritmos circadianos, a própria espécie ou o estadió de desenvolvimento. A variabilidade das respostas com base nestes parâmetros fisiológicos levou à necessidade de identificar outro tipo de marcadores moleculares que fossem mais fiáveis e eficazes na avaliação do stress e bem-estar em peixes de aquacultura, complementares aos indicadores já existentes.

As ómicas como técnicas analíticas de alto rendimento e elevada resolução, em conjunto com a bioinformática, têm sido amplamente utilizadas na descoberta de biomarcadores associados a inúmeros fenótipos em diversos animais, mas sobretudo em humanos, com especial foco na resposta ao cancro. Nos estudos ligados à aquacultura, estas técnicas têm sido utilizadas com enorme sucesso em abordagens relacionadas com a nutrição, rastreabilidade, reprodução, segurança alimentar e bem-estar. Neste trabalho, procedeu-se a uma abordagem “multiómica” visando a integração das técnicas de proteómica, transcriptómica e metabolómica na caracterização da resposta molecular ao stress em diferentes tecidos de dourada, de modo a identificar um conjunto de biomarcadores putativos para diferentes tipos de stress. Para tal, foram estabelecidos três ensaios experimentais com douradas adultas, de uma forma independente: 1) alta densidade, 2) manuseamento repetitivo e 3) hipóxia. Em cada ensaio, testaram-se duas condições de stress (uma de maior intensidade, outra de menor), para além do respetivo grupo controlo. No final de cada ensaio recolheram-se amostras de plasma sanguíneo, fígado e de muco obtido a partir da epiderme. Os capítulos desta dissertação estão organizados de acordo com os diferentes tecidos estudados.

O “Chapter 2” incide sobre a análise proteómica baseada em gel (2D-DIGE) do plasma sanguíneo para avaliar o efeito dos diferentes tipos de stress no sistema imunitário de douradas adultas. Esta análise foi realizada em conjunto com a medição dos níveis de cortisol, glucose e lactato no plasma, bem como a avaliação do pH e rigor mortis no tecido do músculo.

O “Chapter 3” encontra-se dividido em quatro sub-capítulos, focando na análise multiómica de dourada sujeita a diferentes condições experimentais, com o objetivo de estudar e identificar os diferentes mecanismos moleculares de regulação exercida no fígado em resposta ao stress, a nível do genoma e metaboloma. No “Chapter 3.1” foi avaliado o potencial da técnica metabolómica de espectroscopia de infravermelhos designada de FTIR (*Fourier Transformed InfraRed spectroscopy*) na obtenção de um perfil espectral de infravermelho específico de peixes submetidos a stress. No “Chapter 3.2”, a técnica 2D-DIGE foi novamente utilizada, desta vez na comparação do proteoma de fígado de peixes sujeitos a stress em relação a uma condição controlo. Paralelamente, foram ainda medidos os níveis de glicogénio no fígado, assim como os níveis de transcritos específicos (através da técnica de reação de polimerase em cadeia em tempo real, RT-PCR) escolhidos com base nas respetivas proteínas

diferencialmente acumuladas em resposta ao stress. Nos “Chapters 3.3 e 3.4” foi realizada uma análise multiómica do fígado, integrando os dados de proteómica (*label-free shotgun proteomics*), transcriptómica (*RNA sequencing*) e metabolómica (*untargeted LC-MS/MS*), recorrendo a diferentes ferramentas de bioinformática.

O “Chapter 4” incide sobre a descoberta com base em proteómica “shotgun”, de um conjunto de potenciais biomarcadores de stress no muco de dourada, específicos para cada condição experimental. O poder discriminante e preditivo da resposta ao stress de diferentes proteínas foi avaliado com base em modelos de regressão logística. Esta matriz biológica serviu de base à identificação de biomarcadores minimamente invasivos, por se tratar de uma barreira semipermeável entre a epiderme do organismo e o meio envolvente que faz parte do sistema imunitário inato. O facto de o muco ser um biofluido externo facilita a recolha de amostras diminuindo assim o stress associado ao manuseamento dos peixes.

No seu conjunto, este estudo demonstra que a dourada é capaz de se adaptar mais rapidamente a situações de alta densidade (até 45 kg m⁻³), exigindo menos alterações a nível do sistema imunitário e do metabolismo, comparativamente à exposição ao manuseamento repetitivo e a baixas concentrações de oxigénio na água. No que respeita a estas duas últimas condições, a resposta ao stress em dourada aponta para a conservação de energia, sendo esta canalizada para as vias de sinalização típicas de resposta de stress celular (autofagia, endocitose, resposta de stress associada ao retículo endoplasmático e interrupção da replicação do DNA e do ciclo celular), assim como para a síntese de proteínas envolvidas nessas mesmas vias. A nível do sistema imunitário a resposta foi distinta, havendo uma ativação do sistema inato nos peixes expostos a manuseamento repetitivo, nomeadamente do sistema hemostático, e uma imunossupressão nos peixes em condições de hipóxia. Verificou-se, no entanto, uma regulação positiva do metabolismo do ferro, que está associada a respostas anti-inflamatórias, nos peixes expostos aos três tipos de stress, sugerindo um papel importante na regulação da resposta imune e da resposta ao stress. É de salientar ainda a elevada variabilidade de respostas dos indicadores plasmáticos, reforçando assim a necessidade de complementar estes parâmetros com outro tipo de indicadores de stress. Por fim, foram identificadas 28 proteínas a partir do muco da pele, como potenciais biomarcadores específicos para cada tipo de stress. Estes poderão vir a ser validados futuramente como indicadores de bem-estar laboratoriais, promovendo assim uma avaliação precoce do nível de stress em peixes

de aquacultura, de uma forma mais eficaz, robusta, fiável e holística, essenciais na prevenção de doenças e promoção de um cultivo sustentável das espécies alvo.

Palavras-chave: Aquacultura; Dourada; Metabolómica; Proteómica; Stress; Transcriptómica.

TABLE OF CONTENTS

ACKNOWLEDGMENTS	i
FUNDING	iii
DISSEMINATION	iv
SUMMARY	vii
RESUMO.....	viii
TABLE OF CONTENTS	xiii
LIST OF FIGURES	xxi
LIST OF TABLES	xxviii
LIST OF ABBREVIATIONS AND ACRONYMS	xxix

CHAPTER 1 – General Introduction..... 1

1.1. THE STATE OF AQUACULTURE	3
1.2. AQUACULTURE AND SUSTAINABILITY	5
1.3. FISH WELFARE: ORIGIN OF THE CONCEPT AND DEFINITIONS.....	7
1.4. A GLIMPSE INTO SENTIENCE AND CONSCIOUSNESS IN FISH.....	9
1.5. FISH FARMING AND WELFARE: WHERE ARE WE?	11
1.6. FISH WELFARE AND AQUACULTURE SUSTAINABILITY	12
1.7. FISH WELFARE AND STRESS PHYSIOLOGY.....	14
1.7.1. Stability through change	14
1.7.2. The stress response	16
1.7.2.1. <i>The stress response at mucosal surfaces</i>	18
1.8. INDICATORS OF FISH WELFARE	19
1.8.1. Operational and lab-based welfare indicators	19
1.8.2. Physiological stress markers and their reliability as welfare indicators	21
1.9. OMICS IN AQUACULTURE WITH A FOCUS ON FISH WELFARE.....	23
1.9.1. Proteomics	23
1.9.2. Transcriptomics	27
1.9.3. Metabolomics	29
1.9.4. Multiomics	30

1.10. IDENTIFICATION OF STRESS BIOMARKERS	32
1.11. OBJECTIVES	34

CHAPTER 2 – Protein changes as robust signatures of fish chronic stress: a proteomics approach to fish welfare research..... 37

2.1. ABSTRACT	39
2.2. INTRODUCTION	41
2.3. MATERIALS & METHODS	43
2.3.1. Animals	43
2.3.2. Experimental design	43
2.3.3. Sampling procedure.....	44
2.3.4. Plasma stress indicators’ measurement.....	44
2.3.5. Biochemical and quality characterization of fish muscle	44
2.3.6. Plasma proteomics analysis	45
2.3.6.1. <i>Protein labelling</i>	45
2.3.6.2. <i>Protein separation by 2DE</i>	45
2.3.6.3. <i>Image acquisition and analysis</i>	46
2.3.6.4. <i>Protein identification by MALDI-TOF/TOF MS</i>	46
2.3.7. Protein-protein interaction network and gene ontology enrichment analyses	47
2.3.8. Statistical analyses	47
2.4. RESULTS	48
2.4.1. Fish general condition	48
2.4.2. Plasma stress markers analysis	49
2.4.3. <i>Post-mortem</i> muscle biochemical changes.....	50
2.4.4. Plasma proteomics analysis	51
2.5. DISCUSSION	57
2.6. CONCLUSIONS	63
2.7. SUPPLEMENTARY MATERIAL	63

CHAPTER 3 – Multiomics characterization of the gilthead seabream hepatic stress response 65

CHAPTER 3.1 – Mid-infrared spectroscopic screening of metabolic alterations in stress-exposed gilthead seabream (*Sparus aurata*)

.....67

3.1.1. ABSTRACT69

3.1.2. INTRODUCTION71

3.1.3. MATERIALS & METHODS73

3.1.3.1. Experimental design and sampling.....73

3.1.3.2. Sample preparation and FTIR spectroscopy analysis.....74

3.1.3.3. Spectral preprocessing.....75

3.1.3.4. Multivariate statistical analyses75

3.1.4. RESULTS AND DISCUSSION76

3.1.4.1. FTIR spectra of gilthead seabream liver submitted to stressful conditions77

3.1.4.2. Correlation analysis78

3.1.4.3. Principal component analysis80

3.1.4.4. Feature selection and k-nearest neighbor classification analysis .83

3.1.5. CONCLUSIONS85

3.1.6. SUPPLEMENTARY MATERIAL86

CHAPTER 3.2 – Metabolic plasticity of gilthead seabream under different stressors: analysis of the stress responsive hepatic proteome and gene expression 87

3.2.1. ABSTRACT89

3.2.2. INTRODUCTION91

3.2.3. MATERIALS & METHODS93

3.2.3.1. Ethics93

3.2.3.2. Animals and rearing conditions93

3.2.3.3. Experimental design.....94

3.2.3.4. Sampling94

3.2.3.5. Liver proteomics analysis.....95

3.2.3.5.1.	<i>Protein extraction</i>	95
3.2.3.5.2.	<i>Protein labeling and separation</i>	95
3.2.3.5.3.	<i>Gel image analysis and protein identification</i>	96
3.2.3.5.4.	<i>Proteomics data analysis</i>	96
3.2.3.6.	Quantitative real-time reverse transcription polymerase chain reaction (RT-qPCR) Analysis	97
3.2.3.6.1.	<i>RNA isolation and two step reverse transcription PCR (RT-PCR)</i>	97
3.2.3.6.2.	<i>Gene cloning</i>	98
3.2.3.6.3.	<i>RT-qPCR assay</i>	101
3.2.3.6.4.	<i>Expression stability of reference genes and normalization</i>	101
3.2.3.7.	Hepatic glycogen assessment	102
3.2.3.8.	Univariate statistical analyses	102
3.2.4.	RESULTS	103
3.2.4.1.	Gel-based proteomics analysis of gilthead seabream liver	103
3.2.4.2.	Univariate and multivariate statistical analyses of differential abundant proteins	104
3.2.4.3.	Functional GO annotation of identified proteins	105
3.2.4.4.	PPI network analysis and KEGG pathway enrichment	106
3.2.4.5.	Expression stability of candidate reference genes	110
3.2.4.6.	Amplification specificity and efficiency, and absolute quantification	110
3.2.4.7.	Liver glycogen levels	112
3.2.5.	DISCUSSION	112
3.2.5.1.	Carbohydrate metabolism	113
3.2.5.2.	Amino acid metabolism	115
3.2.5.3.	Lipid metabolism	118
3.2.5.4.	Antioxidant system	119
3.2.5.5.	Cellular stress response	120
3.2.5.6.	Protein synthesis	121
3.2.6.	CONCLUSIONS	122
3.2.7.	SUPPLEMENTARY MATERIAL	123

CHAPTER 3.3 – Gilthead seabream liver integrative proteomics and metabolomics analysis reveals regulation by different prosurvival pathways in the metabolic adaptation to stress 125

3.3.1. ABSTRACT	127
3.3.2. INTRODUCTION	129
3.3.3. MATERIALS & METHODS	131
3.3.3.1. Ethics	131
3.3.3.2. Fish and stocking conditions	131
3.3.3.3. Experimental design.....	131
3.3.3.4. Sampling	132
3.3.3.5. Sample preparation	132
3.3.3.6. Label-free shotgun proteomics analysis	133
3.3.3.6.1. <i>NanoLC-MS/MS analysis</i>	133
3.3.3.6.2. <i>Protein identification</i>	134
3.3.3.7. Untargeted metabolomics analysis.....	135
3.3.3.8. Univariate and multivariate statistical analyses	136
3.3.3.9. Functional analyses	137
3.3.4. RESULTS	138
3.3.4.1. Proteomics and metabolomics data overview	138
3.3.4.2. Integrated stress response analysis.....	140
3.3.5. DISCUSSION	143
3.3.6. CONCLUSIONS	152
3.3.7. SUPPLEMENTARY MATERIAL	153

CHAPTER 3.4 – Underlining the hepatic transcriptional changes behind *Sparus aurata* responses to different aquaculture challenges: an RNA-seq study 155

3.4.1. ABSTRACT	157
3.4.2. INTRODUCTION	159
3.4.3. MATERIALS & METHODS	161
3.4.3.1. Fish husbandry	161

3.4.3.2. Experimental trials and sampling.....	161
3.4.3.3. Liver RNA sequencing	162
3.4.3.3.1. Total RNA extraction and purification	162
3.4.3.3.2. Library construction and RNA sequencing	163
3.4.3.4. Bioinformatics analysis	163
3.4.3.4.1. Quality assessment, reads mapping and differential expression analysis.....	163
3.4.3.4.2. Functional enrichment analysis	164
3.4.4. RESULTS AND DISCUSSION	165
3.4.4.1. Overview of RNA-seq data and differential expression analysis	165
3.4.4.2. Net handling induced ribosomal assembly stress coupled to inhibition of insulin growth factor signaling in gilthead seabream hepatocytes.....	167
3.4.4.3. Hypoxia-induced DNA replication stress in gilthead seabream hepatocytes is synergistically mediated by the hypoxia-inducible factor and mTORC1	172
3.4.4.4. The dual role of the endoplasmic reticulum in the adaptation to net handling and hypoxia stress: cholesterol biosynthesis and the unfolded protein response	177
3.4.5. CONCLUSIONS	181
3.4.6. SUPPLEMENTARY MATERIAL	182

CHAPTER 4 – A new window into fish welfare: a proteomic discovery study of stress biomarkers in the skin mucus of gilthead seabream (*Sparus aurata*)..... 183

4.1. ABSTRACT	185
4.2. INTRODUCTION	187
4.3. MATERIALS & METHODS.....	189
4.3.1. Ethics.....	189
4.3.2. Animals and stocking conditions	189
4.3.3. Experimental design	189

4.3.4. Fish sampling	190
4.3.5. Protein sample preparation	190
4.3.6. Label-free shotgun proteomics	191
4.3.6.1. nanoLC-MS/MS	191
4.3.6.2. Protein identification.....	192
4.3.7. Statistical and bioinformatic analyses	193
4.3.7.1. Analysis of DAPs	193
4.3.7.2. Annotation of DAPs and PPI network analysis	194
4.3.7.3. Regression and correlation analysis between levels of protein abundance and physiological stress indicators.....	194
4.3.7.4. Feature selection and predictive modeling of the stress response	195
4.4. RESULTS AND DISCUSSION	197
4.4.1. Label-free shotgun proteomics overview.....	197
4.4.2. Skin mucus proteome response to different challenges	197
4.4.3. Functional analysis of skin mucus DAPs.....	198
4.4.3.1. REACTOME pathway analysis	198
4.4.3.2. Stress-responsive PPI network.....	200
4.4.3.3. GO enrichment of proteins highly interconnected in the network	201
4.4.4. Correlation analysis between the skin mucus proteome and physiological stress indicators in plasma	202
4.4.5. Discovery of candidate stress biomarkers in the gilthead seabream skin mucus.....	204
4.4.5.1. Principal component analysis	205
4.4.5.2. Selection of predictor proteins by RFE.....	205
4.4.5.3. Predictive logistic regression model.....	206
4.4.5.4. Evaluation of model performance through ROC curve analysis.....	206
4.4.6. Study limitations and future perspectives	211
4.5. CONCLUSIONS	212
4.6. SUPPLEMENTARY MATERIAL	212

CHAPTER 5 – General Discussion, Main Conclusions and Future Perspectives.....	215
5.1. Farmed gilthead seabream can tolerate rearing densities up to 45 kg m ⁻³	215
5.2. Gilthead seabream netted four times a week activated several prosurvival pathways as an adaptation response to cellular stress	218
5.3. Exposure to 15% DO for 48h induced an “energy-conservation state” through cell cycle arrest in gilthead seabream hepatocytes	220
5.4. Skin mucus is a promisor minimally invasive biological matrix to identify both chronic and acute stress biomarkers	221
5.5. Directions for upcoming research	222
5.5.1. <i>Targeting specific biomolecules</i>	222
5.5.2. <i>Targeting specific levels of regulation</i>	224
5.5.3. <i>Next steps in biomarker identification</i>	225
5.6. Future perspectives and implications for aquaculture sustainability.	226
REFERENCES	227
APPENDIX	269

LIST OF FIGURES

Figure 1.1. World aquaculture production between 1991 and 2020 (Source: FAO, 2022).	3
Figure 1.2. Schematization of aquaculture’s main contributions to the SDGs (Adapted from Troell et al., 2021)	7
Figure 1.3. Five domains revised from the Brambell Report (1965) by UK Farm Animal Welfare Council to ensure and assess welfare of animal reared and kept under artificial conditions (Adapted from FSBI, 2002).	9
Figure 1.4. Radar plot of the average score attributed to the link animal welfare (AW) – sustainable developmental goal (SDG) (0 – consistent, 1 – enabling, 2 – reinforcing, 3 – indivisible) (Source: Keeling et al., 2019)	14
Figure 1.5. Interaction between good and poor welfare and the subjective experiences appraised by the fish: (1) “stability through constancy” strict linear model according to the homeostasis concept; (2) “constancy through change” hyperbolic model according to allostasis framework. Hypostimulation from low environmental challenges may produce poor welfare conditions; Hyperstimulation from high environmental challenges may also produce poor welfare conditions (distress). Certain degrees of environmental challenge (eustress) will improve welfare (represented above the standard welfare line). Allostatic load - beneficial stress conditions that the fish can cope with; allostatic overload - stress conditions that will cause illness, ultimately death (adapted from Korte et al., 2007).	15
Fig. 1.6. Summarized schematization of the stress response in fish. The perception of the stressful stimulus by the brain induces the release of catecholamines and cortisol from the head kidney into the blood stream. These will induce the release of glucose and lactate and further metabolic, immunological, and behavioral changes that if sustained in time may be detrimental for fish welfare.	17
Figure 1.7. Most used operational and lab-based welfare indicators in aquaculture.	21
Figure 1.8. Different possible pathways that a typical proteomics workflow can follow in aquaculture proteomics studies: gel-based top-down and gel-free bottom-up strategies. Both approaches share the sample preparation feature and aim to identify the proteins of interest.	26
Figure 1.9 – Main questions addressed by the different omics platforms applied to the aquaculture research (Source: Canellas et al., 2022)	31
Figure 1.10. Classical biomarker workflow known as “triangular approach”. Discovery proteomics is first employed to identify a wide set of candidate biomarkers, which are then screened by targeted proteomics for confirmation and quantification. The few remaining candidates are then validated through immunological assays. The number of samples usually increases along the pipeline, contrasting with the number of candidate biomarkers.	34

Figure 2.1. Violin plots showing the distributions of plasma cortisol (ng/ml), glucose (mg/dl) and lactate (mg/dl) levels of gilthead seabream (*Sparus aurata*) submitted to different challenges (A – overcrowding, B – net handling, C – hypoxia), in two intensities, and unstressed fish (control) (n = 18). The boxplot inside includes observations from the 25th to the 75th percentiles as determined by R software; the horizontal line indicates the median value. Whiskers extend 1.5 times the interquartile range. Single data points are outlying data. * $p < 0.05$; ** $p < 0.01$; *** $p < 0.001$; **** $p < 0.0001$. NS (not significant) indicates a p -value greater than 0.05.49

Figure 2.2. *Post-mortem* changes in muscle pH and *rigor mortis* of gilthead seabream (*Sparus aurata*) submitted to different challenges (A – overcrowding, B – net handling, C – hypoxia), in two intensities, and unstressed fish (control), stored in ice for 72 h. Data points are the mean \pm SD of n = 9 for each sampling time. Means labelled * are different at $p < 0.05$51

Figure 2.3. Representative pattern of gilthead seabream (*Sparus aurata*) blood plasma on a 12.5% polyacrylamide 2D gel. Black circles represent the 107 proteins identified by MALDI-TOF/TOF MS with significant differences in abundance in NET groups and black squares the 2 proteins with significant differences in abundance in HYP groups ($p < 0.05$).52

Figure 2.4. Volcano plots of the entire set of plasma proteins detected by DIGE analysis on the NET trial samples. Each point represents the difference in abundance (fold-change) between stressed fish (NET2 on the left; NET4 on the right) and control fish plotted against the level of statistical significance. Dotted vertical lines represent a 2-fold variation in abundance, while dotted horizontal line represent the significance level of $p < 0.05$. Red dots represent proteins significantly up- and downregulated. B – PCA performed with the normalized spot volumes of the 107 identified proteins in the plasma samples of gilthead seabream from the NET trial (n = 6). Blue, orange, and red dots represent CTRL, NET2 and NET4 groups, respectively. C – HCA of 107 significantly differential proteins identified in the plasma samples of gilthead seabream from net handling (NET) trial. Rows represent expression patterns of individual proteins, while each column corresponds to a biological replicate (fish). Cell color indicates the normalized Z-scores of the spot volumes.53

Figure 2.5. PPI network generated with 18 differential proteins identified in the plasma of fish from NET trial. Nodes represent proteins and edges the functional associations between them. STRING annotations are described in Table 2.1. Red arrows represent upregulated proteins in both treatments; blue arrows represent downregulated proteins in both treatments. D – GO Enrichment analysis of the 18 proteins showing significantly differential abundance between control and NET treatments (hypergeometric test, FDR < 0.05).55

Figure 3.1.1. FTIR spectra of the liver of gilthead seabream (*Sparus aurata*) submitted to three different stressful rearing conditions (overcrowding, net handling, and hypoxia) and Pearson’s correlation coefficient matrices comparing the assigned bands of the spectra. (A–C) FTIR spectra, for each treatment, are shown as absorbance values (in

arbitrary units (A.U.)) of 8 averaged spectra (solid line) ± standard deviation (shaded ribbon). For easier readability, mean spectra were offset along the absorbance axis. Numbers indicate the bands assigned to biomolecules, listed in Table 3.1.1. Plots in each row are prepared with the same vertical scale. (D–F) Plots are ordered by hierarchical clustering with complete linkage. Numbers indicate the bands assigned to biomolecules, following the same convention as Table 3.1.1. Thicker lines represent clusters. The degree of pairwise correlation concerning Pearson’s correlation coefficient is displayed by the color gradient and dot size, while the colors define the signal of the correlation (positive or negative). The significance of the correlation is indicated by the label “*” inside the dots (*0.05 < p < 0.01, **0.01 < p < 0.001, *** p > 0.001).79

Figure 3.1.2. PCA on the FTIR spectra collected from the livers of gilthead seabream (*Sparus aurata*) submitted to three different stressful rearing conditions (overcrowding, net handling, and hypoxia). (A–C) Score scatter plots on PC1 and PC2 computed for each trial with the 3600–950 cm^{-1} spectral range. Each point represents the projection of one spectrum, and each treatment is identified by a unique color, as indicated in the legend. Percentages indicate the proportions of explained variance. Ellipses represent an 80% probability of samples being within the shape. (D–F) PC loadings along the corresponding wavenumber for each trial. (G–I) Ranking of the spectral features according to the SVM-RFE method for feature selection, along the wavenumber range of 3600–950 cm^{-1} . Most well classified features in the ranking are shown in dark blue, while least important features are colored in yellow.82

Figure 3.1.3. Classification analysis performed by the k-nearest neighbor (KNN) algorithm on the FTIR spectra collected from the livers of gilthead seabream (*Sparus aurata*) submitted to three different stressful rearing conditions ((a) OC trial, (b) NET trial, (c) HYP trial). Predictive performance of the models is presented as mean classification accuracy (%) of training and testing sets for each subset of selected features by SVM-RFE. Error bars represent the standard deviation obtained by ten-fold cross validation (CV) of the initial data splitting.....85

Figure 3.2.1. Summary of the protein spots identified in the 2D-gels of the proteomics analysis performed with the liver of gilthead seabream (*Sparus aurata*) submitted to different challenges, and their expression profiles..... 103

Figure 3.2.2. Proteomics data analysis of OC trial. (A) Volcano plots of the differential proteins detected by 2D-DIGE analysis on the OC trial liver samples ($n = 6$). Dotted vertical lines represent a 1.5-fold variation in abundance, while the dotted horizontal line represents the significance level of $p < 0.05$ (Student’s t -test). Triangles represent proteins significantly up- and downregulated. (B) HCA of the 36 significantly different spots (One-way ANOVA, followed by Dunnett’s test, $p < 0.05$) in the liver of gilthead seabream from OC trial. Rows represent proteins’ expression patterns, while each column corresponds to a biological replicate (fish). (C) Functional GO classification of the identified proteins. Pie chart shows the level 2 GO annotations of biological process. 105

Figure 3.2.3. Proteomics data analysis of NET trial. (A) Volcano plots of the differential proteins detected by 2D-DIGE analysis on the NET trial liver samples (n = 6). Dotted vertical lines represent a 1.5-fold variation in abundance, while the dotted horizontal line represents the significance level of $p < 0.05$ (Student's t -test). Triangles represent proteins significantly up- and downregulated. (B) HCA of the 165 significantly different spots (One-way ANOVA, followed by Dunnett's test, $p < 0.05$) in the liver of gilthead seabream from NET trial. Rows represent proteins' expression patterns, while each column corresponds to a biological replicate (fish). (C) Functional GO classification of the identified proteins. Pie chart shows the level 2 GO annotations of biological process. (D) PPI network generated with 34 DAPs identified in the liver of fish from NET trial. Nodes represent proteins and edges the functional associations between them. Colored areas indicate enriched KEGG pathways (FDR < 0.05). (E) Bubble plot representing the statistical significance and number of proteins belonging to each KEGG enriched pathway (lower level) overrepresented in the PPI network. BC, betweenness centrality 107

Figure 3.2.4. Proteomics data analysis of HYP trial. (A) Volcano plots of the differential proteins detected by 2D-DIGE analysis on the HYP trial liver samples (n = 6). Dotted vertical lines represent a 1.5-fold variation in abundance, while the dotted horizontal line represents the significance level of $p < 0.05$ (Student's t -test). Triangles represent proteins significantly up- and downregulated. (B) HCA of the 59 significantly different spots (One-way ANOVA, followed by Dunnett's test, $p < 0.05$) in the liver of gilthead seabream from HYP trial. Rows represent proteins' expression patterns, while each column corresponds to a biological replicate (fish). (C) Functional GO classification of the identified proteins. Pie chart shows the level 2 GO annotations of biological process. (D) PPI network generated with 26 DAPs identified in the liver of fish from HYP trial. Nodes represent proteins and edges the functional associations between them. Colored areas indicate enriched KEGG pathways (FDR < 0.05). (E) Bubble plot representing the statistical significance and number of proteins belonging to each KEGG enriched pathway (lower level) overrepresented in the PPI network. BC, betweenness centrality 109

Figure 3.2.5. Expression profiles of 13 different transcripts in the liver (n = 6) of gilthead seabream (*Sparus aurata*) exposed to different challenges (A) OC trial, (B) NET trial, (C) HYP trial, obtained by RT-qPCR. The normalized absolute copy numbers of the target genes are presented in $\log_2(\text{fold-change treated-control})$. Bars labeled * indicate statistically significant differences when compared with the control group (One-way ANOVA, followed by Dunnett's test, * $p < 0.05$; ** $p < 0.01$). 111

Figure 3.2.6. Boxplots showing the distribution of glycogen levels in the liver of gilthead seabream (*Sparus aurata*) submitted to three different challenges (A) OC trial, (B) NET trial, (C) HYP trial. The boxplots include observations (n = 9) from the 25th to the 75th percentiles as determined by R software; the horizontal line indicates the median value. Whiskers extend 1.5 times the interquartile range. Single data points represent outlying data. Lower case letters indicate statistically significant differences ($p < 0.05$). 113

Figure 3.2.7. Schematic representation of the metabolic pathways affected by the different challenges. Yellow, red, and green arrows represent differences in abundance (One-way ANOVA, followed by Dunnett's test, $p < 0.05$) in the liver of *Sparus aurata* from OC, NET and HYP trials, respectively. Dark orange pathway names indicate affected metabolic pathways, while light orange pathway names indicate non-affected pathways. Pointed arrowed lines indicate substrate transport across the mitochondria's membrane, while dashed arrowed lines represent more than one enzymatic reaction. a-KG, α -ketoglutarate; 4-HOG, 4-hydroxy-2-oxoglutarate; 4-HPP, 4-hydroxyphenylpyruvate; 4-MAA, 4-maleyl-2-acetoacetate; DHAP, dihydroxyacetone phosphate; F1,6-BP, fructose 1,6-biphosphate; F1P, fructose-1-phosphate; F6P, fructose-6-phosphate; GA3P, glyceraldeyde-3-phosphate; G1P, glucose-1-phosphate; G2P, glyceraldehyde-2-phosphate; G3P, glycerol-3-phosphate; G6P, glucose-6-phosphate; L-2-HG, L-2-hydroxyglutarate; PEP, phosphoenolpyruvate; UDP-D-GlcUA, UDP-D-glucuronate; UDP-G, UDP-glucose..... 116

Figure 3.3.1. PCA biplots of the liver proteomics and metabolomics data of gilthead seabream subjected to overcrowding (OC), net handling (NET) and hypoxia (HYP) challenges. Each point represents a biological replicate's projection, and experimental groups within trials are represented by a unique color, as indicated in each legend. The largest point represents the group mean. The axes' percentages indicate the proportions of explained variance. The arrows depict the top-five most weighted variables. 139

Figure 3.3.2. A gene-concept network of enriched KEGG terms (FDR < 0.05) within the differential abundant proteins (DAPs) and metabolites (DAMs) identified in the liver of gilthead seabream subjected to the net handling (NET) challenge. Central nodes represent the enriched term, with color and size representing FDR and the number of associated biomolecules, respectively. The concept nodes represent biological concepts, where shape corresponds to the omics modality and color to the regulation of that biomolecule, determined by Student's *t*-test with FDR controlled at 0.05. 140

Figure 3.3.3. Metabolic reaction network generated with the differential abundant proteins and metabolites identified in the liver of gilthead seabream subjected to a net handling challenge. Node shape and color represent the type of biomolecule, according to the legend. Edges represent functional linkages between them. The highlighted clusters, depicted with the MCODE plugin within Cytoscape software, represent the most interconnected regions, with the corresponding overrepresented in KEGG terms (FDR < 0.05). 141

Figure 3.3.4. Integrated proteomics and metabolomics analysis, conducted with DIABLO, of the liver of gilthead seabream subjected to the net handling challenge (NET). (A) Arrow plot of the separation between groups achieved with the first two components of the DIABLO model. Different shapes represent different data modalities. (B) Circos plots representing the Pearson correlation (correlation cutoff = 0.9) between the 10 most-discriminatory proteins and metabolites selected by the first component of the DIABLO model. (C) Voronoi plots obtained with a REACTOME

analysis tool represent two of the most overrepresented high category terms (FDR < 0.05), among the upregulated features selected by DIABLO. The *p*-value scale indicated in the figure legend corresponds to the adjusted *p*-value..... 143

Figure 3.3.5. Overview of the cellular processes and signaling pathways affected by net handling and hypoxia in gilthead seabream hepatocytes. The proteins and metabolites represented were differentially different in abundance, according to a Student's *t*-test with FDR controlled at 0.05..... 147

Figure 3.3.6. Overview of the metabolic pathways affected by net handling and hypoxia in gilthead seabream hepatocytes. The proteins and metabolites represented were significantly different in abundance, according to a Student's *t*-test with FDR controlled at 0.05. 151

Figure 3.4.1. Summary of the exploratory and differential analyses results of RNA-seq data. Biplots represent the principal component analyses (PCA) of the liver transcriptome of gilthead seabream submitted to overcrowding (A), net-handling (B), and hypoxia (C). Experimental groups are distinguished by different colours, as indicated in the legend. Arrows depict the top loadings. MA plots of the shrunken LFCs indicate differentially expressed genes (D – overcrowding, E – net-handling, F – hypoxia). Blue points represent *p*_{adj} > 0.01, and horizontal lines indicate the threshold of log₂|fold-change| > 1.0. 168

Figure 3.4.2. GSEA performed on the RNA-seq data of the liver transcriptome of gilthead seabream submitted to net handling, based on GO (A,D), KEGG (B,E), and REACTOME (C,F) databases, sorted by normalized enrichment score (NES) inferred from permutations of the gene set and false discovery rate (FDR). On the x-axis, the genes were ranked from the most upregulated (left end) to the most downregulated (right end). The y-axis represents the running enrichment score (ES). First line indicates downregulated pathways whereas bottom line indicates upregulated pathways. 171

Figure 3.4.3. Proposed stress response network in gilthead seabream hepatocytes subjected to net-handling and hypoxia. Dashed arrows indicate downregulated pathways, whereas solid arrows represent unchanged or upregulated pathways. .. 173

Figure 3.4.4. GSEA performed on the RNA-seq data of the liver transcriptome of gilthead seabream submitted to hypoxia, based on GO (A,D), KEGG (B,E), and REACTOME (C,F) databases, sorted by normalized enrichment score (NES) inferred from permutations of the gene set and false discovery rate (FDR). On the x-axis, the genes were ranked from the most upregulated (left end) to the most downregulated (right end). The y-axis represents the running enrichment score (ES). First line indicates downregulated pathways whereas bottom line indicates upregulated pathways. 178

Figure 3.4.5. Heatmap of multiomics overrepresentation analysis (ORA): (A) net handling trial, (B) hypoxia trial; listed terms are commonly overrepresented terms between omics datasets. 181

Figure 4.1. Schematization of the methodology workflow, from sample collection to ROC curve analysis.196

Figure 4.2. Circos plots displaying a comprehensive functional characterization of skin mucus DAPs identified in gilthead seabream by label-free shotgun proteomics. Protein functions were annotated according to REACTOME pathways. DAPs within each fish trial i.e., overcrowding (OC), repetitive net handling (NET) and hypoxia (HYP) were assessed by One-way ANOVA followed by Tukey’s test ($p < 0.05$) (see Table S3 - online). Protein annotation into REACTOME pathways is detailed on Table S4 - online.199

Figure 4.3. PPI network of the DAPs identified in the skin mucus of gilthead seabream, submitted to control and repetitive net handling in two intensities, namely “NET2” and “NET4” challenging conditions (Table S3 - online). Nodes represent proteins, and edges, the interactions between them. Betweenness centrality is represented by the size of the nodes, while node color and shape indicate protein regulation and significant differences, respectively, according to the figure legend. Four densely interconnected regions/clusters are highlighted in the squared boxes.201

Figure 4.4. Networks of enriched GO terms (hypergeometric Benjamini & Hochberg FDR correction, $q < 0.05$) in the main clusters depicted in the NET PPI network (Figure 4.3). GO enrichment analysis was performed based on the biological process category.203

Figure 4.5. Sparse partial least squares regression analysis of the skin mucus proteome and the plasma physiological indicators. Networks indicate predictor proteins selected among OC (A), NET (B) and HYP (C) identified proteins with a correlation coefficient higher than 0.75 with the physiological indicators. Proteins (rectangles) are represented by the Protein ID (Table S2 - online). Positive correlations are represented by red edges and negative correlation by green edges.204

Figure 4.6. PCA biplots of the skin mucus proteomics data of gilthead seabream adults from OC (A), NET (B) and HYP (C) trials. Experimental groups within trials are represented by different colors, as indicated in the figure legend. The largest point, in each group, represents the group mean. Axis’ percentages indicate the proportions of explained variance. Arrows represent the top ten features with the highest loading values in the first principal component.206

LIST OF TABLES

Table 1.1. Main factors affecting fish welfare and most common indicators of impaired fish welfare (adapted from Silva et al., 2013)	13
Table 2.1. STRING annotations and fold-changes of the proteins in the PPI network. Bold lettering in the “FC” column indicates significant fold-changes (> 1.0 and < -1.0). List is given in ascending order of spot number.....	56
Table 3.1.1. Tentative assignment of spectral bands to molecular vibrations of functional groups and biochemical compounds, based on similar biological systems described in the literature (Cakmak et al., 2006; Ceylan et al., 2014; Palaniappan et al., 2010; Rodriguez-Casado et al., 2007; Sánchez-Alonso et al., 2012; Silva et al., 2014)	78
Table 3.2.1. Primers used for the RT-PCR and RT-qPCR analyses of the candidate reference genes and the target genes, and expected amplicon sizes	99
Table 3.2.2. Expression stability analysis of each candidate reference gene for gilthead seabream liver RT-qPCR analysis, based on different algorithms.....	110
Table 3.4.1. Summary statistics of the comparison between the experimental transcriptome assembled with Stringtie and the <i>Sparus aurata</i> reference genome, achieved with gffcompare	166
Table 4.1. Logistic regression and ROC curve analyses of predictor proteins selected by the feature selection algorithm (RFE). Values of accuracy and area under the curve (AUC) of the training and testing sets are the mean of 10-fold cross validation. Proteins, represented by STRING annotations, highlighted in blue correspond to downregulated proteins while the ones highlighted in red represented upregulated proteins.	209

LIST OF ABBREVIATIONS AND ACRONYMS

2D-DIGE	Two-dimensional difference gel electrophoresis
A2ML	Alpha-2-macroglobulin
ACN	Acetonitrile
ADP	Adenosine diphosphate
AGC	Automatic gain control
AGXTB	Serine-pyruvate aminotransferase
AHCY	Adenosylhomocysteinase
ALDH2.2	Aldehyde dehydrogenase 2
AMP	Adenosine monophosphate
AMPK	(AMP)-activated protein kinase
ANOVA	Analysis of variance
APP	Acute phase proteins
ARRIVE	Animal Research: Reporting of In Vivo Experiments
ASNS	Asparagine synthetase
ATF4	Activating transcription factor 4
ATF6	Activating transcription factor 6
ATP	Adenosine triphosphate
AUC	Area under the curve
BHMT	Betaine-homocysteine S-methyltransferase
bp	Base pairs
BP	Biological process
BSA	Bovine serum albumin
CAD	Carbamoyl phosphate synthetase 2-aspartate transcarbamoylase-dihydroorotase
CALR	Calreticulin
CCT8	T-complex protein 1 subunit theta
CHAPS	3-[(3-Cholamidopropyl) dimethylammonio]-1-propanesulfonate
CME	Clathrin-mediated endocytosis
CPTAC	Clinical Proteomic Tumor Analysis Consortium
CTRL	Control
CTSD	Cathepsin d
CV	Coefficient of variation/Cross validation
Da	Daltons
DAMs	Differentially abundant metabolites
DAPs	Differentially abundant proteins
DDA	Data dependent acquisition
DEA	Differential expression analysis
DEGs	Differentially expressed genes
DGAV	Direção-Geral de Alimentação e Veterinária
DIA	Data independent acquisition
DIABLO	Data Integration Analysis for Biomarker discovery using Latent components

DMF	Dimethylformamide
DNAJB11	Dnaj heat-shock protein family member B11
DO	Dissolved oxygen
DTT	Dithiothreitol
EDTA	Ethylenedinitrilotetraacetic acid
EIF3A	Eukaryotic initiation factor 3a
ELISA	Enzyme-linked immunosorbent assay
ENO1	Alpha-enolase
ER	Endoplasmic reticulum
ERAD	ER-associated degradation
ESI	Electrospray ionization
FA	Fatty acid
FABP	Fatty-acid binding protein
FBP1	Fructose 1,6-bisphosphatase
FC	Fold-change
FDR	False discovery rate
FP	Forward primer
FTIR	Fourier transform-infrared
GAPDH	Glyceraldehyde-3-phosphate dehydrogenase
GO	Gene ontology
GR	Glucocorticoid receptor
GRP78/HSPA5	78 kda glucose-regulated protein
GRP94/HSP90B	94 kda glucose-regulated protein
GSEA	Gene set enrichment analysis
GSR	Glutathione-disulfide reductase
HAAO	3-hydroxyanthranilate 3,4-dioxygenase
HAD	Hours after death
HCA	Hierarchical clustering analysis
HCD	Higher-energy collisional dissociation
HIF	Hypoxia inducible factor
HPDA	4-hydroxyphenylpyruvate dioxygenase
HPI	Hypothalamic-pituitary-interrenal
HRE	Hypoxia responsive elements
HSPA8	Heat-shock protein family A (Hsp70) member 8
HYOU1	Hypoxia upregulated 1
HYP	Hypoxia
IAA	Iodoacetamide
IBW	Initial body weight
IEF	Isoelectric focusing
IGF	Insulin growth factor
IGFBP1	Insulin growth factor binding protein 1
IGF1R	Insulin growth factor 1 receptor
IRE1	Inositol-requiring protein-1
ITRAQ	Isobaric Tags for Relative and Absolute Quantification

JPA	Joint pathway analysis
KEGG	Kyoto Encyclopedia of Gene and Genomes
LAB	Ketohexokinase
LABWI	Lab based welfare indicators
LARS	Leucyl-trna synthetase
LC	Liquid chromatography
LFC	Log ₂ fold-change
LOOCV	Leave one out cross validation
LR	Logistic regression
MALDI-TOF/TOF MS	Matrix-assisted laser desorption/ionization Time-Of-Flight Mass Spectrometry
MALT	Mucosa-associated lymphoid tissues
MAPK	Mitogen-activated protein kinase
mTORC1	Mechanistic/mammalian target of rapamycin complex 1
NADPH	Nicotinamide adenine dinucleotide phosphate
NCBI	National Center for Biotechnology Information
NDRG1A	N-myc downstream-regulated gene 1a
NES	Normalized enrichment score
NET	Net handling
NGS	Next generation sequencing
NMR	Nuclear magnetic resonance
NRF2	NF-E2-related factor 2
OC	Overcrowding
ORA	Overrepresentation analysis
OWI	Operational welfare indicators
OXPHOS	Oxidative phosphorylation
PAH	Phenylalanine-4-hydroxylase
PARK7	Protein/nucleic acid deglycase DJ-1
PC	Principal component
PCA	Principal component analysis
PDI	Protein disulfide-isomerase
PE	Paired end
PEP	Phosphoenolpyruvate
PERK	Protein kinase RNA (PKR)-like ER kinase
pI	Isoelectric point
PLS	Partial least squares
PMF	Peptide mass fingerprinting
PMT	Photo multiplier tube
PPI	Protein-protein interaction
PRDX	Peroxiredoxin
PTM	Posttranslational modifications
QC	Quality control
RASTR	Ribosome Assembly Stress Response
REDD1	Regulated in DNA damage and development 1

RFE	Recursive feature elimination
RIN	RNA integrity number
RNA-seq	RNA sequencing
ROC	Receiver operating characteristic
ROS	Reactive oxygen species
RPS6	Ribosomal protein S6
RPs	Ribosomal proteins
RPGs	Ribosomal protein genes
RT-qPCR	Quantitative real-time reverse transcription polymerase chain reaction
SALT	Skin-associated lymphoid tissue
SD	Standard deviation
SDS-PAGE	Sodium dodecyl-sulfate polyacrylamide gel electrophoresis
SNP	Single nucleotide polymorphisms
SNR	Signal-to-noise ratio
SOD	Cu/Zn superoxide dismutase
STEAP4	Six-transmembrane epithelial antigen of the prostate 4
STITCH	Search Tool For The Interactions Of Chemicals
STRING	Search Tool for the Retrieval of Interacting Genes/Proteins
SVM	Support vector machine
TCA	Tricarboxylic acid
TCGA	The Cancer Genome Atlas Program
TF	Transcription factor
TFA	Trifluoroacetic acid
TXN	Thioredoxin
UPR	Unfolded protein response
UPS	Ubiquitin proteasome system
VST	Variance stabilizing transformation
XBP1	X-box-binding protein 1

General Introduction

”

The unseen and unfamiliar life of fish has given them low visibility in civil society, in policy circles, and in the animal welfare movement. Meanwhile, the number of farmed fish outnumbers by far any other sentient animals farmed for food.

— Douglas Waley, Eurogroup for Animals



Part of this chapter has been published as review article in:

Raposo de Magalhães, C.S.F., Cerqueira, M.A.C., Schrama, D., Moreira, M.J.V., Boonanuntanasarn, S., Rodrigues, P.M.L., 2020. A Proteomics and other Omics approach in the context of farmed fish welfare and biomarker discovery. *Reviews in Aquaculture* 12, 122-144. **doi: 10.1111/raq.12308**

1.1. THE STATE OF AQUACULTURE

The world's population has reached a historic milestone of 8 billion people in November 2022, according to the United Nations (UN), and is projected to reach 9 billion by 2037 (Zeifman et al., 2022). Unsurprisingly, this unprecedented demographic growth has had severe consequences on the environment, including global warming, climate change, deforestation, and biodiversity loss. One of the key drivers for slowing down environmental degradation for future generations is the reshaping of the global food production and consumption chain. Aquatic foods are making an increasingly critical contribution to food and nutrition. According to the Food and Agriculture Organization (FAO), global consumption of aquatic foods has outpaced population growth, with an average annual increase of 3% since 1961, compared to the 1.6% growth of the population. In 2020, consumption of aquatic food reached 20.2 kg per capita. Rising incomes and urbanization and changes in post-harvest practices and distribution, coupled with modern dietary trends focused on health benefits, are behind the growing demand for seafood products. Consequently, global fisheries and aquaculture production are at a record high, reaching 214 million tonnes in 2020, of which 122.6 million tonnes are produced by the aquaculture sector. Aquaculture contributed a record 49.2% to global production of aquatic animals in 2020 (FAO, 2022).

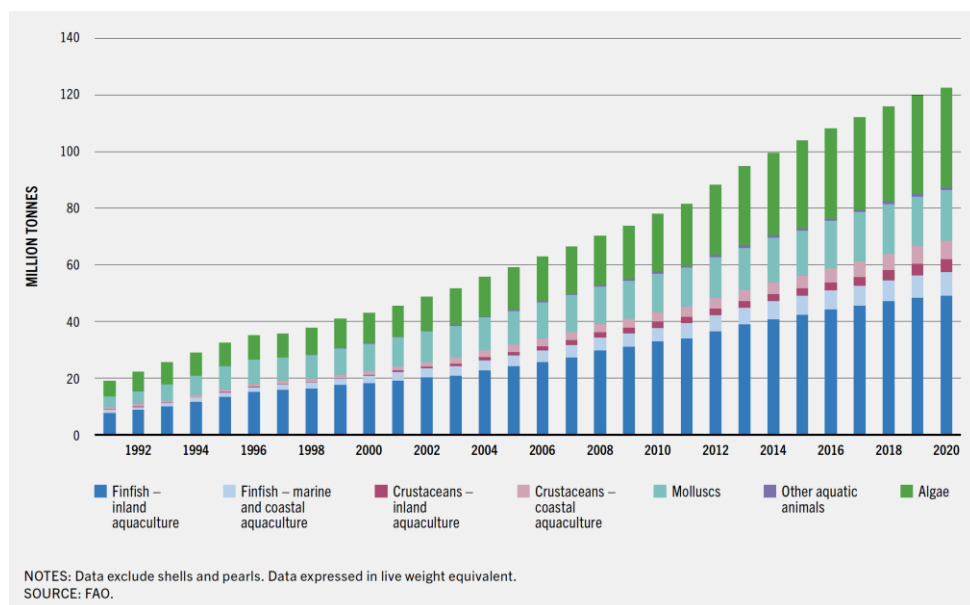


Figure 1.1. World aquaculture production between 1991 and 2020 (Source: FAO, 2022).

Asia remains the main aquaculture producer in the world, accounting for 90% of the total production of aquatic animals, with China leading this region. Europe contributed 3.74% to the world's production of aquatic animals, with Norway being the top-producing country, accounting for 46% of Europe's production, compared to 33% of the European Union (EU). Regarding the main species groups, finfish dominate 90% of the world's inland aquaculture production, while in the case of marine and coastal aquaculture, mollusks are the most produced. Nevertheless, in the case of European aquaculture, production from marine and coastal systems is five times higher than that from inland aquaculture, and finfish species remain the most produced. On a global scale, grass carp (*Ctenopharyngodon idellus*) is the most produced finfish species in the world, with 5,792 thousand tonnes of live weight in 2020, while in the case of marine and coastal aquaculture, Atlantic salmon (*Salmo salar*) leads the production in the same year (2,720 thousand tonnes) (FAO, 2022). In Portugal, a positive aquaculture growth was observed for the period of 2000-2018, with an annual percentage rate (APR) growth between 2.5% and 5% (Hough, 2022). In 2020, aquaculture production in Portugal registered 17 thousand tonnes, an increase of 18.6% compared to the previous year, with turbot (*Scophthalmus maximus*), gilthead seabream (*Sparus aurata*), and European seabass (*Dicentrarchus labrax*) dominating the remaining produced species (INE & DGRM, 2021). According to strategic goal 4 of the National Ocean Strategy 2021-2030, which defines the course for the public ocean policy for the next decade, Portugal aims to increase aquaculture production to 25 thousand tonnes/year.

Gilthead seabream (*Sparus aurata*) was the chosen species in this study as it is one of the most produced species in marine Mediterranean aquaculture (Hough, 2022), which represents 16% of the total European production (Federation of European Aquaculture Producers, 2022). Globally, this species occupies the fourth place among the most produced species in marine and coastal aquaculture systems (168.8 thousand tonnes of live weight in 2020) (FAO, 2022). Gilthead seabream cage farming dominates Mediterranean aquaculture, with Turkey (39% of global production) and Greece (21%) being the largest producers and exporters by volume (Hough, 2022). In Portugal, gilthead seabream production registered 1.8 thousand tonnes (approximately 2% of EU production) in 2020 (INE & DGRM, 2021). In 2018, the country represented 12.4% of the imports of this species by European countries, only surpassed by Italy (31.4%) and Spain (14.5%) (Hough, 2022). *Sparus aurata*

(Linnaeus, 1758) is a ray-finned euryhaline species that belongs to the *Sparidae* family and is mainly distributed along the Eastern Atlantic and Mediterranean Sea at depths of approximately 30 m. It is a protandric hermaphrodite species that first matures as male, and then as female, at approximately 3 years of age, living either solitarily or in small aggregations. Valuable traits, such as robustness, plasticity, diet adaptability, and illness resistance, render it able to adapt to different conditions, making it ideal for aquaculture. Gilthead seabream is mainly farmed in intensive systems, such as raceways, tanks, and offshore sea cages, at average densities of 15-25 kg m⁻³ (Pavlidis & Mylonas, 2011).

1.2. AQUACULTURE AND SUSTAINABILITY

In 1987, the Brundtland Report, also known as “Our Common Future”, coined the concept of sustainable development and defined it as a “(development that) meets the needs of the present without compromising the ability of future generations to meet their own needs” (Keeble, 1988). This publication also established the three pillars of sustainability that aquaculture must adhere to: economy, society, and environment. With almost 90% of global marine fish stocks fully exploited or overfished, aquaculture has emerged as a responsible and sustainable complement to the traditional fishing industry. Aquaculture helps to meet the growing global demand for seafood while reducing the pressure on wild fish stocks, and is a key cornerstone of global food security, ensuring safety, affordability, and traceability of fish products (Béné et al., 2016; CONSENSUS, 2009; Risius et al., 2017; Valenti et al., 2018). International policies, best practices guidelines, and EU initiatives have been developed to ensure sustainable aquaculture practices, such as the FAO’s “Code of Conduct for Responsible Fisheries” (FAO, 1995), the “Strategic Guidelines for a More Sustainable and Competitive EU aquaculture”, and the EU’s “Farm to Fork”, “Blue Growth”, and “Farmed in the EU” strategies. Furthermore, “Blue Growth” pointed out aquaculture as one of the sectors with elevated potential for creating sustainable jobs and growth (EC, 2012), while the European Green Deal recognizes aquaculture as a source of protein for food and feed with a low-carbon footprint (EC, 2021).

The rise in consumer awareness regarding the potential environmental impacts of aquaculture has driven the development of a portfolio of third-party certification schemes to recognize companies' sustainability efforts. These schemes, such as the Aquaculture Stewardship Council (ASC), Best Aquaculture Practices (BAP/GAA),

Friend of the Sea, and GlobalG.A.P., are based on a set of principles and criteria for responsible aquaculture that align with or complement the FAO Technical Guidelines on Aquaculture Certification (FAO, 2011). These organizations provide a verification process for seafood producers, assessing their farming practices based on environmental and social impacts, including resource conservation, animal welfare, and community relations. The adoption of these certification schemes allows companies to demonstrate their commitment to sustainable practices, whereas consumers can make informed decisions and support responsible aquaculture.

On September 25, 2015, the UN introduced the 17 Sustainable Development Goals (SDGs) of the 2030 Agenda for Sustainable Development to protect the planet and promote prosperity. The SDGs, intended to be met by world leaders by 2030, are based on at least one of five major tenets - People, Planet, Prosperity, Peace, and Partnership – which address critical issues such as climate change, poverty, hunger, equality, and ecological responsibility. To drive the achievement of the SDGs in the food and agriculture sector, which includes aquaculture, the FAO created an action plan to guide decision makers (FAO, 2018). FAO's approach comprises 20 actions distributed across five key principles that map to several SDGs: (1) increase productivity, employment, and value addition in food systems; (2) protect and enhance natural resources; (3) improve livelihoods and foster inclusive economic growth; (4) enhance the resilience of people, communities, and ecosystems; and (5) adapt governance to new challenges. As summarized in Figure 1.2, aquaculture plays a prominent role in this universal policy agenda and can contribute to almost all the SDGs to different degrees.

Aquaculture is known for its high feed efficiency and to be one of the most sustainable animal protein production systems (Fry et al., 2018). However, the industry still faces sustainability challenges such as fish escaping, use of antibiotics, disruption of ecosystems, long-term viability of fishmeal in aquafeeds, and animal welfare issues. Another criticism of the industry is that certification schemes tend to focus on large production sites, while neglecting smaller fish farmers. Moreover, with aquaculture production projected to reach 106 million tonnes of aquatic animals by 2030, compared to 87.5 million tonnes in 2020 (FAO, 2022), rapid scale-up could have devastating effects on the environment, animal welfare, and public health, if not managed sustainably.

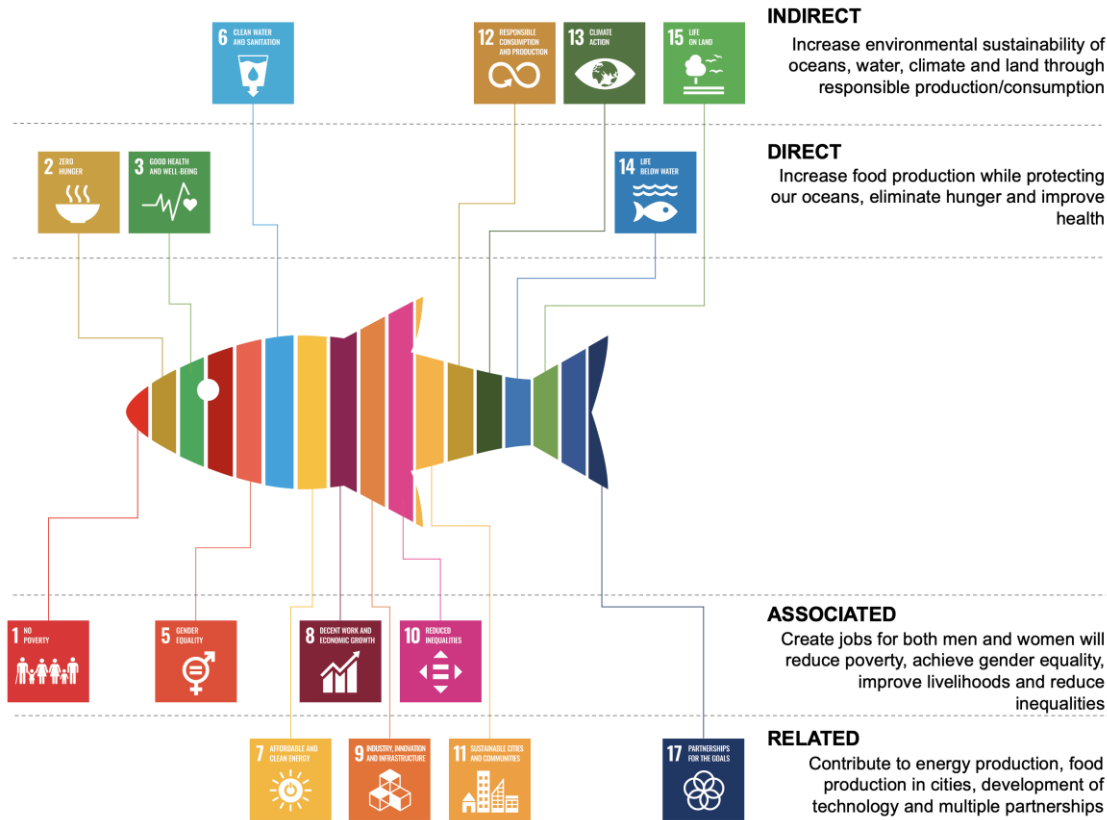


Figure 1.2. Schematization of aquaculture’s main contributions to the SDGs (Adapted from Troell et al., 2021)

Animal welfare is already recognized as a key factor in responsible production and social acceptability of animal production systems. Research on fish cognition and suffering has lent great insights into the lives of fish, leading to increased consumer concern about fish welfare. This has been the main driving force behind increased discussion, research, and initiatives on this topic. In fact, the term “fish welfare” was rarely used in aquaculture research before the turn of the century, yet currently, a brief search on Scopus with this term generated over 3,000 document results.

1.3. FISH WELFARE: ORIGIN OF THE CONCEPT AND DEFINITIONS

The concept of fish welfare originated in public, researchers, consumers, and animal caretakers’ concerns about how animals were kept and raised in intensive aquaculture production systems. It was the book “Animal Machines”, published by Ruth Harrison in 1964, that played a significant role in the history of the animal welfare concept with relevant social, political, and scientific consequences. The scientific basis of animal welfare was then established through the “Brambell report” in 1965, which thoughts like “behavior assessment” or “animal’s needs” were exposed (Brambell,

1965; Rollin, 1989). The “Five Freedoms” described in this report were long recognized as the gold standard in animal welfare: (1) freedom from hunger and thirst; (2) freedom from discomfort; (3) freedom from pain, injury, or disease; (4) freedom to express normal behavior and (5) freedom from fear and distress. A refined version of the five freedoms, now known as the five domains, was then revised by the UK Farm Animal Welfare Council (FAWC) to include a feeling-based definition of animal welfare (Figure 1.3). This concept has been the reference for the development of recommendations and legislation worldwide concerning fish welfare (McCulloch, 2013) and has been used as the basis for animals to be considered sentient beings in the Lisbon Treaty of 2007 (Union, 2007). According to this framework, achieving good fish welfare and health in aquaculture requires these five conditions to be respected, maintained, and improved (Mellor & Stafford, 2001). Nevertheless, this model is criticized because it suggests that the optimum environment is completely free of stress. This framework has its grounds in strict homeostatic principles in which control of stress predicts a linear relationship between stress-related welfare and stress load, which raises controversy regarding the plasticity of fish (further detailed in Section **1.7.1. Stability through change**).

Since then, various definitions have been proposed for animal welfare. Recently, a more general approach has emerged that describes welfare as being related to an animal’s quality of life and subjective experiences (Prunet et al., 2012). However, there is still no single universally accepted framework; most definitions fall into one of the following three categories: (1) feelings-based, which links welfare to the emotional (or emotional-like) state of the animal, and requires a balance between negative experiences, such as pain or fear, and positive experiences, such as the presence of counterparts in the case of social species; (2) function-based, which focuses on the animal’s ability to adapt to its present environment and requires the animal to be in good health, with its biological and physiological systems functioning properly, and not being forced to respond beyond their capacity; and (3) nature-based, which takes into account each species’ inherent biological nature and requires animals to be able to express their natural behavior and lead a natural life (Galhardo & Oliveira, 2009; Prunet et al., 2012). These categories broaden the concept of welfare beyond physical health and the absence of stress. However, it is important to note that in a fish farming context these definitions can be impractical since it is an environment that is

not completely devoid of negative experiences and tracking fish emotional states can be challenging.

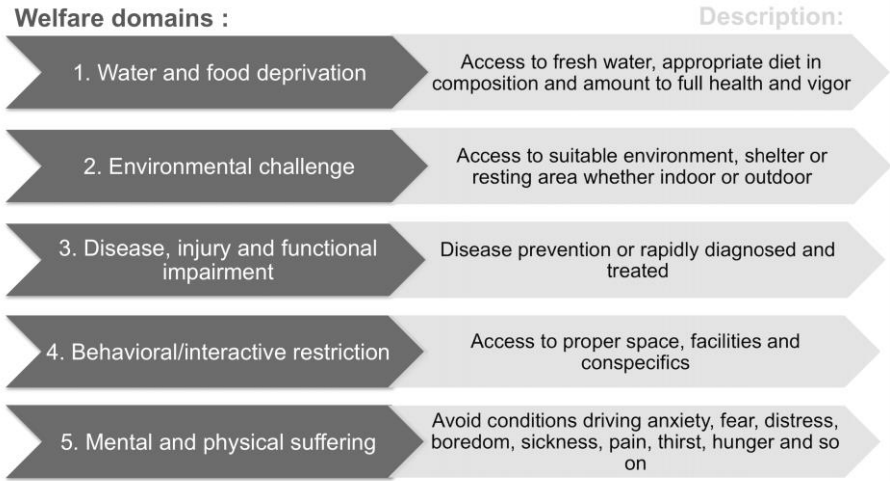


Figure 1.3. Five domains revised from the Brambell Report (1965) by UK Farm Animal Welfare Council to ensure and assess welfare of animal reared and kept under artificial conditions (Adapted from: FSBI, 2002)

1.4. A GLIMPSE INTO SENTIENCE AND CONSCIOUSNESS IN FISH

Fish pain was first politicized by J. L. B. Smith during the 1960s in its book “Our Fishes”, published posthumously in 1968, in response to animal-rights groups’ opposition to angling (Vettese et al., 2020). Even though Smith defended that fish could not feel pain because their brains lacked the frontal lobes found in the mammalian neocortex, he structured the ensuing debate on this controversial topic that would continue until today.

Despite the fact that the number of fishes farmed for human consumption greatly outnumbered that of land animals (approximately 35 times more), fish are not easily fathomed, and they are surely not offered the same level of attention and concern. The fact that fish lack detectable facial expressions, and we do not frequently observe fish lives as we do with terrestrial animals since they live underwater, may be behind our lack of empathy towards fish. However, studies have shown that fish are sentient creatures with consciousness, totally aware of their surroundings, able to feel pain, express emotions, socialize, play, and use tools (Balcombe, 2016). In fact, teleosts share multiple structural and physiological homologies with higher vertebrates, such as humans, including genome homologies, cognitive behaviors, and cellular structures(Howe et al., 2013). However, in practice, welfare assessment of farmed fish

has been mainly based on a function-based approach that focuses on the maintenance of physiological functions, normal growth, behavior, and good health. This approach does not fully consider the feelings-based definition of welfare. Thus, to ensure a comprehensive welfare assessment of fish, it is essential to investigate the mental processes of fish and examine the extent to which they can make conscious choices based on positive or negative expectations (Ashley, 2007; Huntingford et al., 2006; Mejdell et al., 2007; Sneddon, 2007).

Research on fish sentience has been conducted over the last few years to assess the aptitudes of these taxa to consciously experience the surrounding environment, including both suffering and pain, as well as positive states (Braithwaite & Boulcott, 2007; Braithwaite & Huntingford, 2004; Dawkins, 1998; Rose et al., 2012; Sneddon, 2004). Despite lacking a developed neocortex, self-awareness, and the same level of cognitive abilities as mammals, research suggests that fish are capable of sensing noxious stimuli and experiencing pain and fear, to some extent (Sneddon, 2009), perceiving their environment (Millot et al., 2014) and expressing states similar to emotions (Cerqueira et al., 2017). Recently, researchers have described the capacity of zebrafish (*Danio rerio*) to express emotional fever, a physical reaction triggered by stressful situations that is similar to fever and is normally used to identify consciousness in mammals (S. Rey et al., 2015). The extensive evidence of fish behavioral, cognitive, and pain perception abilities, combined with these studies, underscores the importance of considering animal welfare in aquaculture from an ethical perspective (Brown, 2015; Bshary & Brown, 2014; Grigorakis, 2009) rather than only pragmatically.

In summary, evidence of fish sentience, pain, fear, consciousness, cognition, and socialization skills has been continuously demonstrated and extensively reviewed in previous studies (Braithwaite & Ebbesson, 2014; Brown, 2015; Sneddon, 2009, 2015). In addition, it supported the inclusion of these taxa in the national welfare legislation worldwide (Mejdell et al., 2007). Moreover, the New York Times 2016 Bestseller by ethologist Jonathan Balcombe, entitled “What a Fish Knows: The Inner Lives of Our Underwater Cousins” presents an array of fish studies conducted by numerous researchers who concluded that fish are conscious and do feel pain (Balcombe, 2016).

1.5. FISH FARMING AND WELFARE: WHERE ARE WE?

Nowadays, protecting the welfare of farmed animals, including fish, has unequivocally entered the public policy mainstream in a rising number of countries. In Europe, the EU Council Directive 98/58/EC of 20 July 1998 has set minimum standards for the protection of animals reared or kept for farming purposes, including fish. In 2005, the Council of Europe implemented a recommendation on farmed fish welfare, and in 2008, the World Organization for Animal Health (OIE) adopted guidelines and policies for fish welfare. In 2009, the European Food Safety Authority (EFSA) Panel on Animal Health and Welfare (AHAW) issued an opinion on the general approach to fish welfare and the concept of sentience in fish (Algers et al., 2009). The European Directive 2010/63/EU, amended in 2019 by Regulation (EU) 2019/1010 (European Parliament, 2010), has established guidelines and practical indications to ensure optimal conditions for animals kept for scientific purposes. Moreover, the Federation of European Aquaculture Producers (FEAP) has developed a Code of Conduct with guidelines for responsible aquaculture (Federation of European Aquaculture Producers, 2008), which is just one example of how farmers and consumers have become increasingly concerned with fish welfare. Several EU initiatives and projects have also been launched to promote high welfare principles for farmed fish, including “Fish Welfare”, “Wealth”, “Benefish” (Berrill et al., 2009), the COST action “Welfare of fish in European Aquaculture, and more recently in 2022 “Cure4Aqua” and “SEA2SEE” projects. In Portugal, the project “WELFISH” in which this work is included, intends to identify new ways to assess welfare in two important Mediterranean species, gilthead seabream and European seabass (<http://welfish.com/>).

However, implementing these welfare guidelines or protocols across the aquaculture sector and across all cultured species requires much work, as we are only beginning to understand what constitutes positive welfare. This is still recognized as a gap in welfare research, and building a bridge between the scientific community, ethicists, and the fish farming industry has become fundamental to its resolution. In this sense, the ongoing FishEthoBase project (<http://fishethobase.net>) has emerged to meet this need by providing concrete solutions and pointing out welfare criteria for farmed species based on scientific literature in areas such as ethology, ecology, physiology, and general biology (Saraiva et al., 2019). Nevertheless, worldwide efforts to incorporate high welfare standards as an integral component of the “sustainability” labelling in existing certification schemes are currently underway. The Aquatic Life

Institute (ALI) created the Aquatic Animal Alliance (AAA) in 2020, a coalition of 110 animal welfare organizations worldwide. The AAA advocates the inclusion of the highest welfare standards in certification programs as well as clear and informative labelling for consumers. GlobalG.A.P., RSPCA Assured, and Friend of the Sea have started to cover animal welfare in their certification schemes. GlobalG.A.P. released a new welfare standard for Atlantic salmon aquaculture and imposed a ban on shrimp eyestalk ablation. Friend of the sea introduced species-specific welfare standards for fish rearing, slaughter, transport, and handling. In addition, the ASC has launched its fish welfare project and is seeking public input on the key impacts on farmed fish welfare to develop new and improved standards. So far, the project has resulted in the inclusion of humane slaughter standards for fish and a ban on the use of ice slurry.

1.6. FISH WELFARE AND AQUACULTURE SUSTAINABILITY

Welfare and stress are intimately connected, because exposure to potentially stressful conditions in aquaculture can affect fish welfare (further detailed in section **1.7. Fish Welfare and Stress Physiology**) and, consequently, the sustainability of production. Routine procedures (e.g., handling, grading), environmental factors (e.g., hypoxia, temperature), health-related factors (e.g., parasites and wounds), and social aspects (e.g., competition and aggressiveness) can be stressful (Table 1.1) for farmed fish, depending on their nature, species, and resilience (Ashley, 2007; Baldwin, 2010; Conceição et al., 2012; Conte, 2004; Eissa et al., 2017; Iversen et al., 2005; M. Pavlidis et al., 2003; Sangiao-Alvarellos et al., 2005). In 2008, the EFSA issued a scientific opinion report on different aspects of husbandry systems (e.g., dissolved oxygen (DO) and stocking densities) in gilthead seabream and European seabass production (Algers et al., 2008). In the natural environment, fish can also be subjected to many types of stressful stimuli (e.g., injuries, diseases, parasites, floods, storms, predators, or larger conspecifics). The main difference regarding common practices in aquaculture that can become stressful is that these are mostly unavoidable and chronic, and do not allow the animal to recover.

Reducing stress in aquaculture and improving fish welfare can consequently improve fish health and decrease their susceptibility to diseases and parasites. This, in turn, reduces the need for antibiotics, antimicrobials, and other medicines, which is one of the main concerns in aquaculture. This will ultimately ensure food safety (SDG 3) and reduce the diffusion of toxic residues into the wastewater (SDGs 6, 12, and 15).

Improving fish welfare will lead to increased productivity and efficiency (SDGs 2 and 12) and income generation (SDG 1), while reducing feed waste (SDG 12) and the impact on marine ecosystems (SDG 14).

Table 1.1. Main factors affecting fish welfare and most common indicators of impaired fish welfare (adapted from Silva, 2013)

	Factors impairing welfare
Environment	Temperature; pH; salinity; photoperiod
	O ₂ ; CO ₂ ; NH ₃ ; PO ₄ ²⁻
	Xenobiotics and pollutants
Health	Pathogens
	Somatic/fin lesions
	Disease treatments
	Vaccination side-effects
Nutrition	Food deprivation
	Malnutrition
	Anti-nutritional factors
Management practices	Sorting, Handling, Grading
	Transporting; harvesting
	Slaughtering; Sampling
	Stocking densities
Social dynamics	Sorting/grading
	Enforced social contact
	Genetic factors
	Agonistic behaviors/competition

Research has demonstrated that although animal welfare is not explicitly mentioned in the SDGs, improving animal welfare is compatible with achieving the SDGs (Keeling et al., 2019) (Figure 1.4). In September 2021, the ALI issued a report specifically on the benefits of aquatic animal welfare for sustainability, stating that “animal welfare considerations serve as a cross-cutting solution to many of the sustainable development challenges we face today” (Aquatic Life Institute, 2021). In November 2022, the World Federation for Animals, which represents 42 members, published a position paper to support negotiations at the 27th Conference of the parties (COP27) with the United Nations Framework Convention on Climate Change (UNFCCC), and to show how animal welfare improvement can play a key role in climate change mitigation (World Federation for Animals, 2022). Therefore, managing stress and improving fish welfare in aquaculture can undoubtedly contribute to the economic, social, and environmentally sustainable development of the sector.

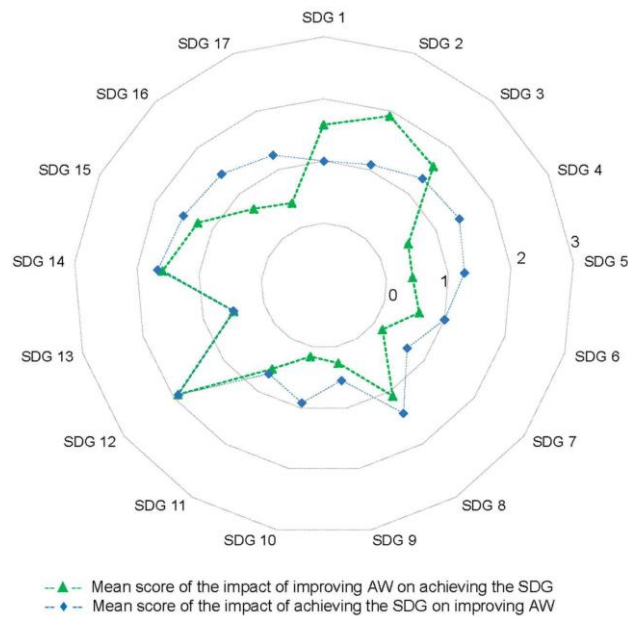


Figure 1.4. Radar plot of the average score attributed to the link animal welfare (AW) – sustainable developmental goal (SDG) (0 – consistent, 1 – enabling, 2 – reinforcing, 3 – indivisible) (Source: Keeling et al., 2019)

1.7. FISH WELFARE AND STRESS PHYSIOLOGY

1.7.1. Stability through change

In 1956, Hans Selye first coined the “stress” concept as a “nonspecific response of the body to any demand placed upon it”. However, this lack of specificity of the stress response has been highly contested, and many other definitions have emerged thereafter. Richard Lazarus later introduced the concept of “appraisal”, which can be defined as the process that detects the stimulus and prepares the body to react in response (Lazarus, 1999). In 2004, Ursin and Eriksen proposed the “Cognitive Activation Theory of Stress” (CATS), which suggests that the stress response involves “neurophysiological activation and arousal and is regarded as a healthy process, if not sustained over time” (Eriksen et al., 2005). Since then, several reviews on stress have been published, discussing concepts and definitions (Koolhaas et al., 2011).

Fish have been demonstrated to be able to adapt and evolve with changing environments, and to require occasional biological challenges to improve resilience and achieve optimal well-being. In fact, rather than continuously making every effort towards a static state, organisms have “the ability to achieve stability through change” in a process called “allostasis” (McEwen & Wingfield, 2003), which accurately explains the adaptive and dynamic nature of biological systems. Fundamentally, this dynamic process refers to the re-tuning of neural, physiological, and behavioral mechanisms to

successfully adapt to predictable and unpredictable stressors (McEwen & Wingfield, 2010; Sterling, 2012). In contrast to homeostasis, allostatic parameters are thus not maintained within narrow ranges but instead fluctuate according to demand. Hence, this concept explains how fish welfare is related to the stress load in a hyperbolic manner (Figure 1.5), where:

- Too low and too high stress loads, i.e., “distress”, negatively impact welfare by hypo-stimulation (aka “use it or lose it”) and unsuccessful coping (aka “wear and tear”), respectively.
- An intermediate range of stress loads, i.e., “eustress”, improves welfare by rewarding successful coping, stimulating learning and neurogenesis, and improving future coping ability (Korte et al., 2007).

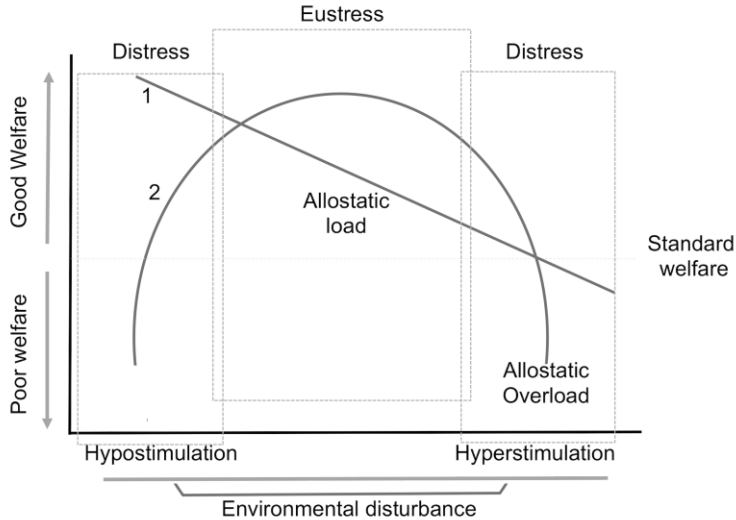


Figure 1.5. Interaction between good and poor welfare and the subjective experiences appraised by the fish: (1) “stability through constancy” strict linear model according to the homeostasis concept; (2) “constancy through change” hyperbolic model according to the allostasis framework. Hypostimulation from low environmental challenges may produce poor welfare conditions; Hyperstimulation from high environmental challenges may also produce poor welfare conditions (distress). Certain degrees of environmental challenge (eustress) will improve welfare (represented above the standard welfare line). Allostatic load - beneficial stress conditions that the fish can cope with; allostatic overload - stress conditions that will cause illness, ultimately death (adapted from Korte et al. 2007).

This way, the allostatic framework complements the Five Freedoms concept, which is considered outdated since it disregards the evidence of animals’ ability to adapt to variations in the environment and the need for biologically relevant challenges to maintain or achieve good physical and mental health and welfare. Fish welfare is guaranteed when the regulatory range of allostatic mechanisms equals environmental

demands and predicts environmental challenges, requiring the prediction of fish perception based on earlier experiences. (Korte et al. 2007; Schulkin 2004).

1.7.2. The stress response

When a fish perceives an internal or external stimulus, a series of behavioral and physiological adjustments occur to help the fish cope. This biphasic response, globally termed “stress response” is triggered by a chain of neurological and endocrine processes (Figure 1.6). First, the challenge is perceived by the fish and the arousal response is activated. The sensory systems in the fish brain will narrow the attention to the stimulus, evaluate it, and compare it with the actual state of the organism and previous stress experiences (Galhardo & Oliveira, 2009). Second, if the stimulus is interpreted as threatening to the fish internal homeostasis, the brain immediately activates the hypothalamus-sympathetic-chromaffin cell (HSC) axis, inducing a rapid release of catecholamines (adrenaline and noradrenaline) from the chromaffin tissue located in the head kidney. These hormones increase cardiac and blood pressure and induce the release of glucose from the liver into the bloodstream, mainly through the activation of the glycogenolysis pathway. Third, almost simultaneously, the brain activates the hypothalamic-pituitary-interrenal (HPI) axis, inducing the secretion of corticosteroids (cortisol in teleost fish). This is followed by a longer latency, but usually a more prolonged elevation in plasma cortisol levels following *de novo* synthesis by the interrenal tissue in the head kidney (Wendelaar Bonga, 1997). Cortisol acts synergistically with the previous hormones in mobilizing glucose, through the activation of the gluconeogenesis pathway, enhancing the organism’s resistance to stress and fueling a “fight-or-flight” response. Consequently, higher muscular activity results in the release of lactate into the blood stream. Cortisol typically exerts his actions through classical genomic action but in addition there is evidence for rapid non-genomic action via G-protein coupled membrane receptors (Aluru & Vijayan, 2009; C. Das et al., 2018; Faught & Vijayan, 2016). Following this alarm stage, secondary responses are manifested by physiological and behavioral adjustments to support adaptation processes. These include alterations to the overall metabolism, such as carbohydrate metabolism (glucose release), as mentioned, as well as protein turnover, amino acid metabolism, and lipolysis (Mommsen et al., 1999). These readjustments then induce a wide range of hematological, respiratory, osmoregulatory, cellular responses, and immunological changes. Finally, tertiary responses correspond to the cumulative

results of prolonged stress exposure and are reflected in whole-animal performance. At this stage, the fish response is mainly characterized by an overall exhaustion and shutdown of metabolism, severely affecting the immune system, reproduction, welfare, and growth, and can even culminate in death (Ashley, 2007; Barton, 2002; Iwama, 2007). The immunosuppressive effect of chronic stress can either be an attempt to attenuate autoimmune damage or conserve the energy needed for processes critical for survival when the organism is struggling to maintain homeostasis (Sapolsky et al., 2000).

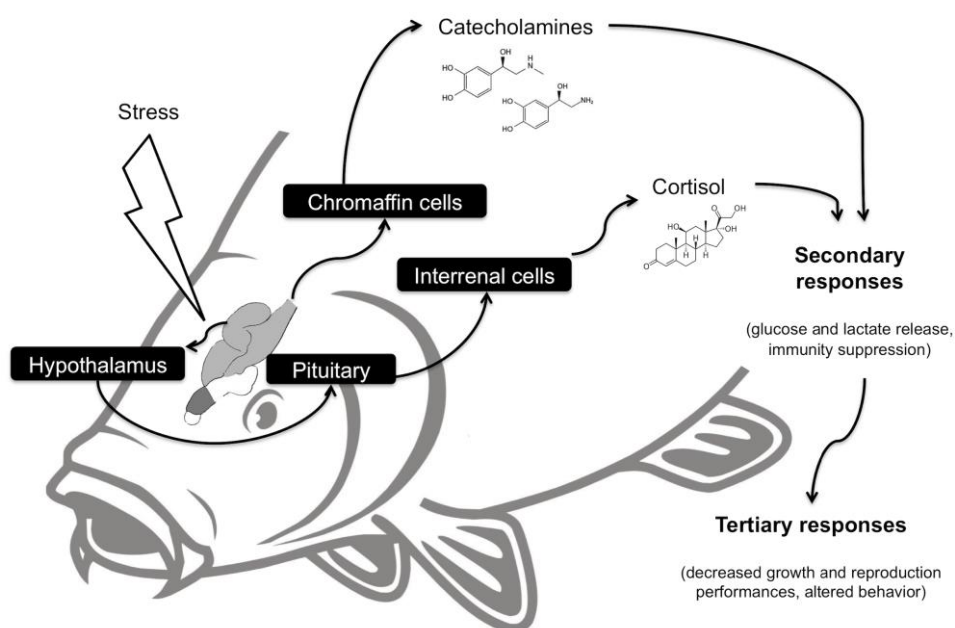


Figure 1.6. Summarized schematization of the stress response in fish. The perception of a stressful stimulus by the brain induces the release of catecholamines and cortisol from the head kidney into the bloodstream. These induce the release of glucose and lactate, and further metabolic, immunological, and behavioral changes that, if sustained in time, may be detrimental for fish welfare.

The extent of the impact of the stress response on fish can be difficult to predict and diagnose because of the heterogeneity of the response. In the short term, a biological challenge may elicit a stimulatory and restorative response (eustress) and allow fish to learn from the experience (Iwama et al., 2006). However, in the case of prolonged exposure to stress or an increase in challenge severity, an overload of the physiological and regulatory systems of the fish can occur, and the animal may no longer be able to adapt (distress), impairing its welfare. What defines this threshold may be individual-related, factors such as the species and level of domestication, sex, developmental stage, and SCS, or stressor-related, i.e., predictability, intensity,

duration, frequency, and type of disturbance (physiological or physical) (Alfonso et al., 2020; Barton, 2002; Castanheira et al., 2017; Conte, 2004; Galhardo & Oliveira, 2009; Martins et al., 2011).

1.7.2.1. The stress response at mucosal surfaces

A lion's share of the work that has been published on the fish stress response over the decades, since evidence of fish sentience has emerged, focuses on central organs and tissues, such as the liver, head kidney, brain, muscle, and plasma. The liver is the central organ that mediates most metabolic rearrangements taking place during fish stress response. It plays a fundamental role in energy substrate administration, since the hepatic tissue synthesizes glucose for non-hepatic tissues during periods of stress, as well as in somatic growth regulation, immune response, and detoxification (Faught & Vijayan, 2016; Madison et al., 2015; Moon, 2004; Nakano et al., 2013; Olivares-Rubio & Vega-López, 2016; Philip & Vijayan, 2015). Most biological molecules produced in different organs during this response are released into the plasma, as described in the previous section. Fish blood plasma, as in other vertebrates, has important biological functions such as distribution of hormones, nutrients, and proteins, excretion, and immunological defense, making it especially important to understand the impact of stress on fish immunity. On the other hand, it was only recently that the fish mucosal surfaces have started to gain attention regarding their potential role during the fish stress response.

The mucosal epithelial barriers in teleost fish serve as the first line of defense against the aquatic environment, which is constantly changing (Peterson, 2015). The main mucosa-associated lymphoid tissues (MALT) are the gut-associated lymphoid tissue (GALT), skin-associated lymphoid tissue (SALT), the gill-associated lymphoid tissue (GIALT), and the recently revealed nasopharynx-associated lymphoid tissue (NALT) (Salinas, 2015). The general aspects of MALT and innate and adaptive mucosal immune responses in teleost fish have been extensively reviewed (Gomez et al., 2013; Salinas, 2015).

The skin is the largest immunologically active organ in fish, and epidermal mucus, its extrinsic layer, is the biochemical barrier between the skin and water (Ángeles Esteban & Cerezuela, 2015). It serves crucial functions in immunity, sensory perception, locomotion, respiration, osmoregulation, and excretion (Ángeles Esteban, 2012; Reverter et al., 2018). Fish skin mucus is mainly composed of O-glycosylated

proteins (GPs), called mucins, which determine its viscoelasticity and rheology, and are secreted by goblet cells, club cells, and sacciform cells in the fish epithelium (Ángeles Esteban, 2012; Ángeles Esteban & Cerezuela, 2015; Y. Xiong et al., 2020). It also comprises other biologically active compounds, such as proteins, carbohydrates, lipids, metabolites, and antimicrobial components (e.g., lysozyme, immunoglobulin, complement proteins, lectins, C-reactive proteins, proteolytic enzymes, and proteases) (Dash et al., 2018). Recently, a review detailing the function of all its bioactive compounds has been performed, and it has been proposed that fish skin mucus is a promising biological matrix for fish health monitoring (Reverter et al., 2018; Santoso et al., 2020).

Research has shown that stress can affect the viscosity, exudation, and composition of fish skin mucus (Benktander et al., 2021; Cone, 2009; Cordero et al., 2016; Easy & Ross, 2010; Fernández-Montero et al., 2020; R. Jia et al., 2016; Khansari et al., 2018; L. Liu et al., 2013; Ordóñez-Grande et al., 2021; Pérez-Sánchez et al., 2017; Rajan et al., 2013; Van Der Marel et al., 2010). Studies on numerous fish species have demonstrated that skin mucus is a promising complementary matrix to look for molecular markers of stress (De Mercado et al., 2018; Franco-Martinez et al., 2022; Guardiola et al., 2016; Reyes-lópez et al., 2021; Sanahuja & Ibarz, 2015). Additionally, its minimally invasive sampling technique makes it ideal for welfare assessment. Furthermore, skin mucus has been proposed to be part of a peripheral cutaneous stress response system in fish (CSRS) (Kulczykowska, 2019), which may be more immediate than the metabolic shift occurring in central organs during stress or physical injury (H. Guo & Dixon, 2021).

1.8. INDICATORS OF FISH WELFARE

1.8.1. Operational and lab-based welfare indicators

Although it may be impossible to eliminate all stressors in aquaculture production, it is important to monitor the impact of stress on the welfare of fish from ethical, environmental, and economic perspectives, as previously explained. As the definition of welfare has evolved, so has the number of variables used to assess the state of the fish. Welfare indicators should include readily, and reliably recognizable aspects related to the behavioral, psychological, and physiological performance of captive individuals. Therefore, knowledge of the ethology and biology of farmed fish is of utmost importance to correctly assess welfare. Several parameters relevant to

welfare assessment have been recognized in previous reviews (Conte, 2004; Toni et al., 2017, 2018). Another recent review classified emerging fish welfare indicators according to their invasiveness (Barreto et al., 2022).

Indicators that can be assessed on-site are known as Operational Welfare Indicators (OWI), which can be environmental- or animal-based. The latter can still be divided into group- and individual-based methods (Figure 1.7). Animal-based indicators are also sometimes known as outcome welfare indicators because they are usually linked to tertiary stress responses; that is, most of the time, they become apparent once the animal is already experiencing negative welfare. In contrast, environmental indicators may help to predict future problems. However, even these minimally invasive and easy-to-assess measures have some disadvantages, such as observer bias, the qualitative nature of most indicators, and the fact that group-level indicators (e.g., behavior) do not always accurately reflect the experiences of individual animals. On the other hand, lab-based welfare indicators (LABWI) are quantifiable measures that, if collected on a regular basis as part of a monitorization/management plan, could more accurately predict an internal disturbance on the animal than the former (Figure 1.7) (Noble et al., 2018). Comparatively, these are less explored than the OWI, mainly because they include collecting samples from the water or the animals, which requires trained personnel, suitable protocols to minimize fish stress during sampling, and specialized equipment. Optimal species-specific protocols integrating both OWI and LABWI would be valuable early warning systems to detect issues in production in a timely manner to improve fish welfare and avoid potentially permanent consequences. However, appropriate combinations of welfare indicators validated for specific species and developmental stages are limited. Nonetheless, welfare assessment indices, based mainly on OWI, have been proposed for Atlantic salmon, lumpfish (*Cyclopterus lumpus*), and grass carp (*Ctenopharyngodon idella*) (Gutierrez Rabadan et al., 2021; Noble et al., 2018; Pedrazzani et al., 2022).

The consistency and effectiveness of welfare indicators and the development of multidisciplinary assessment protocols are critical factors for ensuring the sustainability of the industry and the quality of farmed fish.

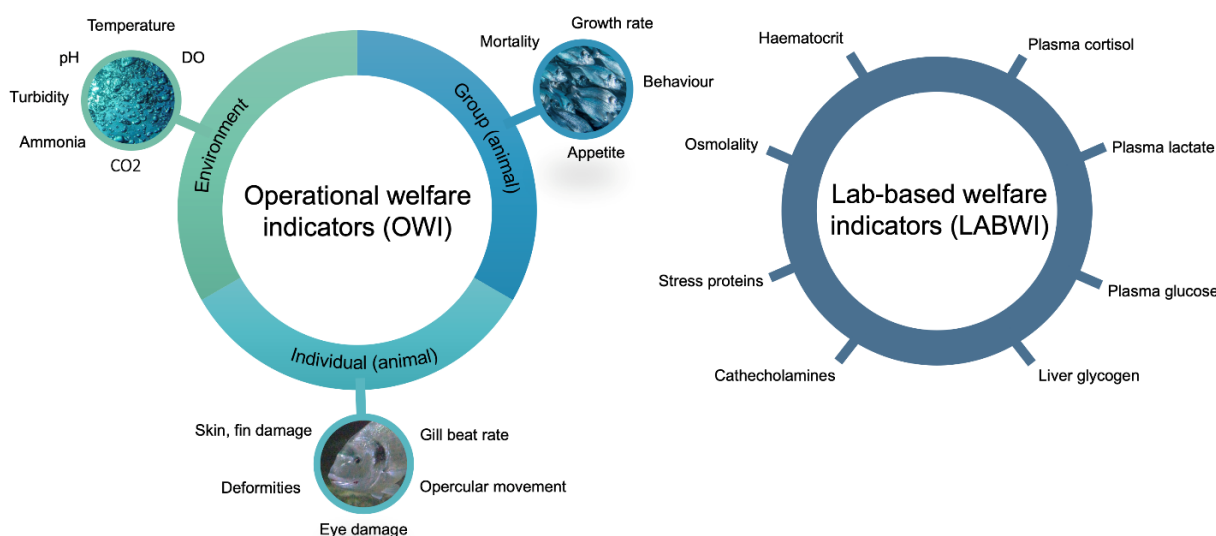


Figure 1.7. Most used operational and lab-based welfare indicators in aquaculture.

1.8.2. Physiological stress markers and their reliability as welfare indicators

The difference between resting and post-stressor cortisol levels is a commonly used measure of physiological stress and is sometimes used as a welfare indicator (LABWI). However, it should be noted that this autonomic rise in plasma cortisol levels is merely indicative of arousal of the HPI axis and is not specific to distress and negative welfare. Cortisol is a central hormone for the maintenance of allostasis, as it supports other hormones during basal conditions and has a stress-induced regulatory role (Mommsen et al., 1999) (see section 1.7.2. **The stress response**). Nevertheless, this information alone is not sufficient to assess fish welfare, as cortisol also has an adaptive physiological role, and several factors can trigger its release in response to stressful conditions (Barton, 2002). Several constraints on the use of cortisol as a single measure of distress and negative welfare can be identified, which can limit the statistical power and skew the interpretation of data.

(1) Response to a stressor is a dynamic process that cannot be described by unimodal trajectories. Hormonal measurements represent only a snapshot (i.e., the maximum response may not be captured) and may not be representative of the stress that was truly experienced.

(2) Cortisol levels may be biased during sampling, as fish capture, handling, and blood collection may constitute a source of stress (Baker & Vynne, 2014).

(3) Most fish display a common pattern of increased cortisol levels when exposed to a source of stress, followed by a return to basal levels within hours when

the stressor is removed, which can be useless in the case of chronic stress. This occurs because cortisol regulates the HPI axis by a series of negative feedback loops, with cortisol mainly acting back at the hypothalamus, pituitary gland, and interrenal tissue to inhibit its own synthesis (Galhardo & Oliveira, 2009).

(4) Habituation to chronic stress or impairment of the HPI axis, i.e., exhaustion of the endocrine stress axis, can also occur. In this case, downregulation of the cortisol response is observed because the interrenal tissue of stressed fish becomes less sensitive to the action of pituitary hormones (Madaro et al., 2015; Mommsen et al., 1999). However, although a cortisol response is not detected, the fish may never re-establish the exact same pre-stress homeostatic ranges, leading to immunocompetence loss and creating ideal conditions for disease development (Einarsdottir et al., 2000; Segner et al., 2012).

(5) The basal cortisol level itself is very context-dependent and is affected by factors such as feeding, season, maturation, domestication, photoperiod, circadian rhythm, and unknown stressors (Galhardo & Oliveira, 2009).

(6) Both basal cortisol levels and the degree of cortisol induction during stressful events display a high degree of inter-individual variation under the same challenging situation (explained through the proactive-reactive continuum). Different behavioral phenotypes and their resilience to stressful events have been related not only to inherent predispositions but also to the cognitive appraisal that individuals often take from complex and dynamic environmental stimuli, that is, the way individuals perceive their surroundings (Faustino et al., 2015).

(7) Mechanistic connections between cortisol and any secondary/tertiary measures are not always straightforward, as the same cortisol level at the same time point may culminate in different outcomes (i.e., for one individual, it can indicate a trajectory to death and for another a trajectory to recovery) (Schreck et al., 2016).

(8) The rate of cortisol clearance in the liver may be affected by extrinsic factors (Mommsen et al., 1999).

Other plasma metabolites associated with secondary stress responses, such as glucose and lactate, are sometimes used as proxy measurements of stress, as their levels are also enhanced under adverse conditions (see section **1.7.2. The stress response**). However, these complementary indicators should also be interpreted with caution (Martinez-Porchas et al., 2009), as problems similar to ones related to the cortisol response may also arise. First, defining reliable reference or threshold values

for these metabolites may not be simple, again, due to extrinsic and intrinsic factors to the animal such as species, developmental stage, diet, time since last feeding, among others (Iwama, Afonso, & Vijayan, 2004). Second, different hepatic glycogen stores, which are related to the species and nutritional status of the animal, may also affect the glucose release. Finally, both glucose and lactate levels can show different cortisol increase and recovery profiles. In the case of lactate, it has also been demonstrated that plasma cortisol levels may rise without any change in plasma lactate levels, and vice versa, and *in situ* recycling of muscle lactate, with limited release into the bloodstream, may also occur (Thomas et al., 1999; Wright et al., 2007).

This suggests that cortisol, glucose, and lactate should be used with caution when evaluating the magnitude of stress response in fish. Therefore, it is necessary to complement these indicators with other molecular measurements to draw reliable conclusions about the stress phenotype of fish and obtain a more complete picture of the welfare of the individuals.

1.9. OMICS IN AQUACULTURE WITH A FOCUS ON FISH WELFARE

High-throughput omics technologies perform in-depth analysis of multiple biological molecules in one or more samples simultaneously. The use of omics technologies, such as genomics, transcriptomics, proteomics, metabolomics, lipidomics, and multiomics, has grown at an astonishing rate in the last decade and has been shown to be a powerful tool for gathering important knowledge regarding biological systems and physiological aspects of organisms. Various omics approaches have been used in many aquaculture research fields, with a wide range of applications, such as traceability, nutrition, health, authentication, reproduction, allergens, and welfare (Canellas et al., 2022; Sundaray et al., 2022; Tripathy et al., 2021). With rapidly expanding capabilities and diversity of analytical platforms coupled with bioinformatics, omics approaches allow us to obtain and mine huge amounts of data previously unattainable and are likely to soon revolutionize the aquaculture research field.

1.9.1. Proteomics

Proteomics has emerged to provide a more complete description of what occurs in living cells by offering the possibility of working with the whole proteome instead of a single protein and providing relevant information concerning the organism's physiological state at a given moment (Rodrigues et al., 2012; Tripathy et al., 2021).

Proteomics has been used to study all kinds of farmed animals, from cattle and poultry to aquaculture, while helping reach common goals in any farming production, such as high productivity and efficiency, and a high-quality and safe food product, accepted by the final consumers (Almeida et al., 2014; Marco-Ramell et al., 2016; Nissa et al., 2021). However, the use of proteomics technologies in the aquaculture field is relatively recent compared to human research, since they have only emerged in the 21st century, with a more accentuated increase in the number of related publications in the last decade (Eckersall et al., 2012; Rodrigues et al., 2012). The availability of fish proteomes is expected to proceed at a slower pace than genome sequencing for several reasons: (1) high dependency on sequenced genomes; (2) higher complexity of protein structures, functions, and interactions compared to nucleic acids; (3) greater number of protein species compared to the number of genes in an organism; (4) lack of an amplification method for proteins; and (5) elevated cost of certain techniques, instruments, and specialized staff for maintenance (Campos & de Almeida, 2016; X. Zhou et al., 2012). Recent research consortia were crucial in trying to overcome these difficulties as for the dissemination of proteomic advances in this area, like the FA1002 - Farm Animal Proteomics COST action (<http://www.cost-faproteomics.org/>) and the PRIME-XS initiative (<http://www.primexs.eu/>).

Most welfare-related proteomic studies are concerned with environmental sources of stress related to common aquaculture production systems, such as diseases and parasites (Buján et al., 2015; G. Chen et al., 2011; X. Chen et al., 2010; Chongsatja et al., 2007; Ji et al., 2013; Lü et al., 2014; Ni et al., 2010; Riera-Ferrer et al., 2022; Somboonwiwat et al., 2010; X.-P. Xiong et al., 2011; D. Xu et al., 2015; Yeh et al., 2008), hypoxia (Doux fils et al., 2012; H. Jiang et al., 2009; Pédrón et al., 2017; Tiedke et al., 2015; G. Zhang et al., 2017), anoxia (R. W. Smith et al., 2009; Wulff et al., 2008), temperature (Chang et al., 2016; Ghisaura et al., 2019; Ibarz et al., 2010; Nuez-Ortín et al., 2018; Richard et al., 2016; Schrama et al., 2017), high stocking densities (Alves et al., 2010; Cordero et al., 2016; E. Jia et al., 2022; Naderi et al., 2018), handling procedures (Alves et al., 2010; Cordeiro et al., 2012a; B. Yang et al., 2015), and pre- and post-slaughter stress (Morzel et al., 2006).

Contrarily to the fixed genome, the proteome is in a constant state of flux to maintain proteostasis. Protein turnover mechanisms and post-translational modifications (PTMs), which are, in major part, a result of extrinsic factors to the animal, can markedly alter the localization, function, and activity of a protein (Bassols

et al., 2014). Thus, the final amount of protein can differ greatly from that of transcripts derived from a gene of interest. However, information at the genomic level is required for the interpretation of proteomic results, which is a bottleneck in aquaculture proteomics because of the lack of farmed fish species with fully sequenced genomes (Crollius & Weissenbach, 2005; Wenne et al., 2007). Protein identification is in this case achieved through homology searches.

Proteomics allows the easy separation of a complex mixture of proteins present in each biological sample. This separation can be achieved by different techniques (i.e., gel-based, or gel-free approaches) at the protein level (top-down approach) (Westermeier & Naven, 2002) or at the peptide level (bottom-up approach) (Gevaert & Vandekerckhove, 2011) (Figure 1.8). In gel-based approaches, proteins can be separated by one- or two-dimensional gel electrophoresis (1/2DE) and protein spots in the gel are detected using visible or fluorescent staining methods (e.g., colloidal Coomassie, silver stain, Sypro™, Flamingo, and Deep Purple™) or through direct detection of fluorescent dyes (e.g., difference gel electrophoresis (2D-DIGE)). The latter uses amino-selective fluorescent dyes with different excitation wavelengths and relies on an internal standard to eliminate gel-to-gel variability and increase reproducibility (Minden, 2012). The intensity of protein spots is then evaluated by means of dedicated software (e.g., Progenesis or SameSpots). Those with significantly different intensities are excised and analyzed by mass spectrometry (e.g., matrix assisted laser desorption ionization-time of flight (MALDI-TOF MS)).

The field of proteomics has witnessed an increase in the popularity of gel-free strategies, also known as MS-based techniques, attributed to ongoing concerns about quantitative reproducibility and limitations in studying certain classes of proteins using gel-based methods. MS has shown tremendous progress in proteomics and is a key tool for the analysis of complex protein samples. However, these approaches should be regarded as complements rather than replacements of gel-based methods. Instead of being previously separated, peptides are typically fractionated in tandem with MS, usually through high dimensional chromatography (e.g., ion-exchange chromatography (IEC) and liquid chromatography (LC)). Quantification and identification of proteins are achieved by MS analysis using label-based or label-free methods (Soares et al., 2012). In the first approach, proteins can be metabolically or chemically labelled (Bantscheff et al., 2007), depending on whether the protein label is introduced *in vivo* by the growth medium (e.g., Stable Isotopic Labelling with Amino

Acids in Cell Culture (SILAC)), or if the proteins or peptides are tagged on a chemical reaction (e.g., Isotope-Coded Affinity Tag (iCAT), Isobaric Tags for Relative and Absolute Quantification (iTRAQ), and Tandem Mass Tag (TMT)) (Schulze & Usadel, 2010), respectively. On the other hand, label-free approaches (e.g., LC-MS), also called shotgun proteomics, are appealing alternatives since they are amenable to almost all types of biological samples, are simpler and less time-consuming, reproducible, cost-effective, and less prone to errors and side reactions related to the labelling technique (Abdallah et al., 2012). Two analytical methods for data acquisition can be distinguished: (1) data-dependent analysis (DDA), in which scanning of all precursor peptide ions during the survey scan (MS1) is performed, followed by precursor ion selection, based on its intensity, for subsequent fragmentation (MS2); quantification is then achieved through spectral counting or peak intensities; and (2) data-independent analysis (DIA) (also known as sequential window acquisition of all theoretical mass spectra (SWATH-MS)), in which no parent ion is selected and data acquisition of all charge states of eluted peptides is performed by a rapid switching of the collision energy between low- and high-energy states (Krasny & Huang, 2021). Lastly, peptide identification is performed by assigning fragment ion spectra to peptide sequences to generate a set of Peptide-Spectrum Matches (PSM) using database search engines, such as Mascot, SEQUEST and X!Tandem. Following, protein inference is achieved by assembling the identified peptide sequences into a set of confident proteins (T. Huang et al., 2012).

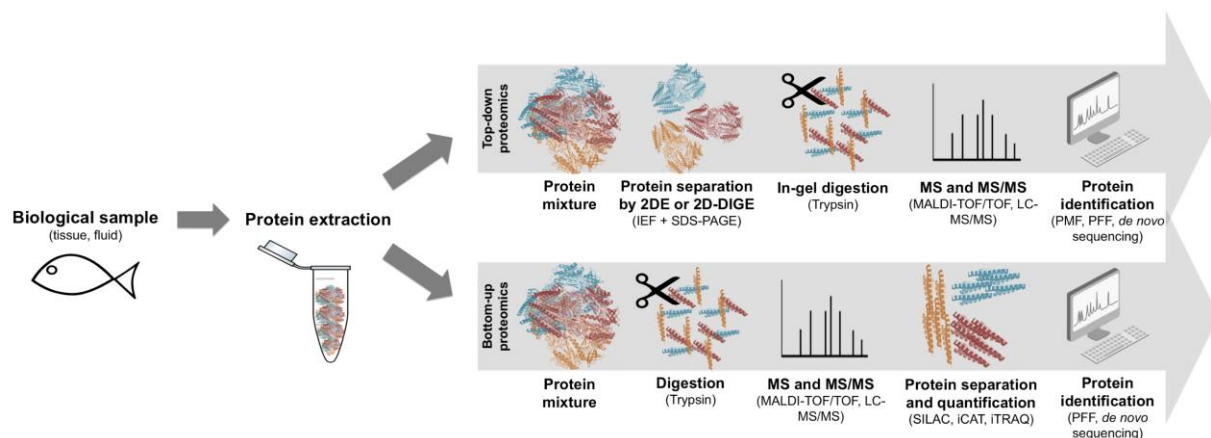


Figure 1.8. Different possible pathways that a typical proteomics workflow can follow in aquaculture proteomics studies: gel-based or top-down and gel-free or bottom-up strategies. Both approaches share the sample preparation feature and aim to identify the proteins of interest.

1.9.2. Transcriptomics

Transcriptomics is the systematic study of an organism's transcriptome, the total RNA content of a cell, and the product of the genome, providing an overview of active and dormant cellular processes through differences in gene expression. In contrast to the relatively stable genome, variations in the transcriptome can be observed following changes in physiological conditions, developmental stages, and the external environment of an organism, offering a correlation between genotype and phenotype. Conventional microarray techniques present major shortcomings related to the need to have the genomic sequence available, high background noise, and are extremely time-consuming. Currently, more advanced techniques of whole-transcriptome sequencing, such as RNA sequencing (RNA-seq), present clear advantages over existing approaches (X. Qian et al., 2014). The introduction of next-generation sequencing (NGS) has significantly increased the number of available reference genomes and transcriptomes and has allowed the detection of single nucleotide polymorphisms (SNPs) and other molecular markers. It is undoubtedly nowadays the most used technique, including in the aquaculture research field (Chandhini & Rejish Kumar, 2019; Ye et al., 2018; Yue & Wang, 2017). The COST action "Functional Annotation of Animal Genomes" (FAANG) (<http://faang-europe.org/>), closed in 2020, aimed at improving the functional annotation of domesticated animal genomes to improve the livestock sector, medical research, and animal welfare. The gilthead seabream genome was first sequenced in 2018 using NGS (Pauletto et al., 2018). In 2019, a genome and transcriptome sequencing study revealed that half of the genes showed multiple copies, with the majority not corresponding to the evolutionary duplication event that took place in teleost fish (whole-genome duplication) (Glasauer & Neuhauss, 2014), but are instead specific to the species and are mainly involved in generating a response to environmental changes, such as immune or sensory responses, as well as in genomic transcription. These genetic duplications may explain the high plasticity and capacity of the species to adapt to diverse farming conditions (Pérez-Sánchez et al., 2019).

In fish welfare research, most studies have been related to the response of the stress transcriptome to xenobiotics and environmental pollutants (Colli-Dula et al., 2018; Hook et al., 2018; Uren Webster et al., 2017; X. Zhang et al., 2017), temperature (Hu et al., 2016; J. Huang et al., 2018; Mininni et al., 2014; Song & McDowell, 2021; Y. Wang et al., 2019; T. Zhou et al., 2019), alkalinity stress (Y. Zhao et al., 2015),

salinity (Z. Xu et al., 2015; X. Zhang et al., 2017), diseases and parasites (Y. Da Wang et al., 2014; Ye et al., 2018), rearing densities (Ellison et al., 2020; Rodriguez-Barreto et al., 2019), ammonia (Z. X. Zhu et al., 2019), fasting (Y. F. Dai et al., 2021; B. Qian et al., 2016), and hypoxia (J. S. Huang et al., 2022). However, studies on the transcriptional effects of other aquaculture stressors are lacking. Stress-related RNA-seq studies on gilthead seabream have focused on the effects of ultraviolet B radiation exposure in the skin (Alves & Agustí, 2022), gill tissue response to an ectoparasite (Piazzon et al., 2019), whole-brain analysis of food-deprived individuals (Ntantali et al., 2020), and the effects of mild hypoxia in the muscle (Naya-Català et al., 2021).

Isolation of total RNA with sufficient integrity for library construction is a critical step in any transcriptome analysis, as impure or degraded RNA will perform poorly in subsequent enzymatic applications. The phenol-chloroform (Trizol) method followed by DNase treatment is the most used RNA purification technique (Tan & Yiap, 2009). The RNA is then disintegrated into short fragments (approximately 150 bp), reverse transcribed into cDNA with an adapter attached into one or both ends, and finally sequenced from one end (single-end sequencing) or both ends (paired-end sequencing). Library construction prior to sequencing, can be performed using one of two methods: depletion of rRNA or selection of polyadenylated RNA, using oligo dT primers (Z. Wang et al., 2009). Widely used NGS platforms for library sequencing are Illumina, Roche 454, and AB SOLid (L. Liu et al., 2012). After quality control analysis of the sequenced reads using dedicated software (e.g., FASTQC), reads can be filtered and trimmed if needed (e.g., FASTp, Trimmomatic), following mapping into the reference transcriptome/genome, if a sequenced genome is available (e.g., STAR, Bowtie2, HISAT), or otherwise *de novo* assembled (e.g., Trinity). After proper assembly, the reads can be counted (e.g., HTSeq and RSEM), and differential gene expression analysis can be performed using edgeR or DESeq2.

Real-time quantitative reverse transcription polymerase chain reaction (qRT-PCR) is used for the targeted expression analysis of specific genes and validation of RNA-seq studies. Appropriate normalization in qRT-PCR (i.e., the expression ratio of a target gene in relation to a reference gene) is needed for the accurate quantification of the gene of interest by minimizing the experimental variation derived mainly from the different initial amounts of RNA and performance of cDNA synthesis (Kozera & Rapacz, 2013). Generally, housekeeping genes, the basic metabolic genes involved in cell survival, are used as reference genes for internal control. However, in welfare

studies, since stress might affect basic physiological and/or metabolic pathways, a common housekeeping gene would not be appropriate for use as a reference gene for normalization (Chervoneva et al., 2010).

1.9.3. Metabolomics

Metabolomics is the study of global metabolite profiles, that is, small molecules produced by cellular metabolic functions, such as amino acids, fatty acids, and carbohydrates, in a system under certain conditions (Dunn & Ellis, 2005; German et al., 2005). Metabolomics usually involves the study of small molecules within a mass range of 50 – 1500 daltons (Da). As the final downstream product of gene transcription, the metabolome amplifies changes in both the transcriptome and proteome and is currently one of the cornerstones of postgenomic techniques for integrative quantitative analyses and data validation. One of the main advantages of metabolomics, compared to proteomic and transcriptomic analyses, is that it involves less sample preparation and has shorter turnaround times from sample collection to data interpretation (Alfaro & Young, 2018). Another positive point is that most metabolites are not species-specific, unlike many genes and proteins, and thus the analytical assay does not need to be optimized for every animal model, and there is no need to have a sequenced genome. However, some limitations of these techniques are mainly their semi-quantitative approach, inability to differentiate isomers, high cost, and challenges in novel compound identification and data interpretation.

Metabolomic approaches can be targeted or untargeted, and the two most common techniques used in data acquisition are nuclear magnetic resonance (NMR) and mass spectrometry coupled with gas or liquid chromatography (GC/LC-MS). MS-based approaches are advantageous because of their higher sensitivity and higher number of detectable metabolites; however, NMR-based analyses are usually favored because they have higher reproducibility and almost no sample pretreatment is required (Young & Alfaro, 2018).

Fourier transform infrared (FTIR) spectroscopy, a form of vibrational spectroscopy, is an established metabolic fingerprinting technique and another common approach in metabolomics, often of qualitative nature. Although it does not result in comprehensive data at the metabolite level, it provides relevant chemical information to rapidly and reproducibly discern prominent changes in the metabolome. It has a low-cost value for consumables and requires small amounts of samples (Talari

et al., 2017). It has been successfully applied to differentiate functional biochemical groups in the livers of fish exposed to different rearing conditions (Ceylan et al., 2014; T. S. Silva et al., 2014).

Metabolomics, besides being the most recent addition to omics strategies, is already widely used in different aquaculture areas. Metabolomic stress and welfare studies have mainly addressed the effects of alkalinity stress (Y. C. Sun et al., 2018), thermal stress (Jiao et al., 2020; M. Song et al., 2019), pollutants (Cappello et al., 2016; Ziarrusta et al., 2018), and transport (Alfaro et al., 2021). Metabolomics studies of gilthead seabream include a study on the identification of biomarkers of nutritional status (Gil-Solsona et al., 2017) and another on metabolic responses to low temperatures (Melis et al., 2017).

1.9.4. Multiomics

Most omics studies have focused on single-data-type designs without considering the intricate relationships among the regulatory layers. The integration of biological data from different omics layers, i.e., multiomics (Figure 1.9), as compared to limiting studies of a single omics type, offers the opportunity to understand the complete flow of information of the organism of study, adopting important hypothesis-generating experiments that have greatly enhanced our knowledge and understanding of physiological processes (Horgan & Kenny, 2011). Combining biological data from as many different hierarchical levels as possible is currently considered the most desirable approach to obtain an accurate picture of the physiological pathways and the state of an organism; however, it also means having datasets with very different data modalities, with their inherent challenges (e.g., different data scaling and normalization), exponentially increased dimensionality, high computational burden, and data storage issues. Multiomics data can be analyzed by integrating the findings of single omics datasets (e.g., integration of enriched biological functions) or by modelling omics datasets together. In the latter, robust integrative frameworks and algorithms should be employed to avoid biased analysis towards a data modality with significantly more features (e.g., Data Integration Analysis for Biomarker discovery using Latent components (DIABLO), Multi-Omics Factor Analysis (MOFA), and joint and individual variation explained (JIVE)). Additionally, weak correlations can often occur between different data modalities, particularly between proteomic and transcriptomic data. This is mainly due to the complex protein kinetics (e.g., PTMs) as

to RNA splicing processes and variations in transcript half-lives and translation products (Greenbaum et al., 2003; Haider & Pal, 2013). Thus, coincident results may be confirmatory, but conflicting data must not be entirely interpreted as contradictory but rather as complementary. The complexity of data analysis, coupled with many other challenges that are amplified by an integrative multiomics approach, explains the difficulty of benchmarking standard bioinformatics methods. A review of the available resources, as well as the main challenges and pitfalls of this approach, was recently published (Krassowski et al., 2020).

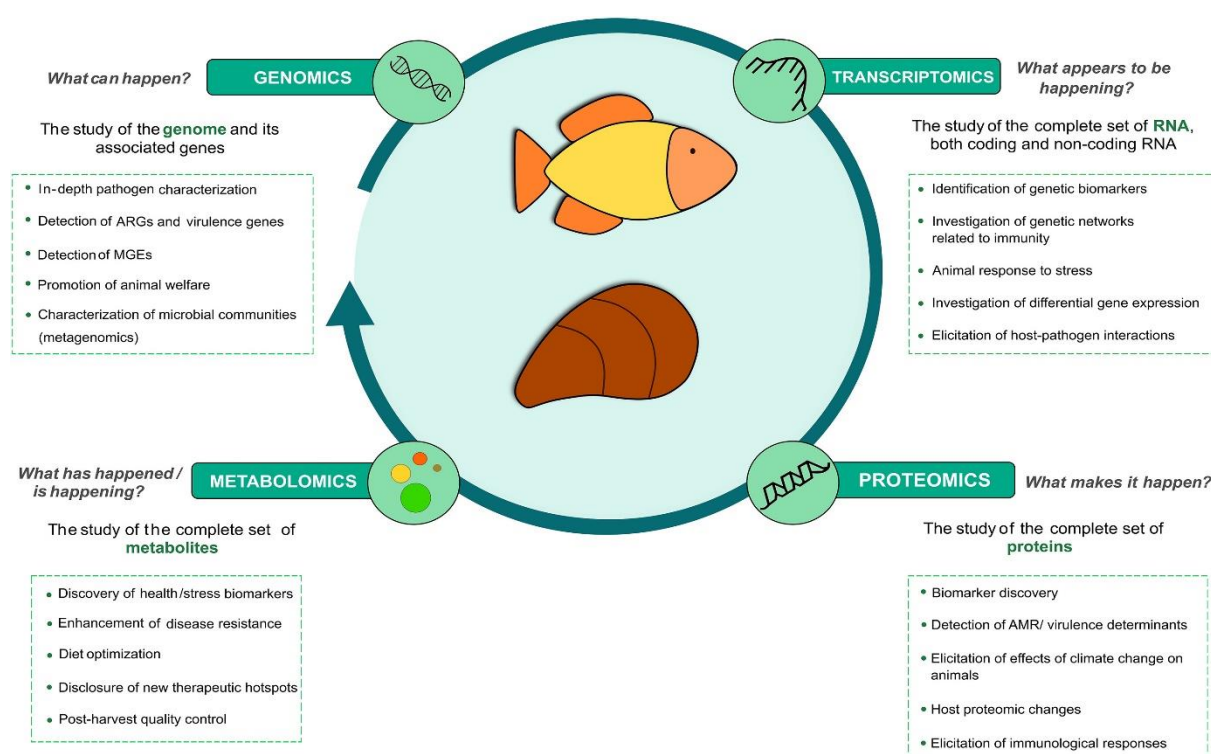


Figure 1.9. Main questions addressed by the different omics platforms applied to the aquaculture research (Source: Canellas et al., 2022)

Despite these challenges, these integrative multiomics approaches, although mostly with two omics types, are already being applied in aquaculture research and fish stress studies, demonstrating their advantages compared with single-omics studies (Colás-Ruiz et al., 2022, 2023; Dale et al., 2020; Karlsen et al., 2011; Lazado et al., 2021; J. Li et al., 2022; Y. Liu et al., 2022; Natnan et al., 2021; Roh et al., 2020; Stentiford et al., 2005; Wen et al., 2019; E. jun Yang et al., 2022; Y. Zhang et al., 2022; Z. X. Zhu et al., 2019). These strategies are also important for biomarker discovery because they consider a complex system as a whole while simultaneously investigating multiple molecules, offering a powerful approach to study biological

pathways related to stress responses to discover candidate biomarkers in fish stress and welfare.

1.10. IDENTIFICATION OF STRESS BIOMARKERS

One of the main goals of omics approaches in aquaculture welfare studies is to identify molecular signatures as biological markers of the fish stress status (Di Girolamo et al., 2014; Sanahuja & Ibarz, 2015). As demonstrated in sections **1.8.1** and **1.8.2**, the identification of fish molecular stress markers (e.g., genes, epigenetic marks, SNPs, proteins, and metabolites) would be extremely useful and complementary to the existing physiological stress markers that are based on primary and secondary stress responses (Marco-Ramell et al., 2016). These would constitute a set of reliable LABWI aimed at providing complete and holistic species-specific welfare assessment protocols, together with OWI. Martins and colleagues stated that “Welfare indicators that are relevant for inclusion in an operational welfare assessment system should be science-based, should measure welfare over extended time periods, should be measurable on a commercial farm within a realistic framework and should be relevant as a decision support system for the farmer” (Martins et al., 2012).

Biomarkers can be classified into four types: predisposition, diagnostic, prognostic, and predictive biomarkers, according to the information they provide. High-quality biomarkers should meet the following criteria: quantifiable, sensitive, inducible, or repressible, highly accurate, and reproducible (Benninghoff, 2007). Since proteins' expression, localization, and activity are ubiquitously affected by environmental factors, proteomics provides an attractive avenue for biomarker research (Oskoueian et al., 2016; Simpson et al., 2009). Studies related to the detection of these markers proposed already potential candidates for stress biomarkers in farmed fish through proteomics, like microglobulins, macroglobulins, apolipoproteins, alpha-1-antitrypsin, transferrins, hemopexins, heat shock proteins (HSPs), plasminogen and complement system proteins (Alves et al., 2010; Bendixen et al., 2011; Bohne-Kjersem et al., 2009; Brunt et al., 2008; Kumar et al., 2009; Metzger et al., 2016; Russel et al., 2006). However, none of these biomarkers has yet reached subsequent phases of verification and validation.

A typical biomarker development proteomics study is divided into three phases: discovery, verification, and validation (Figure 1.10). As the study moves along the pipeline, fewer proteins are measured, and more samples are used to increase

statistical power because individual heterogeneity is one of the main challenges in biomarker identification. The discovery phase focuses on the identification of a large number of candidate biomarkers, typically through untargeted label-free proteomics coupled with data modelling. Candidate biomarkers for further validation are selected by data-driven and knowledge-driven approaches to derive the most discriminative proteins (McDermott et al., 2013). The verification step is usually performed using targeted proteomics (e.g., selected reaction monitoring (SRM)), to confirm that a candidate biomarker is indeed present and to provide a quantitative measurement of the protein. At this step, a threshold for the difference in absolute abundance (i.e., fold change) should be established to consider a candidate biomarker as confidently detectable. Additionally, verification should be performed on the same samples as well as on other samples from a different trial (i.e., the same species, developmental stage, tissue, and experimental condition). Finally, the validation phase is usually carried out using immunological assays, such as enzyme-linked immunosorbent assay (ELISA), to confirm the usefulness, robustness, and reproducibility of the biomarker. In this step, 1-10 candidates are usually evaluated. It is also important to determine whether an assay produces similar results when performed by different individuals and laboratories. In every step, the number of samples depends on several factors, including the number of candidate biomarkers to be tested; thus, it should always be determined by power analysis. Finally, a biomarker, or a combination of biomarkers is identified. As environmental factors and diseases do not affect only a single protein, a panel of biomarkers is usually preferred, as it can more accurately predict a condition and increase sensitivity and specificity. Several critical checkpoints should be considered during the preparation of a biomarker study design, which was recently addressed in a review (Nakayasu et al., 2021).

A validated stress biomarker should preferably have a minimally invasive measurement method, such as in skin mucus, to facilitate welfare status monitoring with any/reduced losses (refinement of the three Rs principle). In this sense, skin mucus was the chosen biofluid in this work for stress biomarker discovery in gilthead seabream. Notably, multiple studies have already demonstrated the potential of skin mucus as an alternative biological matrix to identify minimally invasive stress biomarkers in gilthead seabream using omics technologies (Cordero et al., 2017; Reyes-lópez et al., 2021; Sanahuja & Ibarz, 2015).

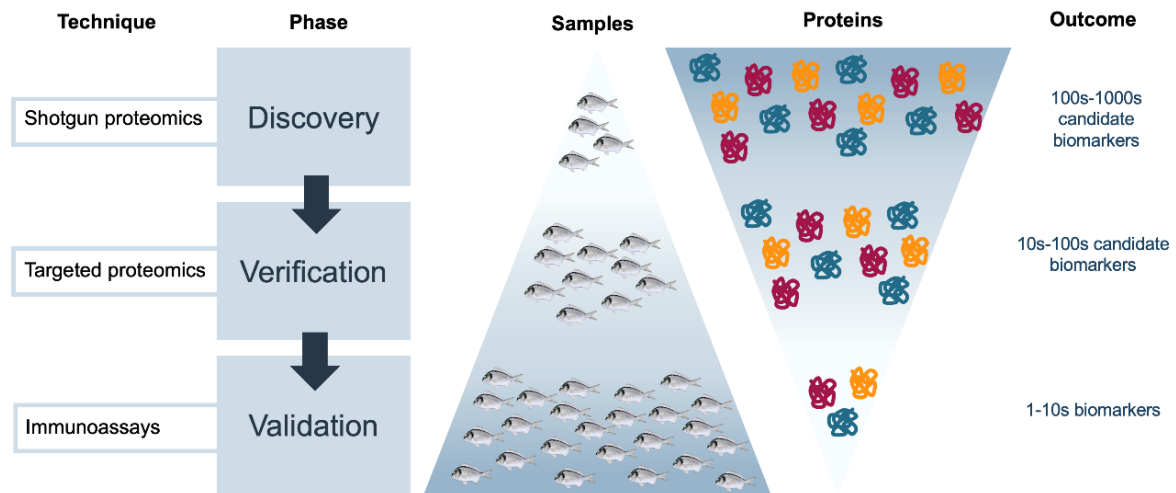


Figure 1.10. Classical biomarker workflow known as “triangular approach”. Discovery proteomics is first employed to identify a wide set of candidate biomarkers, which are then screened by targeted proteomics for confirmation and quantification. The few remaining candidates are then validated through immunological assays. The number of samples usually increases along the pipeline, contrasting with the number of candidate biomarkers.

1.11. OBJECTIVES

The sustainability of the aquaculture industry relies heavily on fish welfare. However, comprehensive measures of species-specific welfare indicators are limited, indicating a need to optimize current farmed fish welfare assessment methods. Gilthead seabream, an important Mediterranean species, is projected to experience growing demand for production. Therefore, understanding the stress response of this species and identifying molecular stress markers to be used as lab-based welfare indicators would greatly contribute to the sustainable growth of production while considering fish welfare. In this study, fish were exposed to different challenges typical in aquaculture production, including overcrowding, net handling, and hypoxia. The gilthead seabream stress response was characterized in different organs and body fluids, such as plasma, liver, and skin mucus, using different omics approaches (i.e., proteomics, metabolomics, transcriptomics, and multiomics) to reveal the underlying molecular mechanisms of stress adaptation in this species from a systems biology perspective. Following, minimally invasive candidate stress biomarkers were identified in the skin mucus. Based on the understanding gained from this work, the primary objective is to support future stress studies on this species and improve stress management protocols, as well as to provide the basis for validating and establishing a reliable stress biosignature for the development of future detection devices of stress status. These devices would allow to assess fish welfare quickly, efficiently, and

accurately in the field, ultimately enhancing the sustainability of aquaculture practices. To achieve this overarching goal, the following objectives were pursued in this PhD thesis:

- **Chapter 2**, aimed to measure physiological stress indicators based on primary and secondary stress responses and analyze the plasma stress-responsive proteome.
- **Chapter 3**, focused on performing a multiomics characterization of the gilthead seabream hepatic stress response. This chapter comprises four sub-chapters:
 - **Chapter 3.1** involved the analysis of the comparative metabolic profiling of the fish liver using vibrational spectroscopy.
 - **Chapter 3.2**, aimed to assess the fish hepatic stress response using gel-based proteomics and expression analysis of specific stress-related genes.
 - **Chapter 3.3** aimed to provide an integrative analysis of the liver stress-responsive proteome and metabolome.
 - **Chapter 3.4**, focused on the transcriptomic analysis of the liver stress response and multiomics integration.
- Finally, **Chapter 4** aimed to discover candidate stress biomarkers in the skin mucus through shotgun proteomics and bioinformatics.

Protein changes as robust signatures of fish chronic stress: a proteomics approach to fish welfare research



What we know about fishes is only a tiny slice of what they know.

— Jonathan Balcombe in “What a Fish Knows”

 **BMC** Series
BMC Genomics

This chapter has been published as research article in:

Raposo de Magalhães, C., Schrama, D., Farinha, A.P., Revets, D., Kuehn, A., Planchon, S., Rodrigues, P.M., Cerqueira, M., 2020. Protein changes as robust signatures of fish chronic stress: a proteomics approach to fish welfare research. BMC Genomics 21, 309. **doi: 10.1186/s12864-020-6728-4**

2.1. ABSTRACT

Aquaculture is a fast-growing industry and therefore welfare and environmental impact have become of utmost importance. Preventing stress associated to common aquaculture practices and optimizing the fish stress response by quantification of the stress level, are important steps towards the improvement of welfare standards. Stress is characterized by a cascade of physiological responses that, in turn, induce further changes at the whole animal level. These can either increase fitness or impair welfare. Nevertheless, monitorization of this dynamic process has, up until now, relied on indicators that are only a snapshot of the stress level experienced. Promising technological tools, such as proteomics, allow an unbiased approach for the discovery of potential biomarkers for stress monitoring. Within this scope, using gilthead seabream (*Sparus aurata*) as a model, three chronic stress conditions, namely overcrowding, handling and hypoxia, were employed to evaluate the potential of the fish protein-based adaptations as reliable signatures of chronic stress, in contrast with the commonly used hormonal and metabolic indicators. A broad spectrum of biological variation regarding cortisol and glucose levels was observed, the values of which rose higher in net-handled fish. In this sense, a potential pattern of stressor-specificity was clear, as the level of response varied markedly between a persistent (crowding) and a repetitive stressor (handling). Gel-based proteomics analysis of the plasma proteome also revealed that net-handled fish had the highest number of differential proteins, compared to the other trials. Mass spectrometric analysis, followed by gene ontology enrichment and protein-protein interaction analyses, characterized those as humoral components of the innate immune system and key elements of the response to stimulus. Overall, this study represents the first screening of more reliable signatures of physiological adaptation to chronic stress in fish, allowing the future development of novel biomarker models to monitor fish welfare.

2.2. INTRODUCTION

Managing welfare of fish in captivity is of increasing importance, both for productivity and sustainability reasons (Huntingford et al., 2006). There is still no clear consensus on how welfare should be defined or objectively measured, given the complexity and controversy of the concept (Branson, 2008; Carezzi & Verga, 2009). Challenges like divergent coping mechanisms, the incomplete knowledge regarding the nociceptive system of fish (e.g., emotional-like states; cognitive abilities, pain, suffering) (Braithwaite & Ebbesson, 2014; Castanheira et al., 2017; Cerqueira et al., 2017; Rose et al., 2012) and the lack of reliable physiological indicators of fish welfare, make its investigation even more difficult (Conte, 2004).

An aquaculture rearing facility deals with multiple stressful situations (stressors) that are inherent to daily routines and can compromise fish well-being. These situations are usually unpredictable and uncontrollable for the animal and can range in duration and severity (Conte, 2004; Selye, 1950). Fish launch a physiological response when faced with these threatening situations (Schreck, 2010; Selye, 1950). This adaptive mechanism, known as stress response, involves a cascade of reactions and enables the fish to cope with the stressor. However, when a stressful event is repeated or prolonged, it exceeds the organism's natural regulatory capacity and the fish fails to regain homeostasis, consequently impairing welfare (Ashley, 2007; Korte et al., 2007).

The physiological stress response starts with the immediate activation of the sympathetic response, followed by a slightly delayed activation of the HPI axis. As a result, catecholamines and corticosteroids (cortisol in teleosts), respectively, are released into the bloodstream (Mommsen et al., 1999; Wendelaar Bonga, 1997). These hormones lead to a series of downstream responses involving alterations in the energy metabolism and respiratory and immune functions (Pottinger, 2008). The rapid mobilization of energy substrates such as glucose (the fuel needed for the coping mechanisms) is caused by the activation of both the glycogenolysis in the liver or muscle, and the hepatic gluconeogenesis, by the catecholamines and cortisol, respectively (Fabbri & Moon, 2016; Vijayan et al., 2010). Stressful stimuli can also lead to strenuous exercise fueled by anaerobic glycolysis in the muscle, generating lactate, which is then released into plasma (Milligan & Girard, 1993; C. M. Wood et al., 1983). Prolonged exposure to the stressor will inevitably lead to alterations that are reflected in the whole-animal's performance, like perturbations at the reproduction, immunological, growth and behavior levels (Boonstra, 2013).

The plasma levels of cortisol, alongside glucose and lactate, are the most commonly used physiological indicators to assess stress in fish (T. Ellis et al., 2012). Nevertheless, some inconsistencies have been reported in several experimental studies. This demonstrates the unreliability of these indicators, mainly in cases of chronic stress, which is mostly due to: (i) a high variability of response levels; (ii) a decrease of the cortisol levels to basal levels within minutes/hours following an acute stressor; (iii) the fact that fish can adapt, to certain extent, to chronic stress and the cortisol response is therefore attenuated; and (iv) the intrinsic and extrinsic factors (e.g. age, sexual maturity, social status, level of domestication, prior experience, nutritional status) that can affect cortisol secretion (Bonier et al., 2009; Davis Jr & McEntire, 2006; Fast et al., 2008; Koakoski et al., 2012; Madaro et al., 2016; Martinez-Porchas et al., 2009). In this sense, it is vital to complement the existing behavioral, biochemical, and physiological measures for a correct interpretation of the welfare status of the fish. This will be crucial to form a robust welfare assessment and to allow, in the future, the development of targeted recommendations and legislation. With the increasing research into the welfare of cultured fish, more advanced technologies are gaining popularity. Proteomics are promising alternatives for the discovery of candidate molecular markers that can indicate physiological alterations due to stress exposure (Marco-Ramell et al., 2016). Despite the limitations to the use of these technologies in the aquaculture field (Almeida et al., 2014), several studies prove already the huge potential of proteomics for the identification of stress signatures (Alves et al., 2010; Brunt et al., 2008; Cordeiro et al., 2012b; Metzger et al., 2016; Sanahuja & Ibarz, 2015).

There is very little data available concerning the process of long-term coping with a chronic stressor and indicators used in this case. Considering this gap in research, we aim, in the present study, to comparatively assess the stress responses of fish at different levels (i.e., plasma stress markers, changes in plasma proteins' abundance and muscle biochemistry). Using gilthead seabream (*Sparus aurata*) as model, three chronic stress conditions were employed, and proteomics was used to benchmark potential signatures of stress adaptation in the plasma proteome since several proteins resulting from physiological events are released into circulation. Gilthead seabream was the chosen species in this study since it is one of the most important species in European aquaculture with high commercial value. This work aims to pioneer a better understanding of the underlying molecular mechanisms behind fish physiological adaptation to long-term stress. Additionally, it aims to bridge the gap

between the scientific community and the industry by paving the way for the development of novel biomarkers to monitor fish welfare.

2.3. MATERIALS & METHODS

2.3.1. Animals

Gilthead seabream (*Sparus aurata*) were obtained from a commercial fish farm (Maresa, Mariscos de Estero S.A., Huelva, Spain) and kept under quarantine conditions for a 2-week period at the Ramalhete Research Station (CCMAR, University of Algarve, Faro, Portugal). The fish were then individually weighed and distributed among conical fiberglass tanks (500 L), according to the density requirements of each trial. The tanks were supplied with natural flow-through seawater from Ria Formosa and kept under natural temperature (13.4 ± 2.2 °C) and photoperiod, salinity at 34.7 ± 0.8 ‰, and artificial aeration (dissolved oxygen above $5 \text{ mg} \cdot \text{L}^{-1}$). Fish were fed by hand once a day, with a diet manufactured by AquaSoja Portugal, following the species' nutritional requirements.

2.3.2. Experimental design

The study was performed in three separate trials: (1) Overcrowding (OC), (2) Net handling (NET) and (3) Hypoxia (HYP), due to logistic issues. Each trial followed a 2-week acclimation period, and the initial rearing density was established at 10 kg m^{-3} (except in the experimental groups of high stocking densities). In the OC trial, during the 54 days of experiment, fish (initial body weight (IBW) = 372.33 ± 6.55 g) were stressed using different high stocking densities, by increasing the number of fish in the tanks. Three different experimental groups were tested in triplicate: Control – 10 kg m^{-3} (OCCTRL), medium density – 30 kg m^{-3} (OC30), high density – 45 kg m^{-3} (OC45). The NET trial lasted for 45 days, and the fish (IBW = 375.69 ± 11.88 g) were stressed by 1-min air exposure, using nets designed to fit inside the tanks and to be lifted to perform the stressful event. The experimental groups were established, in triplicate, as follows: Control – undisturbed fish (the net was also placed in the tanks but not lifted) – (NETCTRL), fish air-exposed twice a week (NET2) and fish air-exposed four-times a week (NET4). In the HYP trial, fish (IBW = 397.99 ± 16.56 g) were subjected to low levels of saturated oxygen, by injection of nitrogen in the water, for 48 h, according to the following experimental groups (in triplicate): Control – 100% saturated oxygen – (HYPCTRL), 30% saturated oxygen (HYP30) and 15% saturated oxygen (HYP15).

Different trial times are due to differences in the nature and severity of the stressor, to which rearing protocols had to be adjusted accordingly.

2.3.3. Sampling procedure

Prior to the sampling day, fish were starved for 48 h to clean the digestive tract. Nine random fish per tank were lethally anaesthetized with tricaine methanesulfonate (MS-222; Merck KGaA, Darmstadt, Germany) for the following sampling procedures: 3 fish for *rigor mortis* index assessment, 3 fish for muscle pH measurement and 6 fish for blood collection. Blood samples of approximately 2 ml were collected from the caudal vein with a heparinized syringe and immediately centrifuged at 2000 g for 20 min. Plasma samples were immediately frozen at – 80 °C until posterior analyses. Fish for the measurement of *post-mortem* biochemical changes (pH and *rigor mortis*) were stored in polystyrene boxes with ice during the sampling period (72 h). All fish were weighed and measured.

2.3.4. Plasma stress indicators' measurement

Plasma cortisol levels were quantified using a commercial Cortisol ELISA kit RE52061 (IBL International, Hamburg, Germany), following the manufacturer's instructions. Measurements were registered at 450 and 620 nm along with a prepared standard curve on a microplate reader Biotek Synergy 4 Hybrid Technology™ (Biotek Instruments Inc., Winooski, USA). Plasma glucose and lactate levels were assessed through commercial colorimetric kits (Spinreact, Girona, Spain), following the manufacturer's instructions.

2.3.5. Biochemical and quality characterization of fish muscle

Muscle pH measurements were performed (n = 3 per tank), using a waterproof pH spear for food testing (Oakton® Instruments, Nijkerk, Netherlands), in the dorsal muscle, at 0, 1, 2, 4, 6, 8, 24, 48 and 72 h after death (HAD), approximately 1–2 cm apart. At the same *post-mortem* periods, *rigor mortis* was assessed (n = 3 per tank) by the rigor index (RI), as previously described (Erikson, 2001), using the formula:

$$RI (\%) = (L_0 - L_t) / L_0 \times 100$$

L_0 (cm) refers to the vertical distance between the base of the caudal fin and the table surface (where the anterior half of the fish is placed), measured immediately after death, whereas L_t (cm) corresponds to the same distance, however at selected time

intervals. Fish were carefully handled during the measurements to avoid an interference with the rigor onset.

2.3.6. Plasma proteomics analysis

2.3.6.1. Protein labelling

Plasma samples were diluted 80X in DIGE buffer (7 M urea, 2 M thiourea, 4 % 3-[(3-Cholamidopropyl) dimethylammonio]-1-propanesulfonate (CHAPS), 30 mM Tris pH 8.5) and the protein content measured with Bradford assay using the BioRad Quick Start Bradford Dye Reagent 1X (Bio-Rad Laboratories, Hercules, California, USA) and bovine serum albumin (BSA) as standard, BioRad Bovine Serum Albumin Standard Set (Bio-Rad Laboratories). Samples' pH was checked with a pH indicator paper, Sigma-P4536 (Sigma Aldrich) and adjusted to 8.5 using 0.1 M NaOH. DIGE minimal labelling of 50 µg of protein was carried out using the CyDye™ DIGE fluor minimal labelling kit 5 nmol (GE Healthcare, Little Chalfont, UK), with 400 pmol fluorescent amine reactive cyanine dyes freshly dissolved in anhydrous dimethylformamide (DMF), following the manufacturer's instructions. Labelling was achieved on ice for 30 min, in the dark, and the reaction quenched with 1 mM of lysine for 10 min. For each trial, six samples per experimental condition were labelled with Cy3 and six with Cy5 to reduce the impact of label difference, while an internal standard consisting of a pool of all samples, with equal amounts, was labelled with Cy2. Samples were randomly sorted to avoid labelling bias.

2.3.6.2. Protein separation by 2DE

For each strip, 150 µg of protein (50 µg from each dye) were loaded along with rehydration buffer (8 M urea, 2% CHAPS, 50 mM dithiothreitol (DTT), 0.001% bromophenol blue, 0.5% Bio-lyte 3/10 ampholyte (Bio-Rad Laboratories)) to complete 450 µL. Passive rehydration was conducted for 15 h on 24 cm Immobiline™ Drystrips (GE Healthcare) with linear pH 4–7, on an IPG Box (GE Healthcare). Following, isoelectric focusing (IEF) was performed in 5 steps: 500 V gradient 1 h, 500 V step-and-hold 1 h, 1000 V gradient 1 h, 8000 V gradient 3 h and 8000 V step-n-hold 5h40 for a total of 60,000 Vhr using Ettan IPGphor at 20 °C (GE Healthcare). Focused strips were reduced and alkylated with 6 ml of equilibration buffer (50 mM Tris-HCl pH 8.8, 6 M urea, 30% (v/v) glycerol and 2% SDS) with 1% (w/v) DTT or 2.5% (w/v) iodoacetamide (IAA) respectively for 15 min each, in constant agitation. Strips were

then loaded onto 12.5% Tris-HCl SDS-PAGE gels and ran in an Ettan DALTSix Large Vertical System (GE Healthcare) at 10 mA/gel for 1 h followed by 60 mA/gel until the bromophenol blue line reaches the end of the gel, using a standard Tris-Glycine-SDS running buffer.

2.3.6.3. *Image acquisition and analysis*

CyDye-labeled gels were scanned on a Typhoon™ laser scanner 9400 (GE Healthcare) at 100 μm resolution, with the appropriate laser filters for the excitation and emission wavelengths of each dye (i.e., Cy2–488/520 nm; Cy3–532/580 nm; and Cy5–633/670 nm), according to the manufacturer's recommendations. The voltages of the Photo Multiplier Tube (PMT) were adjusted to obtain a maximum image quality with minimal signal saturation and clipping. Gel images were checked for saturation during the acquisition process using the ImageQuant TL software (GE Healthcare). The final images were analyzed with SameSpots software (TotalLab, Newcastle, UK), including background subtraction (average normalized volume $\leq 100,000$ and a spot area ≤ 500), filtering, spot detection, spot matching, normalization, and statistical analysis. Spot volume ratios that showed a statistically significant difference (abundance variation of at least 1.0-fold, $p < 0.05$ - One-way analysis of variance (ANOVA) on log₂-transformed normalized spot volumes) were processed for further analysis. Protein spots with statistically different intensities were manually excised from preparative gels and identified by matrix-assisted laser desorption/ionization time-of-flight/time-of-flight mass spectrometry (MALDI-TOF/TOF MS).

2.3.6.4. *Protein identification by MALDI-TOF/TOF MS*

Spots from SYPRO® Ruby-stained (Invitrogen™, Carlsbad, CA, USA) gilthead seabream plasma 2D gels were picked and subjected to in-gel tryptic digestion, similar as reported before (Schiener et al., 2018). In this study, gel plugs were washed twice with 50 mM ammonium bicarbonate solution in 50% (v/v) methanol (MeOH) for 20 min and dehydrated twice for 20 min in 75% acetonitrile (ACN). Proteins were then digested with 8 μL of a solution containing 5 ng/ μL trypsin (trypsin Gold, Promega, Madison, WI, USA) in 20 mM ammonium bicarbonate for 6 h at 37 °C. A 0.1% trifluoroacetic acid (TFA) solution in 50% ACN and a solution of 7 mg/mL α -cyano-4-hydroxycinnamic acid (CHCA) in 50% ACN/0.1% TFA were used for peptide extraction and spotting respectively. MALDI TOF/TOF analysis was performed with a TOF/TOF™ 5800 (AB

SCIEX, Redwood City, CA, USA) mass spectrometer in MS and MS/MS mode. For each spot, the 10 most intense peaks of the MS spectrum were selected for MS/MS acquisition. Database interrogation was carried out over with ProteinPilot v4.5 (AB Sciex) on an in-house Mascot server version 2.6.1 (Matrix Science Ltd., London, UK). Mass lists were searched against NCBI nr database restricted to the taxonomy “other *Actinopterygii*” (tax ID 7898 excluding 31,033 and 7955) with the following parameters: maximum 2 missed cleavages by trypsin, peptide mass tolerance ± 100 ppm, fragment mass tolerance set to 0.5 Da, carbamidomethylation of cysteine selected as fixed modification and tryptophan dioxidation, histidine, tryptophan and methionine oxidation, and tryptophan to kynurenine as variable modifications. Protein hits not satisfying a significance threshold ($p < 0.05$ and a total ion score > 60) were further searched against vertebrate EST (expressed sequence tags) database also restricted to the taxonomy “other *Actinopterygii*”.

2.3.7. Protein-protein interaction network and gene ontology enrichment analyses

The theoretical molecular masses and isoelectric points (pI) of the MS identified proteins were calculated using the amino-acid sequences (in one-letter code) on the ProtParam Tool (<http://us.expasy.org/tools/protparam.html>). A significance cutoff was applied for the identified proteins at log-fold change ± 1.0 . Following, the identified proteins were blasted against *Danio rerio*, on the UniprotKB database, using the FASTA protein sequences as queries. The orthologs were mapped using Search Tool for the Retrieval of Interacting Genes/Proteins (STRING) web tool v11.0 (Szklarczyk et al., 2019) to screen for protein-protein interactions (PPI). Gene ontology (GO) enrichment analysis and network visualization and analysis were performed on Cytoscape v3.7.1 (Shannon et al., 2003) with the BiNGO plug-in (Maere et al., 2005). Important hub proteins were screened by counting the degree of connectivity of each node in the network. Overrepresented GO terms were identified, using *B. rerio* as reference, by selecting the hypergeometric test with a significance threshold of 0.05 after Benjamini & Hochberg FDR correction.

2.3.8. Statistical analyses

All univariate and multivariate statistical analyses were performed using R v3.5.3 for MacOSX (<https://www.rproject.org>). Statistical analyses of the plasma

parameters and the *post-mortem* muscle biochemical changes were performed using plasma cortisol, glucose and lactate levels, muscle pH and *rigor* index as dependent variables, and the stress treatment as factor. Statistical differences between treatments were analyzed independently for each trial (OC, NET and HYP). For *rigor* index and muscle pH, data were processed separately for each sampling time. Differences in plasma and muscle parameters between treatments were assessed by a One-way ANOVA on log₁₀-transformed data, except for *rigor mortis* data, which was transformed by arcsine square root. Multiple comparisons were carried out by the *post hoc* Tukey HSD test. When transformed data failed the Shapiro-Wilk normality test, the non-parametric Kruskal-Wallis on ranks was used, followed by Dunn's test. When transformed data did not verify homoscedasticity assumption by Levene's test, statistical significance was analyzed by Welch's ANOVA, followed by Games-Howell. A significance level of $\alpha = 0.05$ was used in all tests performed. Experimental data is expressed as mean \pm standard deviation (SD). Principal component analysis (PCA) and hierarchical clustering analysis of the identified proteins were performed on the log₂-transformed normalized spot volumes obtained from SameSpots software, with autoscaling. Heatmap was generated by comparing Z-scores of normalized spot volumes and hierarchical clustering of samples and protein spots was performed using the Euclidean distance and the maximum cluster agglomeration method as distance metrics.

2.4. RESULTS

2.4.1. Fish general condition

Fish were monitored every day during the trials. The experimental periods reached the end with a 100% survival rate. The overall condition and growth performance of the fish were also monitored (Additional file 1 - [online](#)), and initial (IBW) and final body weights (FBW) were recorded for each experiment. The average body weight was reduced by the end of the net handling (NET) and hypoxia (HYP) trials, in all groups, including the control. However, there were no significant differences in final body weights between the control group and any of the stressed groups ($p > 0.05$), suggesting that weight reductions were unrelated to the stressor.

2.4.2. Plasma stress markers analysis

Circulating cortisol, glucose, and lactate levels were measured in gilthead seabream submitted to different chronic stressors and in control fish (Figure 2.1). The overall levels of these metabolites showed a high variability of biological responses in all trials, with several data points considered outliers (outside of the interquartile range). Cortisol levels presented the highest intervals of values.

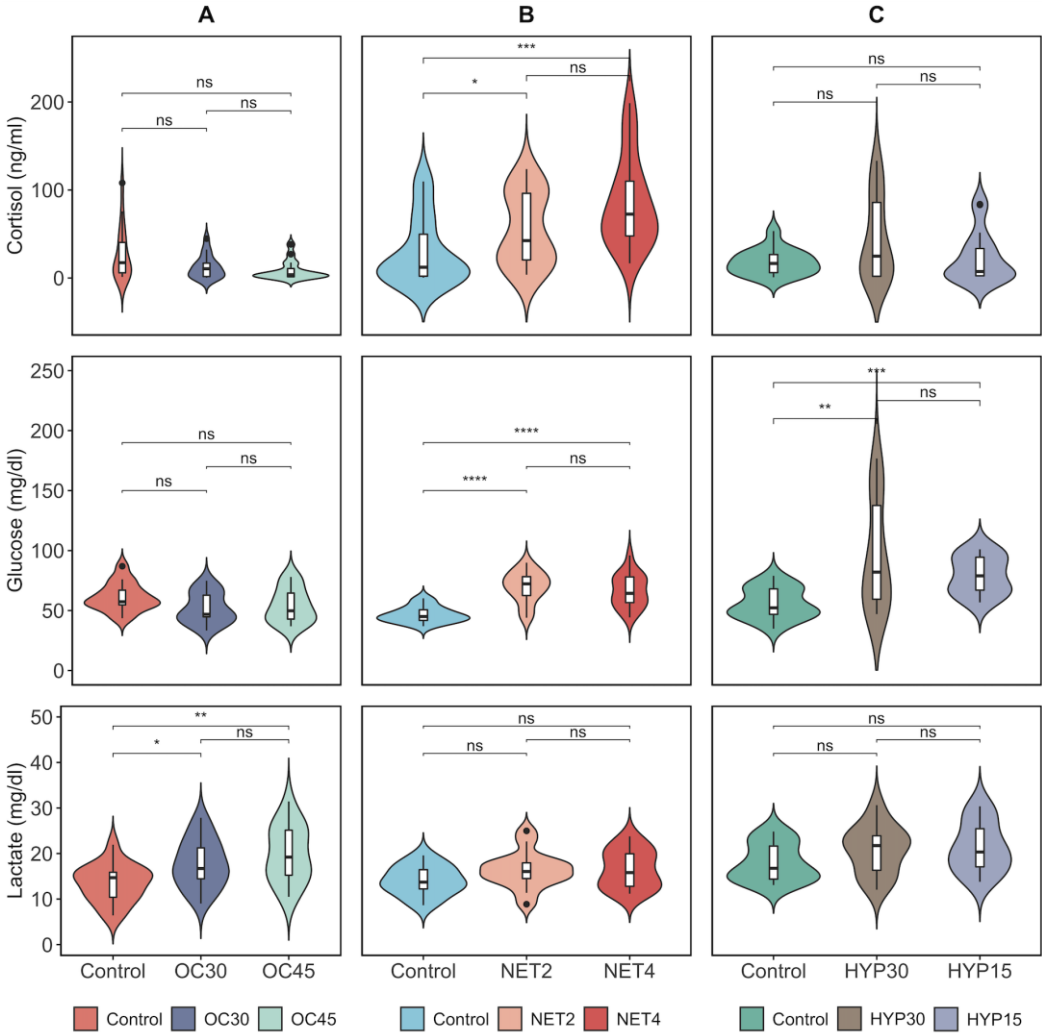


Figure 2.1. Violin plots showing the distributions of plasma cortisol (ng/ml), glucose (mg/dl) and lactate (mg/dl) levels of gilthead seabream (*Sparus aurata*) submitted to different challenges (A – overcrowding, B – net handling, C – hypoxia), in two intensities, and unstressed fish (control) (n = 18). The boxplot inside includes observations from the 25th to the 75th percentiles as determined by R software; the horizontal line indicates the median value. Whiskers extend 1.5 times the interquartile range. Single data points are outlying data. *p < 0.05; **p < 0.01; ***p < 0.001; **** p < 0.0001. NS (not significant) indicates a p-value greater than 0.05.

In the OC trial, only lactate plasma levels presented statistically significant differences, both between control and challenged groups (Lactate_{CTRL} – 13.46 ± 4.07, Lactate_{OC30} – 17.79 ± 5.29, Lactate_{OC45} – 19.89 ± 6.19, $p = 2.89e^{-3}$). Curiously, in the case of cortisol, although not significant, stressed fish showed decreased levels compared to control (Cortisol_{CTRL} – 28.03 ± 30.78, Cortisol_{OC30} – 12.51 ± 13.13, Cortisol_{OC45} – 8.54 ± 10.92, $p = 1.20e^{-1}$). In the NET trial, statistically significant differences were registered for the cortisol and glucose plasma levels, again between control and the challenged groups (Cortisol_{CTRL} – 29.38 ± 38.06, Cortisol_{NET2} – 55.69 ± 41.05, Cortisol_{NET4} – 84.83 ± 50.77, $p = 5.15e^{-4}$; Glucose_{CTRL} – 46.57 ± 6.58, Glucose_{NET2} – 69.76 ± 12.90, Glucose_{NET4} – 66.60 ± 13.74, $p = 2.06e^{-6}$). In the HYP trial, significant differences were only observed in the glucose levels (Glucose_{CTRL} – 55.85 ± 12.72, Glucose_{HYP30} – 96.22 ± 45.53, Glucose_{HYP15} – 79.30 ± 15.78, $p = 1.07e^{-4}$). Cortisol values are presented as mean ± standard deviation (SD) in ng/ml, and glucose and lactate values in mg/dl.

2.4.3. *Post-mortem* muscle biochemical changes

Muscle pH declined over 72 HAD, in gilthead seabream stored in ice. Values ranged from an average of 7.4, 7.7 and 7.4 immediately after slaughtering, to 6.3, 6.5 and 6.4 at the last sampling time, in fish from OC, NET and HYP trials, respectively. Significant differences between conditions were found for the NET trial at 4 ($p_{NET2-NET4} = 0.032$) and 72 HAD ($p_{CTRL-NET2} = 0.008$), and for the HYP trial at 0 ($p_{CTRL-HYP15} = 0.021$), 8 ($p_{CTRL-HYP15} = 0.003$, also in HYP30-HYP15 with lower significance), 48 ($p_{CTRL-HYP15} = 0.006$) and 72 HAD ($p_{HYP30-HYP15} < 0.001$) (Figure 2.2). The onset and resolution of *rigor mortis* (Figure 2.2) showed significant differences between treatments in the NET and HYP trials, specifically at 8 HAD ($p_{CTRL-NET4} < 0.001$), and at 8 ($p_{HYP30-HYP15} < 0.001$) and 24 HAD ($p_{HYP30-HYP15} = 0.020$), respectively. In the OC trial, fish reached an average maximum *rigor* strength at 24 HAD. In the NET trial, averaged maximum *rigor* strength was reached at 48 HAD in CTRL and NET2, and at 24 HAD in NET4 group. In the HYP trial, all groups reached averaged maximum *rigor* strength at 48 HAD.

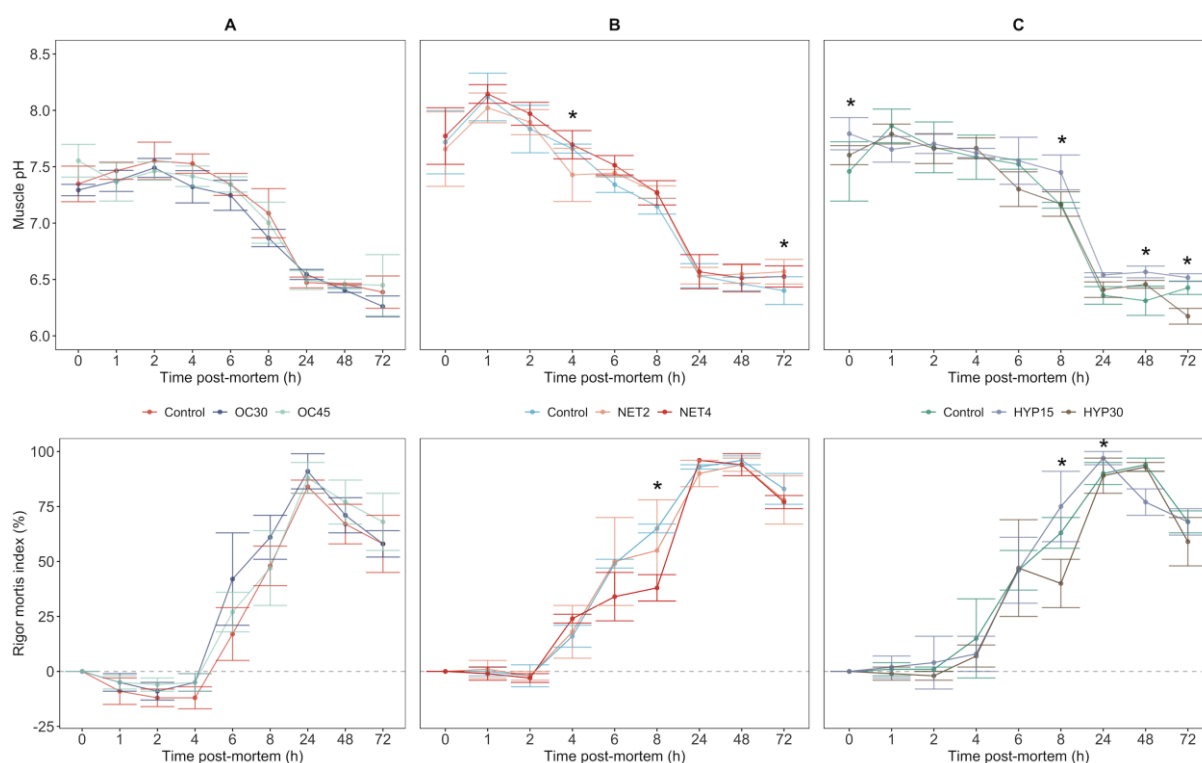


Figure 2.2. Post-mortem changes in muscle pH and *rigor mortis* of gilthead seabream (*Sparus aurata*) submitted to different challenges (A – overcrowding, B – net handling, C – hypoxia), in two intensities, and unstressed fish (control), stored in ice for 72 h. Data points are the mean \pm SD of $n = 9$ for each sampling time. Means labelled * are different at $p < 0.05$.

2.4.4. Plasma proteomics analysis

A comparative proteomics analysis of the gilthead seabream plasma between the control and the stress treatments detected, 681, 752 and 681 protein spots for the OC, NET and HYP trials, respectively, within the pH range of 4–7 and a molecular mass range of 11–114 kDa. After statistical analysis, 19, 360 and 34 protein spots within the OC, NET and HYP trials, respectively, were found to present significantly differential abundance (significance threshold at $p < 0.05$) between experimental conditions. From these, seven, 171 and 12 were manually excised from the 2D gels for MALDI-TOF/TOF MS analysis. No proteins were identified with significance for the OC trial. For the NET and HYP trials, 107 and two differential protein spots, respectively, were successfully identified by a combination of peptide mass fingerprinting (PMF) and MS/MS search, with significant scores (protein score > 76 , total ion score > 60 , $p < 0.05$). Among the spots identified from the NET trial, 13 showed more than one significant protein identification (202, 326, 521, 559, 586, 604, 677, 877, 950, 959, 990, 996 and 1157), indicating that multiple proteins migrated to the same spots on the gel. The identified proteins are listed in an additional file (see additional

file 2 - [online](#)). A representative 2D gel of the gilthead seabream plasma proteome is shown in Figure 2.3.

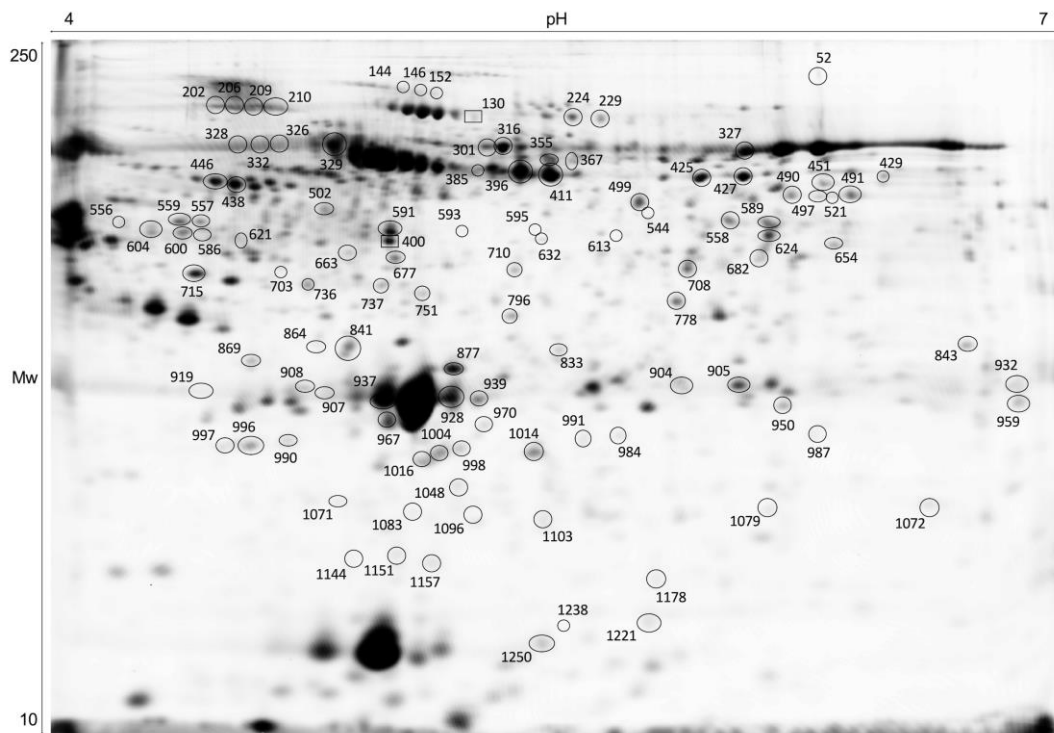


Figure 2.3. Representative pattern of gilthead seabream (*Sparus aurata*) blood plasma on a 12.5% polyacrylamide 2D gel. Black circles represent the 107 proteins identified by MALDI-TOF/TOF MS with significant differences in abundance in NET groups and black squares the 2 proteins with significant differences in abundance in HYP groups ($p < 0.05$).

Considering the number of identifications in each trial, only the 107 identified protein spots from the NET trial were considered for further statistical and bioinformatics analyses. At this step, a log-fold change cutoff of ± 1.0 ($p < 0.05$) was applied (Figure 2.4.A) and a total of 56 identified protein spots (corresponding to 20 single entries) were considered significant. Of these, 19 were upregulated in stressed fish and 34 were downregulated. Three spots (502, 990 and 1021) showed multi-expression patterns and could not be classified as up- or downregulated. Seventeen protein spots (502, 715, 841, 905, 908, 919, 937, 939, 967, 997, 1004, 1016, 1021, 1151, 1221, 1238 and 1250) were identified as apolipoprotein A-I, whereas 13 were downregulated in stressed fish. Four spots (864, 869, 990 and 996) were identified as apolipoprotein Eb and two were upregulated. Complement factor B was identified in 4 spots (144, 146, 152 and 737) and complement component C3 in 5 spots (591, 593, 595, 1048 and 1083) from which three from each were upregulated. Two protein spots

(796 and 833) were identified as warm-temperature acclimation-related 65 kDa, 1 down- and one upregulated. Three spots (202, 206 and 209) identified as inter-alpha-trypsin inhibitor heavy chain H3, 2 spots (224 and 229) as alpha-2-macroglobulin and five (558, 751, 843, 904 and 1079) identified as transferrin were downregulated. Two spots (663 and 710), identified as haptoglobin, were found to be upregulated. Fibrinogen alpha-chain was identified in two spots (521 and 544) and were both upregulated. Alpha-1-antitrypsin homolog, apolipoprotein B-100, beta-actin, calcium/calmodulin-dependent protein kinase type II, leucine-rich alpha-2-glycoprotein, fetuin-B-like, hemopexin-like, hyaluronic acid-binding protein 2 and pentraxin were identified in a single protein spot each.

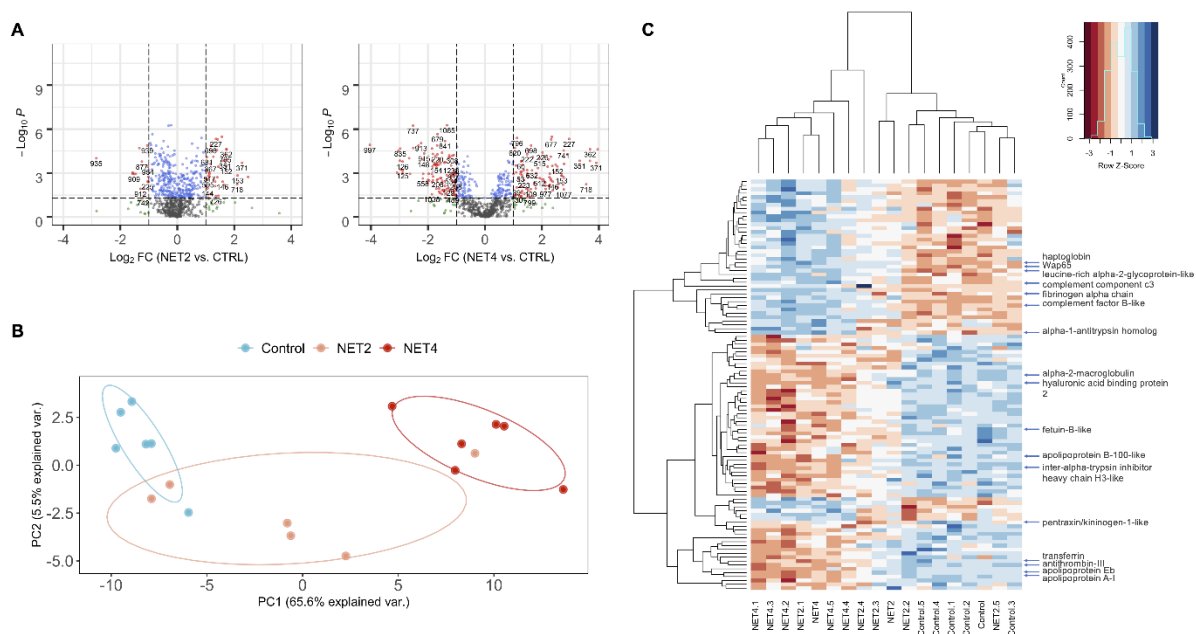


Figure 2.4. Volcano plots of the entire set of plasma proteins detected by DIGE analysis on the NET trial samples. Each point represents the difference in abundance (fold-change) between stressed fish (NET2 on the left; NET4 on the right) and control fish plotted against the level of statistical significance. Dotted vertical lines represent a 2-fold variation in abundance, while dotted horizontal lines represent the significance level of $p < 0.05$. Red dots represent proteins significantly up- and downregulated. B – PCA performed with the normalized spot volumes of the 107 identified proteins in the plasma samples of gilthead seabream from the NET trial ($n = 6$). Blue, orange, and red dots represent CTRL, NET2 and NET4 groups, respectively. C – HCA of 107 significantly differential proteins identified in the plasma samples of gilthead seabream from net handling (NET) trial. Rows represent expression patterns of individual proteins, while each column corresponds to a biological replicate (fish). Cell color indicates the normalized Z-scores of the spot volumes.

Hierarchical clustering (HCA) and PCA analyses were performed for the identified 107 proteins spots with differential relative abundance across NET groups to

check how well the samples grouped based on the expression patterns of the protein spots. The PCA (Figure 2.4.B) showed two main clusters belonging to the control and NET4 samples, while two biological samples belonging to the NET2 group clustered together with the control samples and one with the NET4 samples. The 107 differential protein spots were centralized into two principal components (PC), PC1 and PC2, which represented the maximum variation (65.6%) and the next highest variation (5.5%), respectively. The HCA (Figure 2.4.C) likewise revealed two main groups regarding the biological replicates, as observed by the top dendrogram. The protein spots were also grouped into two main clusters, one displaying a pattern of higher relative abundance and the other of lower relative abundance in stressed fish, when compared to the control. As described above for the PCA, higher variability in NET2 was also shown in the HCA.

For the network and GO enrichment analyses the subset of 20 single protein identifications mentioned above was blasted against *Danio rerio* in the UniprotKB database. A PPI network (Figure 2.5.A) was generated on the STRING web tool revealing 61 edges among 18 nodes/proteins (two proteins had no interaction with the main network), with a clustering coefficient of 0.677 and a very significant enrichment value ($p < 1.0e^{-16}$). The analysis was performed on Cytoscape and specific topological parameters were selected to demonstrate the importance and distribution of the nodes in the network: a darker color intensity of the nodes indicates higher degree, while the size was estimated using the variation in protein abundance (fold-change). For every single entry, one protein spot was chosen as the most representative of each protein (Table 2.1), based mainly on the protein score and experimental molecular weight and pI close to the theoretical ones. From these 18 spots, 11 were down- and seven were upregulated, however, these differences in abundance were mostly significant (log-fold change > 1.0 or < -1.0 , q -value < 0.05) for the NET4 treatment (only two were exclusively significant for the NET2 treatment and two were significant for both treatments). Thus, the fold-change of these 18 spots between NET4 and CTRL groups was used to estimate the size of the nodes on the PPI network, which ranged from -4.04 to $+2.78$. SERPINC1 (antithrombin-III), TFA (transferrin) and FGA (fibrinogen alpha-chain) occupied the most central positions in the network having the highest number of interactions, while APOA1 (apolipoprotein A-I) showed the highest number of experimentally demonstrated interactions, mainly with APOEB (apolipoprotein Eb), APOBB (apolipoprotein B-100) and FGA. GO Enrichment analysis (Figure 2.5.B)

revealed 19 overrepresented (hypergeometric test, $FDR < 0.05$) GO Biological Process (BP) terms, mostly linked to the immune system and response to stimulus. No annotations were retrieved for alpha-1-antitrypsin, leucine-rich alpha-2-glycoprotein-like, apolipoprotein A-I, apolipoprotein B-100-like, haptoglobin, pentraxin and hyaluronic acid binding protein 2. In the horizontal bar plot (Figure 2.5.B), only the nine most significant terms are represented. GO Molecular function enrichment analysis accounted for eight terms with five main proteins (alpha-1-antitrypsin, antithrombin-III, inter-alpha-trypsin-inhibitor, kininogen and alpha-2-macroglobulin) while GO Cellular component revealed four enriched terms with two main proteins (fibrinogen alpha-chain and alpha-2-macroglobulin). A complete list of all GO terms is described on the additional file 3 - [online](#).

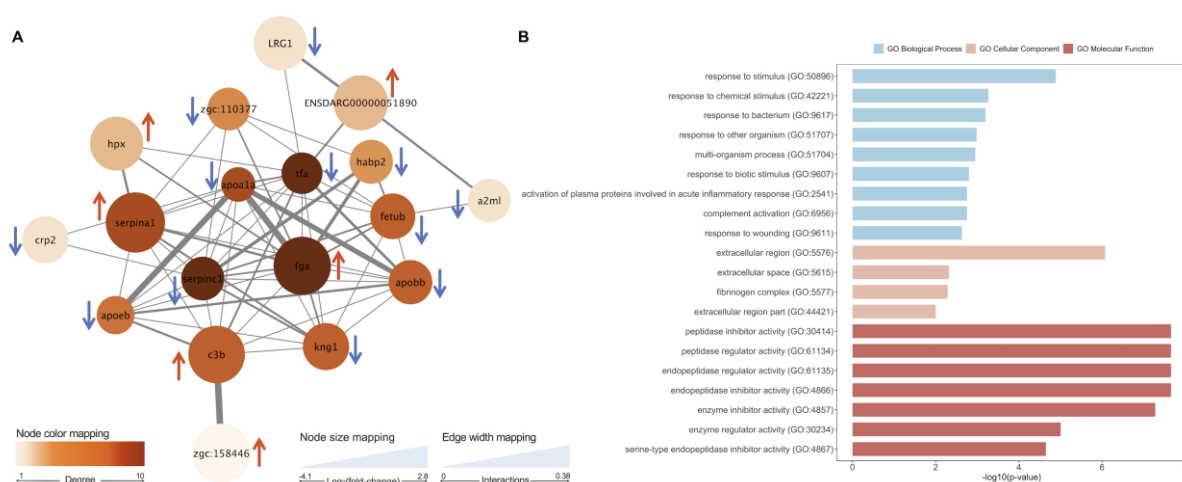


Figure 2.5. PPI network generated with 18 differential proteins identified in the plasma of fish from NET trial. Nodes represent proteins and edges the functional associations between them. STRING annotations are described in Table 2.1. Red arrows represent upregulated proteins in both treatments; blue arrows represent downregulated proteins in both treatments. D – GO Enrichment analysis of the 18 proteins showing significantly differential abundance between control and NET treatments (hypergeometric test, $FDR < 0.05$).

Table 2.1. STRING annotations and fold-changes of the proteins in the PPI network. Bold lettering in the “FC” column indicates significant fold-changes (> 1.0 and < -1.0). List is given in ascending order of spot number.

Spot ^a	Accession no. ^b	Protein ID ^c	FC ^d		<i>Danio rerio</i> homolog (UniprotKB identifier)	STRING annotation
			NET2	NET4		
152	XP_008277007.1	PREDICTED: complement factor B-like [<i>Stegastes partitus</i>]	1.72	2.54	F1QFT0	zgc:158446
202	XP_010753395.2	PREDICTED: antithrombin-III [<i>Larimichthys crocea</i>]	-0.36	-1.61	Q8AYE3	serpinc1
209	XP_019111370.1	PREDICTED: inter-alpha-trypsin inhibitor heavy chain H3-like [<i>Larimichthys crocea</i>]	-0.49	-1.76	F1QTF9	zgc:110377
224	XP_017260893.1	alpha-2-macroglobulin, partial [<i>Kryptolebias marmoratus</i>]	-0.62	-1.74	A0A0R4IDD1	a2ml
316	AWP20152.1	putative apolipoprotein B-100-like isoform 2 [<i>Scophthalmus maximus</i>]	-0.88	-1.46	Q5TZ29	apobb
367	XP_023285742.1	alpha-1-antitrypsin homolog [<i>Seriola lalandi dorsalis</i>]	1.17	2.78	Q6P5I9	serpina1
544	KKF22678.1	Fibrinogen alpha chain [<i>Larimichthys crocea</i>]	1.33	2.26	B8A5L6	fga
556	XP_018550494.1	PREDICTED: leucine-rich alpha-2-glycoprotein-like [<i>Lates calcarifer</i>]	0.51	1.20	Q5RHE5	LRG1
558	AEA41139.1	transferrin [<i>Sparus aurata</i>]	-0.46	-2.18	A0A2R8RRA6	tfa
595	ADM13620.1	complement component c3 [<i>Sparus aurata</i>]	1.08	2.06	Q3MU74	c3b
710	ARI46218.1	haptoglobin [<i>Sparus aurata</i>]	1.39	1.53	F8W5P2	ENSDARG00000051890
736	AJW65884.1	Hyaluronic acid binding protein 2 [<i>Sparus aurata</i>]	-0.33	-1.53	Q1JQ29	habp2
796	ACN54269.1	warm temperature acclimation-related 65 kDa protein [<i>Sparus aurata</i>]	0.85	1.13	Q6PHG2	hpx
877	BAM36361.1	pentraxin [<i>Oplegnathus fasciatus</i>]	-1.24	-0.73	Q7SZ53	crp2
	XP_022604055.1	kininogen-1-like [<i>Seriola dumerilii</i>]	-1.24	-0.73	Q5XJ76	kng1
996	APO15792.1	apolipoprotein Eb [<i>Sparus aurata</i>]	-0.10	-3.04	O42364	apoeb
997	XP_010742296.3	apolipoprotein A-I [<i>Larimichthys crocea</i>]	-0.92	-4.04	O42363	apoa1a
1072	XP_020489366.1	fetuin-B-like [<i>Labrus bergylta</i>]	-0.47	-1.07	E7FE90	fetub

^a Spot no. – number of the spot in the 2D gel (Figure 2.3), attributed by the SameSpots software.

^b Accession number – NCBI accession number

^c Protein ID – protein identification by MALDI-TOF/TOF MS

^dFC – Log₂(fold-change) - significant changes in protein abundance (treated/control). Bold lettering indicates significant fold-changes (> 1.0 and < -1.0).

2.5. DISCUSSION

In this study, the stress response of farmed gilthead seabream adults to chronic stress conditions was primarily assessed by observing both changes in the concentration of routine plasma stress indicators, namely cortisol, glucose and lactate, and post-mortem biochemical parameters, explicitly pH and *rigor mortis*. To evaluate the existence of possible unbiased and reliable markers of chronic stress, proteomics was used to verify the potential of fish protein-based adaptations.

Cortisol is the most commonly used physiological indicator of the primary response to stress (T. Ellis et al., 2012). However, it has been shown that this corticosteroid is not a reliable biomarker of long-term stress exposure (T. Ellis et al., 2002; Martinez-Porchas et al., 2009; Naderi et al., 2017; Zahedi et al., 2019). In this study, gilthead seabream that endured high stocking densities over 54 days showed a possible reconfiguration of the cortisol response. This is supported by the observed downward trend of this metabolite, as compared to unstressed fish. This is suggestive of either a non-activated or an altered responsiveness of the HPI axis, which sometimes leads to the hyporeactivity of the corticosteroid response (Rotllant et al., 2000). The same outcome was observed in juvenile gilthead seabream confined for 14 days at 26 kg m⁻³ (Barton et al., 2005) and in meagre, cultured at different stocking densities for 40 days (Millán-Cubillo et al., 2016). In the NET trial, however, apart from the wide dispersion of observations, plasma cortisol levels were significantly higher in handled fish. This result suggests that the fish were not able to appropriately adapt to the handling stressor. Its persistence, unpredictability, and severity could have prevented the possibility of habituation. Regarding the HYP trial, no effect of the 48 h of hypoxia was reflected in these fish. This suggests an acclimation to the low oxygen environment by a possible adjustment of the oxygen requirement (e.g., reduction of high energy behaviors).

Overall, the aforementioned observations suggest that the cortisol response and the capacity of adaptation are modulated by the nature, duration and intensity of the stressor. However, other factors like species, age, sex, and individual coping mechanisms seem to be ubiquitous and impact their adaptive processes (Fast et al., 2008; Houslay et al., 2019; Rotllant et al., 2000). This process of stress habituation was already suggested and demonstrated in other studies (Tort et al., 2001; Zahedi et al., 2019), but this mechanism is not yet well-understood. High individual variability was also observed in each trial, most likely due to individual differences in the stress

response related to intrinsic factors of the animal (e.g., coping styles, cognitive perception) (Barton, 2002; Barton et al., 2005; Castanheira et al., 2017). Additionally, values registered for control fish, in every trial, are higher than the reference values reported in the literature for this species (Yildiz, 2009). These discrepancies may have several causes, which is why cortisol should be used with caution when evaluating the magnitude of the stress response. Moreover, the difficulty of measuring resting cortisol levels is also acknowledged to be one of the causes of these discrepancies. The lack of proper planning when sampling cortisol, or the manipulation needed to net and anaesthetize the fish, can result in high “control” cortisol levels that do not correspond to the “genuine” basal levels i.e., the non-manipulated fish levels. Also, it is well-established that following the perception of an acute stressor, the levels of circulating stress markers increase within the first minutes or hours of stress response, returning to basal levels as time elapses, usually within 24 h (Fanouraki et al., 2011; Naderi et al., 2018; Vijayan et al., 2010).

Secondary physiological responses are characterized by an increase in glucose and lactate levels in blood plasma to satisfy the increased energy expenditure. Changes in glucose usually follow similar trends as cortisol after the stressor (Wendelaar Bonga, 1997). This is corroborated in this study by the levels of plasma glucose registered in all trials (Figure 2.1). Glucose levels, besides following the same trend as cortisol levels, are, in general, below the basal values for this species (Yildiz, 2009). This could be related to the fish’s inability to maintain the same levels of glucose in the blood due to the high demand for glucose mobilization to other tissues. The decrease of plasma glucose levels in OC agrees with the decrease in the cortisol levels, supporting the hypothesis of habituation or exhaustion of the endocrine system (Martinez-Porchas et al., 2009). The significant increases in the plasma glucose levels of stressed fish from NET and HYP trials are consistent with previous studies. These showed that glucose rises during air exposure or low oxygen levels, due to stimulation of muscle glycogenolysis and hepatic gluconeogenesis, where glucose is synthesized to maintain the energetic substrates’ demand (Omlin & Weber, 2010). Similar to cortisol, glucose and lactate circulating levels also return to basal levels within hours post-stressor, which further makes these metabolites unreliable markers in case of prolonged stressors (Gesto et al., 2013; López-Patiño et al., 2014). Additionally, studies also demonstrate that glucose variations in the blood are not only hormonal-induced due to stressful practices. Factors like variations in the water temperature and

pH, anesthesia, diet composition or fasting can also affect plasma glucose levels (Gesto et al., 2008; Polakof et al., 2012).

When insufficient oxygen is available to maintain the aerobic ATP production, fish resort to anaerobic metabolism to meet cellular requirements. This shift consequently leads to lactate accumulation in the muscle (Weber et al., 2016; C. M. Wood et al., 1983). In this study, changes in the circulating lactate levels do not follow the same trends of cortisol and glucose variations. Statistically significant differences in the lactate levels were only observed in the OC trial. In this case, if the cortisol response is indeed lower due to HPI axis acclimation, as suggested before, the lactate recycling rate in the hepatic glycogenolysis is reduced, explaining the significant plasma lactate increase in stressed fish. Additionally, previous studies show that during hypoxia or intense swimming activity, fish produce lactate in the muscle at a higher rate than it can be processed by other tissues (Weber et al., 2016).

Post-mortem muscle pH and *rigor mortis* have been used as tissue indicators of *ante-mortem* stress in numerous fish species (Acerete et al., 2009; Bahuaud et al., 2010; Poli et al., 2005). After the fish death, both blood circulation and oxygen supply cease. The major source of ATP to the muscle is thus lost since glycogen can no longer be oxidized. However, for a limited time after death, ATP in the muscle is maintained at a definite level by creatine kinase. Consequently, the depletion of ATP reserves stimulates the breakdown of glycogen by anaerobic glycolysis in the muscle, in order to maintain the energy expenditure. This process results in the accumulation of lactic acid, generating H⁺ ions and consequently lowering muscle pH (Bagni et al., 2007). Glycolysis continues until all glycogen is consumed or the glycolytic enzymatic system is made inactive by the low pH. Hence, the magnitude and rate of this pH fall depend on the fish's energy reserves prior to death. These energy reserves can be influenced by the intensity and duration of the stress while fish is alive. To our knowledge, no studies were performed with gilthead seabream regarding the effects of long-term chronic stressors on the evolution of *post-mortem* biochemical processes in the muscle. Results from this study (Figure 2.2) followed the same pH trends as previous studies on gilthead seabream (Matos et al., 2013; T. S. Silva et al., 2012), however, comparing this with the existent studies on pre-slaughter stress (Bahuaud et al., 2010; Matos et al., 2010; Wilkinson et al., 2008), muscle pH values immediately after death are lower than the ones found in this study, suggesting that stress at slaughter was low in our fish. (Poli et al., 2005) state that in cases of exposure to a chronic stressor for a

long time before death, the lactic acid produced can be gradually cleared from the muscle, but simultaneously the energy sources, like glycogen, will likewise gradually become exhausted. Hence, when the fish is killed, muscle pH does not suffer a dramatic fall due to an early end of *post-mortem* anaerobic glycolysis caused by energy source scarcity. This might explain the significant differences found in the HYP trial, where the highest pH values were observed in the highly stressed fish (HYP15), suggesting that these fish had lower energy reserves. Nevertheless, pH values registered after the 24 HAD, in every treatment, agree with the reported by previous studies in this species at the same sampling times (Ayala et al., 2010; Matos et al., 2013).

Rigor mortis is inextricably correlated with muscle ATP and the pH decline. The onset of *rigor mortis* occurs with ATP depletion. When ATP reaches low levels, actin, and myosin in the muscle bind together, forming the actomyosin complex and causing stiffness of the fish body (Delbarre-Ladrat et al., 2006). A strong relationship between low muscle pH immediately after death, and a rapid onset of the rigor state was demonstrated in a range of fish species (Bagni et al., 2007; Wilkinson et al., 2008). In this study, the evolution of *rigor mortis* (Figure 2.2) was similar between treatments and significant differences were only found in the NET and HYP trials at 8, and at 8 and 24 HAD, respectively. A delayed onset was observed, starting between 2 and 6 HAD in every trial and reaching the maximum *rigor* index between 24 and 48 HAD. This delay is in agreement with the high muscle pH registered immediately after death, supporting the hypothesis of low energetic reserves in our fish at the time of death. Measuring glycogen and ATP content in the fish muscle and liver would be a complementary assessment to infer about the energetic reserves and corroborate our hypothesis.

Plasma proteins were evaluated in this study since blood plasma is a very informative biological fluid, acting as a mirror of the physiological condition of the organism. Stress and stress-related hormones are recognized as modulators of the fish immune system (Eslamloo et al., 2014), however, responses depend on the intensity and duration of the stressor. The innate immune system is a fundamental defense mechanism in fish (Bayne & Gerwick, 2001). The acute phase response is part of this system, and it is mainly regulated by cytokines and glucocorticoids (Cray et al., 2009). This response is characterized by the release of acute-phase proteins (APP), by the hepatocytes, into circulation (Charlie-Silva et al., 2019). APP can be

classified as “positive” or “negative” depending on whether their plasma concentration increases or decreases during activation of this response (Gabay & Kushner, 1999). The response profile of our fish demonstrated the same tendency of protein changes.

In this study, the pattern of protein changes observed in the plasma indicates that the fish immune system was affected mainly by net handling and hypoxia challenges. Nevertheless, net handling was shown to be the most impacting. The levels of 20 different plasma proteins (distributed by 56 significantly differential spots), all related with immunological processes, were shown to be modulated by repetitive net handling, compared to two proteins modulated by hypoxia. As mentioned previously, the same proteins were often detected from different spots on the 2D gels. Such a phenomenon may be due to existent isoforms or caused by adaptive changes of the proteome to maintain cellular homeostasis. This adaptation may involve changes at the level of protein degradation, localization, function, and activity – all of which can be modulated by posttranslational modifications (PTMs) (Karve & Cheema, 2011). PTMs can regulate fundamental biochemical processes and be more energetically efficient than altering protein abundance, constituting potential interesting signatures of stress. Studies on PTMs in fish are still scarce.

The changes detected in protein abundance (listed in additional file 2 - [online](#)), along with the PPI network and GO enrichment analyses (Figure 2.5) performed, confirmed the involvement of several components of the innate immune system in the physiological adaptation to these stressors. Proteins considered to be “positive” APP were likewise shown to be increased in abundance in the plasma of fish stressed by net handling (fibrinogen alpha-chain, complement component C3, haptoglobin, complement factor B, warm-temperature acclimation 65 kDa protein, alpha-1-antitrypsin), while proteins considered as “negative” were decreased (transferrin, interalpha-trypsin inhibitor, apolipoprotein A-I) (Roy et al., 2016). A diverse number of proteins involved in the APR was also found previously to be modulated in chronically stressed gilthead seabream (Pérez-Sánchez et al., 2017).

Apolipoprotein A-I (Apo-AI) was modulated only by net handling stress. Seventeen proteoforms were identified in the plasma proteome map, being mostly decreased in abundance when comparing with the unstressed fish. Apo-AI is the main protein constituent of the high-density lipoprotein (HDL), playing a role in lipid metabolism and participating in the reverse transport of cholesterol from tissues to the liver (Concha et al., 2003; Piñeiro et al., 2007). Apo-AI was also found to be decreased

in abundance in crowded Atlantic salmon (Veiseth-Kent et al., 2010). In cod (*Gadus morhua*) it acted as a negative regulator of the complement system (Magnadóttir & Lange, 2004). Other two apolipoproteins were also found to be downregulated in the plasma of fish from NET2 and NET4 groups (Apolipoprotein Eb and apolipoprotein B-100).

The complement system is an essential part of the innate immune system which can be activated through three pathways: the classical, alternative and lectin pathways (Boshra et al., 2006). Fish display a plethora of complement components, mainly complement component C3 (C3), which may present around five proteoforms in a single species (Sunyer et al., 1997). C3 is one of the most abundant proteins in the plasma and plays a central role in the innate immune system, supporting the activation of all three pathways (Boshra et al., 2006). In this study, C3, identified in 5 proteoforms, and complement factor B (Bf), identified in 4, were found to be increased in abundance by net handling. Contrarily, C3 was downregulated in fish exposed to low oxygen levels. Bf also plays a role in complement activation by acting as the catalytic subunit of C3 convertase, an enzyme responsible for the proteolytic cleavage of C3, in the classical and alternative pathways (Boshra et al., 2006).

Several metal-binding proteins, existent in the plasma of vertebrates, can chelate iron, zinc, and copper, which are essential elements for the virulence of bacteria (Porcheron et al., 2013). Alpha-2-macroglobulin (A2M) is a multifunctional protein (Funkenstein et al., 2005) found to be downregulated in the plasma of fish submitted to handling stress. It is mostly known to act as a broad range serine proteinase inhibitor and to bind metal ions (Porcheron et al., 2013). Contrarily, haptoglobin, which is also responsible for the sequestration of iron by binding to hemoglobin, was found to be increased in the plasma of handled fish. Similarly, warm-temperature acclimation-related 65 kDa protein (Wap65), which is involved in the scavenging of free heme (Dietrich et al., 2018), was increased in abundance by net handling and hypoxia stressors. Wap65 in fish is the homologue of mammalian hemopexin (Kinoshita et al., 2001) and in most teleosts presents two proteoforms (Diaz-Rosales et al., 2014). In this study, two spots were also matched to this protein suggesting the presence of these two proteoforms. Transferrin (Tf) decreased in abundance in the plasma of fish stressed by net handling. Tf is a plasma protein also capable of binding iron and an important constituent of the iron homeostasis (Sanahuja & Ibarz, 2015).

In fish, antiproteases are important participants of the non-specific humoral immune defense mechanism (Roy et al., 2016). A2M is an important factor in this mechanism. Alpha-1-antitrypsin is a serine protease inhibitor, upregulated in net-handled fish, which is responsible for negatively regulating blood clotting molecules to prevent thrombosis (Rebl & Goldammer, 2018). Inter-alpha-trypsin inhibitor H3 is also a serine protease inhibitor, which was found to be downregulated in the plasma of fish from NET groups. The same pattern of protein changes was verified for fetuin-B, a cysteine proteinase inhibitor recently described in teleosts (C. Li et al., 2017). Finally, fibrinogen alpha-chain, a beta-globulin involved in blood clotting, an integral part of innate immunity (Rebl & Goldammer, 2018), was found to be upregulated in the plasma of fish belonging to NET groups.

2.6. CONCLUSIONS

In summary, the overall results suggest that physiological changes were higher in fish exposed to repeated handling, while mild and permanent stressors might have allowed the fish to refine their physiological processes and adapt to certain challenges. The variability in the response levels of cortisol, glucose, and lactate, in fish from the same groups, alongside the possible adaptation suggested by the results, demonstrate that these indicators may not be the most robust in case of chronic stress monitoring. On the other hand, plasma proteomics allowed the detection of a cohesive network of protein changes associated with essential immunological pathways in stressed fish. These proteins will be useful in understanding the biological processes behind protein-based stress adaptation in fish and may, therefore, represent the first screening for potential biomarker candidates of chronic stress in gilthead seabream. This work is the first step for a more scientific and reliable assessment of fish welfare. A multidisciplinary approach, and the study of the stress response from the molecular to the behavioral level might just be the holistic approach needed to achieve such a goal.

2.7. SUPPLEMENTARY MATERIAL

Supplementary tables are available for this paper at <https://bmcbgenomics.biomedcentral.com/articles/10.1186/s12864-020-6728-4#Sec22>

Multionics characterization of the gilthead seabream hepatic stress response



Nothing in life is to be feared, it is only to be understood. Now is the time to understand more, so that we may fear less.

— Marie Curie

3.1

Mid-infrared spectroscopic screening of metabolic alterations in stress-exposed gilthead seabream (*Sparus aurata*)



...the number of fish killed (and reported) each year by humans is between 1 and 2.7 trillion. To get a handle on the magnitude of a trillion fishes, if the average length of each caught fish is that of a dollar bill, and we lined them up end to end, they would stretch to the sun and back...

— Jonathan Balcombe in “What a Fish Knows”

**SCIENTIFIC
REPORTS**
nature research

This chapter has been published as research article in:

de Magalhães, C.R., Carrilho, R., Schrama, D., Cerqueira, M., Rosa da Costa, A.M., Rodrigues, P.M., 2020. Mid-infrared spectroscopic screening of metabolic alterations in stress-exposed gilthead seabream (*Sparus aurata*). Scientific Reports 10, 16343. **doi: 10.1038/s41598-020-73338-z**

3.1.1. ABSTRACT

Stress triggers a battery of physiological responses in fish, including the activation of metabolic pathways involved in energy production, which helps the animal to cope with adverse situations. Prolonged exposure to stressful farming conditions may induce adverse effects at the whole-animal level, impairing welfare. Fourier transform infrared (FTIR) spectroscopy is a rapid biochemical fingerprinting technique, that, combined with chemometrics, was applied to disclose the metabolic alterations in the fish liver as a result of exposure to standard stressful practices in aquaculture. Gilthead seabream (*Sparus aurata*) adults exposed to different stressors were used as model species. Spectra were preprocessed before multivariate statistical analysis. PCA was used for pattern recognition and identification of the most discriminatory wavenumbers. Key spectral features were selected and used for classification using the k-nearest neighbor (KNN) algorithm to evaluate whether the spectral changes allowed for reliable discrimination between experimental groups. PCA loadings suggested that major variations in the hepatic infrared spectra responsible for the discrimination between the experimental groups were due to differences in the intensity of absorption bands associated with proteins, lipids, and carbohydrates. This broad range technique can thus be useful in an exploratory approach before any targeted analysis.

3.1.2. INTRODUCTION

Intensive and controlled fish production is necessary to meet the ever-increasing demand for quality protein (FAO, 2020). However, intensification of production, mainly by the aquaculture industry, inevitably leads to environmental and welfare issues. Management practices often induce some level of disturbance, which can elicit a stress response in fish and may result in more severe long-term complications at the growth, reproduction, health, and behavior levels (Wendelaar Bonga, 1997). Therefore, proper monitoring of stress in fish is crucial to reduce the adverse effects of production routines. Also, a more in-depth knowledge of the physiology of fish stress becomes fundamental.

Stress in fish has been extensively studied (Schreck et al., 2016), but only recently, more modern, and sensitive techniques started to be applied in this endeavor. High-throughput technologies have been gaining popularity to unveil the main changes occurring in farmed fish metabolism caused by stressful rearing conditions (Raposo de Magalhães, Schrama, et al., 2020). Among them is metabolomics, which allows for the non-selective chemical analysis of metabolites in a given biological system (Alfaro & Young, 2018). Metabolomics in fish research has been focused mainly on the environmental impacts on fish health (C. Guo et al., 2014; Southam et al., 2008) and welfare (Karakach et al., 2009; Mushtaq et al., 2014). Metabolic fingerprinting is one common approach in metabolomics, often of comparative nature, that can provide qualitative information on the metabolic alterations caused by biotic or abiotic factors (D. I. Ellis et al., 2007). Among different techniques, FTIR spectroscopy, a form of vibrational spectroscopy, is one common analytical platform used in metabolic fingerprinting. It has been successfully applied to differentiate functional biochemical groups in the liver of fish exposed to different rearing conditions (Ceylan et al., 2014; T. S. Silva et al., 2014), to determine the changes caused by spoilage in gilthead seabream (Fengou et al., 2019) and salmon (Saraiva et al., 2017), and to identify alterations provoked by toxic chemicals, in rainbow trout (Çakmak et al., 2003; Coccia et al., 2019), Mozambique tilapia (Velmurugan et al., 2018) and catfish (Matouke, 2019). Furthermore, FTIR spectroscopy was also applied to assess cod liver oil quality (Guillén et al., 2008) and characterize hake lipids and lipid changes during frozen storage (Sánchez-Alonso et al., 2012). Although the use of FTIR spectroscopy in fish research is still in its infancy, these studies with such diverse contexts underline the applicability of this technique to study different fish tissues.

Vibrational spectroscopy is based on the ability of certain compounds, presenting covalent bonds, to selectively absorb unique frequencies of electromagnetic radiation, exciting the molecule to a higher vibrational state. Each chemical bond can vibrate in numerous ways, and each vibration is called a vibrational mode (e.g., stretching or bending). This absorption of energy by the vibrating chemical bond results in an infrared spectrum. The most used techniques based on vibrational energy are Raman and infrared spectroscopies (Keisham et al., 2014).

FTIR spectroscopy is a fast and relatively simple technique, with a low-cost value regarding consumables (H. Zhao et al., 2004) and requiring a small amount of sample (Talari et al., 2017). First, an interferogram is collected from a sample signal using an interferometer. Then a Fourier transform (a mathematical algorithm) is applied to the raw data (interferogram) to obtain the actual infrared spectrum, in the mid-infrared region (D. I. Ellis et al., 2007). Hence, this technique allows to analyze changes in band positions, widths, and intensities to obtain information on the metabolic changes with alterations in main compounds, such as lipids, proteins, and carbohydrates (B. C. Smith, 2011).

No reference has been found in the literature regarding the use of FTIR spectroscopy to investigate the metabolic alterations in farmed fish induced by everyday aquaculture production stressors. However, previous studies on the effects of stressful conditions in algae (Stehfest et al., 2005), yeast (Corte et al., 2010), bacteria (Portenier et al., 2005), and fish toxicology (Velmurugan et al., 2018) demonstrate the potential of its application in this field. One great advantage of this spectroscopic technique is its ability to provide a broad outlook on fish metabolism without any preconceptions. Additionally, its holistic nature can offer a global overview of the classes of biochemical compounds responding directly to external stimuli, which can be extremely useful before any targeted and more accurate analysis.

In the present work, gilthead seabream (*Sparus aurata*) adults, a widely cultured species in European aquaculture, were submitted to three different stressful rearing conditions, namely overcrowding, net handling and hypoxia. These stressors were demonstrated before to induce significant changes in the levels of specific metabolites, known to be associated with the physiological stress response in fish, and stress-related proteins, in the blood plasma of farmed gilthead seabream (*Sparus aurata*) (Raposo de Magalhães, Schrama, et al., 2020). In this work, potential metabolic changes were investigated in the liver of the challenged fish, since this organ plays a

key role in the metabolic responses triggered by the stress response, mainly in the supply of energy for the animal to cope with adverse situations (Wendelaar Bonga, 1997). FTIR spectra were obtained from liver tissue samples and different chemometric techniques were employed for the efficient processing of the high-dimensional datasets generated. This untargeted approach aimed to explore the potential of this technique to screen for spectral changes in the fish liver's metabolic profile and provide a broad overview of the alterations caused by specific farming conditions.

3.1.3. MATERIALS & METHODS

3.1.3.1. Experimental design and sampling

The experiments were conducted at the Ramalhete Experimental Research Station of CCMAR, in Faro, Portugal. For each trial, nine homogeneous groups of gilthead seabream (*Sparus aurata*) adults (supplied by a commercial fish farm — Maresa, Mariscos de Estero S.A., Huelva, Spain) were randomly stocked in indoor 500 L conical fiberglass tanks supplied with flow-through seawater. Each trial was conducted in a different period. Throughout the trials, the physicochemical parameters varied within a natural regime (natural photoperiod, temperature at 13.4 ± 2.2 °C, salinity at 34.7 ± 0.8 ‰ and dissolved oxygen level above 5 mg L^{-1}). Fish were fed by hand once daily, in the morning, according to the fish initial body weight and the water temperature, with commercially available 6 mm feed (AquaSoja, Sorgal, S.A., Ovar, Portugal).

Following a 2-week acclimation period, three stress trials were established: OC — Overcrowding, NET — Net handling, and HYP — Hypoxia. Each tank, with an initial rearing density of 10 kg m^{-3} (except for the high stocking groups), was randomly allocated to one of the three treatments, in triplicate. The OC trial lasted for 54 days, and the fish, with an IBW of 372.33 ± 6.55 g, were subjected to high stocking densities over the entire experimental period, by increasing the number of fish in the tanks. Two intensities were tested, having as experimental groups: OCCTRL — 10 kg m^{-3} , OC30 — 30 kg m^{-3} and OC45 — 45 kg m^{-3} . For the NET trial, fish, with IBW of 375.69 ± 11.88 g, were challenged for 45 days. Specific nets were designed, fitted inside the tanks, and lifted to air-expose the fish for 1 min. The experimental groups were established according to the number of times that the fish were lifted: NETCTRL — undisturbed fish (the net was likewise fitted inside the tanks but not lifted), NET2 — fish air-exposed

twice a week, and NET4 — fish air-exposed four-times a week. In the HYP trial, fish, with an IBW of 397.99 ± 16.56 g, experienced low levels of saturated oxygen over 48 h. Nitrogen was injected in the water according to the experimental groups' requirements: HYPCTRL— 100% saturated oxygen, HYP30 — 30% saturated oxygen, and HYP15 — 15% saturated oxygen. Data regarding zootechnical parameters were previously published by the authors (Raposo de Magalhães, Schrama, et al., 2020).

At the end of each experimental period, three fish per tank ($n = 9$ per treatment) were lethally anaesthetized using MS-222 (Merck KGaA). The livers of the sampled fish were collected for FTIR analysis and immediately frozen at $- 80$ °C. Before harvesting, fish were starved for 48 h to clean the digestive tract.

This study was approved by the ORBEA Animal Welfare Committee of CCMAR and the Portuguese National Authority for the Animal Health (DGAV) on August 26th, 2019. The experiment described was conducted in accordance with the European guidelines on the protection of animals used for scientific purposes (Directive 2010/63/EU) and the Portuguese legislation for the use of laboratory animals, under a “Group-1” license (permit number 0420/000/000-n.99–09/11/2009) from the Veterinary Medicine Directorate, the competent Portuguese authority for the protection of animals, Ministry of Agriculture, Rural Development and Fisheries, Portugal and following category C FELASA recommendations.

3.1.3.2. Sample preparation and FTIR spectroscopy analysis

Prior to FTIR analysis, liver samples were lyophilized for 48 h in a FreeZone 6 L Freeze Dry System (LabConco, Kansas City, MO, USA), to prevent peaks derived from O–H molecular vibrations of water molecules. Lyophilized samples were ground in an agate mortar and pestle and blended with potassium bromide (Sigma Aldrich) until homogeneous, in a 1:3 ratio. The mixture was then placed in an evacuated die (13 mm diameter) and pressed (6×10^6 Pa) for 2 min to obtain approximately a 1 mm-thick translucent pellet, which was then used for analysis by solid-phase transmissive FTIR spectroscopy.

Two individual FTIR spectra were acquired per biological sample (at distinct points of the pellet), in the transmission mode, using a FTIR Spectrophotometer (TENSOR 27 series, Bruker Optik GmbH, Ettlingen, Germany) controlled by the OPUS software (v5.5, Bruker Optik GmbH). To enhance the signal-to-noise ratio (SNR), interferograms were averaged for 32 scans at 4 cm^{-1} resolution, over the middle-

infrared wavenumber range of 4000–600 cm^{-1} , to obtain a single spectrum. Atypical observations (extreme outliers potentially due to technical errors during sample preparation and/or spectral acquisition) were immediately inspected and repeated if needed. Transmittance spectra generated were exported for further analysis.

3.1.3.3. Spectral preprocessing

The .dpt files from OPUS were imported into R v3.5.3 for MacOSX where all data preprocessing, univariate and multivariate statistical analyses were performed. Each spectrum was corrected with a straight line fitted between 2410 and 2270 cm^{-1} to compensate for the atmospheric CO_2 peaks, converted from transmittance to absorbance ($A = \log_{10} 1/T$) and truncated to the spectral region of interest between 3600 and 950 cm^{-1} . De trending was applied for baseline correction and standard normal variate (SNV) transformation, followed by smoothing over 25 points with the Savitzky–Golay filter (Figure S3.1.1 - [APPENDIX](#)). All preprocessing techniques were applied using the *prospectr* package (Stevens & Ramirez-Lopez, 2013). Outlier spectra detection was carried out by a robust PCA through the projection pursuit approach and using the GRID algorithm (Filzmoser et al., 2008). One bad leverage point and one orthogonal outlier were removed from the corresponding datasets (Figure S3.1.2 - [APPENDIX](#)). The functions *PCAgrid* and *pcaDiagplot* used for this analysis belonged to the *pcaPP* and *chemometrics* packages (Filzmoser et al., 2018; Filzmoser & Varmuza, 2017), respectively. Data points considered outliers were removed from further analyses. FTIR spectra from technical replicates were averaged by arithmetic mean. Determination of FTIR band positions (wavenumber (cm^{-1})) was performed, per averaged spectrum, according to the center of weight, using the peak-picking function of the Essential FTIR software (free trial version, Operant LLC, Madison, WI, USA). Tentative assignments of spectral features to classes of biochemical compounds are described in Table 3.1.1.

3.1.3.4. Multivariate statistical analyses

For statistical analyses, FTIR wavenumbers and absorbance values were treated as independent and dependent variables, respectively. Each trial was analyzed separately. To assess metabolic patterns between assigned bands, the Pearson's correlation coefficient and its significance were calculated for the FTIR band matrix using the *rcorr* function, from package *Hmisc* (Harrell, 2019). The correlation matrix

was illustrated through a correlogram using the function `corrplot` from package `corrplot` (T. Wei & Simko, 2017). Detection of structural relationships between variables and pattern recognition was carried out through an exploratory PCA, using the standard `prcomp` R function in the auto-scaled matrices. The ordination diagram was generated for each trial with the assigned object scores relative to each principal component (PC1 and PC2). The loadings corresponding to the most discriminative PCs were plotted to visualize and identify the most informative spectral features. Finally, a supervised classification analysis was performed to investigate whether the spectral changes allowed for the reliable discrimination between experimental groups. Feature selection was adopted to retain relevant information and deduct irrelevant information. This was achieved by support vector machine based on recursive feature elimination (SVM-RFE) and the top-ranked spectral features used as inputs for the KNN classifier. Data splitting into training (70%) and testing (30%) sets was ten-fold cross validated to ensure that every observation was incorporated into the testing set. Each training set was normalized by centering and scaling, and the parameters used to normalize the test set. Every training dataset was then used to train a model, and re-sampling was achieved by leave-one-out cross-validation (LOOCV). External validation was finally performed on a testing dataset, with control as the positive class. The optimal number of neighbors (k) was also determined by inner LOOCV on the training sets, using accuracy as the parameter for selection, from 1 to 5, with a step of 2. Feature selection was performed using the package `sigFeature` (P. Das et al., 2020), and the classification analysis using the functions `trainControl` and `train` from the `caret` package (Kuhn, 2020). Categorization was predicted by the function `predict` from the same package.

3.1.4. RESULTS AND DISCUSSION

In this study, gilthead seabream adults were submitted to three different rearing conditions in separate trials. The chosen challenges are commonly encountered in aquaculture production routines: overcrowding (OC), net handling (NET) and hypoxia (HYP). The livers of stressor-exposed fish were compared to those of control fish using FTIR spectroscopy (D. I. Ellis & Goodacre, 2006), which allows to perform a rapid screening of the biological system under investigation and thus to detect unforeseen metabolic alterations. Hence, this analysis generates a 'holistic' overview of the potential changes in major functional groups retrieved from the challenged fish, making

FTIR spectroscopy a suitable technique to be used prior to any targeted analysis (B. C. Smith, 2011). To the best of our knowledge, this is a pioneering work using FTIR spectroscopy to screen for the effects of stressors associated with standard aquaculture practices in the metabolic profile of farmed fish.

3.1.4.1. FTIR spectra of gilthead seabream liver submitted to stressful conditions

Overall, the FTIR spectra of the fish liver from the three trials showed the typical complex metabolic patterns with several overlapping bands observed mainly at two frequency regions: 3600–2800 cm^{-1} and 1800–950 cm^{-1} . Only the spectral region between 3600 and 950 cm^{-1} was used for further analysis as both the head and end of the spectra showed excessive noise (Figure S3.1.1 - [APPENDIX](#)). For each experimental treatment, 18 spectra were recorded. The acquisition of spectra in transmission mode can be affected by several factors such as sample uniformity and homogeneity, and thickness of the KBr pellet (Diem, 1994). Therefore, spectra were pre-processed before multivariate statistical analyses. Variations were thus minimized by detrending, which also removed the effects of baseline shifts, and the noise reduced with Savitzky–Golay filtering. Raw and treated spectra are shown in Figure S3.1.1 - [APPENDIX](#). The total spectrum was characterized by 15 bands (Figure 3.1.1.A-C) which were assigned to specific vibrational modes, functional groups and biochemical compounds based on the correlation analysis performed and similar biological systems described in the literature (Cakmak et al., 2006; Ceylan et al., 2014; Palaniappan et al., 2010; Rodriguez-Casado et al., 2007; Sánchez-Alonso et al., 2012; T. S. Silva et al., 2014) (Table 3.1.1). Different chemometric techniques were employed to discriminate the different spectral regions and experimental treatments.

Table 3.1.1. Tentative assignment of spectral bands to molecular vibrations of functional groups and biochemical compounds, based on similar biological systems described in the literature (Cakmak et al., 2006; Ceylan et al., 2014; Palaniappan et al., 2010; Rodriguez-Casado et al., 2007; Sánchez-Alonso et al., 2012; T. S. Silva et al., 2014)

Band	Wavenumber (cm ⁻¹)	Vibrational modes and functional groups	Main biochemical compounds	Other biochemical compounds
1	3315-3290	N-H stretching of amides (Amide A) O-H stretching of polysaccharides	Proteins	Carbohydrates
2	3065	Olefinic =C-H stretching	Unsaturated fatty acids	Aromatics
3	3010	Olefinic =C-H stretching	Unsaturated fatty acids	Aromatics
4	2926	CH ₂ , CH ₃ asymmetric stretching	Saturated lipids	Proteins, carbohydrates, nucleic acids
5	2858	CH ₂ , CH ₃ symmetric stretching	Saturated lipids	Proteins, carbohydrates, nucleic acids
6	1750-1739	C=O stretching of esters and aldehydes	Triglycerides, cholesterol esters	Lipids, phospholipids
7	1655	C=O stretching of amides (Amide I) C=C stretching of unsaturated hydrocarbons	Proteins	Unsaturated fatty acids
8	1541	N-H bending and C-N stretching of amides (Amide II) C=C stretching of aromatic hydrocarbons	Proteins	Aromatics
9	1455	CH ₂ symmetric and asymmetric bending	Lipids	Proteins
10	1415-1395	COO ⁻ symmetric stretching	Amino acids and fatty acids	Other carboxylates
11	1305	Olefinic C-H bending P=O stretching in phosphates	Unsaturated fatty acids	Alcohols, aromatic amino acids organic phosphates, carboxylates
12	1240	PO ₂ asymmetric stretching	Nucleic acids	Phospholipids
13	1155	CO-O-C asymmetric stretching of esters and glycogen =C-H bending in aromatics	Phospholipids and Carbohydrates	Aromatics, cholesterol esters
14	1085	C-O stretching of glycogen PO ₂ symmetric stretching	Carbohydrates	Phospholipids
15	1045-1025	C-O stretching of glycogen	Carbohydrates	

3.1.4.2. Correlation analysis

Correlation analysis of the 15 bands assigned to specific biomolecules (Table 3.1.1) revealed four major clusters in the OC trial, with significant Pearson's correlation coefficients greater than 0.71 for all band pairs (Figure 3.1.1.D). Cluster 1 ($r > 0.95$, $p < 0.001$), counting from the top of the matrix, is comprised exclusively of carbohydrate-

like bands, whereas cluster 2 ($r > 0.71$, $p < 0.001$) of bands assigned to proteins. The third cluster ($r > 0.76$, $p < 0.001$) consisted of four bands assigned to lipids, with band n° 13 assigned to carbohydrates and phospholipids. The fourth ($r > 0.77$, $p < 0.001$) is a cluster of three bands, of which two are assigned to unsaturated fatty acids and the third to nucleic acids and phospholipids.

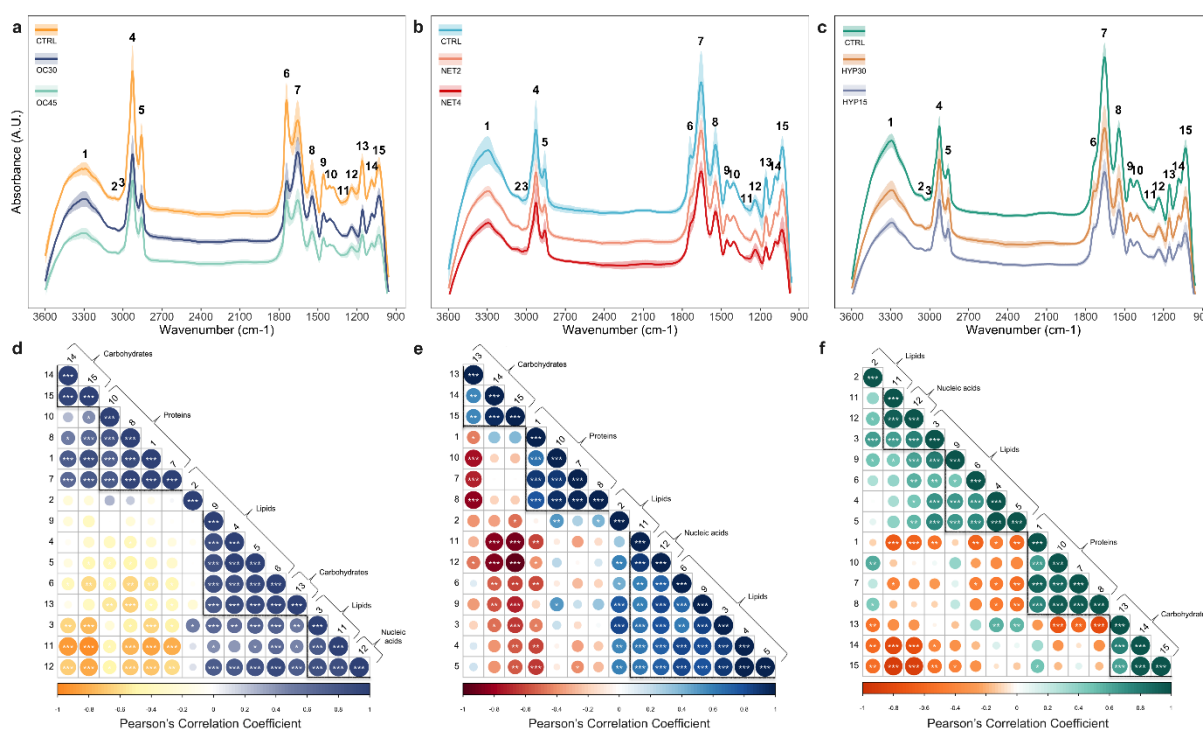


Figure 3.1.1. FTIR spectra of the liver of gilthead seabream (*Sparus aurata*) submitted to three different stressful rearing conditions (overcrowding, net handling, and hypoxia) and Pearson's correlation coefficient matrices comparing the assigned bands of the spectra. (A–C) FTIR spectra, for each treatment, are shown as absorbance values (in arbitrary units (A.U.)) of 8 averaged spectra (solid line) \pm standard deviation (shaded ribbon). For easier readability, mean spectra were offset along the absorbance axis. Numbers indicate the bands assigned to biomolecules, listed in Table 3.1.1. Plots in each row are prepared with the same vertical scale. (D–F) Plots are ordered by hierarchical clustering with complete linkage. Numbers indicate the bands assigned to biomolecules, following the same convention as Table 3.1.1. Thicker lines represent clusters. The degree of pairwise correlation concerning Pearson's correlation coefficient is displayed by the color gradient and dot size, while the colors define the signal of the correlation (positive or negative). The significance of the correlation is indicated by the label “*” inside the dots (* $0.05 < p < 0.01$, ** $0.01 < p < 0.001$, *** $p > 0.001$).

For the NET trial, the correlation analysis originated three very well-defined clusters, with significant Pearson's correlation coefficients greater than 0.58 for all band pairs (Figure 3.1.1.E). The first cluster ($r > 0.58$, $p < 0.001$) grouped three bands assigned to carbohydrates, cluster 2 ($r > 0.66$, $p < 0.001$) consisted of four bands assigned exclusively to proteins, and cluster 3 ($r > 0.58$, $p < 0.001$) was formed mainly

by bands assigned to lipids and band n° 12, which was assigned to nucleic acids and phospholipids. In the HYP trial case, the correlation analysis grouped the bands in four clusters, with significant Pearson's correlation coefficients greater than 0.47 for all band pairs (Figure 3.1.1.F). Clusters 1 ($r > 0.65$, $p < 0.001$) and 2 ($r > 0.47$, $p < 0.02$) were mainly formed by bands assigned to lipids and band n° 12, which was assigned to nucleic acids and phospholipids. Similarly to the NET trial, clusters 3 ($r > 0.66$, $p < 0.001$) and 4 ($r > 0.63$, $p < 0.001$) consisted of bands assigned to carbohydrates and proteins, respectively. Band n° 2 presented low correlations in the OC trial. Absorption band n° 13 can be attributable to either carbohydrate and/or phospholipids. However, the correlation analysis suggests that in the OC trial, it is more likely to represent changes in the phospholipids' content. Contrarily, in the NET and HYP trials, it seems to correspond to carbohydrates.

3.1.4.3. Principal component analysis

PCA is an unsupervised method, with no *a priori* knowledge of experimental structure, primarily used to reduce the dimension of the feature space, detect structural relationships between variables and find potential clusters of observations. The original correlated variables are transformed into a set of orthogonal uncorrelated variables, linear combinations of the first ones (Jolliffe, 1986). In this study, PCA was employed for exploratory analysis. A score scatter plot was generated, for each trial, with the projection of the samples onto the first two principal components (PCs), which accounted for 78%, 79.4% and 78.2% of the total variability of the data from OC, NET and HYP trials, respectively (Figure 3.1.2.A–C). The analysis of the samples' grouping in the score plots suggests that the separation between the corresponding control samples and those belonging to the OC30 (OC trial) and NET4 groups (NET trial) occurred along the PC1 axis. At the same time, PC2 appears to be responsible for the dissimilarities between the control group and the HYP15 group (HYP trial). Observations from groups OC45, NET2, and HYP30 are largely overlapped with the other experimental groups. Loading plots in Figure 3.1.2.D–F, illustrate the weight of each of the original variables (wavenumbers) on the PCs, and thus, the contribution of each spectral feature to discriminate the mentioned pairs of treatments. Positive loading values in the OC30 and NET4 plots (Figure 3.1.2.D,E) indicate a higher concentration, in challenged fish, of the biomolecules corresponding to the indicated spectral ranges. The inverse is verified for the HYP trial loading plot (Figure 3.1.2.F).

The various lobes observed in the plots with high absolute loading values suggest that the separation of the two most distinct groups, observed in the score plots, is based on different spectral regions. The PC1-loadings belonging to the OC trial (Figure 3.2.D), revealed the strongest negative loadings in the 3020–2800 cm^{-1} , 1740 cm^{-1} and 1450 cm^{-1} spectral regions, which correspond to vibrational bands highly associated to lipids (bands n° 3, 4, 5, 6 and 9), and the strongest positive loadings in the regions 1600–1500 cm^{-1} and 1030 cm^{-1} (bands n° 7, 8 and 15), which were attributed to proteins and carbohydrates' bands, respectively. The NET trial's PC1-loading plot (Figure 3.1.2.E) shows the main positive loading peaks at 3060, 1710, 1450 and 1400 cm^{-1} (bands n° 2, 9 and 10), which correspond to bands assigned to vibrational modes of proteins and lipids, and the higher negative loading peaks around 1150 and 1030 cm^{-1} (bands n° 13 and 15), corresponding to the carbohydrate characteristic region. The PC2-loadings of the HYP trial (Figure 3.1.2.F) show the most intense positive peak in the region between 3300 and 3400 cm^{-1} , and the strongest negative loadings at 3000–2800, 1740 and 1350–1150 cm^{-1} , corresponding mainly to lipid-assigned bands (bands n° 3, 4, 5, 6, 11, 12 and 13). These potential changes in these absorption bands appear to be all correlated and suggest a metabolic reprogramming in the fish system to deal with the increase of energy demand during adverse situations. The plasma levels of specific metabolites associated with the physiological response to stress were assessed in these fish in a previous study and published elsewhere (Raposo de Magalhães, Schrama, et al., 2020). Activation of the HPI-axis was previously suggested and supports the hypothesis of a potential metabolic reprogramming to deal with the stressors that fish were exposed to (Raposo de Magalhães, Schrama, et al., 2020). When fish is exposed to a challenging situation, a physiological response initiates to compensate and/or adapt to the new situation (Wendelaar Bonga, 1997). When the coping capacity is surpassed, the so-called stress response mechanism is initiated by the rapid release of catecholamines into the bloodstream, followed by the delayed response of cortisol, which further wide spreads effects on various tissues (Aluru & Vijayan, 2007, 2009).

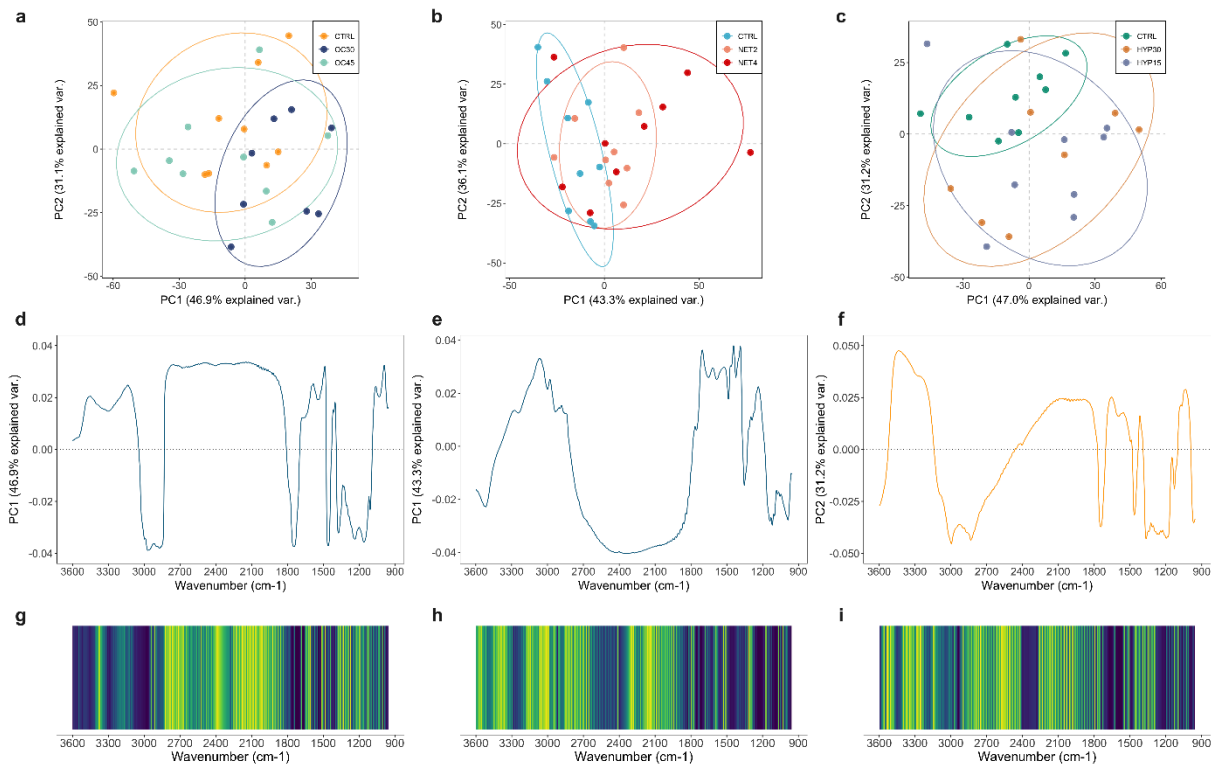


Figure 3.1.2. PCA on the FTIR spectra collected from the livers of gilthead seabream (*Sparus aurata*) submitted to three different stressful rearing conditions (overcrowding, net handling, and hypoxia). (A–C) Score scatter plots on PC1 and PC2 computed for each trial with the 3600–950 cm⁻¹ spectral range. Each point represents the projection of one spectrum, and each treatment is identified by a unique color, as indicated in the legend. Percentages indicate the proportions of explained variance. Ellipses represent an 80% probability of samples being within the shape. (D–F) PC loadings along the corresponding wavenumber for each trial. (G–I) Ranking of the spectral features according to the SVM-RFE method for feature selection, along the wavenumber range of 3600–950 cm⁻¹. Most well classified features in the ranking are shown in dark blue, while least important features are colored in yellow.

Carbohydrates are essential and rapid sources of energy for fish in stressful situations (Schreck et al., 2016). A potential hepatic carbohydrate increment in fish from OC30 group suggests the constant activation of the major gluconeogenic pathway by the chronic cortisol release. This leads to the synthesis of glucose in the liver, which, if not used or exported, can be stored in the form of glycogen (glycogenesis) (Vijayan et al., 2010). Contrarily, the suggested decrease in hepatic carbohydrate content in NET4 fish is consistent with the stressor's physically more intense nature. This reduction suggests the use of glycogen stores, by glycogenolysis, to synthesize glucose, and its immediate uptake, for energy production, or outflow (López-Patiño et al., 2014; Wendelaar Bonga, 1997). These results are consistent with previously reported plasma glucose levels for these fish (Raposo de Magalhães, Schrama, et al., 2020). Proteins and amino acids are essential non-carbohydrate substrates for the gluconeogenesis and have been described as hepatic energy fuels in fish under

different stressful conditions (Vijayan et al., 2010). Results suggest that the protein and amino acid contents increased in the liver of OC30 and NET4 fish, which can be indicative of a cortisol-mediated increased proteolytic activity and consequent mobilization of amino acids to the liver to be used as gluconeogenesis precursors. To some extent, this pattern reinforces the hypothesis of the activation of this pathway. Nonetheless, increased protein content can also be explained by a higher protein turnover and/or synthesis of proteins involved in gluconeogenesis (Mommensen et al., 1999). Finally, the OC and HYP trials PC-loadings suggested that the separation between control and OC30/HYP15 groups might be due, mainly, to potential differences in the spectral bands associated to vibrational modes of lipids. Lipid metabolism in fish is also modulated by cortisol (Vijayan et al., 2010). Glycerol, resulting from the catabolism of triacylglycerols is a suitable precursor for gluconeogenesis, while fatty acids are used as sources of energy in peripheral tissues (T. S. Silva et al., 2012). These differences suggest a cortisol-mediated activation of hepatic lipolysis and the posterior use of the lipids as substrates for gluconeogenesis and/or mobilization to other tissues (Vijayan et al., 2010). Other studies with fish exposed to high stocking densities report a reduction in hepatic lipid content and/or increased exportation of fatty acids into the bloodstream (Hernández-Pérez et al., 2019; Montero et al., 1999). Previous studies on different fish species also report a mobilization of lipids to the liver during exposure to prolonged hypoxia (Gracey et al., 2011; Mustafa et al., 2015). More targeted hypothesis-driven approaches will be interesting to confirm the effects of these farming conditions on the described metabolic pathways.

3.1.4.4. Feature selection and k-nearest neighbor classification analysis

To assess if the spectral features suggested to be responsible for the separation between the groups in the score plots generated by the unsupervised PCA were indeed discriminatory, a supervised classification analysis was performed. A full infrared spectrum contains hundreds or thousands of variables, and the neighboring wavenumbers are always collinear. Hence, selecting the most discriminatory wavenumbers and discarding the uninformative ones can improve the accuracy and robustness of multivariate analyses and classification models (Q. Dai et al., 2015). Spectral feature selection was achieved by a support vector machine based on SVM-RFE (Guyon et al., 2002). Compared with other feature selection methods, SVM-RFE

is a scalable and efficient wrapper method. Firstly, linear SVM is trained on the initial set of features while assigning weights (w) to each one, and then RFE selects feature subsets by recursively considering smaller subsets of features at each time (Duan et al., 2005). Features were incrementally selected 5–30 features with five steps, according to the importance of ranking, as input data to the classifier.

Plots displaying the importance of each spectral feature in the ranking are shown along with the wavenumber range of 3600–950 cm^{-1} in Figure 3.1.2.G–I for comparison with the loadings generated by PCA. Selection of the most informative wavenumbers is generally in accordance with PC loadings, except for the regions between 3200–3000 and $\sim 3300 \text{ cm}^{-1}$, in the spectra from NET and HYP trials. The supervised classification analysis with the KNN algorithm was carried out for each trial, using only two out of the three classes: “control” and the experimental group that presented the clearest separation in the corresponding score plots (i.e., OC30, NET4 and HYP15, in the case of OC, NET and HYP trials, respectively). The KNN algorithm is a non-parametric supervised classification method that allows categorizing unknown samples based on multivariate proximity to other samples of pre-assigned classes (majority voting) (Mucherino et al., 2009). The unknown sample’s identity is based on the class of the nearest known samples, where each class represents an experimental group. In this process, 6 models were built, for each trial, with different subsets of features. The optimal number of neighbors (k) was calculated by LOOCV, where one point in the data set is set as the test data, and the remaining points are set as the training data. The classifier’s performance is shown in Figure 3.1.3 and presented as the mean prediction accuracy \pm SD for the train and test datasets along the different subsets of selected features. The highest accuracy values were obtained for the classification analysis of the OC groups, with a subset of 10 spectral features (87% and 80% for the train and test datasets). Overall, the classification models for the NET4 and HYP15 trials had a satisfactory/poor performance in the discrimination of the experimental groups, which appears to be due, mainly, to high variability of biological responses. Increasing the number of observations per group could potentially improve the classification models’ performance and predictive ability.

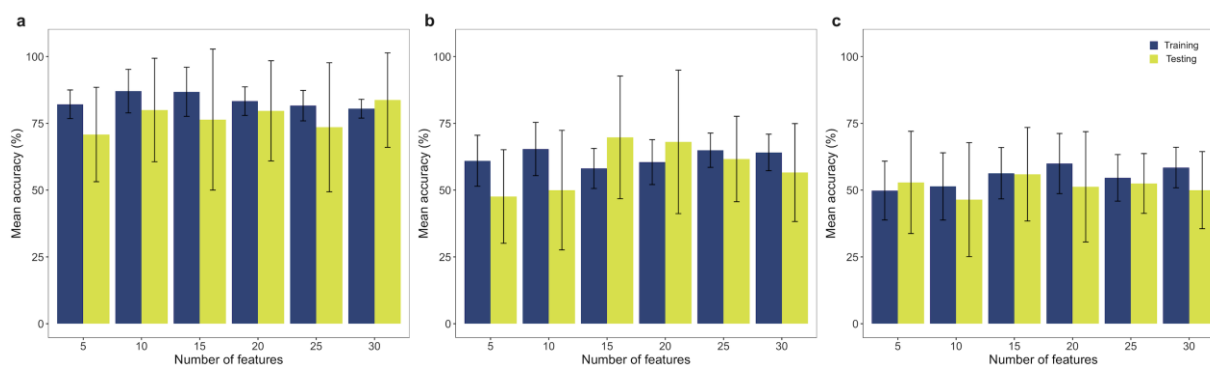


Figure 3.1.3. Classification analysis performed by the k-nearest neighbor (KNN) algorithm on the FTIR spectra collected from the livers of gilthead seabream (*Sparus aurata*) submitted to three different stressful rearing conditions ((a) OC trial, (b) NET trial, (c) HYP trial). Predictive performance of the models is presented as mean classification accuracy (%) of training and testing sets for each subset of selected features by SVM-RFE. Error bars represent the standard deviation obtained by ten-fold cross validation (CV) of the initial data splitting.

3.1.5. CONCLUSIONS

In light of the present findings, FTIR spectroscopy coupled with chemometric analysis of spectral data presents itself as an exploratory starting approach for the collective screening of alterations in the metabolism of proteins, lipids and carbohydrates simultaneously. Moreover, its holistic nature makes this technique a suitable analysis to be employed prior to any targeted approach. This study showed the main spectral differences in the liver of gilthead seabream exposed to high rearing densities (30 kg m^{-3}), net-handled four times a week and exposed to low levels of saturated oxygen (15%) when compared to the control groups. These alterations point towards a potential activation of the fish stress response and a consequent global rearrangement of the metabolism of the main biochemical compounds. Finally, a supervised classification analysis demonstrated that the ten most informative wavenumbers could discriminate between control and crowded fish with relatively reasonable classification accuracy. However, increasing the number of samples of the experimental treatments could benefit the overall predictions. This work introduces FTIR spectroscopy in fish stress research as a rapid broad-range tool to extract untargeted information regarding alterations on the hepatic infrared spectra of fish exposed to challenging farming conditions. Validation analysis will greatly contribute to link these spectral changes to the fish liver biochemistry and potential alterations in specific biochemical compounds and metabolic pathways involved in the fish physiological stress response.

3.1.6. SUPPLEMENTARY MATERIAL

Supplementary figures can be found in the [APPENDIX](#).

3.2

Metabolic plasticity of gilthead seabream under different stressors: analysis of the stress responsive hepatic proteome and gene expression



...to continue to eat large wild fish at the rate we've been eating them we would need "four or five" oceans to support the current human population.

— Paul Greenberg in “Four Fish: The Future of the Last Wild Food”



This chapter has been published as research article in:

Raposo de Magalhães, C., Schrama, D., Nakharuthai, C., Boonanuntanasarn, S., Revets, D., Planchon, S., Kuehn, A., Cerqueira, M., Carrilho, R., Farinha, A.P., Rodrigues, P.M., 2021. Metabolic plasticity of gilthead seabream under different stressors: analysis of the stress responsive hepatic proteome and gene expression. *Frontiers in Marine Science* 8, 676189. doi: [10.3389/fmars.2021.676189](https://doi.org/10.3389/fmars.2021.676189)

3.2.1. ABSTRACT

Hepatic metabolic adjustments are key adaptive mechanisms to stress in fish targeting at increasing energy availability for the animal to efficiently cope with a stressor. Teleosts exhibit a broad variety of these metabolic responses, depending on the species biology, individual experiences, and the challenge's characteristics. Nevertheless, the molecular response to a prolonged stress can be more heterogeneous and far more complex to interpret than that to an acute stress. A comparative proteomics analysis was employed to discover the set of liver proteins involved in the adaptive processes that tune the physiological response of *Sparus aurata* to different suboptimal rearing conditions and physical challenges. Three separate trials were established where fish were submitted to different conditions (overcrowding, net handling, and hypoxia). The response at the transcript level of 13 genes was also assessed. Mass spectrometric analysis revealed 71 differential abundant proteins distributed among the trials. Prolonged exposure to stress seems to have induced widespread changes in amino acid, carbohydrate, and lipid metabolisms, antioxidant response and protein folding, sorting, and degradation processes. Two genes corresponding to heat-shock proteins were found to be differently expressed in net handled fish. These results shed light on the dynamics and extent of this species' metabolic reprogramming under different challenges, supporting future studies on stress markers' discovery and fish welfare research.

3.2.2. INTRODUCTION

Gilthead seabream (*Sparus aurata*) is one of the most economically important marine species for the Mediterranean aquaculture industry. In 2018, it was the fourth major species of finfish produced in Europe (FAO, 2020), with the largest amount coming from intensive farming systems (Matos et al., 2017). Intensification of the aquaculture sector may have deleterious effects on fish welfare and consequently on the environment, ecosystems, and merchantable traits of the final product (Huntingford et al., 2006). Routine procedures, such as manipulation and confinement are unavoidable farming practices that can represent stressful situations for the fish (Conte, 2004). Moreover, cumulative effects of these challenging conditions can be reflected on behavior and physiology and jeopardize fish health and survival (Eslamloo et al., 2014). The importance of managing stress in farmed fish is already being recognized by the industry, as consumers are becoming increasingly aware of fish sentience, raising concerns regarding fish welfare and sustainability. However, the knowledge on the physiology of stress of the farmed species needs to be improved to develop accurate recommendations for best practices.

When a stimulus is perceived as a serious threat by the fish, an adaptive mechanism is triggered, known as physiological stress response. In the short-term it elicits a stimulatory and restorative response (eustress) that helps the individual to cope with the challenge and restore homeostasis, not necessarily equating impaired welfare (Iwama et al., 2006). The immediate activation of the neuroendocrine pathway is the first step following initiation of the physiological response, resulting in the release of catecholamines and cortisol into the bloodstream (Mommensen et al., 1999). It is well known that these hormones induce further changes in the metabolism, supplying energy and glucose to compensate for the coping mechanisms, while other energy-demanding processes such as growth and immune responses are concomitantly suppressed (Fabbri & Moon, 2016; Vijayan et al., 2010). Therefore, if the stressful stimulus persists and/or increases in severity, the stress response becomes maladaptive (allostatic overload), and in this case, vital biological functions can be altered or inhibited and welfare can be compromised (Boonstra, 2013; Korte et al., 2007). The coping capacity and the extent of the impact of the stress response on the fish physiology depends on the species biology, on the individual's previous subjective experiences and coping styles, on the severity of the stressor, among other factors (Galhardo et al., 2009). This heterogeneity of the stress physiology and the myriad of

mechanisms that are consequently modulated in the organism's biological system enhances the difficulty of defining a status of impaired welfare, especially after a long-term or a repetitive stressor exposure (Ashley, 2007; Carenzi & Verga, 2009). Knowledge about the network of proteins involved in the modulation of energy-mobilizing metabolic pathways, cellular processes and molecular mechanisms when affected by specific stressors, could be an important step toward the study of fish chronic stress and the future discovery of new stress indicators. Proteins are ubiquitously affected by abiotic and biotic stimuli, resulting in alterations in protein abundance and in post-translation modifications. As these changes occur over a slower timescale, comparing with endocrine responses, proteomics can thus be a promising alternative to find indicators of an adaptive long-term stress response instead of an early response (e.g., hormones), as that used in acute stress assessment (Cowan & Vera, 2008; Marco-Ramell et al., 2016). The number of studies employing a proteome-wide characterization to unveil the molecular adaptations behind the physiological response to stress in fish has been considerably increasing (Raposo de Magalhães, Cerqueira, et al., 2020). However, the effects on metabolism and hepatic proteome have been studied mainly as a response to environmental stimuli, xenobiotics, diseases, and acute stressors (Causey et al., 2018; Gandar et al., 2017; Ghisaura et al., 2019; Ibarz et al., 2010; Mahanty et al., 2016; Malécot et al., 2011; Naderi et al., 2018; Pédrón et al., 2017; Wiseman et al., 2007; X. Zhang et al., 2017).

The hallmark of the stress response is the activation and regulation of energy-mobilizing pathways and posterior reallocation of resources. Thus, we considered the importance of the liver and its multifaceted role in mediating metabolic adjustments that promote the rewiring of energetic resources toward the stress response and used it as the target tissue in this study. In this sense, we exposed gilthead seabream (*Sparus aurata*) adults to different suboptimal rearing conditions and physical challenges, specifically high rearing densities, net handling, and hypoxia. A previous metabolic fingerprinting of these same fish's liver samples demonstrated alterations in the hepatic infrared spectra of the challenged fish, compared with undisturbed fish, suggesting a challenge-specific metabolic reprogramming (de Magalhães et al., 2020). Here, a 2D-DIGE gel-based proteomics analysis was employed to disclose the set of liver proteins involved in the gilthead seabream adaptive response to these challenges. Validation was achieved by quantitative real-time polymerase chain reaction (RT-qPCR) and the assessment of the hepatic glycogen storage. In this study we provide

for the first time a comprehensive analysis of the gilthead seabream liver proteome involved in adaptive metabolic reprogramming as a response to challenging conditions common to an aquaculture rearing facility. This work provides a fingerprint of proteins that can be further investigated as robust physiological indicators of stress, which could complement the currently used stress assessment measures and contribute for the future development of suitable stress management protocols for this species.

3.2.3. MATERIALS & METHODS

3.2.3.1. Ethics

This study was approved by the ORBEA Animal Welfare Committee of CCMAR and the Portuguese National Authority for the Animal Health (DGAV) on August 26, 2019. The experiment described was conducted in accordance with the European guidelines on the protection of animals used for scientific purposes (Directive 2010/63/EU) and the Portuguese legislation for the use of laboratory animals, under a “Group- 1” license (permit number 0420/000/000-n.99–09/11/2009) from the Veterinary Medicine Directorate, the competent Portuguese authority for the protection of animals, Ministry of Agriculture, Rural Development and Fisheries, Portugal and following category C FELASA recommendations.

3.2.3.2. Animals and rearing conditions

Three separated fish trials were conducted at the Ramalhete Experimental Research Station of CCMAR, in Faro, Portugal. Nine homogeneous groups of gilthead seabream (*Sparus aurata*) adults (supplied from the commercial fish farm Maresa, Mariscos de Estero S.A., Huelva, Spain) were randomly distributed, per trial, in indoor 500 L fiberglass tanks supplied with flow-through seawater. Each trial was conducted in a different time period (from November to March). Physicochemical parameters varied within a natural regime (natural photoperiod, water temperature at 13.4 ± 2.2 °C, salinity at 34.7 ± 0.8 ‰ and dissolved oxygen level above 5 mg L^{-1}). Fish were fed by hand once daily, in the morning, with commercial feed (Standard Orange 6, AquaSoja, Sorgal, S.A., Ovar, Portugal), manufactured according to the species’ nutritional requirements. During the trials, feeding amounts were adjusted according to the fish initial body weights and the daily water temperature (varying between 1 and 1.5% of the tank biomass).

3.2.3.3. Experimental design

After a 2-week acclimation period for each trial, three challenging rearing conditions were tested, namely: OC – Overcrowding, NET – Net handling and air exposure, and HYP – Hypoxia. Each tank was set-up with an initial rearing density of 10 kg m⁻³ (except for the high-stocking groups) and randomly allocated to one of the three experimental groups, in triplicate. The OC trial lasted for 54 days, and the fish, with an average IBW of 372.33 ± 6.55 g, were submitted to high stocking densities, in two intensities, by increasing the number of fish in the tanks. Experimental groups were established as described: OCCTRL – 10 kg m⁻³, OC30 – 30 kg m⁻³ and OC45 – 45 kg m⁻³. For the NET trial, fish, with an average IBW of 375.69 ± 11.88 g, were challenged for 45 days. Nets were designed for the purpose, fitted inside the tanks, and lifted to air-expose the fish for 1 minute. The experimental groups were established according to the number of times, per week, that the fish were challenged: NETCTRL – undisturbed fish (the net was also fitted inside the tanks but not lifted), NET2 – fish air exposed twice a week, and NET4 – fish air-exposed four-times a week. The last stress event was applied 72 h before sampling. In the HYP trial, fish, with an average IBW of 397.99 ± 16.56 g, experienced low levels of saturated oxygen over 48 h. The required saturations were achieved by nitrogen injection into the water: HYPCTRL – 100% saturated oxygen, HYP30 – 30% saturated oxygen, and HYP15 – 15% saturated oxygen. During the 48 h, the levels of saturated oxygen in the water were measured every 30 min. If these were higher than the treatment's requirement, nitrogen was injected, while in contrast, if the levels were lower than the requirement, the water flow was increased.

3.2.3.4. Sampling

At the end of each trial, three fish were collected from each tank, with a net, and immediately anesthetized with a lethal dose of MS-222 (Merck KGaA). The livers of the sampled fish were collected, cut into small pieces, and divided by different 2 ml eppendorf tubes according to the different subsequent analyses. Sample tubes were immediately frozen in liquid nitrogen and stored at -80 °C until further analysis. Before harvesting, fish were starved for 48 h to clean the digestive tract. All sampled fish were weighed and measured. Data concerning zootechnical parameters, such as specific growth rate, were previously published by the authors (Raposo de Magalhães et al., 2020).

3.2.3.5. Liver proteomics analysis

3.2.3.5.1. Protein extraction

For total protein extraction, 50 mg of gilthead seabream liver tissue (n = 6, two samples from each tank, randomly selected) were mixed with 500 ml of extraction buffer (7 M urea, 2 M thiourea, 4% CHAPS detergent, 30 mM Tris pH 8.5), along with 5 ml of protease inhibitor cocktail (Merck KGaA) and 2 ml of ethylenedinitrilotetraacetic acid (EDTA) 250 mM. Sample homogenization was achieved with an Ultra-Turrax IKA T8 (IKA-WERG, Germany) for 5 cycles of 15 s, followed by ultrasound disruption. Homogenates were incubated on ice for 30 min and centrifuged at 13,000 g, 4 °C for 15 min to remove insoluble material. Liver extracts were diluted in the initial buffer and the protein content measured with Bradford assay using BioRad Quick Start Bradford Dye Reagent 1X (Bio-Rad) and BSA, BioRad Bovine Serum Albumin Standard Set (Bio-Rad), as standard. Extracts were then depleted of non-protein contaminants (using 500 mg of protein) with a ReadyPrep™ 2D Cleanup kit (Bio-Rad) and resuspended in the initial buffer. The pH of the cleaned extracts was checked with a pH-indicator paper, Sigma-P4536 (Merck KGaA) and adjusted to 8.5 using 0.1 M NaOH, if necessary.

3.2.3.5.2. Protein labeling and separation

Protein separation was achieved by the 2D-DIGE method, as follows. DIGE minimal labeling was performed as described in (Raposo de Magalhães, Schrama, et al., 2020). Passive rehydration was carried out for 18 h on 24 cm Immobiline™ Drystrips (GE Healthcare) with linear pH 4-7, on an IPG Box (GE Healthcare). A total of 150 mg of protein (50 mg from each dye) were loaded onto each strip, along with a rehydration buffer [8 M urea, 2% CHAPS detergent, 50 mM DTT, 0.001% bromophenol blue, 0.5% Bio-lyte 3/10 ampholyte (Bio-Rad)] to fulfill 450 ml. IEF was performed in 4 steps: 250 V gradient 4 h, 1000 V gradient 6 h, 8000 V gradient 3 h 40 min, 8000 V step-n-hold 3 h 20 min for a total of 50,000 Vhr using the Ettan IPGphor at 20 °C (GE Healthcare). Focused strips were reduced and alkylated with 6 ml of equilibration buffer (50 mM Tris-HCl pH 8.8, 6 M urea, 30% (v/v) glycerol and 2% SDS) with 1% (w/v) DTT or 2.5% (w/v) IAA, respectively, for 15 min each, in constant agitation. Strips were then loaded onto 12.5% Tris-HCl SDS-PAGE in-house gels and ran in an Ettan DALTSix Large Vertical System (GE Healthcare), using a standard Tris-Glycine-SDS running

buffer, at 10 mA/gel for 1 h followed by 60 mA/gel until the bromophenol blue line reaches the end of the gel.

3.2.3.5.3. Gel image analysis and protein identification

Gel images of CyDye-labeled 2D gels were acquired using a Typhoon™ laser scanner 9400 (GE Healthcare) as described in (Raposo de Magalhães, Schrama, et al., 2020). The final gel images were analyzed using SameSpots software v4.6.1.218 (TotalLab), including background subtraction (average normalized volume $\leq 100,000$ and a spot area ≤ 500), filtering, spot detection, spot matching, normalization, and statistical analysis. Spots showing volume ratios with a statistically significant difference (relative abundance variation of at least 1.0-fold, $p < 0.05$ - One-way ANOVA on normalized log₂-transformed spot volumes, followed by $p < 0.05$ – Dunnett's *post hoc* test) were manually excised from SYPRO R Ruby stained (Invitrogen™) 2D gels. Subsequently, gel plugs were subjected to in-gel tryptic digestion and identified by MALDI-TOF/TOF MS, as described in (Raposo de Magalhães, Schrama, et al., 2020). The mass spectrometry proteomics data have been deposited to the ProteomeXchange Consortium (Deutsch et al., 2020) via the PRIDE (Perez-Riverol et al., 2019) partner repository with the dataset identifier PXD024804.

3.2.3.5.4. Proteomics data analysis

Using the amino acid sequences (in one-letter code), the theoretical molecular weight (Mw) and isoelectric point (pI) of the identified proteins were computed using the ProtParam Tool (<http://us.expasy.org/tools/protparam.html>). Normalized log₂-transformed spot volumes were imported into R v4.0.3 for MacOSX. Each trial was analyzed separately. Volcano plots were obtained to elucidate about the number of differential proteins between each experimental group and the corresponding control group, using the EnhancedVolcano function from package EnhancedVolcano (Blighe et al., 2021), after computing Student's *t*-test ($\alpha = 0.05$) for statistical significance. HCA was achieved with the heatmap.2 function from package gplots (Warnes et al., 2020). The differential proteins (One-way ANOVA, followed by Dunnett's test, $p < 0.05$) were normalized according to Z-score for hierarchical clustering of samples and protein spots, taking the Euclidean distance as metrics and the average linkage as agglomeration method. Protein functional annotation, including GO classification analysis, on the basis of biological process, was performed using the OmicsBox

software v1.4.11 (BioBam Bioinformatics SL, Valencia, Spain). The FASTA sequences of the identified proteins were used as input and blasted using the NCBI blast C via CloudBlast with *Danio rerio* and *Sparus aurata* as taxonomy filters. The top 10 blast hits for each query protein, with an E-value less than $1.0e^{-3}$ were retrieved. Mapping and annotation were performed based on the Blast2GO annotation methodology (Conesa et al., 2005), using the default settings. Furthermore, the identified proteins were blasted against *Danio rerio*, on the UniprotKB database, using the FASTA protein sequences, previously retrieved, as queries. The STRING web-based tool v11.0 (Szklarczyk et al., 2019) was then used to map the orthologs, screen for potential PPI and perform a Kyoto Encyclopedia of Gene and Genomes (KEGG) pathway enrichment analysis (FDR, $q < 0.05$). Protein nodes showing no interactions were excluded from further analysis. Network visualization and topological analysis were performed on Cytoscape v3.8.1 (Shannon et al., 2003). Important hub proteins were screened and ranked by the degree values and betweenness centrality of each node in the network.

3.2.3.6. Quantitative real-time reverse transcription polymerase chain reaction (RT-qPCR) analysis

3.2.3.6.1. RNA isolation and two step reverse transcription PCR (RT-PCR)

Gilthead seabream liver samples were ground with a mortar and pestle in liquid nitrogen ($n = 6$, corresponding to the same two samples per tank used for the proteomics analysis). Total RNA was extracted from 100 mg of ground material using Trizol R reagent (Invitrogen™) and treated with DNase I (RQ1 RNase-Free DNase; Promega), to remove contaminating DNA, according to the manufacturer's instructions. The yield and purity of the RNA extraction were assessed with a NanoVue Plus spectrophotometer (GE Healthcare) and the quality and integrity were verified by 1% agarose gel electrophoresis. First strand cDNA synthesis was prepared from 1 mg of total RNA using the ImProm-II^T™ Reverse Transcription System kit (Promega), as follows. The complete reverse transcription reaction (20 ml) contained 0.5 mg/reaction of Oligo(dT)15 Primer, 4 ml of ImProm-II^T™ 5X Reaction Buffer, 5.8 ml of kit's MgCl₂, 1 ml of dNTP Mix, 0.5 ml of Recombinant RNasin[®] Ribonuclease Inhibitor, 1 ml of ImProm-II^T™ Reverse Transcriptase and Milli-Q water up to 20 ml. Initially, a portion of this reaction containing only Oligo(dT)15 and total RNA was incubated at 70 °C for 5 min, and immediately chilled on ice before adding the remaining components. The

reaction was carried out at 25 °C for 10 min followed by extension at 42 °C for 1.5 h and posterior inactivation of the reverse transcriptase at 70 °C for 15 min. Primers for RT-PCR and RT-qPCR were newly designed using the GenScript web-based tool (<https://www.genscript.com/tools/pcr-primers-designer>), with a melting temperature of 55 °C and length and GC content range of 19–24 bp and 50-55%, respectively. *In silico* specificity of constructed primers was corroborated by BLAST. The primers and the expected sizes of amplicons to be used as standard templates in absolute quantification assays are listed in Table 3.2.1. PCR amplification of the cDNA was performed using the Takara Ex taq™ DNA polymerase (Takara, Shiga, Japan) in a total volume of 50 µl, along with 0.2 mM of each primer and 5 µl of cDNA template. For the PCR reaction, initial denaturation was conducted at 95 °C for 5 min followed by 24 reaction cycles, each consisting of a denaturation step at 95 °C for 45 s, annealing at 55 °C for 45 sec, and extension at 72 °C for 45 s, with a final elongation step at 72 °C for 5 min.

3.2.3.6.2. Gene cloning

The PCR products of the expected sizes were isolated and purified using the QIAEX II Gel Extraction kit (QIAGEN, Germantown, MD, United States), according to the manufacturer's instructions. The PCR-amplified DNA fragments were cloned onto the pGEM R T-Easy plasmid (Promega), and the products were transformed into *E. coli* DH5a competent cells and subsequently plated onto 2xYT with Ampicillin, X-Gal and IPTG. Transformants were screened by colony PCR using the EmeraldAmpR GT PCR Master Mix (Takara). Bacterial liquid cultures of positive clone products were used for plasmid extraction, using FavorPrep™ Plasmid DNA Extraction Mini Kit (Favorgen, Ping-Tung, Taiwan), and the DNA quantified using the NanoVue Plus spectrophotometer (GE Healthcare). Purified plasmids were then sequenced by Macrogen, Inc. (Seoul, Korea) (Supplementary Material 4 - [online](#)). Raw sequences were checked for alignment with the designed primers using Genetyx software (<https://genetyx.co.jp>) and stored for further use as standards for RT-qPCR.

Table 3.2.1. Primers used for the RT-PCR and RT-qPCR analyses of the candidate reference genes and the target genes, and expected amplicon sizes

Gene acronym	GenBank accession number	Gene name (<i>Sparus aurata</i>)	Primers' sequences 5' to 3' (FP/RP)	Annealing temperature (°C)	Expected amplicon size (bp)	Trial assessed
<i>18s</i>	AY993930.1	18S ribosomal RNA gene	5'-GACTCTTTCGAGGCCCTGTAATTG-3' 5'-AGCTCGATCCCCGAGATCCAACACTAC-3'	55	166	All
<i>actb</i>	X89920.1	actin, beta 2	5'-TCCTGCGGAATCCATGAGA-3' 5'-GTGGGGCAATGATCTTGATC-3'	55	186	All
<i>ef1-a</i>	AF184170.1	elongation factor 1-alpha	5'-GTGACAACATGCTGGAGACCAGTG-3' 5'-GCAGTGTGGTTCCGTTAGCATTGC-3'	55	93	All
<i>aldh</i>	XM_030393853.1	aldehyde dehydrogenase, mitochondrial-like	5'-GTCACTCTGGAGCTTGGAGGAAAG-3' 5'-TCTGCTTGGACAAAGGTGCGAGAG-3'	55	146	NET
<i>calr3</i>	XM_030403713.1	calreticulin 3b	5'-AGGAGGCAGAGGACATTGCAAACG-3' 5'-CTCCTCCAGGTCCTCATCTTCATC-3'	55	176	OC/NET
<i>capns1a</i>	XM_030437890.1	calpain, small subunit 1 a	5'-CTCAATGACCAGCTGTTCCAGATG-3' 5'-GTTTTGAAGGAACGGCACATGGCA-3'	55	122	OC
<i>ctsd</i>	XM_030415368.1	cathepsin D	5'-CCTTCATCGCTGCCAAGTTTGACG-3' 5'-TCCACCTTCTTCTGGCTCATGATG-3'	55	109	OC/NET
<i>ech1</i>	XM_030397255.1	enoyl CoA hydratase 1, peroxisomal	5'-TGGAGCTGAACCGTCCTGAGAAAC-3' 5'-GAAACCACCACCACTCTGCAGTCT-3'	55	182	All
<i>eno1</i>	XM_030422583.1	enolase 1a, (alpha)	5'-GAACTTCAGGCATCCCATCTGAGC-3' 5'-CACAGACCACAGACTTGGACCTTG-3'	55	169	OC
<i>fbp1</i>	XM_030436654.1	fructose-1,6-bisphosphatase 1b	5'-AGCAGATACGTCGGGTCAATGGTG-3' 5'-CTCAGCTTGCCCTTAGGACTCTTG-3'	55	104	NET
<i>ftcd</i>	XM_037091427.1	formimidoyltransferase cyclodeaminase	5'-GGAGGCTGATTCTCCGTTTCATC-3' 5'-CCATGTAGCTGTAAAGGCAGACG-3'	55	87	HYP
<i>grp78</i>	XM_030436382.1	heat shock protein 5	5'-GACAAAGGCACAGGCAACAAGAAC-3' 5'-TCGATCCTCTCCTTACGCCCTCTTG-3'	55	137	NET
<i>grp94</i>	XM_030425489.1	heat shock protein 90, beta (grp94), member 1	5'-AAGGCACAGGCTTACCAGACAG-3' 5'-CTTCAGCATCATCGCCGACTTTC-3'	55	133	NET/HYP
<i>prdx2</i>	XM_030428230.1	peroxiredoxin 2	5'-GTAGTGCTGGCTGTGAGGTTATCG-3' 5'-GGATTTTCATGGGACCCAGACCTC-3'	55	108	NET

<i>ugd</i>	XM_030415148.1	UDP-glucose 6-dehydrogenase	5'-GAAGCTGCTTCCAGAAGGATGTGC-3' 5'-GTGACAGTGTTGAAGAGGCAGTCG-3'	55	160	NET
<i>ywhab</i>	XM_030420665.1	tyrosine 3-monooxygenase/tryptophan 5-monooxygenase activation protein, beta polypeptide a	5'-CATCTCCAGCATCGAGCAGAAGAC-3' 5'-CACGTCCTGGCAGATTTCTTGGAG-3'	55	109	NET/HYP

3.2.3.6.3. RT-qPCR assay

Purified plasmids were linearized by restriction digestion with EcoRI (Takara). To prepare each target gene's standards, plasmid copy numbers were calculated through the Avogadro's constant, using the web-based tool: <http://cels.uri.edu/gsc/cndna.html>, and serial dilutions were prepared to produce a ten-fold eight-point dilutions series ($10^9 - 10^2$). RT-qPCR reactions (in duplicate) were carried out in 96-well plates using the LightCycler R 480 Instrument II system (Roche Molecular Systems, Inc., Indianapolis, IN, United States). Each standard reaction volume was comprised 1 ml of cDNA template, 1 ml of forward primer, 1 ml of reverse primer, 2 ml of ddH₂O and 5 ml of LightCycler R 480 SYBR Green I Master (Roche Molecular Systems, Inc.). RT-qPCR reactions were conducted in duplicate using the following parameters: pre-incubation at 95 °C for 5 min, followed by 40 amplification cycles of 95 °C for 15 s, annealing for 30 s and 72 °C for 30 s. Primers and annealing temperatures used in this analysis are listed in Table 3.2.1. At the end of the amplification process, the specificity was tested using melting curve analysis: 95 °C for 5 s followed by 65 °C for 1 min, then continuous temperature increase (1 °C/15 s) to 97 °C, with fluorescence measurement, and then cooling at 40 °C for 30 s. The specificity of the amplicons was confirmed by the presence of a single peak. Data acquisition was carried out by the LightCycler R 480 Software v1.5 (Roche Molecular Systems, Inc.).

3.2.3.6.4. Expression stability of reference genes and normalization

Standard curves were computed by plotting the logarithm of the known RNA standard concentration against their corresponding quantification cycle (C_q) values. Absolute copy numbers of the target genes (*eno1*, *capns1a*, *ech1*, *calr3*, *ctsd*, *grp94*, *prdx2*, *aldh*, *fbp1*, *ywhaba*, *grp78*, *ugdh*, *ftcd*), chosen based on the corresponding protein's expression profile and their literature-based evidence of stress-related function, in unknown samples were calculated from the respective linear logarithmic regression line equations using the C_q values obtained from duplicate RT-qPCR reactions. Raw C_q values from candidate reference genes, target genes and corresponding standards are shown in Supplementary Material 3 - [online](#). The chosen candidate reference genes, *18s*, *actb* and *ef1-a*, were selected based on their frequent usage for normalization in fish gene expression studies. Their expression stability was evaluated through the commonly used algorithms Delta-CT method (Silver et al.,

2006), BestKeeper (Pfaffl et al., 2004), NormFinder (Andersen et al., 2004), and geNorm (Vandesompele et al., 2002) using the web-based tool RefFinder (Xie et al., 2012) (<https://www.heartcure.com.au/reffinder>). RefFinder integrates the data generated from all the algorithms and provides a comprehensive re-ranking of the genes. Target genes' expression data was normalized to the geometric mean of the most stable endogenous reference genes for each sample. Normalized gene expression data is presented in $\log_2(\text{fold-change}_{\text{treated/control}})$.

3.2.3.7. Hepatic glycogen assessment

Gilthead seabream liver glycogen was assessed using a commercial kit (MAK016; Sigma-Aldrich). Briefly, 10 mg of liver tissue were homogenized in 100 ml of Milli-Q water at 4 °C, using a tissue lyser (VWR, Radnor, PA, United States) and a metal bead for 30 s at 25/s frequency, and boiled for 5 min to inactivate enzymes. Samples were then centrifuged at 13,000 g for 5 min. Assays were then performed on 96-well plates, in duplicate, following manufacturer's instructions, and read at 570 nm along with a prepared standard curve on a microplate reader Biotek Synergy 4 Hybrid Technology™ (Biotek Instruments Inc.). Sample blanks were run simultaneously in the assays, in duplicate, for glucose subtraction from the sample readings.

3.2.3.8. Univariate statistical analyses

Univariate statistical analyses of gene expression data and glycogen levels were performed using R v4.0.3 for MacOSX. Statistical differences between experimental groups and the control group were analyzed independently for each trial (OC, NET, and HYP), by One-way ANOVA on \log_{10} -transformed data. Multiple comparisons of gene expression data were carried out by the *post hoc* Dunnett's test. Normality of the residuals was assessed by a Shapiro-Wilk's test. When transformed data from hepatic glycogen levels did not verify homoscedasticity assumption by Levene's test, statistical significance was assessed by Welch's ANOVA, followed by the *post hoc* test Games-Howell (specifically OC and NET trials). A significance level of $\alpha = 0.05$ was used in all tests performed. The correlation between genes' expression changes and the corresponding products was assessed by Pearson's correlation. All plots were generated using the R package ggplot2 (Wickham, 2016).

3.2.4. RESULTS

3.2.4.1. Gel-based proteomics analysis of gilthead seabream liver

Changes in the liver proteome of gilthead seabream exposed to the different challenges and undisturbed fish were assessed, comparatively, through gel-based proteomics using the 2D-DIGE technique. The number of protein spots identified in each trial is summarized schematically in Figure 3.2.1 to facilitate interpretation.



Figure 3.2.1. Summary of the protein spots identified in the 2D-gels of the proteomics analysis performed with the liver of gilthead seabream (*Sparus aurata*) submitted to different challenges, and their expression profiles.

Analysis of CyDye-labeled gels revealed 1205, 974 and 1060 protein spots for the OC, NET and HYP trials, respectively, within the experimental pH range of 4–7 and molecular weights ranging from 11–90 kDa. Following a statistical analysis, 36, 165, and 59 protein spots within the OC, NET and HYP trials, respectively, showed significantly differential abundances (One-way ANOVA, followed by Dunnett's test, $p < 0.05$) among experimental groups. Spots were manually excised from corresponding preparative gels and identified by MALDI-TOF/TOF MS. From these, 13, 52 and 26 were successfully identified by MS/MS, with significant scores, in two databases (protein score > 76 (NCBI) or > 86 (EST), total ion score > 60 , $p < 0.05$). All the identified proteins and their attributes are listed in Supplementary Material 1 - [online](#). Of the protein spots identified in the OC trial, 7 were upregulated and 6 were

downregulated in challenged fish, compared with control fish, while in the NET trial 22 protein spots were upregulated and 30 were downregulated. Finally, in the HYP trial, 18 of the identified protein spots were upregulated and 8 were downregulated in challenged fish. Among the protein spots of NET trial with significant identifications attributed, 12 showed more than one significant identification, while in the case of the identified protein spots corresponding to the HYP trial, 8 spots also showed more than one significant identification. Regarding the total protein identifications attributed to OC protein spots, 12 corresponded to single entries, from which 7 are protein varying in abundance uniquely in this trial, 2 corresponded to shared identifications with the NET trial (heart-type fatty acid binding protein and calreticulin) and 3 with the HYP trial ($\Delta^{3,5},\Delta^{2,4}$ -dienoyl-CoA isomerase, glutathione S-transferase and proteasome subunit beta). In the case of NET trial, 42 protein identifications corresponded to single entries. Among these, 34 proteins have differential abundance exclusively in this trial, and apart from the 2 protein identifications shared with the OC trial, 6 other protein identifications are also common between NET and HYP trials (14-3-3 protein beta/alpha, actin, cytoskeletal type II keratin 8, elongation factor-1-beta, peroxiredoxin 2 and serine—pyruvate aminotransferase). Apart from the common identifications, 19 additional proteins, corresponding to single entries, were found to be varying in abundance exclusively in the HYP trial.

3.2.4.2. Univariate and multivariate statistical analyses of differential abundant proteins

In order to identify, in each trial, which stress intensity induced the highest number of differentially abundant proteins (DAPs), the fold-change of the protein spots (log₂-transformed) was plotted against their statistical significance (log₁₀-transformed). The originated volcano plots showed that the highest number of DAPs was found between the fish from OC45, NET4 and HYP15, and their corresponding control fish, in the OC (Figure 3.2.2.A), NET (Figure 3.2.3.A) and HYP (Figure 3.2.4.A) trials, respectively. Although, in the case of OC and HYP trials, the highest fold-changes were found between the proteins of OC30 and HYP30 groups and the control group. These same observations were corroborated after HCL analysis. Separation between groups was more evidenced in the NET trial (Figure 3.2.3.B), when compared with OC (Figure 3.2.2.B) and HYP (Figure 3.2.4.B) trials, whereas the most divergent groups were the control and NET4, as observed by the top dendrogram. Protein spots

also grouped into two main clusters, one displaying a pattern of higher relative abundance (including mainly proteins related to protein synthesis, folding and sorting) and the other of lower relative abundance in challenged fish (including mainly proteins involved in the amino acid and carbohydrate metabolisms), when compared to the control.

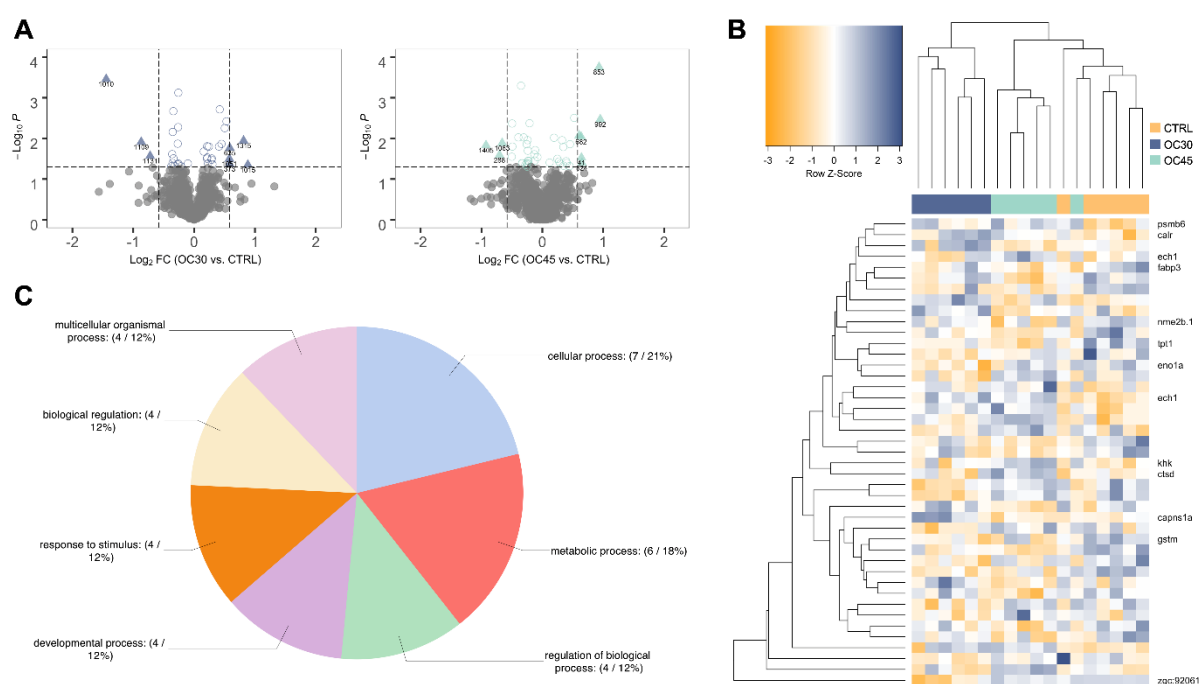


Figure 3.2.2. Proteomics data analysis of OC trial. (A) Volcano plots of the differential proteins detected by 2D-DIGE analysis on the OC trial liver samples ($n = 6$). Dotted vertical lines represent a 1.5-fold variation in abundance, while the dotted horizontal line represents the significance level of $p < 0.05$ (Student's t -test). Triangles represent proteins significantly up- and downregulated. (B) HCA of the 36 significantly different spots (One-way ANOVA, followed by Dunnett's test, $p < 0.05$) in the liver of gilthead seabream from OC trial. Rows represent proteins' expression patterns, while each column corresponds to a biological replicate (fish). (C) Functional GO classification of the identified proteins. Pie chart shows the level 2 GO annotations of biological process.

3.2.4.3. Functional GO annotation of identified proteins

To elucidate about the biological functions of the liver proteins responding to the different challenges in gilthead seabream, a GO classification was performed. Functional GO annotation of the identified proteins revealed, based on the top five level 2 BP GO terms, that the DAPs were mostly implicated in cellular (GO:0009987) and metabolic processes (GO:0008152), response to stimulus (GO:0050896), biological regulation (GO:0065007) and regulation of biological processes (GO:0050789). This is shown in the pie charts of all three OC (Figure 3.2.2.C), NET (Figure 3.2.3.C) and

HYP trials (Figure 3.2.4.C). Multi-level pie charts of BP GO terms of the identified proteins from all three trials are shown in Figure S3.2.1 - [APPENDIX](#). Regarding the OC trial, four out of the 12 unique proteins were involved in the response to stimulus. From these, three are upregulated [calreticulin (CALR), cathepsin (CTSD), and ketohexokinase (KHK)] and one is downregulated [glutathione-S-transferase (GTSM)] in challenged fish. Among the 42 unique proteins identified in the NET trial, 14 were implicated in the response to stimulus, i.e., 78 kDa glucose-regulated protein (HSPA5), protein disulfide-isomerase (P4HB), protein disulfide-isomerase A3 (PDIA3), calreticulin (CALR), 94 kDa glucose-regulated protein (HSP90B1), serine-pyruvate aminotransferase (AGXTB), aldehyde dehydrogenase (ADLH2.2), fructose- 1,6-bisphosphatase (FBP1B), protein/nucleic acid deglycase DJ-1 (PARK7), Cu-Zn superoxide dismutase (SOD1), liver-type fatty acid-binding protein (FABP1B.2), phenylalanine-4-hydroxylase (PAH), peroxiredoxin 2 (PRDX2), and UDP-glucose-6-dehydrogenase (UGDH). The first six proteins described are upregulated in challenged fish, while the last eight are downregulated, when compared with control fish. The HCL analysis also shows that a subset of these proteins, specifically, the first five proteins mentioned, which are implicated in protein folding processes, are all grouped in the same cluster. In the case of the HYP trial, seven differential proteins were implicated in the response to stimulus. From these, four are upregulated in challenged fish, being these AGXTB, rho GDP-dissociation inhibitor (ARHGDI3), erlin-2 (ERLIN2), and glutathione-S-transferase (GSTM), while the other three are downregulated [inositol monophosphatase (IMPA1), peroxiredoxin 2 (PRDX2), and regucalcin (RGN)].

3.2.4.4. PPI network analysis and KEGG pathway enrichment

A PPI analysis was carried out with the unique protein identifications from each trial to elucidate about the biological interactions between the DAPs in the liver of gilthead seabream exposed to the different challenges. The unique proteins were blasted against *Danio rerio* and the orthologs were used to generate a network using the STRING web-based tool. For each unique entry, one protein spot was chosen as the most representative of each protein (Supplementary Material 1 - [online](#)), based mainly on the protein score and the closeness between experimental and theoretical molecular weights and pI. In the case of OC trial, no interactions were found in the STRING database between the identified proteins. Contrarily, in the NET trial, the

generated PPI network (Figure 3.2.3.D) revealed 70 edges among 34 nodes, with a clustering coefficient of 0.501 and a very significant enrichment value ($p < 1.0e^{-16}$).

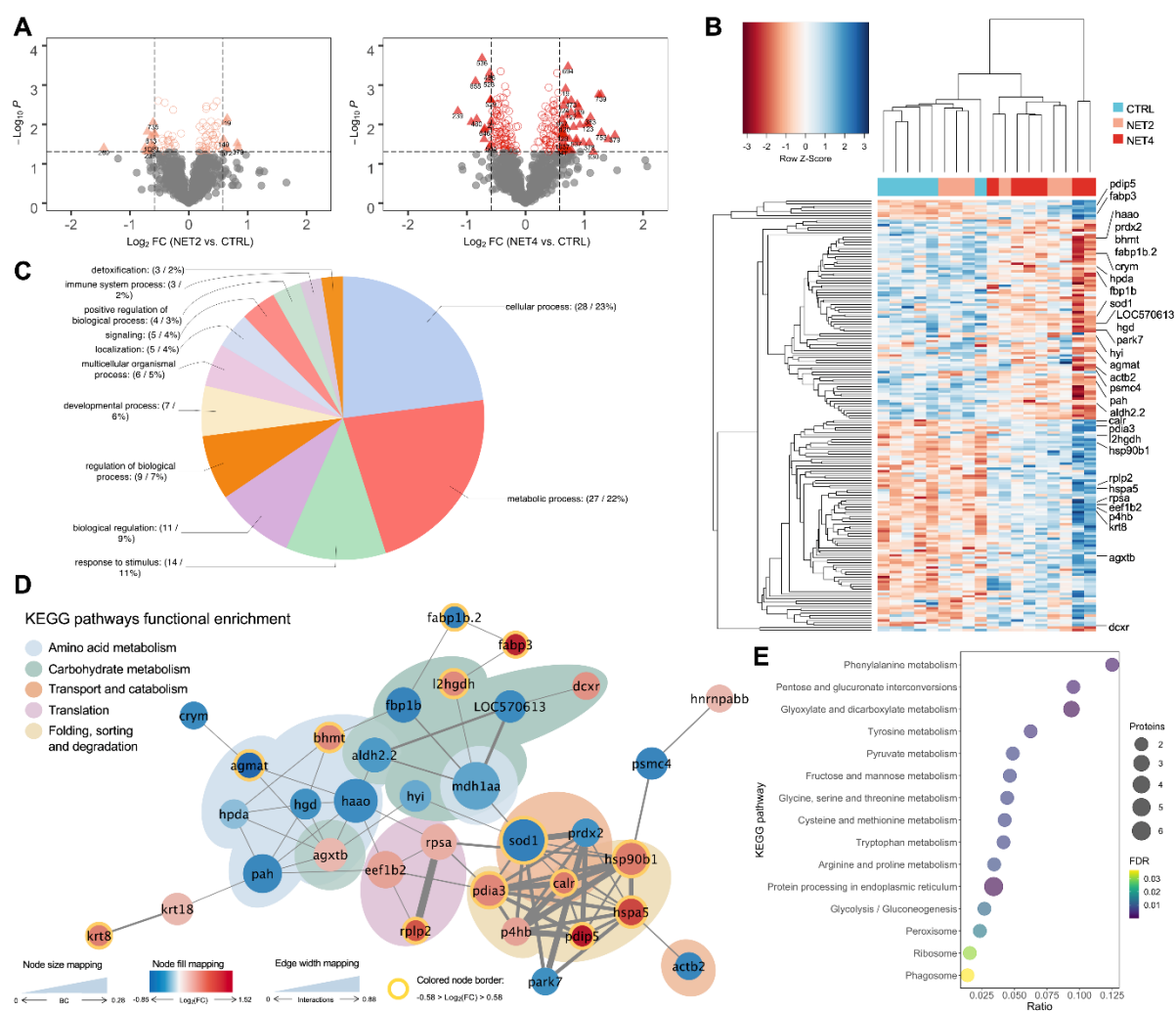


Figure 3.2.3. Proteomics data analysis of NET trial. (A) Volcano plots of the differential proteins detected by 2D-DIGE analysis on the NET trial liver samples ($n = 6$). Dotted vertical lines represent a 1.5-fold variation in abundance, while the dotted horizontal line represents the significance level of $p < 0.05$ (Student's t -test). Triangles represent proteins significantly up- and downregulated. (B) HCA of the 165 significantly different spots (One-way ANOVA, followed by Dunnett's test, $p < 0.05$) in the liver of gilthead seabream from NET trial. Rows represent proteins' expression patterns, while each column corresponds to a biological replicate (fish). (C) Functional GO classification of the identified proteins. Pie chart shows the level 2 GO annotations of biological process. (D) PPI network generated with 34 DAPs identified in the liver of fish from NET trial. Nodes represent proteins and edges the functional associations between them. Colored areas indicate enriched KEGG pathways (FDR < 0.05). (E) Bubble plot representing the statistical significance and number of proteins belonging to each KEGG enriched pathway (lower level) overrepresented in the PPI network. BC, betweenness centrality

Likewise, the HYP PPI network (Figure 3.2.4.D) revealed 28 edges among 26 nodes, with a clustering coefficient of 0.551 and an enrichment value of $1.51e^{-11}$. The

topological analysis of each network was performed separately on Cytoscape and specific coefficients were selected to highlight the importance and distribution of each node in the network, i.e., the size of the nodes indicates betweenness centrality (ranging from 0 to 0.28 in NET and from 0 to 0.62 in HYP), the divergent color mapping was estimated based on the fold-change (\log_2 -transformed) of each protein (ranging from -0.85 to 1.52 in the NET network and from -1.4 to 0.7 in the HYP network), and the colored node border indicates proteins with a fold-change of at least 1.5-fold. In the NET network, 17 of the 34 nodes represent upregulated proteins in challenged fish (red nodes), while the remaining 17 represent downregulated proteins (blue nodes). PDIA3 (protein disulfide-isomerase A3), HSPA5 (78 kDa glucose-regulated protein), and SOD1 (Cu-Zn superoxide dismutase) showed the highest number of established edges (nine), followed by HSP90B1 (94 kDa glucose-regulated protein) with eight, and finally by P4HB (protein disulfide-isomerase) and HAAO (3-hydroxyanthranilate 3,4-dioxygenase) with seven. Regarding the HYP network, 18 nodes represent upregulated proteins in challenged fish (orange nodes) while the remaining eight represent downregulated proteins (green nodes). EIF5A (eukaryotic translation initiation factor 5A), AGXTB, thioredoxin (TXN) and PRDX2 (peroxiredoxin 2) showed the highest degree of connectivity among the nodes, with four edges.

It was also possible to discriminate, in the NET network, five cohesive overrepresented clusters summing up the five enriched KEGG pathways (FDR, $q < 0.05$). The colored areas in the network (Figure 3.2.3.D) indicate the higher level enriched KEGG pathways. The lower level KEGG enriched pathways are represented in the bubble plot in Figure 3.2.3.E. Protein processing in endoplasmic reticulum (term ID: dre04141) was the most overrepresented (FDR = $2.35e^{-6}$) pathway in the liver response to the net handling, accounting for six proteins in the network. Amino acid metabolism accounted for nine proteins in the network, however these were distributed over six lower level KEGG pathway terms, i.e., phenylalanine metabolism (term ID: dre00360), tyrosine metabolism (term ID: dre00350), glycine, serine and threonine metabolism (term ID: dre00260), tryptophan metabolism (term ID: 00389), arginine and proline metabolism (term ID: dre00330), and cysteine and methionine metabolism (term ID: dre00270). Regarding the HYP network, three KEGG pathways were overrepresented (Figure 3.2.4.E), being these glyoxylate and dicarboxylate metabolism (term ID: dre00630), peroxisome (term ID: dre04146), and proteasome (term ID: dre03050). The network community represented by the latter was the most

over-represented KEGG pathway (FDR = $3.5e^{-4}$), which in fact represents a protein complex that integrates the proteasome.

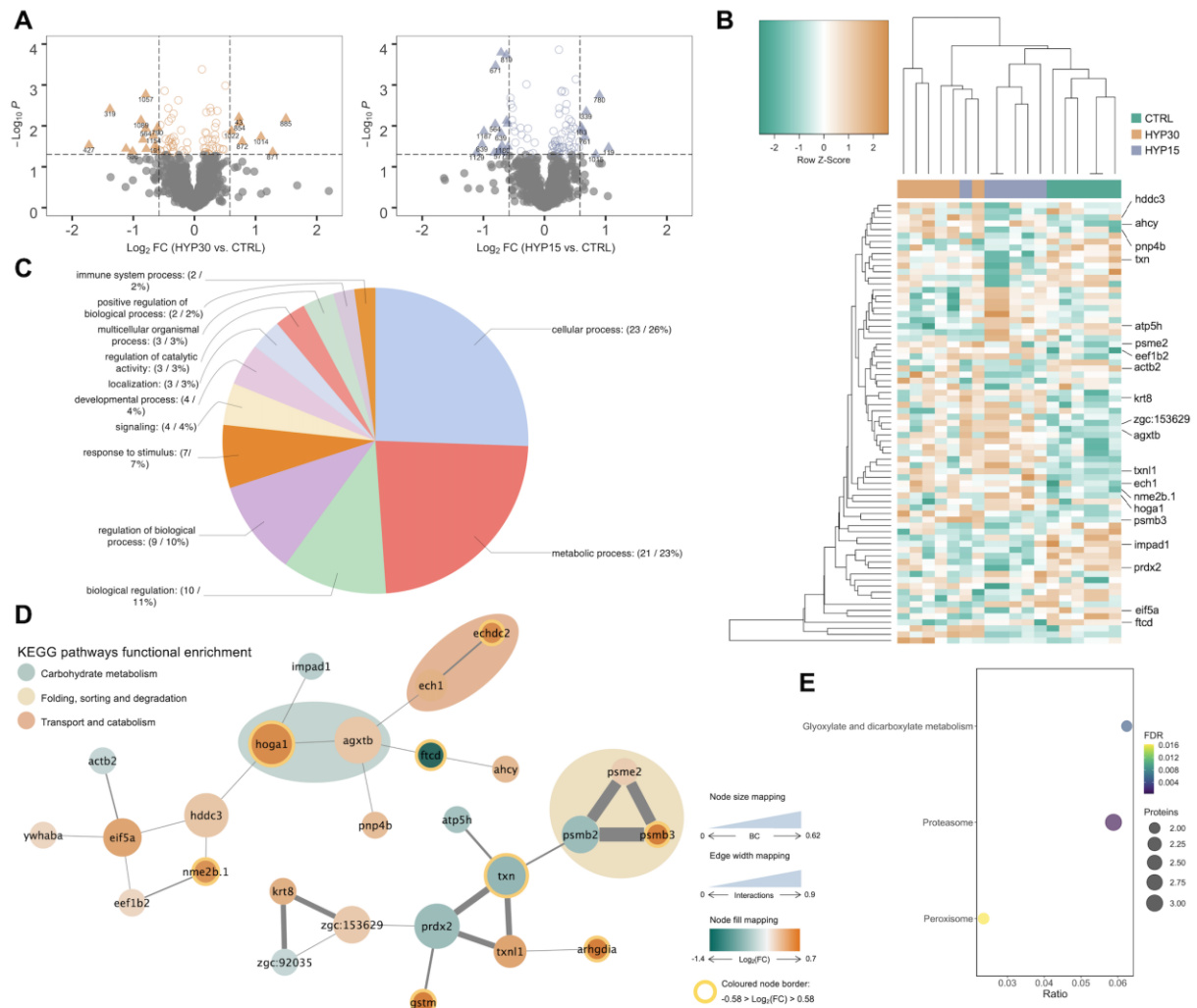


Figure 3.2.4. Proteomics data analysis of HYP trial. (A) Volcano plots of the differential proteins detected by 2D-DIGE analysis on the HYP trial liver samples ($n = 6$). Dotted vertical lines represent a 1.5-fold variation in abundance, while the dotted horizontal line represents the significance level of $p < 0.05$ (Student's t -test). Triangles represent proteins significantly up- and downregulated. (B) HCA of the 59 significantly different spots (One-way ANOVA, followed by Dunnett's test, $p < 0.05$) in the liver of gilthead seabream from HYP trial. Rows represent proteins' expression patterns, while each column corresponds to a biological replicate (fish). (C) Functional GO classification of the identified proteins. Pie chart shows the level 2 GO annotations of biological process. (D) PPI network generated with 26 DAPs identified in the liver of fish from HYP trial. Nodes represent proteins and edges the functional associations between them. Colored areas indicate enriched KEGG pathways (FDR < 0.05). (E) Bubble plot representing the statistical significance and number of proteins belonging to each KEGG enriched pathway (lower level) overrepresented in the PPI network. BC, betweenness centrality

3.2.4.5. Expression stability of candidate reference genes

The raw Cq values of the three candidate reference genes (Supplementary Material 3 - [online](#)) ranged from 7.75 (*18s*) to 18.29 (*actb*), from 7.47 (*18s*) to 19.34 (*actb*), and from 6.55 (*18s*) to 19.58 (*actb*), in the OC, NET and HYP trial assays, respectively. The threshold fluorescence for *actb* was always higher than the other genes, indicating a low expression level. On the other hand, *18s* was the most expressed gene among the candidates. Overall, considerable variations were observed between the expression levels of the different candidate reference genes.

The candidate reference genes were ranked separately for the three trials, according to their expression stability values, using standard algorithms (Table 3.2.2). In general, within each trial, the ranks were consistent across the different algorithms, however, between trials, the results were differential. The geNorm M value of 1.5 was employed as threshold and therefore, only genes with an M value below 1.5 were used as reference genes. Genes *actb* and *18s* were the most stable reference genes across all trials, while *ef1-a* was not used in NET trial since its M value was above the established threshold.

Table 3.2.2. Expression stability analysis of each candidate reference gene for gilthead seabream liver RT-qPCR analysis, based on different algorithms (R - rank).

Gene	Delta-CT		BestKeeper		NormFinder		geNorm		RefFinder	
	R	STDEV	R	Std Dev [± Cp]	R	SV	R	M	R	GM
OC trial										
<i>18s</i>	2	0.932	1	0.222	2	0.672	1	0.786	2	3.000
<i>actb</i>	3	1.008	3	0.815	3	0.844	2	0.934	3	1.414
<i>ef1-a</i>	1	0.862	2	0.648	1	0.408	1	0.786	1	1.189
NET trial										
<i>18s</i>	2	1.654	3	1.395	2	1.053	1	1.243	2	1.861
<i>actb</i>	1	1.570	1	1.019	1	0.662	1	1.243	1	1.000
<i>ef1-a</i>	3	1.981	2	1.031	3	1.777	2	1.735	3	2.711
HYP trial										
<i>18s</i>	3	1.194	3	1.049	3	1.057	2	1.058	3	3,00
<i>actb</i>	2	0.993	2	0.988	2	0.569	1	0.786	2	1.682
<i>ef1-a</i>	1	0.987	1	0.938	1	0.542	1	0.786	1	1.0

3.2.4.6. Amplification specificity and efficiency, and absolute quantification

The gilthead seabream response to the different challenges was also assessed at the transcript level. Based on the DAPs obtained in the liver proteomics analysis, 13 corresponding genes (*eno1*, *capns1a*, *ech1*, *calr3*, *ctsd*, *grp94*, *prdx2*, *aldh*, *fbp1*, *ywhaba*, *grp78*, *ugdh*, *ftcd*) were selected for gene expression analysis by RT-qPCR.

A melting curve analysis was carried out at the end of each amplification and used to determine primer specificity. The resulting melting peaks are shown in Figure S3.2.2 - [APPENDIX](#). The amplification efficiency (E) was calculated for each standard curve used for absolute quantification, which varied from 92 to 110%, with a correlation coefficient (R^2) kept above 0.987 (Supplementary Material 3 - [online](#)).

The absolute copy numbers of the target genes were calculated based on the standard curves constructed with the linearized cDNA plasmids. Subsequently, the absolute copy numbers of the target genes were normalized by the absolute copy numbers of the reference genes, obtained by the geometric mean of the candidate reference genes selected in the expression stability analysis (Table 3.2.2). The higher fold-changes between challenged fish and control fish were found in the NET trial. Statistically significant differences (One-way ANOVA, followed by Dunnett's test, $p < 0.05$) were found exclusively in the NET trial, specifically in genes *grp78* (NET2-CTRL: $p = 0.002$, NET4-CTRL: $p = 0.018$) and *grp94* (NET2-CTRL: $p = 0.001$, NET4-CTRL: $p = 0.027$), which were found to be upregulated in challenged fish from both experimental groups (Figure 3.2.5). These genes correspond to the proteins 78 kDa glucose-regulated protein (HSPA5) and 94 kDa glucose-regulated protein (HSP90B1), respectively, which were also found to be significantly upregulated in the livers of fish from NET4 group. Although no significant differences were found for the other target genes, the expression profiles of gene and protein expression in the NET trial were highly correlated, with a Pearson's correlation coefficient (r) of 0.892 and a statistical significance of 0.0029.

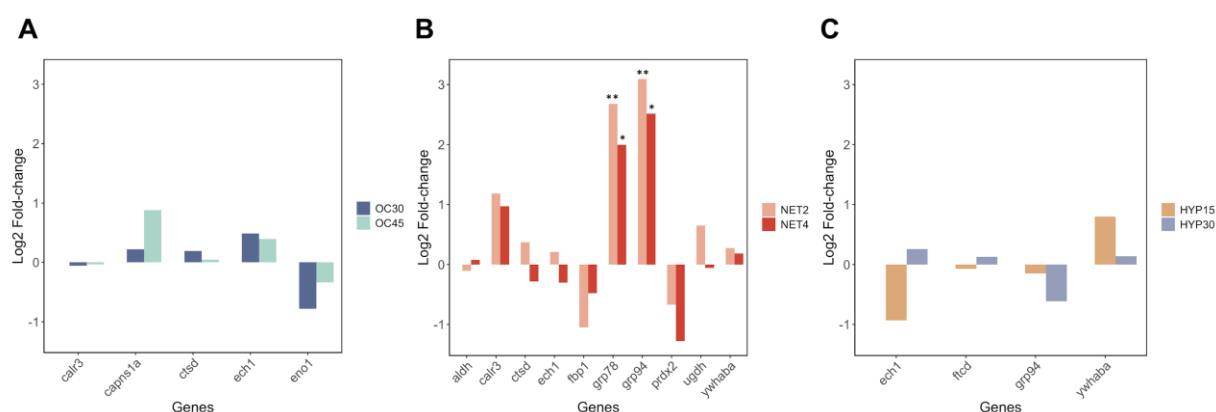


Figure 3.2.5. Expression profiles of 13 different transcripts in the liver ($n = 6$) of gilthead seabream (*Sparus aurata*) exposed to different challenges (A) OC trial, (B) NET trial, (C) HYP trial, obtained by RT-qPCR. The normalized absolute copy numbers of the target genes are presented in $\log_2(\text{fold-change treated-control})$. Bars labeled * indicate statistically significant differences when compared with the control group (One-way ANOVA, followed by Dunnett's test, * $p < 0.05$; ** $p < 0.01$).

3.2.4.7. Liver glycogen levels

Glycogen stores were assessed in the liver of gilthead seabream exposed to the different challenges using commercial kits. Statistical differences were found exclusively for the NET trial (Welch's ANOVA, $p < 0.05$), between control and challenged fish from both experimental groups (Games-Howell *post hoc* test, NET2-CTRL: $p = 0.001$, NET4-CTRL: $p = 0.12$), whereas significantly lower levels were found in the latter group (Figure 3.2.6). High dispersion of biological responses was found for the fish from OC30 (Coefficient of variation (CV) = 25.6%), NET4 (CV = 64.6%), HYP30 (CV = 43.2%) and HYP15 (CV = 46.8%).

3.2.5. DISCUSSION

This study provides a comprehensive characterization of the liver proteome responses and related genes of gilthead seabream exposed to three different challenges, namely, overcrowding, net handling, and hypoxia. Our findings demonstrate that fish respond to stress via a complex regulatory network, rather than relying on a few specific stress-related proteins. Furthermore, the different magnitude of regulatory changes observed among trials suggests a specific response influenced by its severity. This scenario agrees with a previous FTIR exploratory analysis performed on the liver of these fish, where a metabolic reprogramming was proposed to meet the energy demands required during the physiological stress response (de Magalhães et al., 2020).

When an external challenge is perceived by the fish, the HPI axis in the brain is activated, initiating a physiological response which aids the fish to cope with the situation (Wendelaar Bonga, 1997). The inherent release of cortisol and catecholamines influences a diverse array of downstream biological functions, including growth, immune function, reproduction, and metabolism (Pottinger, 2008). A well-studied role of cortisol in fish is the activation of specific metabolic pathways in the liver, aiming to increase the glucose production and its allocation to meet the energy requirements (Vijayan et al., 2010). After stimulation by external factors, a rapid generation of glucose occurs through glycogenolysis by the consumption of hepatic glycogen storage, while long-term production is mainly achieved through gluconeogenesis (Pankhurst, 2011). The regulation of these pathways occurs at multiple levels, such as hormonal, transcriptional, and allosteric regulation, mediated by the action of insulin, glucagon, and cortisol (Faught & Vijayan, 2016).

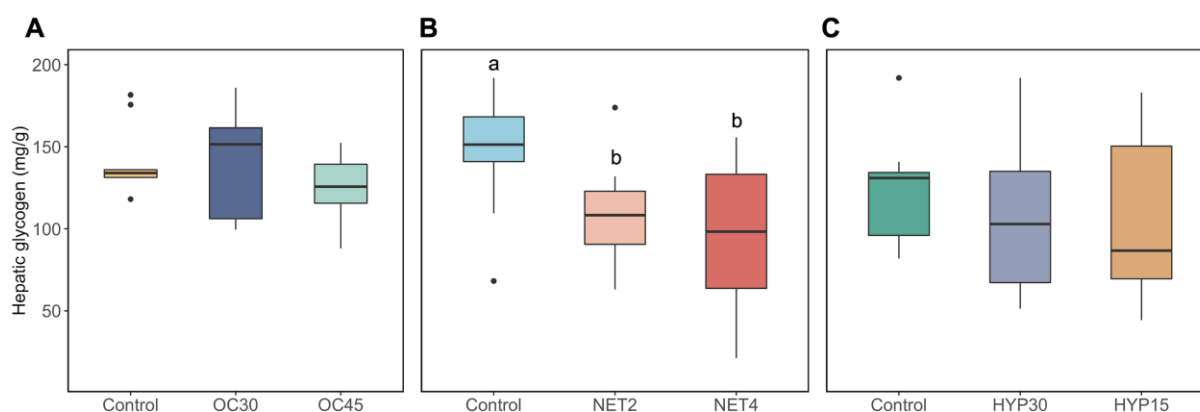


Figure 3.2.6. Boxplots showing the distribution of glycogen levels in the liver of gilthead seabream (*Sparus aurata*) submitted to three different challenges (A) OC trial, (B) NET trial, (C) HYP trial. The boxplots include observations ($n = 9$) from the 25th to the 75th percentiles as determined by R software; the horizontal line indicates the median value. Whiskers extend 1.5 times the interquartile range. Single data points represent outlying data. Lower case letters indicate statistically significant differences ($p < 0.05$).

3.2.5.1. Carbohydrate metabolism

Cortisol activates the gluconeogenic pathway in the liver by genomic and non-genomic signaling, although the former is the most well described mechanism in fish (Faught & Vijayan, 2016). It diffuses through the cell plasma membrane, binds to the glucocorticoid receptor (GR), and then translocates into the nucleus to induce the expression of gluconeogenic genes (Teles et al., 2013). Binding of other transcriptional regulators to these gene promoters is required to activate their transcription, such as those mediated by the hormone glucagon via a complex series of enzymatic reactions (Forbes et al., 2019). Plasma cortisol levels of fish handled four times a week (NET4 group from NET trial), published in another work (Raposo de Magalhães, Schrama, et al., 2020), were significantly increased when compared with control fish. However, proteomics results from this study suggest a downregulation of gluconeogenic activity in these fish. The rate-limiting step of gluconeogenesis is the irreversible dephosphorylation of fructose 1,6-bisphosphate into fructose-6-phosphate, which is catalyzed by fructose 1,6-bisphosphatase (FBP1) (Figure 3.2.7), a key regulatory enzyme (Timson, 2019). This enzyme is tightly regulated beyond transcriptional regulation. It is inhibited by the substrate fructose 2,6-bisphosphate, which it is by itself regulated by the hormone glucagon, via cyclic adenosine monophosphate (cAMP) (Enes et al., 2009). Allosterically, FBP1 is also inhibited by adenosine monophosphate (AMP), when adenosine triphosphate (ATP) levels are decreased, since gluconeogenesis is an energy consuming process (Gizak et al., 2012). FBP1 was

significantly downregulated in the liver of NET4 fish, suggesting that gluconeogenesis was suppressed. Results from the assessment of hepatic glycogen stores (Figure 3.2.6), which show significantly decreased values in the fish from NET4 group, suggest that the glucose required for stress coping processes was most likely being produced through glycogenolysis, by the breakdown of glycogen. The elevated plasma glucose levels for these fish, previously measured and published in another work (Raposo de Magalhães, Schrama, et al., 2020), support these observations. It has been described that the liver is the major organ supplying glucose to the gills and brain under situations of high energy requirement. However, it is important to note that changes in plasma glucose can be influenced by a panoply of other factors, such as diet and muscle glycogenolysis, which under stressful situations is mostly activated by catecholamines (Mommsen et al., 1999). Other proteins (DCXR, LOC570613 and UGDH) involved in the carbohydrate metabolism, specifically in the glucuronate pathway (which is within the enriched KEGG pathway named “pentose and glucuronate interconversions”), were significantly altered in abundance in the liver of NET4 fish. Changes in this pathway were detected in yellow drum liver, exposed to cold and/or starvation stress, to compensate for the energy deficit and convert other carbohydrates into glucose (Jiao et al., 2020).

Similarly, in the OC trial, a repression of the gluconeogenic/glycolytic pathway appears to have occurred in challenged fish, since alpha-enolase (ENO1A), the enzyme responsible for catalyzing the interconversion of phosphoenolpyruvate into glycerate-2-phosphate, was downregulated in challenged fish (Figure 3.2.7). Previous studies on fish stress agree with our observations. Chronic cortisol administration in gilthead seabream repressed the expression of the ENO1 gene (Teles et al., 2013), while in Senegalese sole, repeated handling stress induced the downregulation of the protein ENO1A (Cordeiro et al., 2012b). The RT-qPCR analysis also demonstrated a downregulation of the ENO1 and FBP1 genes, however, no statistically significant differences were found, most likely due to high biological variability in the transcript levels. Another DAPs in the OC trial (significantly upregulated in the liver of fish from OC45 group), identified by the functional GO annotation in this study as being involved in the response to stimulus, is KHK. This protein initiates the fructose metabolism by the phosphorylation of fructose into fructose-1-phosphate (Figure 3.2.7). This substrate can be further converted either into glyceraldehyde-3-phosphate, which serves as a key triose intermediate for the gluconeogenic/glycolytic pathway, or into glycerol-3-

phosphate as substrate for the synthesis of triglycerides (Diggle et al., 2009). This suggests that overcrowded fish might be producing energetic resources from other alternative sources, such as by supplying triose sugars for gluconeogenesis. No significant changes were found for the plasma glucose levels in OC45 fish, when compared with control fish (Raposo de Magalhães, Schrama, et al., 2020), although glucose can be being used by other energy-requiring tissues, such as the brain and muscle. In fact, a gel-based proteomics analysis of the muscle tissue (data not published) showed that the protein beta-enolase was significantly upregulated in these fish (\log_2 fold-change = 0.62; One-way ANOVA, followed by Dunnett's test, $p = 0.0369$), suggesting that muscle glycolysis was most likely taking a part in glucose disposal. The significantly higher plasma lactate levels registered for these fish (Raposo de Magalhães, Schrama, et al., 2020) indicate a potential anaerobic consumption of glucose in the muscle, which results in lactate production.

3.2.5.2. Amino acid metabolism

The carbohydrate and the amino acid metabolisms are intimately linked (Mommsen et al., 1999). In this study, key proteins involved in the catabolism of specific amino acids were found to be significantly downregulated mostly in fish from NET4 group, when comparing with the control group. In fact, carbohydrate metabolism and amino acid metabolism were the two overrepresented higher level KEGG pathways in the NET PPI network comprising the highest number of proteins (Figure 3.2.3.D). Indeed, hepatic gluconeogenesis relies on noncarbohydrate substrates for glucose production, such as lactate, amino acids, fatty acids, and glycerol. Glucogenic amino acids are thus essential precursors for gluconeogenesis and have already been described as hepatic energy fuels in fish under different stressful conditions (Vijayan et al., 2010). Notably, these can enter the gluconeogenic pathway either by conversion into pyruvate or into intermediates of the tricarboxylic acid (TCA) cycle, which, by conversion into oxaloacetate, enter the gluconeogenic pathway. The 4-hydroxyphenylpyruvate dioxygenase (HPDA) and the PAH are two proteins involved in the phenylalanine (Phe) metabolism (Figure 3.2.7). There are two main routes by which Phe can be metabolized: oxidation to tyrosine (Tyr) and transamination to phenylpyruvate (Shafik et al., 2014).

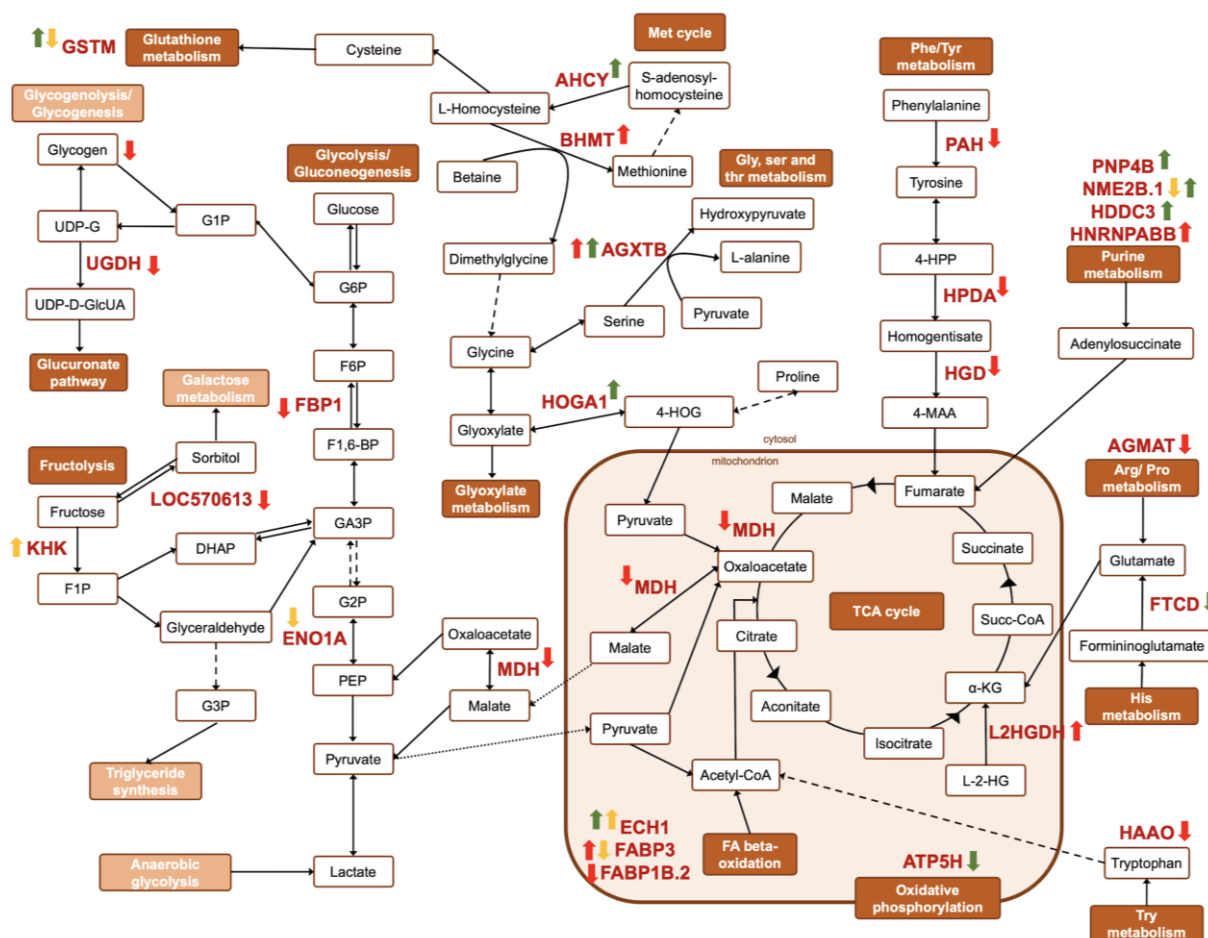


Figure 3.2.7. Schematic representation of the metabolic pathways affected by the different challenges. Yellow, red, and green arrows represent differences in abundance (One-way ANOVA, followed by Dunnett's test, $p < 0.05$) in the liver of *Sparus aurata* from OC, NET and HYP trials, respectively. Dark orange pathway names indicate affected metabolic pathways, while light orange pathway names indicate non-affected pathways. Pointed arrowed lines indicate substrate transport across the mitochondria's membrane, while dashed arrowed lines represent more than one enzymatic reaction. a-KG, a-ketoglutarate; 4-HOG, 4-hydroxy-2-oxoglutarate; 4-HPP, 4 hydroxyphenylpyruvate; 4-MAA, 4-maleyl-2-acetoacetate; DHAP, dihydroxyacetone phosphate; F1,6-BP, fructose 1,6-biphosphate; F1P, fructose-1-phosphate; F6P, fructose-6-phosphate; GA3P, glyceraldehyde-3-phosphate; G1P, glucose-1-phosphate; G2P, glyceraldehyde-2-phosphate; G3P, glycerol-3-phosphate; G6P, glucose-6-phosphate; L-2-HG, L-2-hydroxyglutarate; PEP, phosphoenolpyruvate; UDP-D-GlcUA, UDP-D-glucuronate; UDP-G, UDP-glucose.

HPDA is responsible for converting phenylpyruvate into 2-hydroxyphenylacetate, whereas PAH catalyzes the oxidation of Phe into Tyr. Both proteins were found to be downregulated in fish from NET4 group. Following the cycle, Tyr then enters the tyrosine metabolism, where HPDA also participates, being involved in the conversion of 4-hydroxy-phenylpyruvate into homogentisate (Rüetschi et al., 2000). The latter can then be converted into 4-maleyl-acetoacetate by an enzyme called homogentisate 1,2- dioxygenase (HGD) (Figure 3.2.7). However, this was also

found to be downregulated in the liver of the challenged fish from our NET experiment. Downregulation of Phe and Tyr catabolism has been reported in gilthead seabream exposed to cold stress (Ghisaura et al., 2019; Ibarz et al., 2010) and hepatotoxins (Malécot et al., 2011). The substrate 4-maleyl-acetoacetate can be converted into fumarate, an intermediate of the TCA cycle. Here, fumarate is converted into malate, which is subsequently converted into oxaloacetate to enter the gluconeogenic pathway. The enzyme which reversibly catalyzes the oxidation of malate into oxaloacetate, malate-dehydrogenase (MDH) (Musrati et al., 1998), was found to be downregulated in challenged fish, thus intercepting the TCA cycle at this step (Figure 3.2.7). MDH was also found to be downregulated in the liver of rainbow trout exposed to 24 h of crowding stress (Naderi et al., 2018). Betaine-homocysteine S-methyltransferase (BHMT) was another protein found to be downregulated by stress in the liver of fish from NET4 group. It is important to mention that BHMT was identified as a differential abundant protein in three spots, whereas two were significantly up- and one was downregulated (spot no.373). However, in this last spot more than one significant identification was found. This protein exerts catalytic functions in the methionine (Met) cycle, converting L-homocysteine into Met, by transferring a methyl group from betaine. Met is a key factor in the protection of oxidative stress, reacting with a variety of reactive oxygen species (ROS) to form methionine sulphoxide (MetO), which is then reduced back to Met (Séité et al., 2018). This way, betaine is converted into dimethylglycine, a reaction likewise catalyzed by BHMT (Figure 3.2.7). AGXTB, which converts serine and pyruvate into hydroxypyruvate and alanine (Y. Sun et al., 2019), is another DAP in the same KEGG pathway (Glycine, serine, and threonine metabolism) as the last reaction mentioned. In the case of fish from NET4 group, AGXTB was found to be significantly upregulated. AGXTB was also reported to be upregulated in the kidney of rainbow trout exposed to handling stress (Krasnov et al., 2005). The proteins HAAO, aldehyde dehydrogenase (ALDH2.2) and agmatinase (AGMAT) were other DAPs involved in the amino acid metabolism, specifically in the tryptophan, and in the arginine and proline metabolism (Figure 3.2.7), which were also found to be downregulated in fish from this same group. Additionally, PAH, AGXTB and ALDH2.2 are proteins involved in the response to stimulus, according to the functional GO classification performed (Figure 3.2.3.C). The downregulation of amino acid catabolic pathways in net handled fish suggests that amino acids may be being redirected toward protein synthesis.

Contrarily, in the HYP trial, the pattern of changes in protein abundance suggests an increase of amino acid catabolism. The protein 4-hydroxy-2-oxoglutarate aldolase (HOGA1) is an enzyme that catalyzes the conversion of 4-hydroxy-2-oxoglutarate into pyruvate or glyoxylate, which can enter the TCA cycle or the glyoxylate metabolism, respectively (Figure 3.2.7). Additionally, the enzyme adenosylhomocysteinase (AHCY), is involved in the Met cycle, catalyzing the reversible hydrolysis of S-adenosyl-homocysteine into adenosine and L-homocysteine (Ghisaura et al., 2014). This last intermediate of the cycle can be converted either back to methionine, or into L-cysteine, which can enter the glutathione metabolism (Figure 3.2.7). Both proteins (i.e., HOGA and AHCY) were found to be upregulated in the challenged fish from HYP trial.

3.2.5.3. Lipid metabolism

In addition to energy repartitioning from carbohydrate metabolism, it is also well-known that stress plays a role in enhancing lipid metabolism in fish liver (Mommensen et al., 1999). Cortisol is known to enhance the lipase activity, increasing lipid catabolism and the conversion of triglycerides into glycerol and free fatty acids (FFA). However, the mechanisms behind this action in fish are not fully described (Vijayan et al., 2010). For most fish species, fatty acid (FA) beta-oxidation is the major source of energy, in the form of ATP, which occurs in the mitochondria and peroxisomes. The degradation of FAs originates acetyl-CoA, which supports gluconeogenesis, ketogenesis and ATP production through the TCA cycle (Olivares-Rubio & Vega-López, 2016). Enoyl-coA hydratase is an enzyme which participates in both the mitochondrial and the peroxisomal beta-oxidation, while $\Delta^{3,5},\Delta^{2,4}$ -dienoyl-CoA isomerase is an auxiliary enzyme in the degradation of unsaturated fatty acids (Poirier et al., 2006) (Figure 3.2.7). Both were found to be upregulated in the liver of hypoxia-exposed fish, which agrees with previous studies on Nile tilapia exposed to hypoxia stress (M. Li et al., 2018). Similarly, in the OC trial, $\Delta^{3,5},\Delta^{2,4}$ -dienoyl-CoA isomerase was also found to be upregulated in the liver of overcrowded fish. Fatty-acid binding proteins (FABPs), which are implicated in the transport of these molecules to different cell compartments (Furuhashi et al., 2011), were also found to be differentially abundant in challenged fish from OC and NET trials. FABP3 was significantly downregulated in the liver of overcrowded fish, while in the NET4 group, two protein spots corresponding to this protein were identified as differently abundant, one up- and one downregulated,

making impossible to infer about the expression pattern of this protein in these fish. Contrarily, FABP1B.2 was downregulated in fish from NET4 group. The observed changes in lipid metabolism, similar to the pattern of changes observed in carbohydrate metabolism, add more weight to the different ways energetic resources can be used according to the severity of the challenge.

3.2.5.4. Antioxidant system

Reactive oxygen species (ROS) are generated as byproducts during the normal course of aerobic metabolism. ROS accumulation can lead to DNA mutation, mRNA and protein denaturation, membrane lipid peroxidation and ultimately, cell death (Bhattacharya, 2015). Generation of antioxidant proteins is the primary liver response against oxidative stress, such as SOD, peroxiredoxins (PRDX), thioredoxins (TXN) and glutathione (GSSH) system-related proteins. SOD is the first enzyme involved in ROS scavenging. It is a metalloenzyme responsible for catalyzing the dismutation of superoxide anion (O_2^-) into O_2 and hydrogen peroxide (H_2O_2). Peroxiredoxins catalyze the reduction of peroxides with the help of thioredoxin (Valero et al., 2015). Glutathione-S-transferase (GST) catalyzes the conjugation of cellular components damaged by ROS with reduced glutathione (GSSH) and nicotinamide adenine dinucleotide phosphate (NADPH) (Storey, 1996). All these proteins were found to be downregulated in challenged fish from all 3 trials (GSTM in OC trial, SOD1 and PRDX2 in NET trial, and PRDX2 and TXN in HYP trial), except for GSTM in hypoxia-exposed fish which was upregulated. The transcription levels of SOD1 were also found to be decreased in Atlantic cod exposed to hypoxia (Olsvik et al., 2006), while gilthead seabream exposed to cold stress also showed a decreased abundance of TXN (Ghisaura et al., 2019). This might suggest that FA beta-oxidation, in fish from overcrowding and hypoxia stress, occurred mainly in the mitochondria and not in the peroxisome, since the main byproduct of peroxisomal beta-oxidation would be H_2O_2 (Poirier et al., 2006). Moreover, as previously proposed, dysfunction of the ability to detoxify is itself a reflection of oxidative stress (Banh et al., 2016; Nuez-Ortín et al., 2018). This hypothesis is also supported in NET trial by the downregulation of BHMT which is responsible for maintaining steady levels of the glutathione precursor S-adenosylmethionine and preventing homocysteine accumulation (Obeid, 2013). Additionally, reduction in the abundance of ALDH2.2, which is an important protein in the detoxification of aldehydes (Xiao et al., 2009), may aggravate the effects of

potential oxidative stress in fish from NET4 group. Nevertheless, the secondary response to oxidative stress, characterized by the increased abundance of chaperones, was activated.

3.2.5.5. Cellular stress response

In the current study, a broad scale increase in abundance of chaperones and stress response proteins was observed in response to net handling and overcrowding challenges, whereas the majority was involved in the unfolded protein response (UPR). When there is an excessive accumulation of unfolded and/or misfolded proteins in the endoplasmic reticulum (ER) (ER stress), the UPR is activated to mitigate the situation and avoid apoptosis. This process can thus be interpreted as a quality control of protein conformation, whereas the correctly folded proteins are exported to the Golgi complex. In contrast, incorrectly folded proteins are retained at ER for refolding, by heat shock proteins, or targeted for proteasome-mediated degradation (Ji & Kaplowitz, 2006). The widely studied heat shock protein (HSP) family is composed of proteins with a cytoprotective role that are involved in protein refolding and assembly (Roberts et al., 2010). These proteins are usually upregulated in fish tissues in response to an array of different stressors (Iwama, Afonso, Todgham, et al., 2004; Vijayan et al., 2010). In our study, two different HSPs were significantly upregulated in the liver of net handled fish, the 78 kDa glucose-regulated protein (HSPA5/GRP78) and the 94 kDa glucose-regulated protein (HSP90B/GRP94). Regarding HSPA5, three spots were detected as DAPs, whereas only one presented downregulation in challenged fish (spot no. 319). However, more than one protein was significantly identified in this spot. This same increased regulation was also verified at the transcript level, whereas the RT-qPCR analysis of the corresponding gene expression showed statistically significant differences in GRP78 and GRP94 genes, between the challenged and the control fish from NET trial (Figure 3.2.5.B). The close relation of HSP90 with GR is well established in mammals. In teleosts, HSP90 was proposed to increase the stability of GR before it binds to cortisol (Sathiyaa & Vijayan, 2003). Moreover, *in vitro* exposure of rainbow trout hepatocytes to cortisol showed an upregulation of HSP90 (Aluru & Vijayan, 2007). The high plasma cortisol levels observed in net-handled fish, published in another work (Raposo de Magalhães, Schrama, et al., 2020), corroborates the transcript and corresponding proteins changes observed in this study. Calreticulin (CALR) together with protein-disulfide isomerases (PDI) are also involved in UPR (Grek & Townsend,

2013). CLR is the major calcium-binding protein of the ER (Kales et al., 2007). P4HB, PDIA3 and PDIP5 are different isoforms of the protein-disulfide isomerase family and play a crucial role in catalyzing disulfide bond formation (Grek & Townsend, 2013). These chaperones were significantly upregulated in challenged fish from NET trial, while CALR was likewise upregulated in challenged fish from OC trial. However, differential abundance of proteasome degradation proteins suggests that protein degradation was inhibited in net handled fish, since 26S protease regulatory subunit 6B (PSMC4) was downregulated. In hypoxia-exposed fish, no conclusive hypothesis can be generated since two isoforms of proteasome degradation proteins were identified, being one upregulated (PSMB3 and PSME2) and the other downregulated (PSMB2). Downregulation of proteasome degradation proteins was reported in the liver proteome of Atlantic cod following exposure to elevated temperatures (Nuez-Ortín et al., 2018). Contrarily, in overcrowded fish, proteasome subunit beta type-6 (PSMB6) and CTSD, a lysosomal protein also responsible for protein degradation, were found to be upregulated. CTSD was previously reported to be upregulated in the liver of trout following an acute stressor (Wiseman et al., 2007) and after a cortisol treatment (Aluru & Vijayan, 2007). These significant changes in the chaperones' abundance suggest that the high intensity of these challenges might have compromised the antioxidant defense barrier but enhanced the expression of heat shock proteins since oxidative stress may damage proteins.

3.2.5.6. Protein synthesis

Other proteins showing significant changes in abundance levels were related to the purine and pyrimidine metabolism, including nucleoside-diphosphate kinase (NME2B.1), purine nucleoside phosphorylase (PNP4B), and guanosine-30,50-bis(diphosphate) 30-pyrophosphohydrolase (HDCC3), to transcription [heterogeneous nuclear ribonucleoprotein (HNRNPABB)], and to translation, such as elongation factor-1-beta (EEF1B2), eukaryotic translation initiation factor 5A (EIF5A), 60S acidic ribosomal protein P2 (RPLP2), and ribosomal 40S subunit (RPSA), all undergoing upregulation to different extents in NET and HYP trials, thus indicating an overall increase in protein synthesis.

3.2.6. CONCLUSIONS

Our study demonstrates that the metabolic shift occurring in gilthead seabream liver to cope with a challenge and restore homeostasis, comprises an intricately complex network of proteins involved in different but coordinated metabolic pathways and cellular processes. Long-term exposure to repetitive net handling, coupled with air exposure, was associated with significantly perturbed carbohydrate metabolism and amino acid catabolism, and ER stress. The latter was also associated with overcrowded fish, although to a lower extent, together with alterations in lipid metabolism. In contrast, a shorter-term challenge (hypoxia) induced a different rearrangement of the stress response. However, considering the number of DAPs, net handling was undoubtedly the stressor that caused the highest impact on the liver proteome response. Additionally, two genes were found to be differently expressed in net-handled fish. However, a high variability was verified within the same group, which could be associated to individual biology or sample processing differences. Undeniably, a broader transcriptomic approach would be necessary to evaluate the direct activity of the genome under the conditions tested. Collectively, results suggest a response influenced mainly by the severity of the challenge, which appeared to be tightly associated with the plasma glucocorticoid levels. Differences in the circulating levels of cortisol could explain the different magnitude of proteome alterations after exposure to a continuous (overcrowding) and a repetitive (net handling) challenge. A possible habituation or exhaustion and desensitization by the overcrowded fish can skew interpretation of a “stressed state”. Finally, this work demonstrates the potential of proteomics approaches for the study of protein interactions and their roles in the mounting of the adaptive response to stress. Additionally, it provides a set of proteins that could be further investigated as novel stress markers to complement the currently used stress indicators. However, this data needs to be thoroughly validated before inferring about potential candidate biomarkers. Further integration of other omics modalities could provide a complete picture of the underlying biology behind the stress response modulation, across multiple organizational levels. Establishing, as accurately as possible, resting levels of the desired markers and studying the link between the quantification of the stress response with fitness traits and fish performance metrics would also be necessary. Nonetheless, this will provide a complementary approach to classical physiological and behavioral observations for the future development of a multidisciplinary welfare assessment.

3.2.7. SUPPLEMENTARY MATERIAL

Supplementary figures can be found in the [APPENDIX](#). Supplementary tables are available for this paper at: <https://www.frontiersin.org/articles/10.3389/fmars.2021.676189/full#supplementary-material>

3.3

Gilthead seabream liver integrative proteomics and metabolomics analysis reveals regulation by different prosurvival pathways in the metabolic adaptation to stress



It is a curious situation that the sea, from which life first arose should now be threatened by the activities of one form of that life.

— Rachel Carson in “The Sea Around Us”

This chapter has been published as research article in:

Raposo de Magalhães, C., Farinha, A.P., Blackburn, G., Whitfield, P.D., Carrilho, R., Schrama, D., Cerqueira, M., Rodrigues, P.M., 2022. Gilthead seabream liver integrative proteomics and metabolomics analysis reveals regulation by different pro-survival pathways in the metabolic adaptation to stress. *International Journal of Molecular Sciences*, 23(23), 15395. **doi: 10.3390/ijms232315395**



International Journal of
Molecular Sciences

3.3.1. ABSTRACT

The study of the molecular mechanisms of stress appraisal on farmed fish is paramount to ensuring a sustainable aquaculture. Stress exposure can either culminate in the organism's adaptation or aggravate into a metabolic shutdown, characterized by irreversible cellular damage and deleterious effects on fish performance, welfare, and survival. Multiomics can improve our understanding of the complex stressed phenotype in fish and the molecular mediators that regulate the underlying processes of the molecular stress response. We profiled the stress proteome and metabolome of *Sparus aurata* responding to different challenges common to aquaculture production, characterizing the disturbed pathways in the fish liver, i.e., the central organ in mounting the stress response. Label-free shotgun proteomics and untargeted metabolomics analyses identified 1738 proteins and 120 metabolites, separately. Mass spectrometry data have been made fully accessible via ProteomeXchange, with the identifier PXD036392, and via MetaboLights, with the identifier MTBLS5940. Integrative multivariate statistical analysis, performed with DIABLO, depicted the 10 most-relevant features. Functional analysis of these selected features revealed an intricate network of regulatory components, modulating different signaling pathways related to cellular stress, e.g., the mTORC1 pathway, the unfolded protein response, endocytosis, and autophagy, to different extents according to the stress nature. These results shed light on the dynamics and extent of this species' metabolic reprogramming under chronic stress, supporting future studies on stress markers' discovery and fish welfare research.

3.3.2. INTRODUCTION

Over the past 20 years, global aquaculture has been thriving and developing toward the critical goals of environmental, economic, and societal sustainability. Producing more food (i.e., calories, proteins, amino acids) per unit of land area is the current model for overcoming global population expansion. With the continuous intensification of aquaculture, the welfare of farmed fish is becoming a key issue, for which stress management has become a powerful tool to continue improving the sector's sustainable growth (F. Huntingford, 2008). Exposure to minor stressors is known to promote fish resilience, while major stressors can affect whole-animal performance and, in more severe cases, survival (Iwama et al., 2006). Fish respond to stressful stimuli through an elaborate endocrine machinery that provides the chemical mediation of a hypothalamic combined signal through the action of glucocorticoids, to manage the production and expenditure of energy and allow for a proper fight-or-flight response (Mommsen et al., 1999). The liver is the central organ in the energy management adaptation response, responsible for processes such as the synthesis of glucose and fatty acids degradation, to compensate for coping mechanisms. However, if the severity of the stimulus increases, the stress response can shift to an energy conservation state, and high-energy costly biological functions, such as immunity and growth, are suppressed, which might compromise fish welfare (Boonstra, 2013). At the hepatocyte level, cells undergo immediate changes to help their metabolism adapt and to protect themselves against potential damage. This process is orchestrated through a multilayered cellular program, which involves the concerted action of diverse stress-signaling pathways regulated at different levels of biological organization (Pakos-Zebrucka et al., 2016). The cellular stress response was recently reviewed in fish subjected to salinity (Evans & Kültz, 2020) and temperature stress (Somero, 2020). However, studies addressing the specific signaling pathways supporting the cellular stress response at different organizational levels are scarce.

High-throughput technological advances, such as “omics” approaches, allow for a deeper understanding of the intricate network of signaling pathways involved in the regulatory mechanisms responsible for the specific metabolic adaptation to different stressors. Proteins and metabolites represent the downstream outcome of an organism's genome and its interaction with the environment. Thus, untargeted proteomics and metabolomics analyses can provide a high-resolution snapshot of a fish subjected to a certain stressful stimulus. Proteomics has been extensively used to

study fish hepatic metabolism in response to different stressors (Causey et al., 2018; Gandar et al., 2017; Ghisaura et al., 2019; Naderi et al., 2018; Pédrón et al., 2017; Quan et al., 2021; Raposo de Magalhães et al., 2021; G. Zhang et al., 2017). On the other hand, the use of untargeted metabolomics in fish stress research, although less explored, has been occurring in recent years (Alfaro et al., 2021; Jiao et al., 2020; Ziarrusta et al., 2018). However, integrated multiomics studies are still limited. Combining omics strategies permits a more holistic understanding of the interrelationships of the active biomolecules and their corresponding functions, and it is becoming a powerful tool for life science research. However, in fish and aquaculture research, this approach is still hampered by the lack of genomic data, analytical tools, and comprehensive databases, among other aspects (Raposo de Magalhães, Cerqueira, et al., 2020). Notably, few studies with different fish species, combining different omics platforms, have provided remarkable insights into nutrition (Y. Wei et al., 2021) and exposure to environmental stressors (Colás-Ruiz et al., 2022; Dale et al., 2020; Wen et al., 2019; Z. X. Zhu et al., 2019) and pathogens (Ge et al., 2020; J. N. Li et al., 2020; Long et al., 2015).

Gilthead seabream (*Sparus aurata*) is one of the most produced finfish species in Mediterranean aquaculture and the fourth major species produced in Europe (FAO, 2022). Therefore, molecular insights into the stress physiology of this species could provide the industry with deeper knowledge on welfare conditions, eventually devising stress-mitigation strategies by conventional and modern farming to develop improved recommendations on best practices. To the best of our knowledge, the present work is the first multiomics study to portray signaling and metabolic pathway perturbations in challenged gilthead seabream. Herein, we subjected gilthead seabream adults to different challenges with different severities, simulating standard practices and conditions in an aquaculture farm, such as overcrowding, net handling and hypoxia, and conducted an integrated proteomics and metabolomics analysis of the liver tissue through high-resolution liquid chromatography coupled with mass spectrometry (LC-MS/MS). These data will link the interplay of different stress-signaling pathways to complex stress variation and enhance our understanding of biological stress pathways decoded by the animal stress response. We henceforward envisage an increase in the use of more-integrated approaches within fish stress research built upon the knowledge attained from comprehensive and system-wide studies to improve aquaculture sustainability and bring about a less-damaging food system.

3.3.3. MATERIALS & METHODS

3.3.3.1. Ethics

The present study was officially approved by the Responsible Body for Animal Welfare (ORBEA) of CCMAR and the Portuguese National Authority for the Animal Health (DGAV), on 26 August 2019. The animal experiments followed the European guidelines on the protection of animals used for scientific purposes (Directive 2010/63/EU) and Portuguese legislation for the use of laboratory animals, under a “Group 1” license (permit number 0420/000/000-n.99–09/11/2009) from the Veterinary Medicine Directorate, the competent Portuguese authority for the protection of animals, Ministry of Agriculture, Rural, Development and Fisheries, following the category C FELASA recommendations.

3.3.3.2. Fish and stocking conditions

Sparus aurata adults were randomly distributed in 500 L fiberglass tanks provided with flowthrough seawater from Ria Formosa. Physicochemical parameters varied according to natural fluctuations (natural photoperiod, water temperature at 13.4 ± 2.2 °C, salinity at 34.7 ± 0.8 ‰, and dissolved oxygen level above 5 mg L^{-1}). Fish were fed once daily, by hand, with a commercial feed (Standard Orange 6) from “AquaSoja, Sorgal, S.A” (Ovar, Portugal), according to the species’ nutritional requirements. Experimental trials took place at the Ramalhete Research Station of CCMAR (Faro, Portugal), and fish were supplied by the company “Maresa, Mariscos de Estero S.A.” (Huelva, Spain).

3.3.3.3. Experimental design

Three separate experimental trials were conducted, where fish were subjected to three challenges: OC—overcrowding; NET—repetitive net handling, coupled with air exposure; and HYP—hypoxia. Two experimental groups were set for each trial: (1) control group (CTRL) and (2) challenged group. Triplicate tanks were used for each group (i.e., a total of six tanks per trial), with an initial rearing density of 10 kg m^{-3} (except for the high-rearing-density group, as further described). In the OC trial, fish with average IBW of 373.89 ± 11.04 g were subjected to high stocking densities of over 54 days. Experimental groups were established as follows: (1) CTRL — 10 kg m^{-3} and (2) OC45 — 45 kg m^{-3} . In the NET trial, fish (IBW = 376.52 ± 8.96 g) were challenged for 45 days with specific nets designed for the purpose: (1) CTRL — undisturbed fish

(the net was likewise fit inside the tanks but not lifted) and (2) NET4 — fish netted four times a week (fish were lifted and air-exposed for one min). The last air-exposure challenge was performed 72 h before sampling. In the HYP trial, fish (IBW = 405.74 ± 35.14 g) experienced low levels of saturated oxygen in the water over 48 h. Experimental groups were established as follows: (1) CTRL had 100% saturated oxygen and (2) HYP15 had 15% saturated oxygen. Measurements of saturated oxygen levels were conducted every 30 min to keep track of potential fluctuations and adjust nitrogen injection if necessary. Zootechnical results were previously published by the authors (Raposo de Magalhães, Schrama, et al., 2020).

3.3.3.4. Sampling

At the end of each trial, fish were starved for 48 h to clean the digestive tract, according to normal practice in aquaculture production. Three fish were randomly sampled from each tank and immediately anesthetized with a lethal dose of MS-222 (Merck KGaA). Liver samples were collected, chopped, divided into two Eppendorf tubes (i.e., one for proteomics and one for metabolomics), immediately frozen in liquid nitrogen, and stored at -80 °C until further use.

3.3.3.5. Sample preparation

For proteomics analysis, liver protein extracts ($n = 6$, two fish per tank; tank unit as biological replicate) were obtained from 50 mg of tissue solubilized with 500 μ L of extraction buffer (7 M urea, 2 M thiourea, 4% CHAPS, 30 mM Tris pH 8.5), 5 μ L of proteases' inhibitor (PI) cocktail (Merck KGaA), and 2 μ L of 250 mM EDTA. Sample homogenization was conducted by using a tissue lyser (VWR) with 5 mm metal beads for two cycles of 30 s, at a frequency of 25/s. Homogenates were incubated at 4 °C for 30 min, in constant rotation and centrifuged at 13,000 g and 4 °C for 15 min to remove insoluble material. Liver extracts were diluted in the initial buffer, and the protein content was measured by using the BioRad Quick Start Bradford Dye Reagent and BSA Standard Set (Bio-Rad). Extracts were then depleted of nonprotein contaminants by using the ReadyPrep™ 2D Clean-Up kit (Bio-Rad), following the manufacturer's instructions. The cleaned protein pellet was further resuspended in 100 mM Tris pH 8.5, 1% sodium deoxycholate, 10 mM TCEP, 40 mM chloroacetamide, and protease inhibitors for 10 min at 95 °C at 1000 rpm (Thermomixer, Eppendorf, Hamburg, Germany). Subsequently, samples were prepared according to the solid-phase-

enhanced sample-preparation (SP3) protocol (Hughes et al., 2018). Enzymatic digestion was conducted with 2 µg Trypsin/LysC overnight at 37 °C at 1000 rpm.

For metabolomics analysis, 10 mg of liver tissue (n = 9, three fish per tank; tank unit as biological replicate) were homogenized on a tissue lyser, with chloroform/methanol/water 1:3:1 (v/v/v) at 4 °C and a 5 mm metal bead, for 30 s, at 25/s frequency. Homogenates were incubated at 4 °C for 1 h, in constant rotation, and lastly centrifuged for 3 min at 13,000 g and 4 °C. The supernatant was collected and analyzed by LC-MS/MS. In addition, 10 µL from each supernatant sample was pooled as the quality control (QC) sample.

3.3.3.6. Label-free shotgun proteomics analysis

3.3.3.6.1. NanoLC-MS/MS analysis

Peptides from enzymatic digestion (500 ng) were analyzed through online nanoLC using an UltiMate™ 3000 system coupled with a Q-Exactive Hybrid Quadrupole-Orbitrap mass spectrometer (Thermo Scientific, Bremen, Germany). Samples were loaded onto a trapping cartridge (Acclaim PepMap C18 100 Å, 5 mm × 300 µm i.d., 160454, Thermo Scientific) in the mobile phase (2% ACN, 0.1% FA at 10 µL min⁻¹). After 3 min loading, the trap column was switched inline to a 50 cm by 75 µm inner-diameter EASY-Spray column (ES803, PepMap RSLC, C18, 2 µm, Thermo Scientific) at 250 nL min⁻¹. Separation was achieved by mixing A: 0.1% FA and B: 80% ACN, 0.1% FA, with the following gradient: 5 min (2.5% B to 10% B), 120 min (10% B to 30% B), 20 min (30% B to 50% B), 5 min (50% B to 99% B), and 10 min (hold 99% B). Subsequently, the column was equilibrated with 2.5% B for 17 min. Data acquisition was achieved by using Xcalibur 4.0 and Tune 2.9 software (Thermo Scientific).

The mass spectrometer was operated in data-dependent acquisition (DDA), in positive mode, alternating between a full scan (m/z 380–1580) and a subsequent HCD MS/MS of the 10 most-intense peaks from the full scan (normalized collision energy of 27%). The ESI spray voltage was 1.9 kV and capillary temperature was 275 °C. Global settings were: use lock masses best (m/z 445.12003), lock-mass injection full MS, and chromatography peak width (FWHM) of 15 s. Full scan settings: 70k resolution (m/z 200), AGC target 3e6, and maximum injection time 120 ms. DDA settings: minimum AGC target 8e3, intensity threshold 7.3e4. Charge exclusion: unassigned, 1, 8, > 8, peptide match preferred, exclude isotopes on, dynamic exclusion 45 s. MS2 settings: microscans 1, resolution 35k (m/z 200), AGC target 2e5, maximum injection time 110

ms, isolation window 2.0 m/z, isolation offset 0.0 m/z, dynamic first mass, and spectrum data-type profile. MS analyses were performed at the Proteomics Scientific Platform of i3S, Porto, Portugal.

3.3.3.6.2. *Protein identification*

Raw MS data were processed by using SEQUEST® on Proteome Discoverer™ software 2.5.0.400 (Thermo Scientific) and searched against the UniProtKB Eupercaria database (taxon ID 1489922; Release 2020_05; 651,914 sequences). The SEQUEST HT search engine was used for the identification of tryptic peptides. The ion mass tolerance was set at 10 ppm for precursor ions and 0.02 Da for fragmented ions. A maximum of two missed cleavage sites was allowed, with a minimum peptide length of six amino acids and 144 as maximum. Cysteine carbamidomethylation was defined as constant modification. Methionine oxidation, protein N-terminus acetylation, and loss of methionine and Met-loss+Acetyl were defined as variable modifications. Peptide confidence was set to high. The Inferys rescoring node was considered for this analysis. The processing node Percolator was enabled with the following settings: maximum delta Cn 0.05; decoy database search target FDR \leq 1%, validation based on q-value. Protein label-free quantitation was performed with the Minora feature detector node at the processing step. Precursor ions quantification (TOP3) was performed at the processing step with the following parameters: peptides to use unique plus razor, precursor abundance was based on intensity, normalization mode was based on total peptide amount, and the pairwise protein ratio calculation and hypothesis test were based on a *t*-test (background based). Magellan storage files (.msf) were imported into Scaffold v.4.11.1 (Proteome Software Inc., Portland, OR, USA) to validate MS/MS-based peptide and protein identifications. A second search engine, i.e., X! Tandem algorithm (the GPM, thegpm.org; version X! Tandem Alanine 2017.2.1.4), was applied to all MS/MS samples, by using a reverse-concatenated subset of the UniProtKB Eupercaria database (release 2020_05; 651,914 entries), also assuming Trypsin digestion and parent ion tolerance of 10 ppm and a fragment ion mass tolerance of 0.020 Da. Carbamidomethyl of cysteine was specified as a fixed modification and Glu->pyro-Glu of the N-terminus, ammonia-loss of the N-terminus, gln->pyro-Glu of the N-terminus, oxidation of methionine and acetyl of the N-terminus as variable modifications. Peptide identifications were accepted if they could be established at a greater than 92% probability to achieve an FDR less than 0.1% by the

peptide prophet algorithm (Keller et al., 2002) with Scaffold delta-mass correction; protein identifications were accepted at a minimum 99% probability to achieve an FDR less than 1% by the protein prophet algorithm (Nesvizhskii et al., 2003), containing at least three identified peptides. Proteins containing similar peptides that could not be differentiated based on MS/MS analysis alone were grouped to satisfy the principles of parsimony. The MS proteomics data were deposited on the ProteomeXchange Consortium (Deutsch et al., 2020) via the PRIDE (Perez-Riverol et al., 2019) partner repository with the dataset identifier PXD036392 and 10.6019/PXD036392.

3.3.3.7. Untargeted metabolomics analysis

All samples were analyzed on a Thermo Scientific Q-Exactive Orbitrap mass spectrometer, running in positive/negative switching mode, connected to a Dionex UltiMate™ 3000 RSLC system (Thermo Fisher Scientific, Hemel Hempstead, UK) using a ZIC-pHILIC column (150 mm × 4.6 mm, 5 μm column, Merck Sequant, Gillingham, UK). The column was maintained at 30 °C, and samples were eluted with a linear gradient (20 mM ammonium carbonate in water for A and acetonitrile for B) over 46 min at a flow rate of 0.3 mL/min as follows: 0 min 20% A, 30 min 80% A, 31 min 92% A, 36 min 92% A, 37 min 20% A, and 46 min 20% A. The injection volume was 10 μL, and samples were maintained at 5 °C prior to injection. The MS settings were as follows: resolution 70,000, AGC 1e6, m/z range 70–1050, sheath gas 40, auxiliary gas 5, sweep gas 1, probe temperature 150 °C, and capillary temperature 320 °C. For positive mode ionization: source voltage +3.8 kV, S-Lens RF Level 30.00, S-Lens Voltage 25.00 (V), Skimmer Voltage 15.00 (V), Inject Flatopole Offset 8.00 (V), and Bent Flatopole DC 6.00 (V). For negative mode ionization: source voltage was 3.8 kV. The calibration mass range was extended to cover small metabolites by including low-mass calibrants with the standard Thermo calmix masses (below m/z 138): butylamine (C₄H₁₁N₁) for positive ion electrospray ionization (PIESI) mode (m/z 74.096426) and COF₃ for negative ion electrospray ionization (NIESI) mode (m/z 84.9906726). To enhance calibration stability, lock-mass correction was also applied to each analytical run (positive mode: lock mass (m/z) 144.9822; negative mode: lock mass (m/z) 100.9856). To assess the running of the instrument, the pooled samples (QC) were assessed for reproducibility and were run throughout the sample analysis, every fifth sample.

The raw mass spectrometry data were preprocessed using the polyomics-integrated metabolomics pipeline (PiMP) (Gloaguen et al., 2017). Briefly, data were converted from Thermo proprietary raw files (.raw) to the open format mzXML and uploaded to PiMP. Within PiMP, unique signals were extracted by using the XCMS centwave algorithm (C. A. Smith et al., 2006) and matched across biological replicates based on a mass-to-charge ratio (m/z) and retention time. These grouped peaks were then filtered on the basis of relative standard deviation and combined into a single file. The combined sets were then filtered on signal to noise score, minimum intensity, and minimum detections. The final peak set was then gap filled and displayed in the PiMP user interface. Filters were applied using MZMatch (Scheltema et al., 2011). Metabolite identifications were validated by comparing the chromatographic retention times and the m/z values against a set of in-house standards. The metabolites' level of identification was classified according to the Metabolomics Standards Initiative (MSI) (Table S4 - [online](#)) (Sumner et al., 2007). The MS metabolomics data were deposited on MetaboLights (Haug et al., 2020) with the dataset identifier MTBLS5940.

3.3.3.8. Univariate and multivariate statistical analyses

Protein abundance was estimated based on TOP3 precursor intensity, and normalized values (against the sum of all ion intensities in each sample replicate) were log₁₀ transformed prior to statistical analysis (Farinha et al., 2021). The residuals' normality and homoscedasticity were confirmed by using the SPSS™ Statistics software v.25.0 (IBM™, Armonk, NY, USA). Univariate statistical analyses of proteomics data were performed in the Perseus software (Tyanova et al., 2016), including only proteins quantified in at least four out of six replicates per experimental group. Differences in protein abundance between control group and experimental group, within each trial, were analyzed by using a Student's t -test ($p < 0.05$) with FDR controlled at 0.05. Statistical analyses of the metabolomics data were performed on MetaboAnalyst 5.0 (Pang et al., 2021), using only the metabolites detected in at least six out of nine replicates per experimental group. Prior to univariate hypothesis testing, peak intensities were log₁₀ transformed and Pareto scaled, and the missing values were imputed based on one-fifth of the minimum positive value of each variable. Differential analysis was achieved by a Student's t -test ($p < 0.05$) with FDR controlled at 0.05.

A multivariate statistical analysis was performed by using R v.4.2.0 (R Core Team, 2022) for MacOSX. Group separation and replicates' variability were analyzed, for each data modality, through PCA, using the `prcomp` R function in the auto scaled matrices. Missing values were imputed based on the feature median. Biplots were generated by using the R package `factoextra` (Kassambara & Mundt, 2020). DIABLO algorithm, within the R package `mixOmics` (Rohart et al., 2017), was used to perform the integrative analysis of proteomics and metabolomics datasets (identified proteins and metabolites) and depict the 10 most-correlated and discriminatory features between both data modalities. The parameters of the final DIABLO model were tuned based on three-fold CV repeated five times and using the centroids distance as distance metric.

3.3.3.9. Functional analyses

Joint pathway analysis (JPA) of DAPs and differentially abundant metabolites (DAMs) was performed on MetaboAnalyst 5.0, using the Entrez IDs for proteins and compound KEGG IDs for metabolites as queries and *Danio rerio* as reference. Overrepresentation analysis (ORA) was achieved with two-sided hypergeometric test, followed by Benjamini-Hochberg method for p -value correction and using the combined p -values at the pathway level as integration method. Enriched terms and the corresponding features were visualized on a cnetplot using the R package `enrichplot` (Yu, 2022a). The search tool for the interactions of chemicals (STITCH) (Kuhn et al., 2008) was used to generate, for each trial, a metabolic reaction network (protein-metabolite) of DAPs and DAMs. Protein identifiers from the STRING database (Szklarczyk et al., 2021) and compound names were used as queries. Networks were visualized and topologically analyzed with the Cytoscape software v.3.8.1 (Shannon et al., 2003), using the plugin MCODE (Bader & Hogue, 2003) to extract significant clusters from the main network according to the default parameters. Enriched REACTOME terms within the features selected by the DIABLO model were depicted by using the analysis tool from the knowledgebase REACTOME (Fabregat et al., 2017), with the identifiers projected to human orthologs as queries and visualized as Voronoi plots.

All figures were created by using the open-source graphics editor Inkscape (<http://www.inkscape.org/>).

3.3.4. RESULTS

3.3.3.1. Proteomics and metabolomics data overview

Proteomics analysis of gilthead seabream liver led to a mean of $40\% \pm 2\%$ of peptide spectrum matches (PSM) out of a mean of $27,122 \pm 917$ total spectra per MS/MS sample (Table S1 - [online](#)). About 1738 proteins were identified with a probability higher than 99% to achieve a false discovery rate (FDR) of $< 1\%$ assigned by the protein prophet algorithm, with at least three peptides, on the Scaffold software (Table S2 - [online](#)). From these, 1443, 1435, and 1418 reproducible proteins, present in at least four out of six replicates were selected from OC, NET, and HYP trials, respectively, for further statistical analyses. On the other hand, metabolomics analysis detected 3393, 5846, and 3616 peaks for the OC, NET, and HYP liver samples, respectively, from which 840, 1189, and 894 metabolite-like signals were annotated on the basis of mass and retention time, and 84, 112, and 89 were identified against authentic in-house standards (Table S4 - [online](#)).

A differential analysis of the liver proteomes between the control and challenged groups revealed 40, 349, and 46 differentially abundant proteins (DAPs) (Student's *t*-test, $p < 0.05$, 5% FDR) among the OC, NET, and HYP trials, respectively, from which 20, 202, and 20 were upregulated in the challenged group, and 20, 147, and 26 were downregulated (Table S3 - [online](#)). A Student's *t*-test with 5% FDR correction of the metabolomic data identified 40 and 58 peaks corresponding to confidently identified metabolites, significantly changing in abundance ($p < 0.05$) in NET- and HYP-challenged groups, compared with the corresponding control group. No DAMs were identified between control fish and challenged fish in the OC trial (Table S5 - [online](#)).

The score scatter plots (Figure 3.3.1) of the PCA showed that the first two principal components were able to capture 35.8%, 41.5%, and 27.9% of the total variability of OC, NET, and HYP trials data, respectively. A clear separation between groups was obtained for the NET data along the PC1 axis. The plots display the top-five features with the highest loading values as variable arrows. The PCA of the metabolomics data, conducted with the identified and single-annotated metabolites, showed that PC1 and PC2 were able to explain 38.7%, 41%, and 37.9% of the variability within OC, NET, and HYP datasets, respectively, achieving a better group separation for the NET and HYP trials than the PCA did, according to the proteomics data. In Figure 3.3.1, the top-five features with the highest loading values are displayed as variable arrows in the biplots.

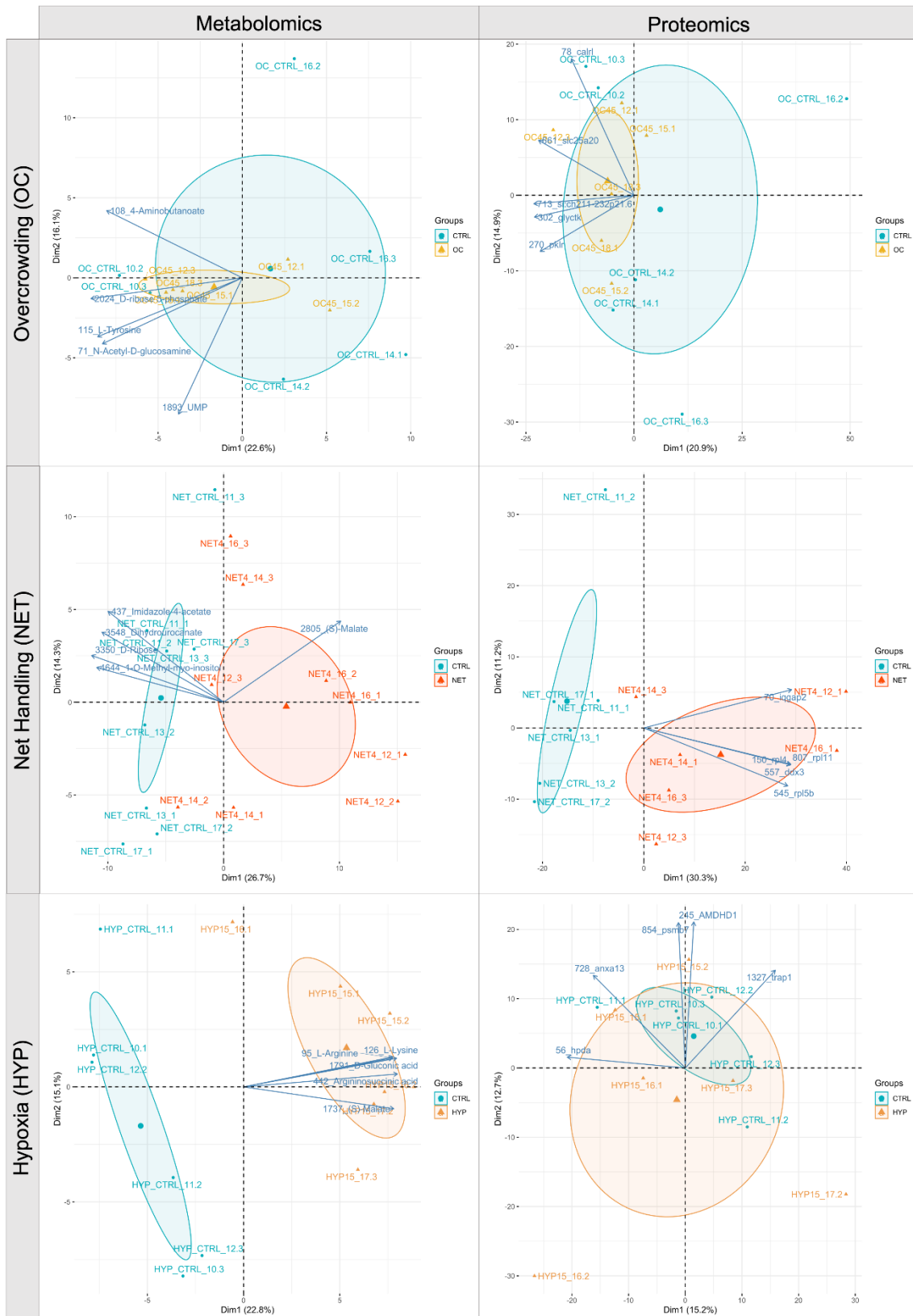


Figure 3.3.1. PCA biplots of the liver proteomics and metabolomics data of gilthead seabream subjected to overcrowding (OC), net handling (NET), and hypoxia (HYP) challenges. Each point represents a biological replicate's projection, and experimental groups within trials are represented by a unique color, as indicated in each legend. The largest point represents the group mean. The axes' percentages indicate the proportions of explained variance. The arrows depict the top-five most weighted variables.

3.3.4.2. Integrated stress response analysis

An overrepresentation analysis (ORA) of differential proteins and metabolites from NET fish liver resulted in 12 overrepresented KEGG terms with FDR < 0.05, the three most enriched being ribosome (FDR = 1.032×10^{-22}), protein processing in ER (FDR = 2.384×10^{-14}), and one-carbon pool by folate (FDR = 0.002) (Figure 3.3.2; Table S6 - [online](#)). Regarding the HYP analysis, 11 enriched terms were revealed: ABC transporters (FDR = 4.926×10^{-08}), aminoacyl-tRNA biosynthesis (FDR = 0.003) and alanine, aspartate, and glutamate metabolism (FDR = 0.003) were the three most enriched (Figure S3.3.1 - [APPENDIX](#)). No joint pathway analysis (JPA) was performed for the OC data because no DAMs were identified by univariate hypothesis testing.

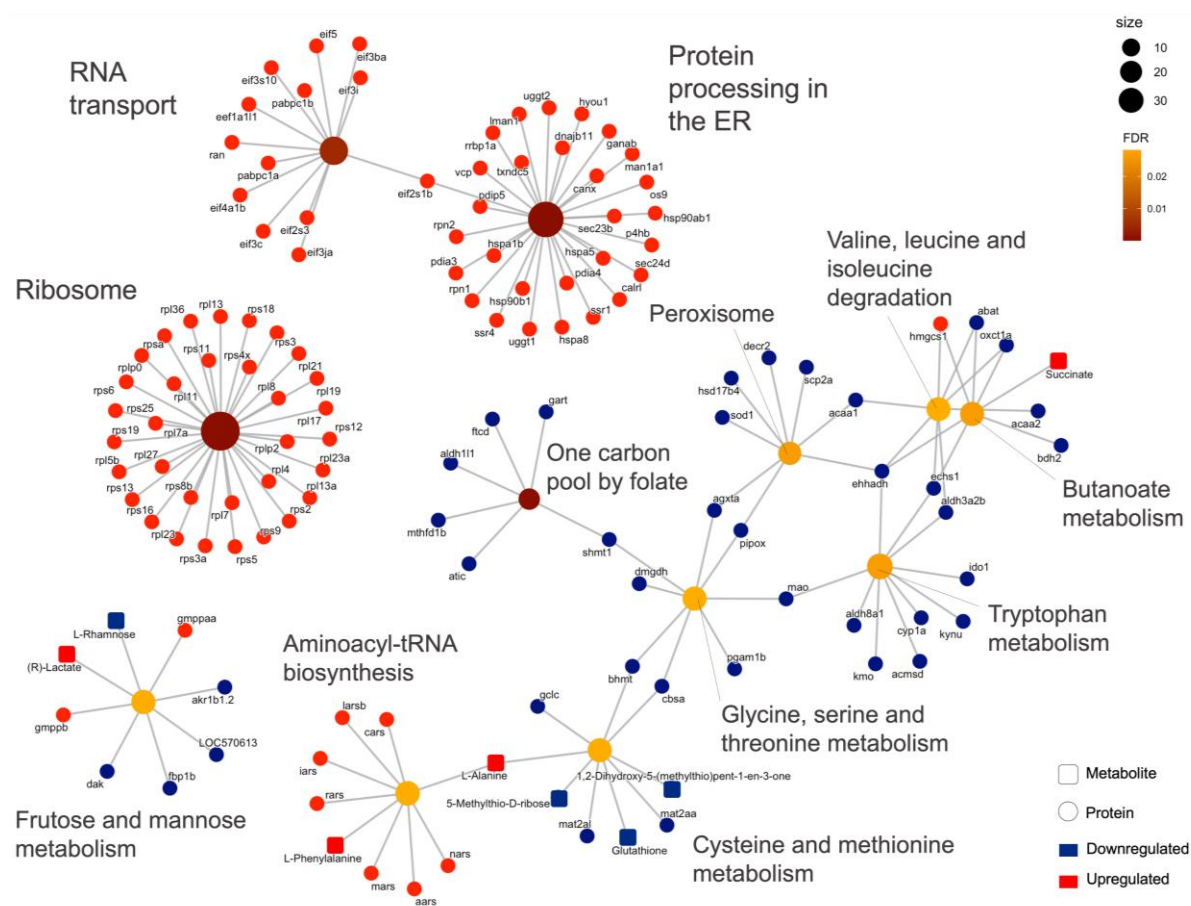


Figure 3.3.2. A gene-concept network of enriched KEGG terms (FDR < 0.05) within the differential abundant proteins (DAPs) and metabolites (DAMs) identified in the liver of gilthead seabream subjected to the net handling (NET) challenge. Central nodes represent the enriched term, with color and size representing FDR and the number of associated biomolecules, respectively. The concept nodes represent biological concepts, where shape corresponds to the omics modality and color to the regulation of that biomolecule, determined by Student's *t*-test with FDR controlled at 0.05.

A metabolic reaction network (metabolite protein) was generated for each trial, i.e., NET and HYP, with the corresponding DAPs and DAMs. The topological analysis on Cytoscape revealed a network with 296 nodes, 3176 edges, and a clustering coefficient of 0.428, for the NET trial, with four main clusters highlighted by MCODE plugin (Figure 3.3.3). The top three nodes with the highest betweenness centrality were succinate, phenylalanine, and alanine. The JPA conducted on each cluster individually showed that the enriched KEGG terms were involved mainly in translation, folding processes, and amino acid metabolism (Figure 3.3.3). The HYP trial DAPs and DAMs generated a network with 71 nodes, 438 edges, a clustering coefficient of 0.704, and one highly interconnected cluster identified by MCODE. Proteins in this cluster were enriched mainly in KEGG terms related to amino acids, nucleotides, and lipid metabolism. The highest betweenness centrality values were attributed to phosphate, ATP, and ADP metabolites (Figure S3.3.2 - [APPENDIX](#)).

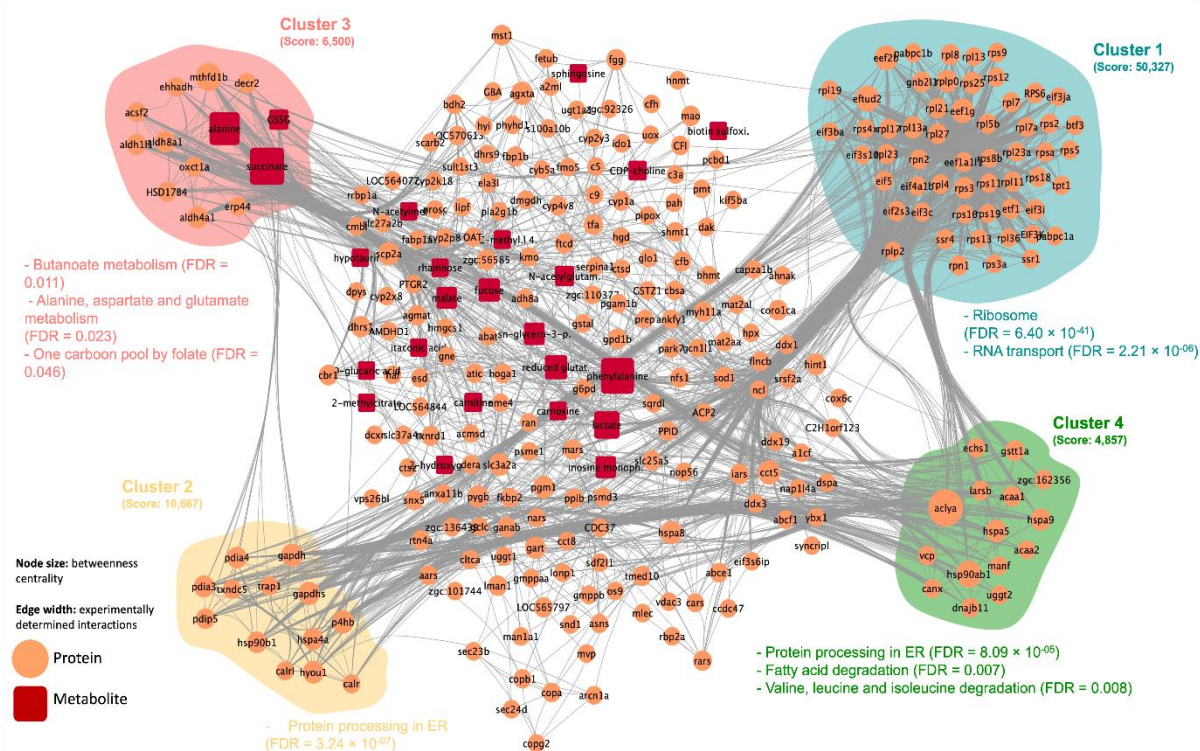


Figure 3.3.3. Metabolic reaction network generated with the differential abundant proteins and metabolites identified in the liver of gilthead seabream subjected to a net handling challenge. Node shape and color represent the type of biomolecule, according to the legend. Edges represent functional linkages between them. The highlighted clusters, depicted with the MCODE plugin within Cytoscape software, represent the most interconnected regions, with the corresponding overrepresented in KEGG terms (FDR < 0.05).

DIABLO was used to perform a correlation analysis between both data modalities and to depict each trial's 20 most discriminatory features (10 metabolites and 10 proteins). The arrow plot (Figure 3.3.4.A) of the first two components of the NET DIABLO model showed that group separation was achieved over the first dimension and that replicates' variability was consistent across omics datasets. Proteomics and metabolomics data showed a Pearson correlation of 0.95 on the first component, with six proteins and five metabolites showing $r > 0.9$, as demonstrated in the circos plot from Figure 3.3.4.B. The features from the first component were then subjected to an ORA on the REACTOME database (Table S7 - [online](#)), according to their expression patterns, to depict the biological functions and pathways that were most affected by the NET challenge (Figure 3.3.4.C).

A total of 106 terms presented $FDR < 0.05$, for the upregulated proteins and metabolites, where transport of small molecules ($FDR = 2.19 \times 10^{-2}$), cellular responses to stimuli ($FDR = 2.19 \times 10^{-2}$) and metabolism of proteins ($FDR = 2.19 \times 10^{-2}$) were the three most enriched higher-level terms. In the case of the downregulated features, 10 lower-level terms showed $FDR < 0.05$, being mostly implicated in the metabolism of certain amino acids and peroxisomal processes. Regarding the HYP trial, the final DIABLO model calculated two components that could separate control from the hypoxia challenged group along the dimension 1 axis, according to the arrow plot in Figure S3.3.3.A - [APPENDIX](#). The Pearson correlation between both data modalities on the first component was 0.96, while four proteins and six metabolites among the selected features demonstrated $r > 0.8$ (Figure S3.3.3.B - [APPENDIX](#)). A REACTOME overrepresentation analysis of the selected upregulated and downregulated features (Figure S3.3.3.C - [APPENDIX](#)) showed that 84 terms were upregulated ($FDR < 0.05$), the transport of small molecules ($FDR = 6.91 \times 10^{-3}$), metabolism ($FDR = 2.16 \times 10^{-2}$), and cellular responses to stimuli ($FDR = 6.47 \times 10^{-2}$) being the most enriched. On the other hand, among the 77 downregulated terms with $FDR < 0.05$, the three most enriched were mainly integrating energy metabolism, protein repair, and the metabolism of vitamins and cofactors.

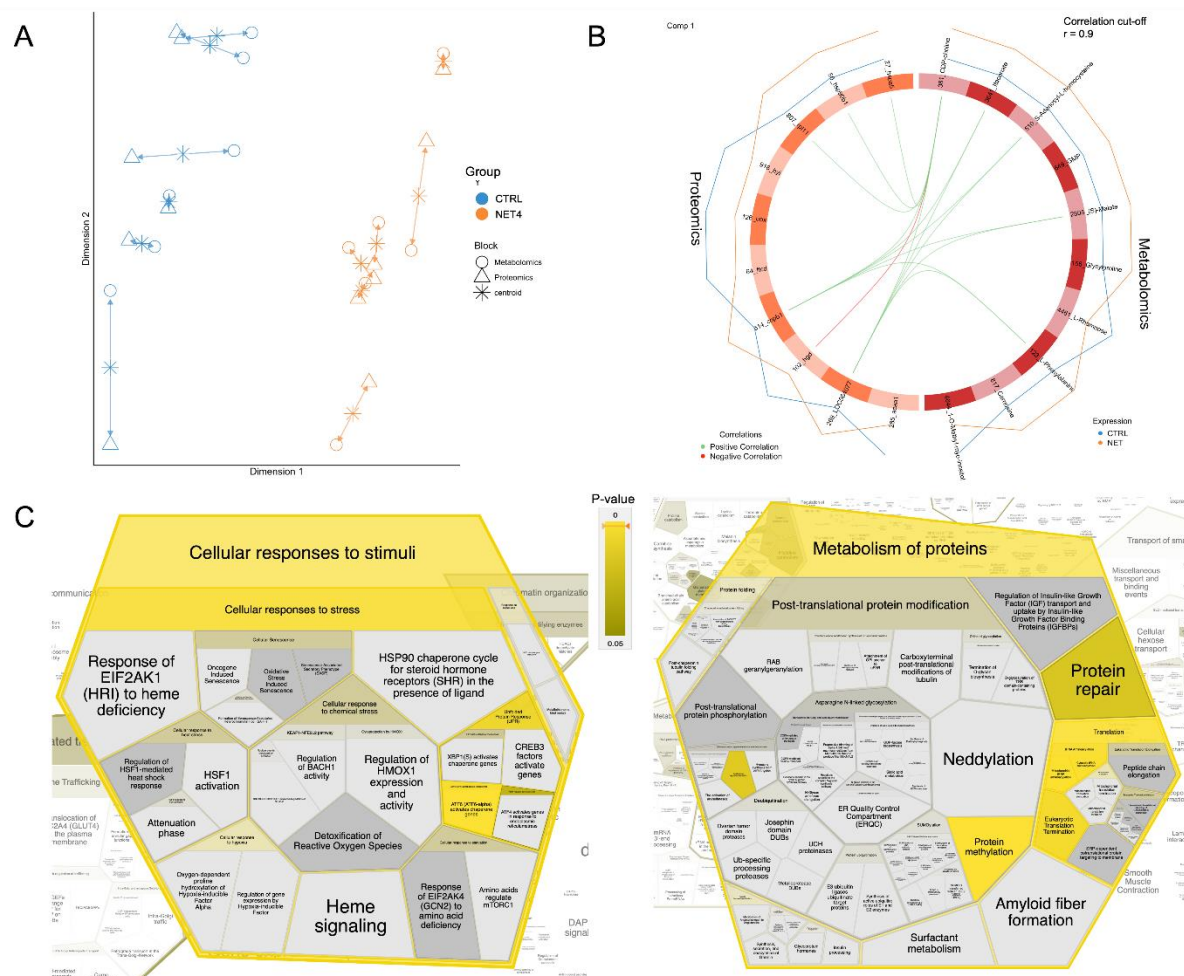


Figure 3.3.4. Integrated proteomics and metabolomics analysis, conducted with DIABLO, of the liver of gilthead seabream subjected to the net handling challenge (NET). (A) Arrow plot of the separation between groups achieved with the first two components of the DIABLO model. Different shapes represent different data modalities. (B) Circos plots representing the Pearson correlation (correlation cutoff = 0.9) between the 10 most-discriminatory proteins and metabolites selected by the first component of the DIABLO model. (C) Voronoi plots obtained with a REACTOME analysis tool represent two of the most overrepresented high category terms (FDR < 0.05), among the upregulated features selected by DIABLO. The *p*-value scale indicated in the figure legend corresponds to the adjusted *p*-value.

3.3.5. DISCUSSION

The stress response is a regulatory mechanism conserved among vertebrates, which comprises a cascade of events from the molecular to the whole individual level. This internal disturbance can either culminate in the organism's adaptation, characterized by a compensating stress response (i.e., reallocation of energy resources with reversible physiological damage and potentially improved fish fitness), or scale up to a metabolic shutdown, characterized by irreversible cellular damage and resulting in permanent deleterious effects on fish performance and survival. What defines this threshold depends on individual (e.g., species, age, previous experiences,

coping styles) and/or stressor-related factors (e.g., severity), increasing the difficulty of defining a stressed phenotype in fish (Wendelaar Bonga, 1997). The molecular regulation of this complex response occurs at different biological levels, and therefore, the integrated approach employed in this study provides a systemic perspective of the main interactions between the hepatic proteome and metabolome and unveils the main pathways underpinning this species' stress response to different challenges. In aquatic animals, the liver is responsible for the storage, production, and reallocation of energy resources and is one of the most profoundly affected organs during a stress response (Vijayan et al., 2010). It has been shown that the magnitude of the liver response greatly depends on the severity of the stimulus (Raposo de Magalhães et al., 2021), specifically acute vs chronic stimuli. At the cellular level, this translates into stress responses that can be manifold, ranging from the activation of survival pathways, which are geared toward helping the cell recover from the insult, to eliciting programmed cell death. The cell's fate critically relies on its ability to mount an appropriate stress response.

In this study, the numbers of dysregulated proteins and metabolites in the liver suggested that net handling was the challenge that induced the most intense metabolic reprogramming in gilthead seabream (349 DAPs and 40 DAMs vs 46 DAPs and 58 DAMs in the HYP trial and 40 DAPs and 0 DAMs in the OC trial), most likely related to its severity (1^{1/2} months compared with the 48 h of the hypoxia challenge). These results might also suggest a multistress effect, as recently proposed (Petitjean et al., 2019), which might have resulted from a synergetic combination of net handling and air exposure. Previous plasma and liver analyses conducted on these same fish, published elsewhere (Raposo de Magalhães et al., 2021; Raposo de Magalhães, Schrama, et al., 2020), also verified this same difference in response to these different challenges. According to the ORA performed with REACTOME on the NET proteins and metabolites selected by the DIABLO model (Table S7 [-online](#)), terms related to the metabolism of amino acids, amino acid transport across the plasma membrane, UPR, and translation were included among the most enriched ones. Notably, pathways related to the catabolism of amino acids were mainly downregulated, whereas pathways related to the biosynthesis of a specific set of amino acids were essentially upregulated. Simultaneously, amino acid transport, translation, and UPR were upregulated (Figure 3.3.4.C). These results suggest that net handling most likely induced cellular stress and that challenged fish coped with the stress by activating this

prosurvival pathway, i.e., UPR. UPR is directly and indirectly related to the other overrepresented pathways through different regulatory processes, in an intricate network of signaling pathways to ensure cell survival and tissue homeostasis, as will be further discussed. The protein–metabolic interaction network also demonstrated this interconnection between these pathways (Figure 3.3.3).

During normal and stressful circumstances, secreted proteins undergo maturation in the ER before being exported to the Golgi apparatus, if properly assembled. Cellular stress may disturb this process, resulting in the accumulation of unfolded/misfolded proteins in the ER and culminating in the orchestration of the UPR. This response is initiated by three ER-resident molecular proteins, most notably inositol-requiring protein-1 (IRE1), protein kinase RNA (PKR)-like ER kinase (PERK), and activating transcription factor 6 (ATF6), which will activate three intracellular signal transduction pathways. PERK phosphorylates eukaryotic initiation factor 2 (eIF2 α) and allows the translation of activating transcription factor 4 (ATF4), which may, in turn, activate the transcription of chaperones and other proteins involved in the regulation of apoptosis (e.g., C/EBP Homologous Protein (CHOP)), autophagy (e.g., autophagy related 12 (ATG12)), and amino acid metabolism (e.g., asparagine synthetase (ASNS)). PERK can also directly phosphorylate the transcription factor NF-E2-related (NRF2), which induces the expression of antioxidant genes (Fulda et al., 2010). In this study, proteins eIF2 α and ASNS were upregulated in NET-challenged fish. Accordingly, in largemouth bass exposed to heat stress, eIF2 α gene was also reported to be upregulated, along with other UPR-related genes (X. Zhao et al., 2022). In contrast, ATF6 is first activated in the Golgi and then acts as a transcription factor of chaperones, such as the 78 kDa glucose-regulated protein (BiP/GRP78/HSPA5) and the 94 kDa glucose-regulated protein (HSP90B1), x-box-binding protein 1 (XBP1), and genes involved in the ER quality control machinery (e.g., calreticulin (CALRL)) (Fulda et al., 2010). HSPA5 and HSP90B1 were upregulated in NET-challenged fish, together with five other heat-shock proteins (HSPs) (Table S3 - [online](#)). In fact, the upregulation of proteins from the HSP family is a commonly reported response to stress in fish (Iwama, Afonso, Todgham, et al., 2004; Vijayan et al., 2010). Corroborating these results, these proteins were previously reported to be upregulated in the liver of these same fish, after a gel-based proteomics analysis, along with a positively correlated expression pattern of the corresponding genes, assessed by real-time polymerase chain reaction (RT-PCR) (Raposo de Magalhães et al., 2021). Lastly, IRE1 catalyzed

the alternative splicing of XBP1 mRNA, leading to the expression of the XBP1 transcription factor (TF). Subsequently, this TF activated the expression of numerous genes, encoding proteins from the ER quality control machinery (e.g., hypoxia upregulated 1 (HYOU1), DnaJ heat-shock protein family member B11 (DNAJB11), protein disulfide-isomerase 6 (PDIP5)), ER-associated degradation (ERAD), and lipid synthesis (Fulda et al., 2010). In summary, in NET-challenged fish, several proteins that participated in these processes, i.e., UPR, protein folding, quality control, protein tracking to Golgi (COPII-dependent anterograde transport), and ERAD, were upregulated, suggesting that NET-challenged fish's hepatic cells activated UPR to attempt to improve the balance between protein load and folding capacity, by translating specific proteins, and consequently to attenuate ER stress. The upregulation of different aminoacyl-tRNA synthetases and several translation-related proteins (Table S3 - [online](#)) corroborated this hypothesis. Furthermore, previous studies have reported an upregulation of ER stress in seawater-transferred rainbow trout livers (Morro et al., 2021), common carp exposed to hydrogen peroxide (R. Jia et al., 2020), rainbow trout following overcrowding stress (Valenzuela et al., 2020), and gilthead seabream exposed to low temperatures (Mininni et al., 2014). On the other hand, PDIP5 was found to be downregulated in hypoxia-exposed fish, exposing again the divergent responses of NET and HYP fish according to the challenge severity. A schematic diagram summarizing these stress mechanisms and the associated dysregulated proteins is depicted in Figure 3.3.5.

The ERAD system mediates the removal of incorrectly folded proteins in a multistep process involving the recognition and targeting of substrates, followed by ubiquitination, retrotranslocation, and degradation (Tepedelen & Kirmizibayrak, 2019). After ubiquitination, protein recycling can occur through autophagy and/or the ubiquitin-proteasome system (UPS) (Kocaturk & Gozuacik, 2018). NET fish presented 12 proteins involved in the ERAD process that were found to be upregulated, suggesting that protein degradation was stimulated in challenged fish. Nevertheless, two proteins belonging to the proteasome showed ambiguous expression patterns (PSMD3 was upregulated, whereas PSME1 was downregulated). The same was verified for HYP fish (PSMD6 was upregulated, whereas PSMD5 was downregulated) (Figure 3.3.5). In OC fish, proteasome subunit beta type-6 (PSMB6) was upregulated. Changes in proteasome subunits were reported in Atlantic cod in response to *V. anguillarum* infection (Rajan et al., 2013) and high-temperature exposure (Nuez-Ortín et al., 2018).

Interestingly, heat-shock protein family A (Hsp70) member 8 (HSPA8), an upregulated protein in NET-challenged fish's ERAD response, is involved in a process called "chaperone-mediated autophagy", which entails the direct delivery of cytosolic proteins, targeted for degradation, to the lysosomes. However, this cellular function has been poorly described in fish because, until recently, it was presumed to be exclusive to mammals and birds (Lescat et al., 2018, 2020). Moreover, the upregulation of HSPA8 was also observed in Senegalese sole following repeated handling stress (Cordeiro et al., 2012b) and in gilthead seabream fed maslinic-supplemented diets (Matos et al., 2013).

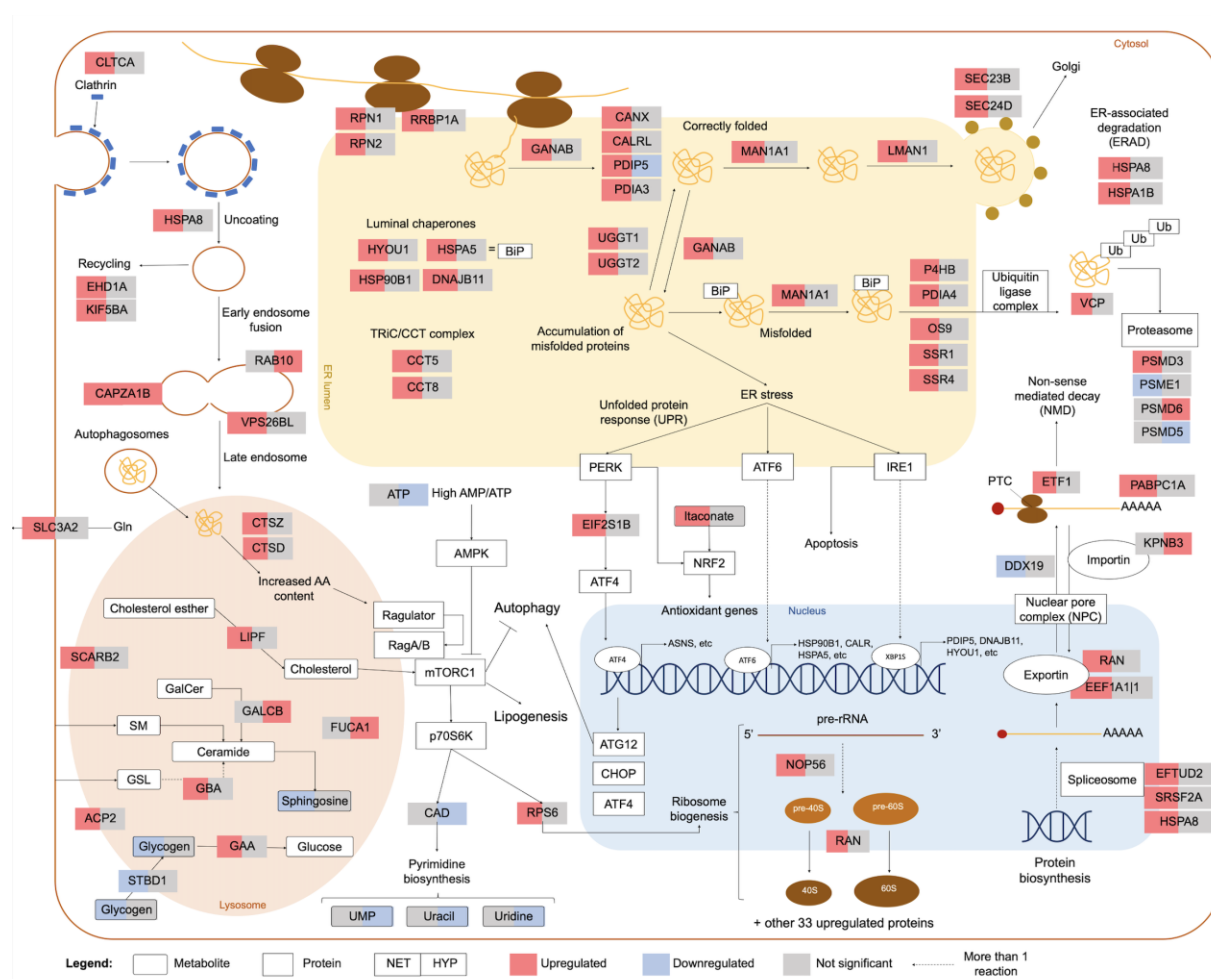


Figure 3.3.5. Overview of the cellular processes and signaling pathways affected by net handling and hypoxia in gilthead seabream hepatocytes. The proteins and metabolites represented were differentially different in abundance, according to a Student's *t*-test with FDR controlled at 0.05.

Macroautophagy, the best-described form of autophagy, is a key pathway in stress-induced metabolic adaptation and damage control. It is responsible for

degrading intracellular substrates, such as organelles or proteins, in bulk or selectively by encasing them in double-membraned vesicles, called autophagosomes, which are then delivered to the lysosome (Cuervo, 2004). On the other hand, the degradation and recycling of extracellular substrates are facilitated by endocytosis. The dynamic remodeling of the plasma membrane proteome is crucial to the cellular adaptation to stress, as many signaling cascades originate at the cell surface receptors. In clathrin-mediated endocytosis (CME), responsible for most of this flux, formed vesicles later fuse with lysosomes for content degradation. CME also contributes to the uptake of material such as metabolites, hormones, and other proteins from the extracellular space (López-Hernández et al., 2020). The degradation in the lysosome is then mediated by the action of hydrolases, including cathepsins. Both NET- and HYP-challenged fish had upregulated proteins involved in these pathways (Figure 3.3.6), suggesting that endocytosis also participated in the cellular stress response to these challenges. Cathepsin d (CTSD) has previously been reported to be upregulated in the liver of trout following an acute stressor (Wiseman et al., 2007). Different cathepsins were also upregulated in fasting gilthead seabream (Salmerón et al., 2015). Additionally, glycogen is also delivered to the lysosomes by selective autophagy, in a mechanism known as “glycophagy”. Glycogen is the main carbohydrate store in fish liver, and a rapid generation of glucose after acute stimuli is usually achieved by glycogen breakdown (Faught & Vijayan, 2016). The lysosomal hydrolytic degradation of glycogen in the liver has been proposed as an alternative route, occurring in parallel to the canonical glycogenolysis pathway in cytosol, to meet high-circulating-glucose demands for systemic utilization. Contrary to glycogenolysis, glycophagy produces non phosphorylated glucose that can be more rapidly used (Mandl & Bánhegyi, 2018). However, in fish, these mechanisms are still poorly described. Nonetheless, glycogen phosphorylase B (PYGB), responsible for catalyzing the phosphorolysis of glycogen in the first step of glycogenolysis, was found to be downregulated in NET fish (Figure 3.3.6). Alongside, lysosomal alpha-glucosidase (GAA), responsible for the breakdown of glycogen in the lysosomes, was upregulated (Figure 3.3.5), suggesting that glycogen degradation was occurring mainly at the lysosomal level. Concomitantly, glycogen levels in NET fish were significantly downregulated, as previously assessed by commercial kits and published in another work (Raposo de Magalhães et al., 2021), whereas plasma glucose levels were significantly upregulated (Raposo de Magalhães, Schrama, et al., 2020). Lysosomes are the control center of catabolic and anabolic

processes in eukaryotic cells, recycling the building blocks of the cargo delivered by endocytic and autophagic pathways and regulating cell physiology. In fact, lysosomes have been recently investigated as signaling hubs and central organelles in the mammalian cellular stress response (Lakpa et al., 2021; Lawrence & Zoncu, 2019; Saftig & Puertollano, 2021). In fish, lysosomal stability has been used as a bioindicator of environmental toxicity (Köhler et al., 2002).

One of the most important regulators of cell metabolism, growth, and proliferation is the mechanistic target of rapamycin complex 1 (mTORC1), which is activated mainly by growth factors and both high amino acid cytosolic and intraluminal content. When activated, mTORC1 is recruited to the cytosolic face of the lysosomal membrane. Henceforth, a complex cascade of tightly regulated reactions switches the metabolism toward anabolic processes such as ribosome biogenesis, protein synthesis, glucose metabolism, and nucleotide and lipid synthesis and inhibits catabolic processes such as autophagy. At a downstream level, mTORC1 activates p70 ribosomal protein S6 kinase1 (p70S6K), which further phosphorylates ribosomal protein S6 (RPS6) and carbamoyl phosphate synthetase 2-aspartate transcarbamoylase-dihydroorotase (CAD), responsible for inducing ribosome biogenesis and *de novo* pyrimidine biosynthesis, respectively (Heberle et al., 2015). Results for NET fish are contradictory regarding mTORC1 signaling, in that RPS6 and several other proteins involved in ribosome biogenesis (35 proteins in total) were upregulated (Figure 3.3.5), whereas some proteins participating in purine and pyrimidine biosynthesis were downregulated. On the one hand, the production of one-carbon units required for *de novo* purine biosynthesis was downregulated (Figure 3.3.2), and on the other hand, the glutamine-leucine SLC3A2-SLC7A5 antitransporter and leucyl-tRNA synthetase (LARS), two proteins known to activate mTORC1 (J. M. Han et al., 2012; Nicklin et al., 2009), were found to be upregulated in these fish. Hence, more analyses would be needed to infer this pathway's regulation on NET fish. Undeniably, mTOR signaling regulation in fish has been extensively described in muscle growth (Johnston et al., 2011; Vélez et al., 2014) and nutrition studies (Farinha et al., 2021; S. L. Han et al., 2020; Sáez-Arteaga et al., 2022). In stress-related studies, genes involved in mTOR signaling were found to be upregulated in the liver of gilthead seabream subjected to hyper- and hypo-osmotic challenges (Martos-Sitcha et al., 2016). However, the mTORC1 regulatory mechanisms in fish during stress remain largely elusive. In contrast, in HYP fish, results suggest that this pathway was

potentially downregulated, as CAD and pyrimidine biosynthesis-related proteins were downregulated, as were adenosine triphosphate (ATP) levels (Figure 3.3.5). Additionally, asparagine, a nonessential amino acid known to stimulate mTORC1 signaling (Yoo et al., 2022), was similarly downregulated (Figure 3.3.6). Low ATP levels inhibit mTORC1 because this complex responds to cellular energy status via the heterotrimeric adenosine monophosphate (AMP)-activated protein kinase (AMPK). When the cellular ATP:AMP ratio is low, which is common in hypoxia stress because of a shortage in oxygen and consequently an impaired mitochondrial respiratory chain, AMPK inhibits mTORC1 to conserve energy because protein biosynthesis consumes the lion's share of energy and cellular resources (Chun & Kim, 2021). In the liver of goldfish subjected to hypoxia, the authors reported that AMPK activity increased by ~5.5-fold, with no increase in protein abundance, suggesting that changes in AMPK activity are most likely due to PTMs. These were accompanied by an increase in the ATP:AMP ratio and a decrease in protein synthesis (Jibb & Richards, 2008). The same was verified for rainbow trout (Williams et al., 2019). The inhibition of the mTOR-signaling pathway was reported in Arctic char exposed to hypoxia, precisely 15% of air saturation, along with a decrease in the rate of protein synthesis (Cassidy & Lamarre, 2019). In humans, the dysregulation of the mTOR-signaling pathway has been associated with aging and several diseases (Laplante & Sabatini, 2012).

During aerobic conditions, pyruvate, resulting from glycolysis, is introduced into the tricarboxylic acid (TCA) cycle, which theoretically generates 36 ATP molecules via a respiratory chain in the mitochondria (Kierans & Taylor, 2021). Inadequate tissue oxygenation inhibits the process of oxidative phosphorylation (OXPHOS), and fish can generate ATP only through substrate-level phosphorylation, which includes converting pyruvate into lactate in the cytosol, and phosphate transfer from intermediates such as creatine phosphate (PCr) (Richards, 2009). Accordingly, in this study, pyruvate carboxylase (PCL), which catalyzes the conversion of pyruvate into oxaloacetate to enter the TCA cycle, was downregulated in hypoxia-exposed fish, whereas lactate and creatine phosphate were upregulated (Figure 3.3.6). The downregulation of isocitrate dehydrogenase (IDH1), an enzyme of the TCA cycle, in these fish also corroborates the suppression of this pathway, together with the upregulation of glucogenic amino acids (e.g., alanine, arginine, proline), which enter the TCA cycle to further produce glucose (Figure 3.3.6). Concomitantly, a 1H-NMR-based metabolomics study revealed an upregulation of lactate, alanine, and PCr in hypoxia-exposed common carp (Lardon

et al., 2013). Interestingly, in NET fish, lactate was likewise upregulated in challenged fish, and cytochrome c oxidase subunit 6C (COX6C), the terminal enzyme of the mitochondrial respiratory chain, was downregulated, suggesting that OXPHOS was also downregulated in net-handled fish (Figure 3.3.6).

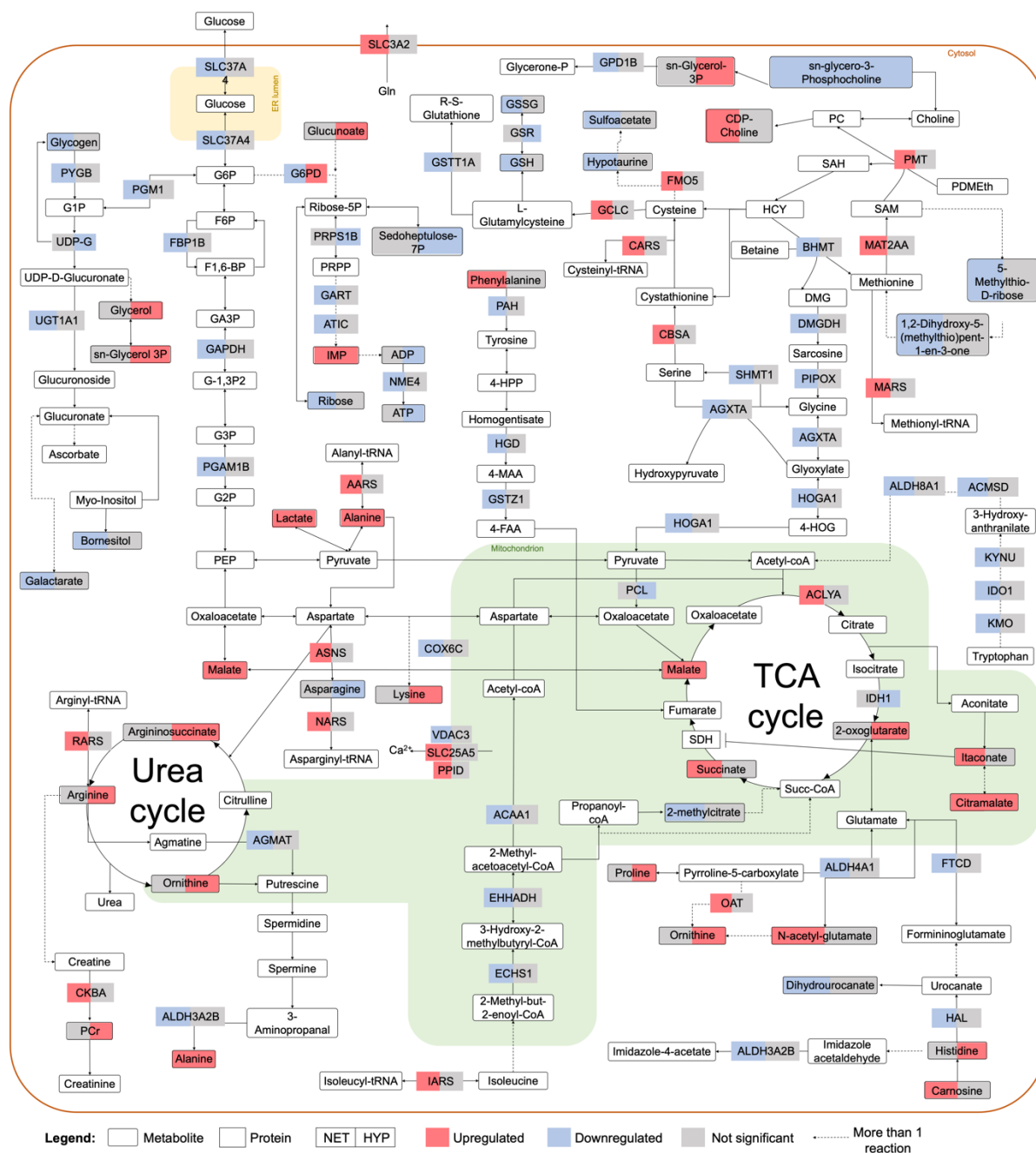


Figure 3.3.6. Overview of the metabolic pathways affected by net handling and hypoxia in gilthead seabream hepatocytes. The proteins and metabolites represented were significantly different in abundance, according to a Student's *t*-test with FDR controlled at 0.05.

Another metabolite involved in OXPHOS is succinate, a substrate of the TCA cycle, which is at the crossroads of numerous other metabolic pathways, such as the

degradation of branched-chain amino acids (BCAAs), GABA shunt, and PTMs, among others. Succinate was found to be upregulated in NET fish (Figure 3.3.6), which might be explained by the fact that succinate dehydrogenase (SDH), responsible for converting succinate into fumarate as part of OXPHOS, is inhibited by the metabolite itaconate (Tretter et al., 2016). Itaconate is derived from the decarboxylation of cis-aconitate, a substrate of the TCA cycle, and it has been described as an important regulatory metabolite of inflammation, modulating innate immunity to limit tissue damage and metabolism. Apart from inhibiting SDH, and consequently OXPHOS and reactive oxygen species (ROS) generation, it also decreases glycolysis by inhibiting key enzymes, i.e., glyceraldehyde-3-phosphate dehydrogenase (GAPDH) and aldolase a (ALDOA). Moreover, it alkylates Kelch-like ECH-associated protein 1 (KEAP1), inducing the release of nuclear factor NRF2, an antioxidant regulator, and has an anti-inflammatory effect by decreasing the levels of inflammatory cytokines (R. Li et al., 2020). In humans, itaconate has been extensively described in macrophages and recently in liver tissue (Yi et al., 2020). Results suggest a potential modulatory effect mediated by itaconate in NET fish, given that the metabolite was upregulated in challenged fish, along with a significant downregulation of GAPDH (Figure 3.3.6). Several proteins implicated in the immune system were regulated by the net handling challenge (Table S3 - [online](#)), including six-transmembrane epithelial antigen of the prostate 4 (STEAP4), a metalloredutase involved in iron and copper homeostasis (Scarl et al., 2017), which was significantly affected by all challenges, i.e., OC, NET, and HYP. Currently, we are unable to corroborate the regulatory effect and importance of itaconate in gilthead seabream metabolism and immunity after stress exposure. However, these are interesting data in light of the evidence that itaconate is such an important regulatory metabolite in humans.

3.3.6. CONCLUSIONS

The fish stress response has been extensively studied at different levels, e.g., behavioral changes, physiological indicators, metabolic adaptations, immune responses, oxidative stress, the genomic and nongenomic effects of glucocorticoids, etc. However, the regulatory mechanisms of cellular stress are less explored, and studies addressing the cellular stress response at different organizational levels are scarce. Stress-related signaling pathways are evolutionarily conserved, playing an important role in maintaining homeostasis and ensuring cell survival.

In this multiomics study, we demonstrated that the gilthead seabream responded to cellular stress through an intricate network of regulatory components, modulating different signaling pathways to different extents, according to the stress nature. Furthermore, mTORC1 signaling appears to be the crosstalk between ER stress and metabolic reprogramming, stimulating/inhibiting a myriad of biosynthetic and catabolic processes, otherwise maintained at basal homeostatic states, depending on the cell resources' availability. Net-handled fish appear to have activated the UPR to deal with an ER flooded with unfolded/misfolded proteins, shutting down most metabolic pathways to shift the energy toward the translation of stress-related mRNAs. Contrarily, hypoxia-exposed fish, because of the low availability of cellular energy, appear to have downregulated protein synthesis in an mTORC1-dependent manner. Notably, endocytosis was an upregulated shared pathway between NET and HYP fish, suggesting an important role in stress homeostasis. Fish exposed to overcrowding showed lower alterations at the proteome level and no significant alterations at the metabolome level, suggesting that gilthead seabream might be more resistant to high rearing densities than to physical stresses or low oxygen availability. Additionally, the integrated analysis depicted the most dysregulated pathways, along with the interconnections between the proteins and the metabolites that were responding to the different challenges. This study shows that both omics validated and complemented each other, presenting a clear advantage over more conventional single-omics analyses and paving the way to more holistic approaches in fish stress research. These findings provide interesting new avenues of investigation for the study of unbiased fish welfare biomarkers, which will not only impact the aquaculture industry resilience by offering better decision-making and stress prevention strategies but also offer higher food safety from aquaculture products.

3.3.7. SUPPLEMENTARY MATERIAL

Supplementary figures can be found in the [APPENDIX](#). Supplementary tables are available for this paper at: <https://www.mdpi.com/article/10.3390/ijms232315395/s1>

3.4

Underlining the hepatic transcriptional changes behind *Sparus aurata* responses to different aquaculture challenges: an RNA-seq study



Life has a way of talking to the future. It's called memory. It's called genes.

— Richard Powers in “The Overstory”

This chapter was submitted as research article to:

Raposo de Magalhães, C., Sandoval, K., Kagan, F., McCormack, G., Schrama, D., Carrilho, R., Farinha, A.P., Rodrigues, P.M., Cerqueira, M. 2023. Underlining the hepatic transcriptional changes behind *Sparus aurata* responses to different aquaculture challenges: an RNA-seq study. BMC Genomics, **Submitted**

 **BMC** Series
BMC Genomics

3.4.1. ABSTRACT

Gilthead seabream (*Sparus aurata*) is an important species in Mediterranean aquaculture. Rapid intensification of its production and other husbandry practices can cause stress, impairing overall fish performance and raising issues related to sustainability, animal welfare, and food security and safety. The advent of next-generation sequencing technologies has greatly revolutionized the study of fish stress biology, allowing a deeper understanding of the molecular stress responses. Here, we characterized for the first time, using RNA-seq, the different hepatic transcriptome responses of gilthead seabream to common aquaculture challenges, namely overcrowding, net-handling, and hypoxia, further integrating them with the liver proteome and metabolome responses. After reference-guided transcriptome assembly, annotation, and differential gene expression analysis, 7, 343, and 654 genes were differentially expressed (adjusted p-value < 0.01, $\log_2|\text{fold-change}| > 1$) in the overcrowding, net handling, and hypoxia challenged groups, respectively. Gene set enrichment analysis (FDR < 0.05) suggested a scenario of challenge-specific responses, that is, net handling induced ribosomal assembly stress, whereas hypoxia induced DNA replication stress in gilthead seabream hepatocytes, consistent with proteomics and metabolomics' results. However, both responses converged upon the downregulation of insulin growth factor signaling and induction of endoplasmic reticulum stress. These results support the high phenotypic plasticity of this species and its differential responses to distinct challenging environments at the transcriptomic level. Furthermore, it provides significant resources for characterizing and identifying potentially novel genes that are important for gilthead seabream resilience and aquaculture production efficiency with regard to fish welfare.

3.4.2. INTRODUCTION

Within genomics and transcriptomics, the advent of next-generation sequencing (NGS) has greatly revolutionized the study of biological systems, allowing for the rapid sequencing of whole genomes, transcriptomes, and molecular markers (e.g., SNPs), including those in aquatic model systems. At the time of this writing, 248 representative fish genome assemblies at the chromosome level were available in the NCBI genome database, with 94% of those released only in the last four years, including the gilthead seabream (*Sparus aurata*) genome. NGS-based RNA sequencing (RNA-seq) has recently become more accessible; however, in fish, transcriptomics is still in the nascent stage. However, besides mapping and annotating fish transcriptomes, it has already offered valuable insights into many biological processes in commercially important fish species and has helped scientists tackle many challenges in aquaculture (Chandhini & Rejish Kumar, 2019; X. Qian et al., 2014). Using solutions such as RNA-seq to integrate the use of various optimization production criteria is pivotal for the sector's sustainability and competitiveness.

Ensuring the sustainable growth and development of aquaculture in response to its evident intensification is at the forefront of priorities for meeting the increasing fish consumption rate of the global population. In fact, aquaculture is currently the most important industry worldwide to compensate for the declining and rapidly accelerating depletion of wild fish stocks. Its production is projected to continue to increase and reach 106 million tonnes of aquatic animals by 2030, compared to 87.5 million tonnes registered in 2020 (FAO, 2022). However, the continued increase in the number of aquatic animals produced poses many challenges for meeting the global demand for fish. Disregarding the overall farming conditions may significantly impact different measures of fish performance, and consequently, productivity (Conte, 2004). Sub-optimal husbandry conditions, such as high rearing densities, can be stressful for some fish species and consequently affect growth rates, trigger aggressive/unwanted behaviors, and reduce disease resistance (Ashley, 2007). Furthermore, prolonged exposure to high stocking densities has been shown to negatively affect the response to subsequent stimuli such as acute net confinement (Ruane et al., 2002). Hypoxia is often associated with overcrowding and is known to induce significant physiological changes such as reduced appetite, depressed metabolic rates and muscle oxidative capacity, and a switch in substrate preference towards more oxygen (O₂)-efficient fuels (Naya-Català et al., 2021). Unpredictable physical stressors such as handling are

common procedures in aquaculture farms that can increase the chances of abrasion, wounds, and infections, thereby causing severe stress (Ashley, 2007).

Fish display different coping mechanisms to deal with environmental challenges through adaptive neuroendocrine and metabolic adjustments, collectively termed stress responses (Galhardo et al., 2009). The hypothalamic-pituitary-interrenal (HPI) axis mediates this response, promoting the synthesis of glucocorticoid hormones (e.g., cortisol) that activate distinct signaling and metabolic pathways responsible for the overall physiological rearrangement needed to adapt to the new internal disturbance (Wendelaar Bonga, 1997). The liver is the leading organ in this response, managing substrate administration by synthesizing glucose and regulating somatic growth, immune response, detoxification, and synthesis of stress-related proteins (Faught & Vijayan, 2016).

High-throughput transcriptomic studies with different fish species have mainly focused on the immunological responses to pathogens and parasites (Ye et al., 2018), and on the effects of alkalinity (Y. Zhao et al., 2015), rearing density (Ellison et al., 2020; Rodriguez-Barreto et al., 2019), temperature (J. Huang et al., 2018; Song & McDowell, 2021; Wang et al., 2019; T. Zhou et al., 2019), salinity (X. Zhang et al., 2017), ammonia (Z. X. Zhu et al., 2019), and fasting (Y. F. Dai et al., 2021; B. Qian et al., 2016). However, studies on the transcriptional effects of other aquaculture stressors are still lacking. Stress-related RNA-seq studies on gilthead seabream have focused on the effects of ultraviolet B radiation exposure in the skin (Alves & Agustí, 2022), gill tissue response to an ectoparasite (Piazzon et al., 2019), whole-brain analysis of food-deprived individuals (Ntantali et al., 2020), and the effects of mild hypoxia in the muscle (Naya-Català et al., 2021). To our knowledge, no study has addressed and compared the hepatic transcriptome response to different aquaculture challenges in gilthead seabream, a highly consumed and produced fish in the Mediterranean region (Hough, 2022).

Therefore, in this study, RNA-seq was employed to assess the transcriptional machinery behind stress adaptation, underlining and quantifying the genes and gene families expressed in the liver of gilthead seabream adults in response to different aquaculture challenges, namely, overcrowding, net handling, and hypoxia. Multiomics integration was further performed to compare the most significant dysregulated biological functions in the proteome, metabolome, and transcriptome. The multi-level characterization of stress adaptation mechanisms provides valuable knowledge for the

future selective breeding of more resilient commercial species that can thrive under changing conditions and adapt well to life in captivity while ensuring high welfare standards.

3.4.3. MATERIALS AND METHODS

3.4.3.1. Fish husbandry

Gilthead seabream (*Sparus aurata*) adults, supplied by the company “Maresa, Mariscos de Estero S.A.” (Huelva, Spain) were maintained at the Ramalhete Research Station of the CCMAR facilities (Faro, Portugal) under standard rearing conditions. Throughout the experimental trials, fish were maintained in 500 L fiberglass tanks with a flow-through system with seawater from the local Ria Formosa (natural photoperiod, water temperature: 13.4 ± 2.2 °C, dissolved oxygen level: > 5 mg L⁻¹, and salinity: 34.7 ± 0.8 psu). Fish were fed once daily by hand (% body weight day⁻¹ adjusted when necessary), with commercial feed (Standard Orange 6) from “AquaSoja, Sorgal, S.A” (Ovar, Portugal), according to the nutritional requirements of the species.

3.4.3.2. Experimental trials and sampling

Three experimental trials were conducted separately, where fish were subjected to three different challenges: OC, Overcrowding, NET, repetitive net handling coupled to air exposure; and HYP, hypoxia. In each trial, fish were randomly assigned to two experimental groups: (1) the control group (CTRL) and (2) the challenged group. Each experimental group was divided into three tanks with an initial rearing density of 10 kg m⁻³ (except for the high rearing density group, as described further). In the OC trial, fish with an average initial body weight (IBW) of 373.89 ± 11.04 g were reared under high stocking densities over 54 days. Experimental groups were established as follows: (1) CTRL – 10 kg m⁻³ and (2) OC45 – 45 kg m⁻³. In the NET trial, fish (IBW = 376.52 ± 8.96 g) were challenged for 45 days with nets designed for the purpose that were fitted inside the tanks: (1) CTRL – undisturbed fish (the net was equally fitted inside the tanks but not lifted) and (2) NET4 – fish were lifted and air-exposed for 1 min, four-times a week. In the HYP trial, fish (IBW = 405.74 ± 35.14 g) were reared under low levels of dissolved oxygen for 48 h. Experimental groups were established as follows: (1) CTRL – 100% saturated oxygen and (2) HYP15 – 15% saturated oxygen. Saturated oxygen levels were measured every 30 min to keep track of potential fluctuations and adjust

the nitrogen injection if necessary. The zootechnical results have been previously published (Raposo de Magalhães, Schrama, et al., 2020).

At the end of each trial, three fish were randomly collected from each tank and immediately anesthetized using a lethal dose of tricaine methanesulfonate (MS-222; Merck KGaA, Darmstadt, Germany). Liver samples were collected, chopped, immediately frozen in liquid nitrogen, and stored at -80 °C until further use. According to standard aquaculture practices, fish were starved for 48 h before sampling to clean the digestive tract.

3.4.3.3. Liver RNA sequencing

3.4.3.3.1. Total RNA extraction and purification

Total RNA was extracted from 70 mg of gilthead seabream liver samples (n = 9, 3 fish per tank; tank unit as a biological replicate) using TRI reagent® (T9424, Sigma-Aldrich, Merck), following the manufacturer's instructions, with slight modifications. Briefly, after homogenizing the tissue with an autoclaved micropestle in 1 ml TRI reagent®, homogenates were centrifuged at 12,000 × g for 10 min at 4 °C and the supernatant was left to stand at room temperature (RT) for 5 min. Phase separation was achieved with 200 µL of cold chloroform (-20 °C), followed by vortexing, incubation for 15 min at RT, and centrifugation at 12,000 × g for 30 min at 4 °C. RNA isolation from the aqueous phase was performed using 500 µL of cold isopropanol (-20 °C), followed by vortexing. For RNA precipitation, samples were allowed to stand for 1 h at -20 °C followed by centrifugation at 12,000 × g for 15 min at 4 °C. The pellets were then washed twice with 1 ml 75% cold EtOH (-20 °C), centrifuged at 12,000 × g for 8 min at 4 °C, and dried for 5-10 min, on ice in a fume hood. The pellets were resuspended in 50 µL of RNase-free water in a ThermoMixer® C (Eppendorf, Hamburg, Germany) at 55 °C for 10 min at 500 rpm. RNA purification and DNase I treatment were performed using the Isolate II RNA Mini Kit (BIO-52073, Meridian BioScience®, Cincinnati, OH, USA), according to the manufacturer's instructions. The yield and purity of extracted RNA were assessed using a NanoVue Plus spectrophotometer (GE Healthcare, Chicago, IL, USA). Total RNA quality and integrity were checked using a 2200 TapeStation (Agilent Technologies, Santa Clara, CA, USA), and all samples with an RNA integrity number (RIN) > 7 were considered for sequencing.

3.4.3.3.2. Library construction and RNA sequencing

RNA-seq libraries were prepared from 1 µg of total RNA using the Illumina TruSeq™ Stranded mRNA Library Prep Kit (Illumina Inc., San Diego, CA, USA) according to the manufacturer's instructions. All RNA-seq libraries were paired-end (PE) sequenced (2 × 151 bp) with dual indexing on an Illumina NovaSeq 6000 System, with poly-A selection, according to the manufacturer's protocol (TruSeq Stranded mRNA Reference Guide # 1000000040498 v00). The sequencer generated BCL/cBCL (base call) binary files, which were then converted into FASTQ files using bcl2fastq. Raw sequenced data were deposited in the ArrayExpress (Athar et al., 2019) database (<http://www.ebi.ac.uk/arrayexpress>) under accession number E-MTAB-12842. Approximately two billion PE reads were obtained from the 54 sequenced samples, with an average of approximately 37 million reads per sample (Additional file 1 - [online](#)). Library construction and RNA sequencing were performed by Macrogen, Inc. (Seoul, South Korea).

3.4.3.4. Bioinformatics analysis

3.4.3.4.1. Quality assessment, reads mapping and differential gene expression analysis

Quality control (QC) analysis of raw reads was performed using FastQC v0.11.9 (Andrews 2010). Raw data were processed using Fastp v0.22.0 (S. Chen et al., 2018) to remove adapters, filter-out low-quality and short reads (cut-off = 100 bp) and perform base correction in overlapped regions. Fastp was also used to calculate the Q20, Q30, GC-content, and sequence duplication levels of the clean data. Trimmed reads were inspected again using FastQC to ensure their quality and were then used for subsequent analyses. Mapping to the *Sparus aurata* reference genome (Genome assembly: GCA_900880675.1, https://www.ensembl.org/Sparus_aurata/Info/Index) was carried out using the splice-aware STAR aligner v2.7.10 (Dobin et al., 2013), with the following settings: overhang – 150 bp, length (bases) of the SA pre-indexing string – 13, minimum intron length – 20, minimum alignment score normalized to read length – 0.4, minimum matched bases normalized to read length – 0.4 and output BAM files sorted by coordinate. Mapped reads were extracted from the BAM files using SAMTools v1.9 (H. Li et al., 2009) and investigated using the genome browser Integrative Genomics Viewer (IGV) v2.15.4 (Robinson et al., 2011). To improve annotation, a reference-guided transcriptome assembly was performed using Stringtie

v2.1.1 (Pertea et al., 2015). Potential transcripts were assembled individually for each sample and merged to generate a non-redundant transcriptome, which was subsequently compared to the reference annotation file (GTF) using gffcompare v0.11.2 (Pertea & Pertea, 2020). A new alignment of the reads was performed using STAR with the new GTF file and the same settings as those described above. Alignment QC was performed using Qualimap v2.2.1 (Okonechnikov et al., 2016). All results from the previous steps were merged with MultiQC v1.13 (Ewels et al., 2016) (the report is provided in Additional file 2 - [online](#)). All analyses were performed using the CCMAR high-performance computing (HPC) facility, CETA.

The number of reads per gene was counted while mapping within STAR using reverse strandedness counts. Differential expression analysis (DEA) was performed by importing the raw read counts of each sample into the R package DESeq2 v1.36.0 (Love et al., 2014) from Bioconductor. Genes with low expression were removed, normalization was performed according to sequencing depth and RNA composition, and variance stabilizing transformation (VST) was applied for visualization. The threshold for differentially expressed genes (DEGs), calculated using Wald's test, was an adjusted p-value (Benjamini-Hochberg correction) < 0.01 and \log_2 [fold-change] (LFC) > 1.0, after Bayesian shrinkage (A. Zhu et al., 2019). PCA was achieved with the Bioconductor R package PCAtools v2.8.0 (Blighe & Lun, 2022).

3.4.3.4.2. Functional enrichment analysis

Annotation of unknown genes and transcripts was performed using the HMMER v3.3 nhmmer tool (Wheeler & Eddy, 2013) for homology search against *Danio rerio* (cut-off threshold of E-value < 0.01). Queries that matched no hits within the threshold were reanalyzed with Pannzer2 (Törönen et al., 2018) (cut-off threshold of positive predictive value (PPV) > 0.5) by first extracting candidate open reading frames (ORFs) of at least 70 amino acids and predicting potential peptides using TransDecoder v5.7.0 (<https://github.com/TransDecoder/TransDecoder>).

Prior to enrichment analyses, *Danio rerio* orthologs of annotated genes were searched for all identifiers using g:Profiler (Raudvere et al., 2019). Gene ontology (GO), Kyoto Encyclopedia of Genes and Genomes (KEGG), and REACTOME overrepresentation analyses (ORA) were performed using enrichGO() and enrichKEGG() functions from the R package clusterProfiler v.4.4.4 (T. Wu et al., 2021) and enrichPathway() from the ReactomePA package v1.40.0 (Yu & He, 2016). All

terms were considered enriched with a cut-off value of < 0.05 for the adjusted p-values (Benjamini-Hochberg correction). Gene set enrichment analysis (GSEA) (A. Subramanian et al., 2005) on the aforementioned knowledgebases was performed using the clusterProfiler package. The genome-wide annotation of zebrafish from Bioconductor (R package org.Dr.eG.db v3.8.2) (Carlson, 2019) was used for mapping in all enrichment analyses. No significantly enriched terms were found for the OC trial; therefore, it was excluded from subsequent analyses. Visualization was achieved with packages ggplot2 v.3.4.0 (Wickham, 2016) and enrichplot v1.16.2 (Yu, 2022b).

Multomics integration was performed using the corresponding and previously published proteomic and metabolomic data from the same fish specimens (Raposo de Magalhães et al., 2022). KEGG and REACTOME ORA of proteomics datasets were likewise performed using the clusterProfiler R package, whereas for metabolomics datasets, analysis was performed using the MetaboAnalyst 5.0 Enrichment analysis web-based tool (Pang et al., 2021) and the REACTOME Analysis tools (Fabregat et al., 2017).

All figures were generated using the open-source graphics editor Inkscape (<http://www.inkscape.org/>).

3.4.4. RESULTS AND DISCUSSION

3.4.4.1. Overview of RNA-seq data and differential expression analysis

Trimming and quality filtering of raw reads resulted in an average of 2.71% discarded reads per sample, mainly due to short size (cut-off was set at 100 bp) and/or low quality. Reads that passed the filter ranged between 14.5 and 22.5 million per sample, with an average length size of 146 bp and a GC content of 49.57%. Regarding the first alignment, more than 90% of the trimmed reads were mapped to the reference genome (uniquely mapped), of which 17.85%, on average, mapped to no features (i.e., unannotated regions of the genome). Reference-guided transcriptome assembly was performed to improve genome annotation, enabling the discovery of 3,637 putative new genes and 5,036 transcripts (i.e., no overlap with any reference gene/transcript) out of a total of 31,834 assembled genes. Summary statistics of the comparison between the assembled transcriptome and the reference genome are displayed in Table 3.4.1. The new alignment with the assembled transcriptome revealed an average mapping rate of 91.79%, with 2.33% of the reads mapping to no features. The alignment QC results also showed an improvement in the genomic origin of the reads,

as those mapped to exonic regions increased from an average of 64% in the first alignment to 89% after the new alignment with the assembled transcriptome. Significant homologies (E-value < 0.01) with *Danio rerio* were retrieved for 24% of the unknown genes.

Table 3.4.1. Summary statistics of the comparison between the experimental transcriptome assembled with Stringtie and the *Sparus aurata* reference genome, achieved with gffcompare

Data summary		
Query mRNAs	125,523 in 32,533 loci (118,947 multi-exon transcripts)	
Reference mRNAs	73,301 in 27,314 loci (70,848 multi-exon)	
Matching intron chains	70,848	
Matching transcripts	73,093	
Matching loci	27,110	
Missed exons	0/378,760 (0.0%)	
Novel exons	44,268/475,793 (9.3%)	
Missed introns	396/321,758 (0.1%)	
Novel introns	21,709/373,737 (5.8%)	
Missed loci	0/27,314 (0.0%)	
Novel loci	6,383/32,533 (19.6%)	
Accuracy estimation		
	Sensitivity	Precision
Base level	100.0	71.3
Exon level	97.6	78.5
Intron level	99.7	85.8
Intron chain level	100.0	59.6
Transcript level	99.7	58.2
Locus level	99.3	79.8

Gene counts were then imported into R for DEA and low expression genes were removed, resulting in three datasets with 17,775, 17,361 and 17,838 assembled genes for OC, NET and HYP trials (Additional file 3 - [online](#)). PCA biplots with VST-transformed counts (Figure 3.4.1) showed a clear separation between control and treated samples for the NET and HYP trials, along the first and the two first principal components (PC), accounting for 37.74% and 40.57% of the total data variance, respectively. Considering the PCA of NET samples, MSTRG.16120, MSTRG.8388, and MSTRG.8386, coding for pentraxin-like and hepcidin-like proteins, were the top three genes with the highest absolute loading values in PC1 (Figure 3.4.1.B). Regarding HYP, the top three genes that presented the highest absolute loading

values in the first PC were MSTRG.16169 and MSTRG.16177, encoding two proteins from the heat shock protein 70 family, and MSTRG.18353 encoding a protein from the cytochrome P450 family 2 (Figure 3.4.1.C). In contrast, in the OC biplot, an overlap between the control and experimental group was observed (Figure 3.4.1.A).

DEA retrieved 7, 343, and 654 DEGs (assembled gene IDs) ($p_{adj} < 0.01$, LFC > 1) among the OC (Figure 3.4.1-D), NET (Figure 3.4.1-E) and HYP (Figure 3.4.1-F) trials, respectively (Additional file 4 - [online](#)). Of these, 1, 15, and 22 genes, respectively, were not annotated. These numbers demonstrate that the overcrowding challenge had a drastically lower impact on the hepatic transcriptome than hypoxia and net handling, possibly suggesting adaptation/habituation of the animals or a higher resistance to this condition in this species. This trend was also observed for both the liver proteome and metabolome, as previously reported (Raposo de Magalhães et al., 2022). The low plasma cortisol levels found and previously reported also corroborate this hypothesis (Raposo de Magalhães, Schrama, et al., 2020). In this context, a recent study compared the response of European seabass and gilthead seabream to chronic overcrowding and found higher resilience of the latter in terms of plasma hormones and gene expression (Samaras et al., 2018). Additionally, a transcriptomic study with gilthead seabream juveniles subjected to food deprivation and high stocking densities also showed that different stressors are handled by different stress pathways (Skrzynska et al., 2018), supporting the challenge-specific responses observed here. This demonstrates the great adaptive plasticity of gilthead seabream in different farming and challenging environments. In fact, the underlying genetic basis of this trait has been recently demonstrated and attributed to high rates of gene duplication and mobile genetic elements, which might favor the acquisition of novel gene functions (Pérez-Sánchez et al., 2019).

3.4.4.2. Net handling induced ribosomal assembly stress coupled to inhibition of insulin growth factor signalling in gilthead seabream hepatocytes

Gene set enrichment analysis (GSEA) based on GO biological processes (BP) (Figure 3.4.2.A,D), KEGG (Figure 3.4.2.B,E), and REACTOME (Figure 3.4.2.C,F) databases revealed 183 enriched terms ($FDR < 0.05$) for NET trial genes (Additional file 5 - [online](#)).

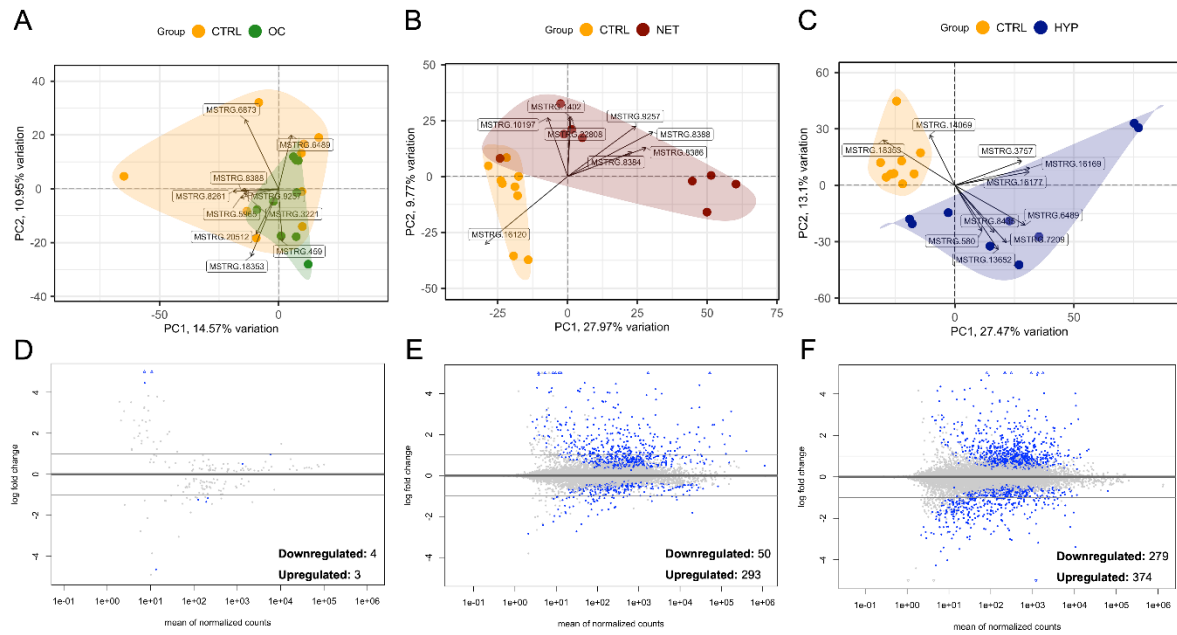


Figure 3.4.1. Summary of the exploratory and differential analyses results of RNA-seq data. Biplots represent the principal component analyses (PCA) of the liver transcriptome of gilthead seabream submitted to overcrowding (A), net-handling (B), and hypoxia (C). Experimental groups are distinguished by different colours, as indicated in the legend. Arrows depict the top loadings. MA plots of the shrunken LFCs indicate differentially expressed genes (D – overcrowding, E – net-handling, F – hypoxia). Blue points represent $p_{adj} > 0.01$, and horizontal lines indicate the threshold of $\log_2|\text{fold-change}| > 1.0$.

The top significantly downregulated processes i.e., those with the lowest normalized enrichment score (NES) in all three databases, were mainly related to rRNA processing, ribosome biogenesis, and translation initiation (Figure 3.4.2.A-C). Interestingly, all of these processes were upregulated at the proteome level, as retrieved by the ORA of the proteomics dataset (Additional file 6 - [online](#)). The simultaneous upregulation of protein homeostasis genes and downregulation of ribosomal protein genes (RPGs), followed by disruption of various steps in ribosome biogenesis (rRNA production, processing, or ribosome assembly), as further explained, suggests that net handling induced ribosomal assembly stress through a response similar to the Ribosome Assembly STress Response (RASTR), previously described in yeast and humans (Albert et al., 2019; Kang et al., 2021). This dysregulation of ribosome biogenesis surveillance mechanisms can result in free ribosomal proteins (RPs) (X. Zhou et al., 2015), which might explain their upregulation at the proteomic level (Raposo de Magalhães et al., 2022). The RASTR regulatory pathway is essential for transcription regulation to maintain proteome homeostasis, thus avoiding the accumulation of defective and/or unassembled ribosomal proteins.

Ribosome assembly is a highly complex process associated with cell growth and proliferation. It monopolizes an enormous fraction of biogenic capacity and requires the coordinated work of rRNA, RPs, and other factors. In eukaryotes, ribosomes are comprised of four rRNAs (28S, 18S, 5.8S, and 5S) and 79 highly conserved RPs organized in a small (40S) and a large subunit (60S). The first three rRNAs are synthesized by RNA polymerase I (Pol I) along with other factors in the nucleolus, while 5S rRNA is transcribed separately by Pol III in the nucleoplasm. The pre-rRNAs are then assembled with RPs and exported to the cytoplasm for final maturation (Pelletier et al., 2017). Unsurprisingly, this process is strictly regulated spatiotemporally through a myriad of quality control checkpoints involving a staggering number of factors (Gnanasundram & Fåhræus, 2018).

Regulation of ribosome biogenesis at the rRNA level can occur through different signaling pathways, such as the PI3K/AKT, MAPK/ERK, and mammalian rapamycin protein kinase (mTOR) pathways (Caron et al., 2010; Gnanasundram & Fåhræus, 2018). Activation/repression of rDNA transcription by these pathways occurs through the transcriptional modulation of both Pol I and III, by interacting with specific transcription factors (TFs) (Gnanasundram & Fåhræus, 2018; Iadevaia et al., 2014). Besides recruiting TFs, the action of the PI3K/AKT pathway on RNA polymerases is also mediated by the factor c-Myc, which is considered a major regulator of ribosome assembly (van Riggelen et al., 2010). Interestingly, *myca*, and the activator protein *mycbp*, were downregulated in net-handled fish (Additional file 4 - [online](#)). The significant upregulation of the pathway “AUF1 (hnRNP D0) binds and destabilizes mRNA (ID: R-DRE-450408)” observed in the proteomics data ORA (Additional file 6 - [online](#)) might corroborate the downregulation of the c-Myc gene, as this complex, i.e., AUF1, binds and destabilizes mRNAs encoding, among others, c-Myc, interleukin-1 beta (IL1B), and cyclin-dependent kinase inhibitor 1 (CDKN1A). Accordingly, the latter (*cdkn1a*) was also significantly downregulated in net-handled fish (LFC = -2.83, padj = 0.006). Maf1 is also a central negative regulator of Pol III transcription. Additionally, it was shown to suppress the transcription of the TATA-binding protein (TBP), a transcription factor used by all nuclear RNA polymerases (Johnson et al., 2007). Genes *maf1* and *tbp* were found to be up- and downregulated, respectively, in net-handled fish (Additional file 3 - [online](#)), although the difference was not statistically significant (padj > 0.01). Furthermore, the downregulation of the pathways “RNA Polymerase III Transcription Initiation From Type 3 Promoter (ID: R-DRE-76071)”,

“FoxO signalling pathway (ID: dre04068)” (Additional file 5 - [online](#)), “PI3K cascade (ID: R-DRE-109704)” and “IGF1R signaling cascade (ID: R-DRE-2428924)” (Additional file 6 - [online](#)) in net-handled fish suggests a downregulation of Pol III and consequently a repression of the 5S rRNA transcription, which may lead to an inability to assemble the ribosomes properly.

Type 1 insulin-like growth factor (IGF1) is an extracellular growth factor that can activate the PI3K/AKT signaling pathway (Figure 3.4.3). In fact, *igf1* and *igf1rb*, coding for the growth factor and its receptor, respectively, were found to be downregulated in the fine flounder (*Paralichthys adspersus*) skeletal muscle after crowding stress (Valenzuela et al., 2018), in the liver of coho salmon (*Oncorhynchus kisutch*) 16h after acute handling stress (Nakano et al., 2013), and in the liver of gilthead seabream exposed to acute confinement (Saera-Vila et al., 2009). Accordingly, these genes were downregulated in net-handled fish, although not significantly ($\text{padj} > 0.01$; Additional file 3 - [online](#)). Moreover, *igfbp1a*, coding for the IGF binding protein 1a, which binds IGF, with high affinity, in the extracellular environment, was significantly upregulated (LFC = 2.46, $\text{padj} = 0.003$). This protein is mainly produced in the liver and prevents IGF1 from binding to its transmembrane receptor (IGF1R) and inducing cellular growth (A. W. Wood et al., 2005). The elevation of this protein in response to stress in the liver of gilthead seabream suggests an important role in adaptation mechanisms, most likely shifting the energy from somatic growth towards stress-responsive pathways to promote survival. In rainbow trout (*Oncorhynchus mykiss*) exposed to handling and confinement stress, reduced IGF1 signaling in peripheral tissues was also observed due to the upregulation of IGFBP1 (S. Liu et al., 2014). The mTORC1 is also known to inhibit IGF1R through a negative feedback loop involving growth factor receptor-bound protein 10 (GRB10) (Ghomlaghi et al., 2021). Concomitantly, the expression of the corresponding gene (*grb10b*) was upregulated in these fish (LFC = 0.62, $\text{padj} = 0.017$).

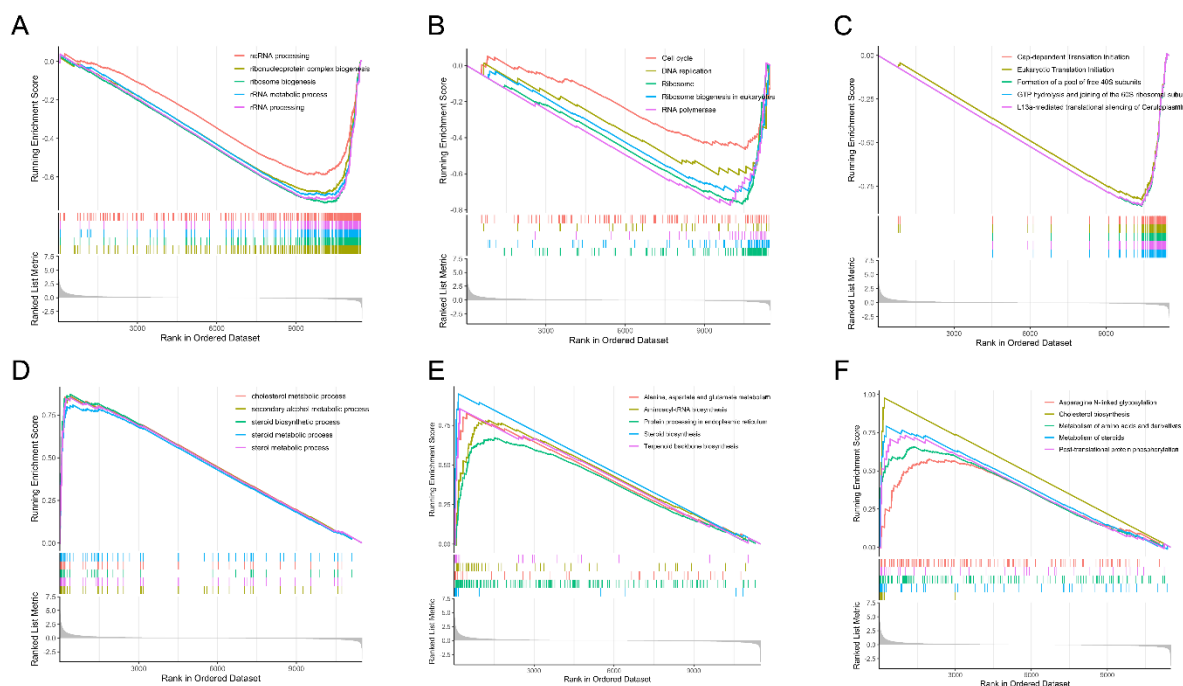


Figure 3.4.2. GSEA performed on the RNA-seq data of the liver transcriptome of gilthead seabream submitted to net handling, based on GO (A,D), KEGG (B,E), and REACTOME (C,F) databases, sorted by normalized enrichment score (NES) inferred from permutations of the gene set and false discovery rate (FDR). On the x-axis, the genes were ranked from the most upregulated (left end) to the most downregulated (right end). The y-axis represents the running enrichment score (ES). First line indicates downregulated pathways whereas bottom line indicates upregulated pathways.

Regulation of RPGs can occur at different levels; however, given their structural complexity, this process is not yet entirely understood in humans. RPGs are among the most highly expressed genes in most cell types, and their architecture increase the complexity of ribosome biogenesis (Pelletier et al., 2017). mTOR signaling regulates RPGs' expression and promotes the synthesis of RPs in two steps. First, it induces the transcription of RPGs and small nucleolar ribonucleoproteins (snoRNPs), necessary for ribosome assembly, through Pol II. Second, by promoting the translation of RPs mRNAs through their 5' terminal oligo-pyrimidine (TOP) motifs, in an RPS6KB1-dependent manner (Iadevaia et al., 2014). Intriguingly, *rps6kb1b* is upregulated in net-handled fish (LFC = 0.82, padj = 0.008) suggesting an upregulated translation, however the GSEA indicated that "Cap-dependent Translation Initiation (ID: R-DRE-72737)" was negatively enriched (Figure 3.4.2.C). This was mainly associated with the downregulated genes encoding for the different subunits of the eukaryotic initiation factor 3 (eIF3). The eIF3 complex specifically targets and initiates the translation of a specialized repertoire of mRNAs involved in cell proliferation. The downregulation of

its transcripts may also be related to the impairment of ribosome assembly, as the 40S subunit is required with eIF3 to form the translation pre-initiation complex (PIC) (Georges et al., 2015). In contrast, the protein levels of the six eIF3 subunits were upregulated, as previously reported (Raposo de Magalhães et al., 2022). Moreover, specific overexpressed RPs have been shown to autoregulate their transcripts by alternative splicing, redirecting them to degradation through different systems, such as nonsense mediated decay (NMD), ribonucleases, or exosomes (Petibon et al., 2021). PTMs are another mechanism of RPG regulation that modifies protein stability and function, with ubiquitination and phosphorylation being the two most commonly occurring processes (Simsek & Barna, 2017). In fact, “Post-translational protein phosphorylation (ID: R-DRE-8957275)” was one of the positively enriched pathways in net-handled fish (Figure 3.4.2.F). At this step, RPs are translated in the cytoplasm, imported into the nucleus for ribosome assembly, and then exported back into the cytoplasm for maturation. Unsurprisingly, this causes substantial demands on nuclear import and export machinery, and any perturbation at these steps can also impair ribosome biogenesis. In net-handled fish, the *ipo7* and *ipo4* genes, that encode the importin 7 and 4 import factors, were found to be downregulated (LFC = -0.39, padj = 0.006 and LFC = -0.58, padj = 0.012, respectively), along with the pathway “Nucleocytoplasmic transport (ID: GO:0006913)” (Additional file 5 - [online](#)).

Overall, these results suggest that inhibition of IGF1 by net handling stress most likely downregulated the PI3K/AKT and mTOR signaling pathways, resulting in the repression of RNA polymerase activity and consequent perturbation of the ribosome assembly process. Dysfunctional ribosomes are associated with a panoply of human disorders called ribosomopathies and are, in fact, behind several cancers (Narla et al., 2011), however this association has not yet been explored in fish. The proposed regulation network is illustrated in Figure 3.4.3.

3.4.4.3. Hypoxia-induced DNA replication stress in gilthead seabream hepatocytes is synergistically mediated by the hypoxia-inducible factor and mTORC1

In the HYP trial, GSEA based on GO biological processes (BP) (Figure 3.4.4.A,D), KEGG (Figure 3.4.4.B,E), and REACTOME (Figure 3.4.4.C,F) databases revealed a total of 249 significantly enriched (FDR < 0.05) terms (Additional file 7 - [online](#)).

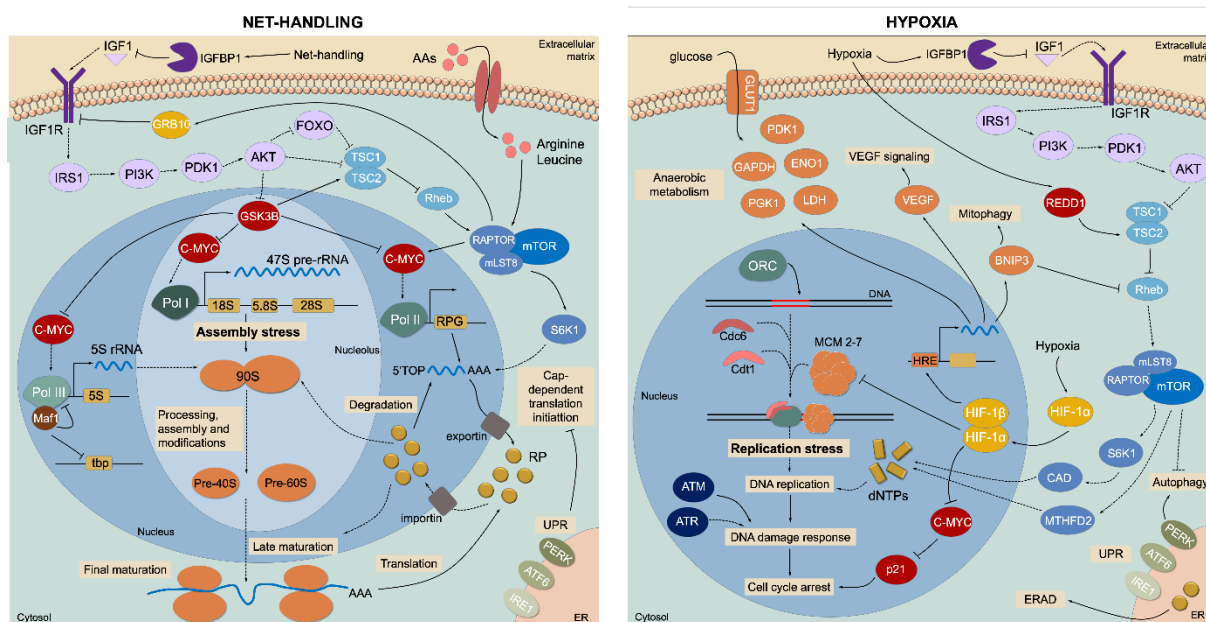


Figure 3.4.3. Proposed stress response network in gilthead seabream hepatocytes subjected to net-handling and hypoxia. Dashed arrows indicate downregulated pathways, whereas solid arrows represent unchanged or upregulated pathways.

DO is one of the main limiting factors in fish farming as it can severely affect many aspects of fish performance and physiology. In ponds, it generally depends on phytoplankton's photosynthesis rate, aquatic organisms' respiration, and/or the atmospheric oxygen diffusion (O_2) (Abdel-Tawwab et al., 2019). De-oxygenation of the world's oceans has also recently been highlighted as a major consequence of climate change, which can impact offshore aquaculture (Townhill et al., 2017). O_2 is crucial in numerous cellular processes such as oxidative metabolism, energy supply through ATP generation, and cell survival. One of the many impairments caused by inefficient tissue oxygenation is genomic instability, which drives DNA replication stress. The negative enrichment of the pathways "DNA replication (ID: GO:0006260)", "DNA replication (ID: dre03030)", and "Cell cycle (ID: dre04110)" (Figure 3.4.4.A-C) indicates a potential stalling of DNA replication and a halt or a slowdown of the cell cycle in hypoxia-exposed fish. The "DNA Replication (ID: R-DRE-69306)" pathway was also found to be downregulated in metabolomics, as retrieved by the ORA (Figure 3.4.5.B). DNA replication is the process of genome duplication that a cell undergoes during cell cycle division. In eukaryotes, it is initiated by the binding of the origin recognition complex (ORC) to a replication origin, which then recruits a hexameric DNA helicase (MCM) and a helicase loading factor to form the pre-replicative protein complex (pre-RC) (L. Wu et al., 2014). Downregulation of the REACTOME pathway "Activation of

the pre-replicative complex (ID: R-DRE-68962)” (Figure 3.4.4.C) indicates a potential hypoxia-induced replication arrest due to impaired pre-RC assembly/activation. Several studies in humans have demonstrated that a decrease in dNTP levels accompanies abrogated replication under hypoxic conditions due to downregulation of ribonucleotide reductase (RNR), a key enzyme that mediates the synthesis of deoxyribonucleotides, the key blocks for DNA replication and repair (Ng et al., 2018; Pires et al., 2010). In accordance with these findings, the gene coding for this enzyme, *rrm1*, was significantly downregulated in hypoxia-exposed fish (LFC = -1.77, padj = 0.008). Moreover, metabolites UMP, uracil, and uridine, involved in nucleotide biosynthesis, were significantly downregulated in the liver of these fish, according to a previous metabolomics analysis (Raposo de Magalhães et al., 2022). This is in accordance with the downregulation of the KEGG pathway “Pyrimidine metabolism (ID: dre00240)” in both the transcriptome and metabolome (Figure 3.4.5.B). Previous studies are in accordance with these findings, as nucleotide biosynthetic processes were also downregulated in the gills of golden Pompano (*Trachinotus ovatus*) under hypoxic stress (San et al., 2021). Moreover, *rrm1* was also found to be downregulated in the gills of juvenile Chinook salmon (*Oncorhynchus tshawytscha*) under hypoxic conditions for six days (Akbarzadeh et al., 2020). Hypoxia is also known to induce replication stress (RS) and activate the DNA damage response (DDR) independently of the DNA damage itself. This response relies on surveillance sensor kinases, namely the ataxia-telangiectasia-mutated kinase (ATM), ataxia telangiectasia and Rad3-related protein (ATR), and DNA-dependent protein kinase (DNA-PK), which are activated via PTMs. The activation of these pathways can result in the regulation of DNA repair pathways, cell cycle control, and apoptosis. Depending on the severity of hypoxia, that is, duration and level of oxygen, DNA repair pathways can be activated or repressed at the transcriptional level (Kumareswaran et al., 2012; Ng et al., 2018; Pires et al., 2010). Negative enrichment of the pathways “double-strand break repair via homologous recombination (ID: GO:0000724)”, “Activation of ATR in response to replication stress (ID: R-DRE-176187)”, and “HDR through Single Strand Annealing (SSA) (ID: R-DRE-5685938)” (Figure 3.4.4.A-C; Additional file 7 - [online](#)), parallel with the significant upregulation of genes (e.g., *xrcc5*, *xrcc6*) involved in the canonical non-homologous end-joining repair mechanism (Additional file 4 - [online](#)), suggests a potential selective regulation of the DNA repair pathways, favoring the downregulation of some and the upregulation of others.

The relationship between hypoxia, cell cycle arrest, and DNA repair mechanism inhibition has not yet been completely revealed in teleosts. Nevertheless, downregulation of DNA replication due to hypoxia has also been observed in the gills of spotted seabass (*Lateolabrax maculatus*) (Ren et al., 2022) and liver of threespine stickleback (*Gasterosteus aculeatus*) (Leveelahti et al., 2011). In Nile tilapia (*Oreochromis niloticus*), short and prolonged hypoxia induced DNA damage that was directly proportional to increasing hypoxic concentrations (Mahfouz et al., 2015).

Hypoxia-inducible factor 1 (HIF-1) is a heterodimer composed of HIF-1 α and HIF-1 β subunits that is at the center of almost all hypoxia-induced pathways, acting mainly as a TF to mediate adaptive responses at both cellular and systemic levels. The isoform HIF-1 α is a well-documented key modulator of the hypoxia signaling pathway; after being translocated into the nucleus, it heterodimerizes with HIF-1 β and binds to hypoxia-responsive elements (HREs) located in the promoters of hypoxia-inducible genes, which modulate their expression (B. H. Jiang et al., 1996). In this study, several genes involved in the HIF-1 signaling pathway were significantly upregulated, including *egln1*, *egln2*, *egln3*, *hif1an*, and *hif1al* (Additional file 4 - [online](#)). Accordingly, the positive enrichment of the pathways “response to hypoxia (ID: GO:0001666)”, “Cellular response to hypoxia (ID: R-DRE-1234174)” and “Oxygen-dependent proline hydroxylation of Hypoxia-inducible Factor Alpha (ID: R-DRE-1234176)” (Figure 3.4.4.D-F, Additional file 7 - [online](#)) further supports the activation of HIF-1 α in the liver of hypoxia-exposed gilthead seabream. Furthermore, several DEGs known to be targeted by HIF-1 α and to promote hypoxia adaptation through different mechanisms were also upregulated (Additional file 4), such as *vegfaa*, which initiates the vascular endothelial growth factor (VEGF) signalling pathway (Choi et al., 2011); *epoa*, which stimulates blood cell production, *higd1a* which is responsible for maintaining mitochondrial homeostasis, *slc2a1b* which facilitates cellular glucose uptake (C. Chen et al., 2001), *gapdhs*, *pgk1*, *eno1a*, *slc16a3* and *ldha1*, which are metabolic enzymes that reduce oxygen consumption and promote anaerobic metabolism (Taylor & Scholz, 2022), *pdh1* which inhibits the tricarboxylic acid (TCA) cycle (Kim et al., 2006) and *bnip3lb* which promotes mitophagy (Taylor & Scholz, 2022). These changes can be supported by the positive enrichment of the pathways “Glycolysis/Gluconeogenesis (ID: dre00010)”, “Mitophagy – animal (ID: dre04137)” and “Glycolysis (ID: R-DRE-70171)” (Figure 3.4.4.E; Additional file 7 - [online](#)). In addition to metabolism, HIF-1 α has also been demonstrated to inhibit the activation of the MCM helicase in a non-

transcriptional manner (Hubbi et al., 2013), which might corroborate the downregulation of DNA replication initiation, as genes *mcm2*, *mcm3*, *mcm4*, and *mcm5* were significantly downregulated in hypoxia-exposed fish (Additional file 4 - [online](#)). Additionally, cell cycle arrest can also be induced in a HIF-1 α -dependent manner by displacing c-Myc from the p21 and p27 promoters, two cyclin-dependent kinases (CDKs) inhibitors (Druker et al., 2021). Here, the genes *myca* (LFC = -0.91, padj = 0.006) and *cdkn1a* (LFC = 1.28, padj = 0.004), encoding the proteins c-Myc and p21, respectively, were downregulated and upregulated in response to hypoxia, supporting the action of HIF-1 α in cell cycle arrest.

The relationship between hypoxia-induced activation of HIF-1 and metabolism has also been widely demonstrated in the livers of several fish species exposed to hypoxic conditions, such as *Epinephelus coioides* (Lai et al., 2022), *Procambarus clarkia* (L. Zhang et al., 2022), *Hypophthalmichthys nobilis* (G. Chen et al., 2021), *Salvelinus alpinus* (Cassidy & Lamarre, 2019) and *Danio rerio* (Mandic et al., 2020). Curiously, *hif-1 α* was downregulated in the white skeletal muscle and the heart of gilthead seabream subjected to moderate hypoxia (42-43%) (Martos-Sitcha et al., 2019), suggesting that either only more severe hypoxic conditions, such as the 15% oxygen saturation applied in this study, are able to induce HIF-1 α activation in this species, or that the response of this factor differs significantly among tissues.

Another major signaling pathway that responds to hypoxia and promotes adaptation to low O₂ availability is mTORC1. In another study, mTORC1 signaling has been reported to be downregulated in Arctic char exposed to 15% DO (Cassidy & Lamarre, 2019). Hypoxic conditions are known to lead to a downregulation of OXPHOS and, thus, to a reduction in cellular energy, consequently ceasing high-energy-demanding cellular processes such as translation. A metabolomic analysis of the livers of the same fish confirmed that ATP levels were significantly downregulated (Raposo de Magalhães et al., 2022), indicating a low ATP:AMP ratio. This can lead to an inhibition of the mTORC1, mediated by the metabolic regulator 5' AMP-activated protein kinase (AMPK) and/or the Regulated in DNA damage and development 1 (REDD1) (Saxton & Sabatini, 2017). The first is carried out either through phosphorylation and activation of TSC2 or through the phosphorylation of Raptor, while the latter activates TSC2 by titrating the inhibitory 14-3-3 proteins (Britto et al., 2020). In this study, *ddit4* (LFC = 2.81, padj = 2.20e-10) and *ywhaz* (LFC = 0.89, padj = 0.0007), coding for the proteins REDD1 and 14-3-3, respectively, were significantly

upregulated in hypoxia-exposed fish, suggesting that REDD1 might be important for maintaining cellular energy homeostasis during oxygen challenges. Gene *ddit4* was likewise found to be upregulated in threespine stickleback (*Gasterosteus aculeatus*) (Leveelahti et al., 2011), in the gills and heart of bighead carp (*Hypophthalmichthys nobilis*) (G. Chen et al., 2021), and in the muscle of largemouth bass (*Micropterus salmoides*) (He et al., 2022), exposed to different hypoxia levels. To promote autophagic cell death mTORC1 can also be inhibited by BNIP3, which is transcriptionally activated by HIF-1 α (Y. Li et al., 2007). As previously mentioned, *bnip3lb* was significantly upregulated in hypoxia-exposed fish (LFC = 1.72, padj = 8.48e-08), demonstrating an inhibitory effect of HIF-1 α over mTORC1. A transcriptomic analysis of zebrafish exposed to hypoxia revealed increased levels of *bnip3* in the heart (Marques et al., 2008). Similarly, *bnip3* was also upregulated in channel catfish infected with *Edwardsiella ictaluri* (Yuan et al., 2016). Finally, mTORC1 could also be inhibited by a downregulation of the IGF1 signaling, as *igfbp1a* was also upregulated in response to hypoxia (LFC = 4.20, padj = 2.22e-10), as observed in net-handled fish. Previously *in vivo* and *in vitro* studies with zebrafish embryos demonstrated unequivocal evidence of a causal relationship between elevated IGFBP1 expression and hypoxia-induced embryonic growth and developmental retardation, suggesting that the HIF pathway is responsible for its transcriptional activation (Kajimura et al., 2005). Another study reported that the zebrafish IGFBP-1 promoter contains 13 consensus hypoxia response elements (HREs) (Kajimura et al., 2006). This protein was also upregulated at the mRNA level in Atlantic croaker during hypoxic stress (Rahman & Thomas, 2011). The proposed regulation network is illustrated in Figure 3.4.3.

3.4.4.4. The dual role of the endoplasmic reticulum in the adaptation to net handling and hypoxia stress: cholesterol biosynthesis and the unfolded protein response

Regarding the upregulated pathways in net-handled fish, one of the most enriched in both the GSEA and ORA was steroid and cholesterol biosynthesis (ID: GO:0006695, dre00100, R-DRE-191273), which takes place in the endoplasmic reticulum (ER) (Figure 3.4.2.D-F).

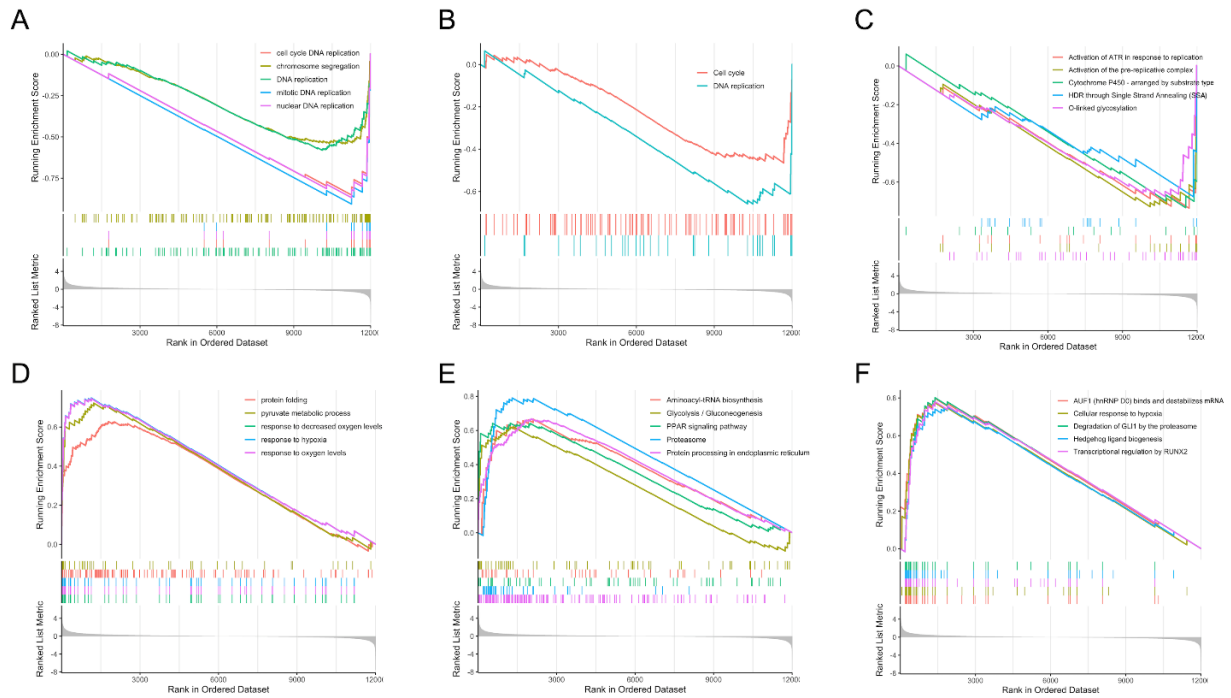


Figure 3.4.4. GSEA performed on the RNA-seq data of the liver transcriptome of gilthead seabream submitted to hypoxia, based on GO (A,D), KEGG (B,E), and REACTOME (C,F) databases, sorted by normalized enrichment score (NES) inferred from permutations of the gene set and false discovery rate (FDR). On the x-axis, the genes were ranked from the most upregulated (left end) to the most downregulated (right end). The y-axis represents the running enrichment score (ES). First line indicates downregulated pathways whereas bottom line indicates upregulated pathways.

Cholesterol, which can be obtained from diet or *synthesized de novo* in the liver, is a crucial component of the cell membranes in vertebrates and a precursor of the stress hormone cortisol (Ikonen, 2008). Sterol responsive element binding protein (SBREBP) is the master transcriptional regulator of cholesterol biosynthesis, mediated by mTORC1 (Düvel et al., 2010). *Sreb1f2*, the gene encoding for this protein, was found to be significantly upregulated in net-handled fish (LFC = 1.18, padj = 0.0001), together with multiple genes involved in steroid and cortisol synthesis and in pathways downstream of cortisol action (*cyp21a2*, *hsd17b7*, *fdft1*, *stard*, *cebpb*, *pck1*, *pck2*, *g6pca.1*) (Additional file 4 - [online](#)). On the other hand, in hypoxia-exposed fish, multiple DEGs involved in steroid and cholesterol biosynthesis were downregulated (*cyp7b1*, *hsd17b7*, *hsd17b1*, *cyp2r1*, and *fdft1*), which could be explained by the likely downregulation of mTORC1, as previously hypothesized. In addition, the plasma cortisol levels of these fish were found to be significantly upregulated in NET fish and unchanged in HYP fish (Raposo de Magalhães, Schrama, et al., 2020). Cortisol, considered the primary stress hormone in fish, is a multifaceted glucocorticoid

synthesized by interrenal cells in the head kidney as a quick response to external stimuli. It is vastly studied in teleost fish and is widely used as a physiological stress marker (Mommsen et al., 1999). However, there is still a lack of studies on the association between cholesterol biosynthesis and cortisol response in stressed fish.

The pathways “Protein processing in endoplasmic reticulum (ID: dre04141)”, “response to endoplasmic reticulum stress (ID: GO:0034976)” and “Asparagine N-linked glycosylation (ID: R-DRE-446203)” (Figure 3.4.2.A-C) were also positively enriched in net-handled fish, suggesting that this challenge might have induced stress in the ER, which is in accordance with the ORA of the proteomics data (Figure 3.4.5.A). In fact, several processes related to ER stress were modulated by the challenge, specifically the N-glycan trimming, the ER quality control, the ER-associated degradation (ERAD), the ubiquitin ligase complex and the unfolded protein response (UPR). Associated to these pathways, 11 genes were significantly upregulated (LFC > 1, padj < 0.01), i.e., *calr*, *calr3b*, *ddost*, *canx*, *prkcsh*, *dnajb11*, *sar1ab*, *hyou1*, *pdia6*, and *pdia4* (Additional file 4 - [online](#)). In addition to being the organelle responsible for lipid synthesis and protein folding, the ER is the most important storage site for intracellular calcium ions. The newly synthesized proteins are translocated into the ER lumen and glycosylated. Correctly folded proteins are then transported to the Golgi complex, while misfolded proteins are targeted by chaperones for refolding or degradation through the ER-associated degradation (ERAD) system if terminally misfolded (Braakman & Bulleid, 2011). When homeostasis is compromised by conditions such as hypoxia, nutrient deprivation, calcium depletion, or accumulation of misfolded proteins, stress is induced, which initiates the unfolded protein response (UPR). Three ER-transmembrane stress sensors mediate this signal transduction pathway: inositol-requiring enzyme 1 (IRE1), pancreatic endoplasmic reticulum kinase (PERK), and activating transcription factor 6 (ATF6). The three branches of the UPR converge to restore homeostatic adaptation; however, in severe cases, they can switch to promote apoptotic cell death (Walter & Ron, 2011). One of the main outputs of PERK signaling is the attenuation of translation through the inhibitory action of EIF4EBP1 (*eif4ebp1*, LFC = -0.47, padj = 0.0099). Specifically, cap-dependent translation is temporarily downregulated in tandem with increased cap-independent translation of many mRNAs, such as activating transcription factor 4 (ATF4) (Corazzari et al., 2017). The ATF6 and IRE1 pathways regulate the expression of genes mainly involved in protein folding and ERAD, which were significantly upregulated by the challenge (e.g.,

calr, *pdia6*, *dnajb11*, and *hyou1*). The results suggest that fish exposed to net handling likely counteracted ER stress by activating the UPR and ERAD and avoiding cell death (Figure 3.4.3).

Similarly to net-handled fish, “Protein processing in the endoplasmic reticulum (ID: dre04141)” was significantly enriched in hypoxia exposed fish and among the top 5 pathways with the highest NES, along with “Asparagine N-linked glycosylation (ID: R-DRE-446203)”, “protein folding (ID: GO:0006457)” and “response to unfolded protein (ID: GO:0006986)” (Figure 3.4.4.D-F; Additional file 3 - [online](#)). Hypoxia can induce protein misfolding due to the lack of oxygen required to form disulphide linkages, leading to ER stress and the consequent activation of the UPR. In this study, several DEGs were involved in distinct processes in the ER, such as *vcp*, *prkcsb*, *uggt1*, *plaa*, *hspa5*, *pdia6*, *calr*, *hsp90aa1.2*, *ero1a*, *hsp70.3*, and *xbp1*. Additionally, seven DEGs encoding proteasome subunits were also significantly upregulated, coupled with the positive enrichment of the pathways “ERAD pathway (ID: GO:0036503)” and “Proteasome (ID: dre03050)” by GSE. These results suggest a hypoxia-mediated response of the ER, based on the activation of the UPR and ERAD pathways, to deal with misfolded proteins and maintain ER homeostasis. In a study using DNA microarrays, UPR was also upregulated in the liver of gilthead seabream exposed to low temperatures (Mininni et al., 2014). Also in gilthead seabream, genes involved in lectin chaperone-mediated protein quality control were found to be upregulated in response to mild hypoxia (Naya-Català et al., 2021). In rainbow trout subjected to heat stress, an RNA-seq study also revealed upregulation of the KEGG pathway “Protein processing in the ER” (J. Huang et al., 2018).

In the case of unresolved and/or sustained ER stress, the kinase domain of IRE1 has been shown to activate the Jun N-terminal kinase (JNK) signaling pathway, which apart from being implicated in ER stress-related apoptosis it also promotes cell survival by inducing autophagy (Ogata et al., 2006). The transcription factor Jun is a central JNK target in the promotion of hepatocyte survival and in this study *junba* and *junbb* encoding this protein were significantly upregulated in fish exposed to both hypoxia (*junba*: LFC = 1.00, padj = 0.006; *junbb*: LFC = 0.84, padj = 0.02) and net handling (*junba*: LFC = 1.79, padj = 3.48e-08; *junbb*: LFC = 0.73, padj = 0.049) challenges, suggesting an important role in stress adaptation in gilthead seabream that requires further investigation. The pathway “autophagy (ID: GO:0006914)” was also positively enriched in hypoxia-exposed fish, which is concomitant with the

downregulation of the mTORC1 pathway. *In vitro* and *in vivo* in mice, have demonstrated that Jun protected the hepatocytes from excessive activation of the ER stress response and subsequent cell death, linking the UPR to autophagy (Fuest et al., 2012). Jun was also significantly upregulated in the liver of rainbow trout exposed to confinement stress (Momoda et al., 2007) and handling (S. Liu et al., 2014).

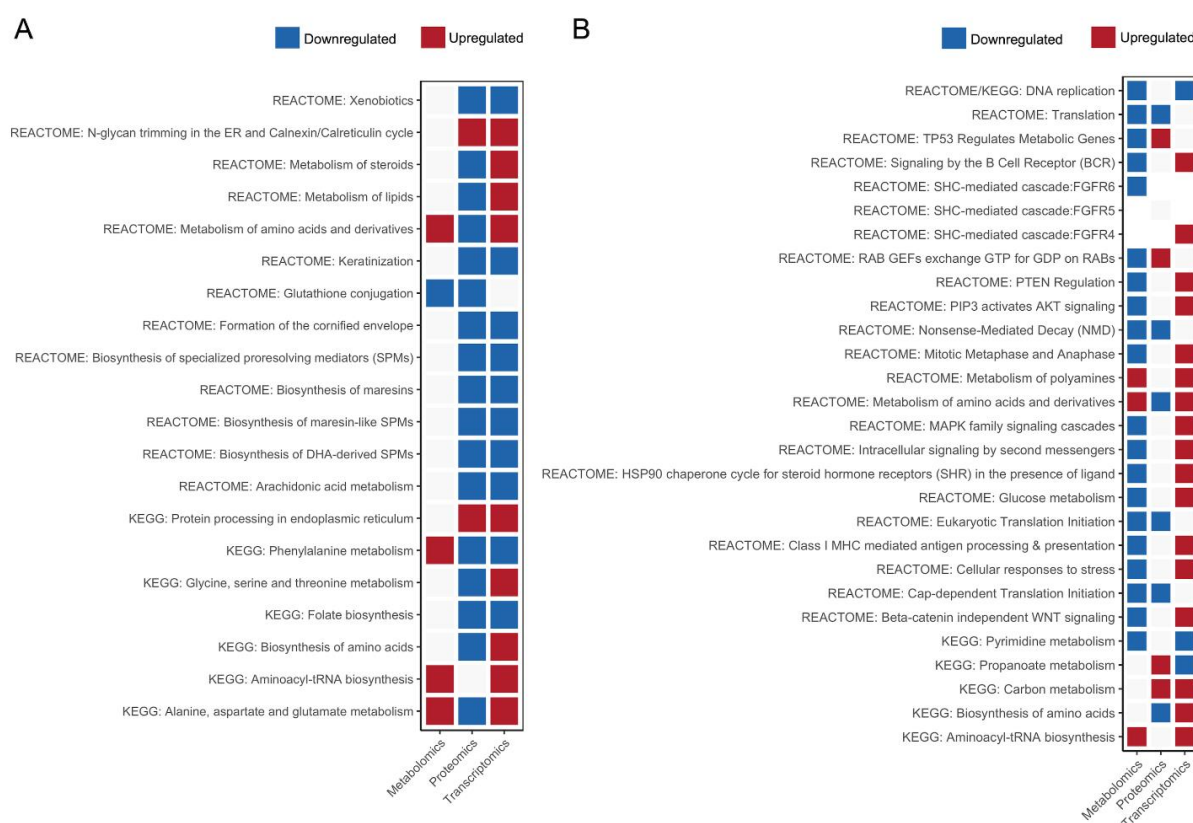


Figure 3.4.5. Heatmap of multiomics overrepresentation analysis (ORA): (A) net handling trial, (B) hypoxia trial; listed terms are commonly overrepresented terms between omics datasets.

3.4.5. CONCLUSIONS

Altogether, the results showed a challenge-specific transcriptional response of the liver of gilthead seabream to the different stimuli imposed, reinforcing the high phenotypic plasticity of this species to the changing environment. The most pronounced difference was observed between the overcrowded fish, and the fish exposed to net handling and hypoxia challenges, in terms of the number of dysregulated genes and gene families. Gilthead seabream has demonstrated high resilience to high stocking densities (45 kg m^{-3}), which might be due to domestication and/or evolutionary adaptation, in contrast to what was observed in fish netted four times a week and exposed to 15% DO. Net-handled and hypoxia-exposed fish also

demonstrated specific responses, such as the ribosome assembly stress response and DNA replication stress, respectively; however, both appeared to converge in the attenuation of translation to avoid proteotoxicity and shift the energy from cell proliferation and somatic growth towards stress-coping pathways. Notwithstanding, the response to both stressors converged in the induction of ER stress and downregulation of insulin growth factor signaling, a pathway that regulates many of the downstream processes described here. It is also important to note that a complete understanding of these responses was only made possible by the integration of biological data from the different complementary molecular levels, showing the promisor role of multiomics in understanding the fate of mRNA and the complete picture of the stress response pathways.

The characterization and identification of potentially novel genes represents the next step towards a more holistic understanding of the coping mechanisms to stressful aquaculture routines. Within this framework, knowledge of the genetic background of commercially important fish species that efficiently adapt to challenging conditions can provide evidence of desirable traits that can be a win-win strategy for overcoming both animal welfare and sustainability issues in aquaculture.

3.4.6. SUPPLEMENTARY MATERIAL

Supplementary tables are available for this paper at: https://ualg365-my.sharepoint.com/:f/g/personal/csraposo_ualg_pt/EvETOi0VDSdDusm9d1q3uMcB6P7GKYYxEnNEFK4m2Bivnw?e=0mUu6b

A new window into fish welfare: a proteomic discovery study of stress biomarkers in the skin mucus of gilthead seabream (*Sparus aurata*)



We must plant the sea and herd its animals using the sea as farmers instead of hunters. That is what civilization is all about - farming replacing hunting.

— Jacques Yves Cousteau

This chapter has been published as research article in:

Raposo de Magalhães, C., Farinha, A.P., Carrilho, R., Schrama, D., Cerqueira, M., Rodrigues, P.M., 2023. A new window into fish welfare: a proteomic discovery study of stress biomarkers in the skin mucus of gilthead seabream (*Sparus aurata*). *Journal of Proteomics*, In Press, **doi: 10.1016/j.jprot.2023.104904**



4.1. ABSTRACT

Fish skin mucus is a dynamic external mucosal layer that acts as the first line of defense in the innate immune system. Skin mucus' exudation and composition change severely under stress, making it a valuable biofluid to search for minimally invasive stress markers. This study focused on the skin mucus proteome response to repetitive handling, overcrowding, and hypoxia, using *Sparus aurata*, an important species in Mediterranean aquaculture, as a model. Biomarker discovery analysis was performed using label-free shotgun proteomics coupled with bioinformatics to unveil the most predictive proteins for the stressed phenotype. A mean of 2166 proteins were identified at a $< 0.2\%$ false discovery rate, from which the DAPs were mainly involved in the immune system and protein metabolism. A sparse partial least squares regression analysis revealed a high correlation between DAPs and plasma physiological stress indicators. Feature selection, performed by recursive feature elimination followed by logistic regression analysis of the selected proteins, disclosed 28 candidate biomarkers with values of area under the curve > 0.75 . These minimally invasive biomarkers could be used in forthcoming species-specific stress management protocols to improve fish welfare and promote farmed fish safety, positive societal outcomes, and business sustainability.

4.2. INTRODUCTION

Global fish consumption has been increasing at an average annual rate higher than that of all other animal protein foods, with aquaculture currently accounting for 56% of the aquatic food produced for human consumption (FAO, 2022). With the rapid development of aquaculture, it is urgent to ensure environmentally sustainable growth (Carballeira Braña et al., 2021; Jennings et al., 2016). Animal welfare is the foremost topic when deliberating on sustainability issues that arise from this industry because unfavorable welfare conditions ultimately result in impaired social, environmental, and animal well-being outcomes. In aquaculture, poor welfare implies more pollution in local waterways, poor fish immunity, and increased disease susceptibility, resulting in reduced global food security (Conte, 2004; Franks et al., 2021; Keeling et al., 2019). Moreover, fish diseases and chemicals used in their prevention and treatment, such as antibiotics, have severe consequences for aquatic ecosystems (Bergqvist & Gunnarsson, 2013; Lieke et al., 2020; Moreira et al., 2017). Increased consumer awareness and ethical concerns about intensive fish management systems, together with evidence that fish are sentient organisms that experience pain and suffering, have contributed to increased research on fish welfare (Browman et al., 2019; Brown, 2015; Lund et al., 2007). Establishing standardized welfare needs and indicators for aquaculture has been a matter of persistent debate and development among researchers and policymakers (Ashley, 2007). Welfare indicators provide information about the extent to which the animal's needs are met, and therefore, the welfare state of the fish. These should be usable, reliable, scalable, easily recognizable, minimally invasive, and evaluated within a reasonable timeframe. Ideally, a comprehensive welfare assessment framework should include both operational and laboratory-based welfare indicators (Stien et al., 2020). However, besides the numerous efforts toward the validation of species-specific welfare indicators, appropriate combinations of these measures are still scarce for most farmed species.

Many biotic and abiotic factors can affect the living conditions of farmed fish throughout their lifecycle and, consequently, their welfare state (Schreck & Tort, 2016). Transportation, handling, and unfavorable husbandry parameters, among others, may act as stressors and can evoke a long-term maladaptive physiological stress response in fish (Huntingford et al., 2006). The orchestration of this response starts with the activation of the neuroendocrine pathway, followed by the release of hormones into the bloodstream, culminating in the activation of energy-mobilizing pathways and

reorganization of resources (Mommsen et al., 1999). These adjustments constitute the adaptive function of the stress response intended to help fish cope with the situation (Iwama, 2007). However, when the challenges are prolonged, chronic deviation from the optimal functional level may reduce the animal's regulatory capacity, while growth, reproduction, and immune function can be affected, compromising welfare (Boonstra, 2013; Korte et al., 2007).

With the advent of holistic omics technologies, remarkable progress has been made in the characterization of fish responses to different challenges (Alfaro & Young, 2018; Cerqueira et al., 2020; de Vareilles et al., 2012; Raposo de Magalhães, Cerqueira, et al., 2020; Raposo de Magalhães et al., 2022; Raposo de Magalhães, Schrama, et al., 2020; Schrama et al., 2017; T. S. Silva et al., 2014), and proteomics has been successfully employed as a powerful toolset for biomarker identification in animal welfare research (Almeida et al., 2014; Cowan & Vera, 2008; Marco-Ramell et al., 2016).

Fish skin mucus is a dynamic external mucosal layer located between the epidermis and the environment, acting as the first line of defense of the innate immune system, as well as in respiration and excretion, among others (Easy & Ross, 2009; Shephard, 1994; S. Subramanian et al., 2007). The skin mucus matrix is mainly produced by goblet cells located in the epithelial tissue of fish. Its exudation and composition are known to change significantly under acute and chronic stress (Fernández-Alacid et al., 2018; Fernández-Montero et al., 2020). Additionally, this biofluid was recently proposed to form part of a cutaneous stress response system in fish (Kulczykowska, 2019), and a few studies have highlighted its potential for stress monitoring in different fish species (Cordero et al., 2016; De Mercado et al., 2018; Easy & Ross, 2010; R. Jia et al., 2016; Pérez-Sánchez et al., 2017; Reyes-López et al., 2021; Sanahuja & Ibarz, 2015).

In this study, we screened for potential stress biomarkers in the skin mucus proteome of gilthead seabream adults subjected to overcrowding, repetitive net handling, and hypoxia challenges using data and knowledge-driven approaches. We benchmarked an array of skin mucus proteins as candidate stress biomarkers for the given species that, according to logistic regression (LR) analysis, were most predictive of an imposed disturbance based on protein abundance values. These biomarkers could leverage the industry with tools to assess stress at early onset using minimally invasive lab-based indicators and contribute to the improvement of species-specific

welfare management protocols for sustainable aquaculture in tandem, boosting the business, acting as a gain for the environment, and improving global food security and safety.

4.3. MATERIALS & METHODS

4.3.1. Ethics

This study was approved by the Animal Welfare Committee of CCMAR (ORBEA) and the Portuguese National Authority for Animal Health, on August 26, 2019. The experiments followed the European guidelines on the protection of animals for scientific purposes (Directive 2010/63/EU) and the Portuguese legislation for the use of laboratory animals, under a “Group-1” license (permit number 0420/000/000-n.99–09/11/2009) from the Veterinary Medicine Directorate, the competent Portuguese authority for the protection of animals, Ministry of Agriculture, Rural Development and Fisheries, following category C FELASA recommendations.

4.3.2. Animals and stocking conditions

Gilthead seabream adults were supplied by “Maresa, Mariscos de Estero S.A.” (Huelva, Spain), and the experiments were conducted at the Ramalhete Research Station of CCMAR (Faro, Portugal), from November to March. Fish were randomly distributed into indoor 500 L fiberglass tanks supplied with flow-through seawater from Ria Formosa. Before each trial, the fish underwent a 2-week acclimation period. Physicochemical parameters varied within the natural regime during the trials (natural photoperiod, water temperature of 13.4 ± 2.2 °C, salinity of 34.7 ± 0.8 ‰ and dissolved oxygen level above 5 mg L^{-1}). Fish were fed once daily (in the morning) by hand, with commercial feed (Standard Orange 6, “AquaSoja, Sorgal, S.A”, Ovar, Portugal), according to the nutritional requirements of the species.

4.3.3. Experimental design

Three independent trials corresponding to challenging rearing conditions were tested: OC – Overcrowding, NET – repetitive net handling and air exposure, and HYP – Hypoxia. In each trial, fish were randomly allocated to three experimental groups: (1) a control group (CTRL), (2) a medium-intensity challenge and (3) a high-intensity challenge group. Fish within each group were distributed into triplicate tanks, and 4 fish per tank were further sampled for proteome analysis, in a total of 12 fish samples.

The initial rearing density was 10 kg m⁻³. In the OC trial, fish with an average IBW of 372.33 ± 6.55 g were subjected to high stocking densities over 54 days. The experimental groups were as follows: (1) OCCTRL – 10 kg m⁻³, (2) OC30 – 30 kg m⁻³ and (3) OC45 – 45 kg m⁻³. For the NET trial, fish (IBW = 375.69 ± 11.88 g) were challenged for 45 days. Nets were designed for this purpose, fitted inside the tanks, and lifted to air-expose the fish for 1 min. The experimental groups were established according to the frequency of the challenge: (1) NETCTRL – undisturbed fish (the net was also fitted inside the tanks but not lifted), (2) NET2 – fish netted twice a week, and (3) NET4 – fish netted four times a week. The last air exposure event was performed 72 h before sampling to ensure a resting period and make sure that any response was not derived from an acute stress but instead chronic. In the HYP trial, fish (IBW = 397.99 ± 16.56 g) were subjected to low saturated oxygen levels for 48 h. Saturations were achieved by nitrogen injection: (1) HYPCTRL – 100% saturated oxygen, (2) HYP30 – 30% saturated oxygen, and (3) HYP15 – 15% saturated oxygen. Saturated oxygen levels were measured every 30 min to keep track of potential fluctuations and adjust the injection rate, if necessary. Zootechnical data have been previously published by the authors (Raposo de Magalhães, Schrama, et al., 2020).

4.3.4. Fish sampling

At the end of the trials, fish were starved for 48 h to clean the digestive tract according to standard practices in aquaculture production. Four fish were randomly sampled from each tank for proteomic analyses and immediately anesthetized with a lethal dose of MS-222 (Merck KGaA). Excess water was removed using paper towels for skin mucus collection. Mucus samples were obtained by gently scraping the fish skin with a cell scraper on both sides of the fish and at the anterior-posterior orientation, avoiding scale removal as well as blood and feces or urine contamination. All samples were immediately frozen in liquid nitrogen and stored at -80 °C until further use.

4.3.5. Protein sample preparation

Skin mucus samples (n = 12, 4 fish per triplicate tank; tank unit as biological replicate) (200 µL) were first diluted with 10% (v/v) Milli-Q water to decrease sample viscosity and then solubilized with 200 µL buffer containing 1.5% (w/v) DTT, 1.5 mM EDTA, and a PI cocktail (Merck KGaA). Samples were homogenized in a ThermoMixer® C (Eppendorf, Hamburg, Germany) at 1400 rpm for 15 min at 4 °C.

Homogenates were centrifuged at 14,000 g, 4 °C, for 30 min, recovering the supernatant for further analysis. Mucus extracts were diluted in the initial buffer, and the protein content was measured using the BioRad Quick Start Bradford Dye Reagent and BSA Standard Set (Bio-Rad). Extracts were then depleted of non-protein contaminants using the ReadyPrep™ 2D Clean-up kit (Bio-Rad) following the manufacturer's instructions. The cleaned protein pellet was resuspended in 100 mM Tris pH 8.5, 1% sodium deoxycholate, 10 mM TCEP, 40 mM chloroacetamide, and protease inhibitors for 10 min at 95 °C at 1000 rpm (Thermomixer, Eppendorf). Samples were then prepared following the solid-phase-enhanced sample-preparation (SP3) protocol, as described elsewhere (Hughes et al., 2018). Enzymatic digestion was performed with 2 µg trypsin/LysC overnight at 37 °C and 1000 rpm.

4.3.6. Label free shotgun proteomics

4.3.6.1. nanoLC-MS/MS analysis

Peptides (500 ng) were analyzed by online nanoLC using an UltiMate™ 3000 system coupled to a Q-Exactive Hybrid Quadrupole-Orbitrap mass spectrometer (Thermo Scientific). Samples were loaded onto a trapping cartridge (Acclaim PepMap C18 100 Å, 5 mm × 300 µm, i.d. 160454, Thermo Scientific) in a mobile phase of 2% ACN and 0.1% FA at 10 µL min⁻¹. After 3 min of loading, the trap column was switched in-line to a 50 cm × 75 µm inner diameter EASY-Spray column (ES803, PepMap RSLC, C18, 2 µm, Thermo Scientific) at 250 nL min⁻¹. Separation was achieved by mixing A: 0.1% FA and B: 80% ACN, 0.1% FA, with the following gradient: 5 min (2.5% B to 10% B), 120 min (10% B to 30% B), 20 min (30% B to 50% B), 5 min (50% B to 99% B) and 10 min (hold 99% B). Subsequently, the column was equilibrated with 2.5% B for 17 min. Data acquisition was controlled by Xcalibur 4.0 and Tune 2.9 software (Thermo Scientific).

The mass spectrometer was operated in data-dependent acquisition (DDA) positive mode alternating between a full scan (m/z 380-1580) and subsequent HCD MS/MS of the 10 most intense peaks from the full scan (normalized collision energy of 27%). ESI spray voltage was 1.9 kV, and the capillary temperature was 275 °C. The global settings were as follows: use lock masses best (m/z 445.12003), lock mass injection Full MS and 175 chromatography peak width (FWHM) of 15 s. Full scan settings: 70k resolution (m/z 200), AGC target 3e6, maximum injection time 120 ms. DDA settings: minimum AGC target 8e3, intensity threshold 7.3e4, charge exclusion:

unassigned, 1, 8, > 8, peptide match preferred, exclude isotopes on, dynamic exclusion 45 s. MS2 settings: microscans 1, resolution 35k (m/z 200), AGC target 2e5, maximum injection time 110 ms, isolation window 2.0 m/z, isolation offset 0.0 m/z, dynamic first mass and spectrum data type profile. MS analyses were performed at the Proteomics Scientific Platform of i3S, Porto, Portugal.

4.3.6.2. Protein identification

Raw MS data were processed using SEQUEST[®] on Proteome Discoverer[™] software 2.5.0.400 (Thermo Scientific) and searched against the UniProtKB Eupercaria database (taxon ID 1489922; Release 2020_05; 651,914 sequences) for protein identification. The SEQUEST HT search engine was used to identify tryptic peptides. The ion mass tolerance was 10 ppm for precursor ions and 0.02 Da for fragmented ions. A maximum of two missed cleavage sites were allowed, with a minimum peptide length of six amino acids and a maximum of 144. Cysteine carbamidomethylation was defined as a constant modification. Methionine oxidation, protein N-terminus acetylation, loss of methionine and Met-loss+Acetyl were defined as variable modifications. Peptide confidence was set to high. The Inferys rescoring node was considered for this analysis. The processing node Percolator was enabled with the following settings: maximum delta Cn 0.05; decoy database search target false discovery rate (FDR) \leq 1%, validation based on *q*-value. Protein label-free quantitation was performed with the Minora feature detector node at the processing step. Precursor ions quantification (TOP3) was performed at the processing step with the following parameters: peptides to use unique plus razor, precursor abundance was based on intensity, normalization mode was based on total peptide amount, pairwise protein ratio calculation and hypothesis test were based on a *t*-test (background based). Processing workflow results i.e., .msf files, were imported into Scaffold (v.5.0.1, Proteome Software Inc.) to validate MS/MS-based peptide and protein identifications. A second search engine i.e., X! Tandem algorithm (The GPM, thegpm.org; version X! Tandem Alanine 2017.2.1.4) was applied to all MS/MS samples, using a reverse concatenated subset of the UniProtKB Eupercaria database (Release 2020_05; 651,914 entries), also assuming Trypsin digestion and parent ion tolerance of 10 ppm and fragment ion mass tolerance of 0.020 Da. Carbamidomethyl of cysteine was specified as a fixed modification, and Glu->pyro-Glu of the N-terminus, ammonia-loss of the N-terminus, gln->pyro-Glu of the N-terminus, oxidation of methionine and acetyl of the N-terminus

were specified as variable modifications. Peptide identifications were accepted if they could be established at greater than 95% probability to achieve an FDR less than 0.02% by the Peptide Prophet algorithm (Keller et al., 2002) with Scaffold delta-mass correction. Alongside, protein identifications were accepted at a minimum 99% probability (protein Decoy FDR of 0.2%) by the Protein Prophet algorithm (Nesvizhskii et al., 2003), containing at least four identified peptides. Proteins containing similar peptides that could not be differentiated based on MS/MS analysis alone were grouped to satisfy the principles of parsimony. Protein abundance was estimated based on the TOP3 Ion Precursor Intensity and normalized against the sum of all ion intensities in each sample replicate. The MS proteomics data have been deposited on the ProteomeXchange Consortium (Deutsch et al., 2020) via the PRIDE (Perez-Riverol et al., 2019) partner repository with the dataset identifier PXD038712 and doi:10.6019/PXD038712.

4.3.7. Statistical and bioinformatic analyses

4.3.7.1. Analysis of DAPs

Univariate and multivariate statistical analyses and bioinformatic analyses were performed using R v.4.2.0 (R Core Team, 2022) for MacOSX. A batch effect was observed among the 12 fish sample replicates within each experimental group, corresponding to two independent batches of six replicate samples each, identified using LC-MS/MS at different times. The batch effect among the two different sets of identified samples (replicate numbers 1 and 2 in the first batch, and 3 and 4, in the second batch) was corrected using the ComBat function within the R package sva (Leek et al., 2012), using the normalized protein abundance values (Figure S4.1 - [APPENDIX](#)). The corrected datasets were then filtered based on valid values (proteins quantified in at least 8 out of 12 replicates per challenging condition) and log₁₀ transformed prior to statistical analysis to ensure a Gaussian distribution of the residuals (Farinha et al., 2021). After assessing the residuals' normality and homoscedasticity, differences in protein abundance across experimental groups within each trial were analyzed by One-way ANOVA followed by *post-hoc* Tukey's HSD test ($p < 0.05$). The relationship between experimental groups was analyzed through PCA, using the `prcomp` R function in the auto-scaled matrices (samples × DAPs). Missing values were imputed based on the feature medians. Biplots were generated using the R package `factoextra` (Kassambara & Mundt, 2020). The most discriminant principal

component loadings were inspected to extract the top 10 features with the highest weights in each dimension.

4.3.7.2. Annotation of DAPs and PPI network analysis

DAPs were annotated based on the REACTOME knowledgebase (Fabregat et al., 2017) using the web-based analysis tool from Reactome v.82. The R packages *circlize* (Gu et al., 2014) and *ComplexHeatmap* (Gu et al., 2016) were used to visualize the results. PPI analysis of DAPs was carried out using the STRING v.11.0 (Szklarczyk et al., 2021). The FASTA sequences were used as queries to map the corresponding *D. rerio* orthologs. Protein nodes that showed no interactions were excluded from further analysis. Subsequently, PPI networks were visualized and analyzed topologically using the Cytoscape software v.3.9.1 (Shannon et al., 2003). The MCODE plugin (Bader & Hogue, 2003) was employed to detect densely connected regions within each network, using the app's default parameters. Clusters were extracted from the main network and analyzed individually. GO enrichment analysis of each cluster based on the Biological Process (BP) category was performed with the Cytoscape app ClueGO v.2.5.8 (Bindea et al., 2009). A two-sided hypergeometric test was used followed by the Benjamini-Hochberg method for p -value correction (FDR < 0.05).

4.3.7.3. Regression and correlation analysis between levels of protein abundance and physiological stress indicators

To evaluate the relationship between the levels of protein abundance from the skin mucus proteome and typical physiological stress indicators in the plasma (cortisol, glucose, and lactate) previously assessed by the authors under the same stress conditions (Raposo de Magalhães, Schrama, et al., 2020), a sparse partial least squares (sPLS) regression analysis (K.-A. L. Cao & Besse, 2008) was performed using the *mixOmics* package (Rohart et al., 2017). The levels of physiological stress indicators (Table S1 - [online](#)) were taken as the response “Y” variable and the identified proteins as the “X” variable. The analysis was performed using the mean values per tank ($n = 3$), as the number of fish replicates per tank was not the same for proteome profiling (four fish per tank) and the assessment of physiological stress indicators (six fish per tank). Model tuning was performed to define the best number of dimensions, based on the Q2 criterion, and the number of variables, based on the correlation

between predicted and actual components, through 10-fold cross-validation (CV) repeated five times. The linear relationship between physiological indicators and selected features was assessed by Pearson's correlation ($p < 0.05$).

4.3.7.4. Feature selection and predictive modeling of the stress response

To identify features that were the most predictive for a biological state, in this case, the stressed versus challenged phenotype, and thus retrieve the most discriminatory and biologically meaningful proteins in each trial, a binary classification algorithm was employed. "Stressed/Challenged" (yes vs. no) was used as the response variable (i.e., medium- and high intensity challenge groups, in each trial, were grouped as a single class) and the proteins' abundance as the explanatory variables. Feature selection was first performed using the recursive feature elimination (RFE) method combined with the Naïve Bayes classifier (Jung, 2016). Datasets (36 samples i.e., 24 "stress" and 12 "control") were first randomly divided into training (26 samples) and testing sets (10 samples) while keeping the same class balance, through 10-fold CV repeated three times. The R packages recipes (Kuhn & Wickham, 2022) and ROSE (Lunardon et al., 2022) were used for training data preprocessing and class imbalance correction, respectively. The models were fitted using the caret (Kuhn, 2020) package, with 5-fold CV repeated five times as a resampling method to select the number of predictor variables within each fold. Models were externally validated on the testing sets. Selected features had to meet the following criteria: selected in at least five out of 10 folds and two out of three repetitions. The final selected features were then compared with the top 10 features with the highest loading values on PCA, the top 20 features with the highest values of betweenness centrality in the PPI network and the features selected by the sPLS analysis of each plasma physiological indicator.

To assess whether the selected features correctly classified the samples into challenged and non-challenged groups (control), a binary logistic regression model was generated using each selected protein individually as a predictor (protein abundance as input). Datasets (36 samples i.e., 24 "stress" and 12 "control") were again divided randomly into training (21 samples) and testing sets (15 samples) while keeping the same class balance and using 10-fold CV. Preprocessing and data augmentation were performed as described previously. Generalized linear models were generated using the caret package with 10-fold CV repeated 10 times as the resampling method and accuracy as metric. The predictive ability of the fitted models

was evaluated on the testing sets in terms of accuracy and area under the receiver operating characteristic (AUC-ROC) curves. ROC curves were generated using the R package pROC (Robin et al., 2011) to evaluate the performance of the model and the AUC, which reflects the potential of the measurement as a diagnostic tool. Accuracy and AUC were averaged across the 10 folds. The overall workflow of the statistical and bioinformatic analyses is summarized in Figure 4.1.

All figures were created using the open-source graphics editor Inkscape (<http://www.inkscape.org/>).

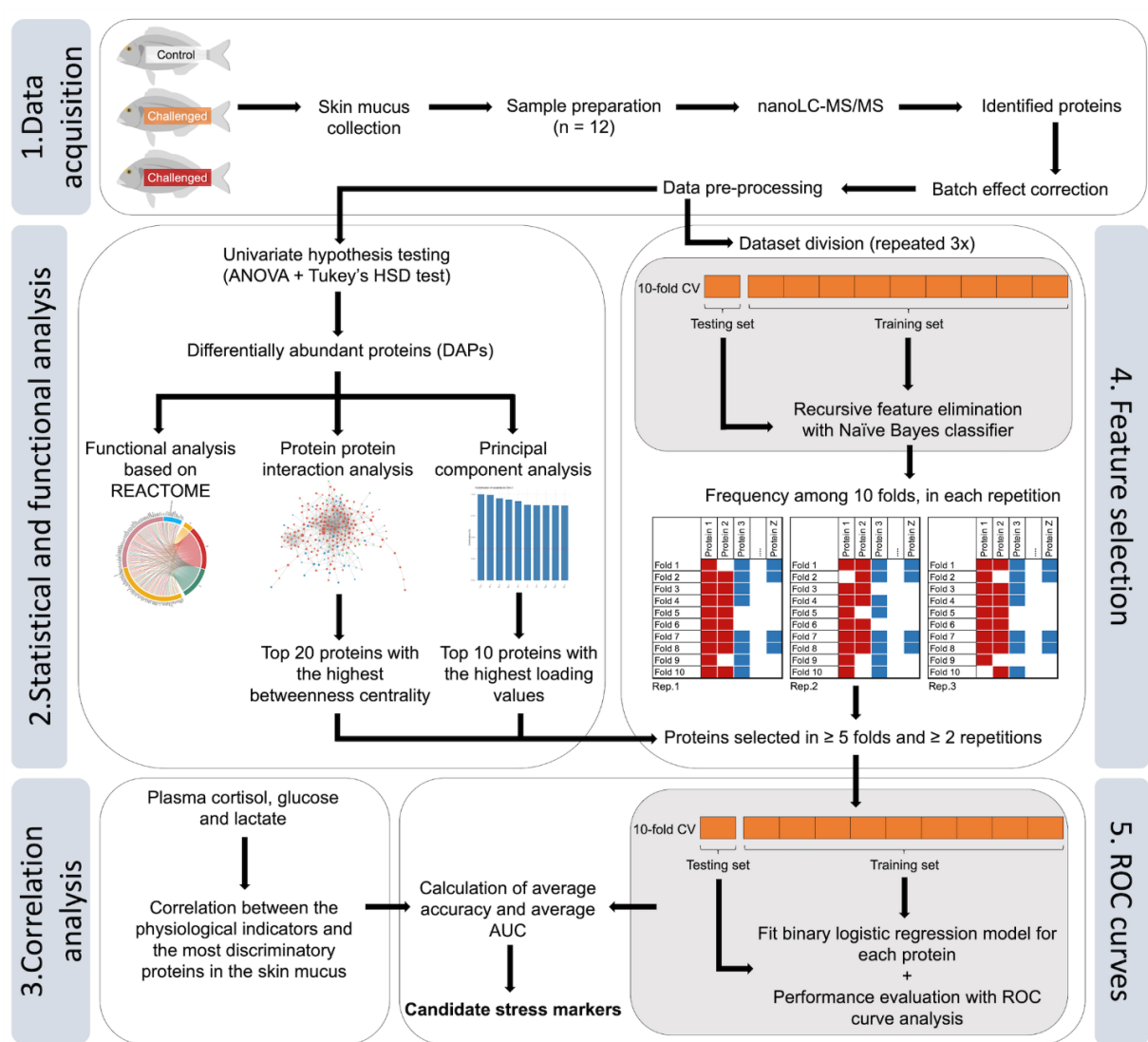


Figure 4.1. Schematization of the methodology workflow, from sample collection to ROC curve analysis.

4.4. RESULTS AND DISCUSSION

4.4.1. Label-free shotgun proteomics overview

Proteome analysis of gilthead seabream skin mucus led to a mean of $45.4 \pm 9.6\%$ PSM out of a mean of $38,866 \pm 6674$ spectra per MS/MS sample (Table S2 - [online](#)). A total of 2,214, 2,156 and 2,127 proteins were identified for the OC, NET and HYP trials, respectively, with a probability higher than 99% (decoy FDR < 0.2%) assigned by the Protein Prophet algorithm, with at least four peptides (decoy FDR < 0.02%) on the Scaffold software v.5.0.1 (Proteome Software Inc.) (Table S3 - [online](#)). From these, 1,857, 1,736, and 1,722 reproducible proteins i.e., present in at least 70% of all replicates (Table S3 - [online](#)) were selected from the OC, NET and HYP trials, correspondingly, for further statistical and functional analyses.

4.4.2. Skin mucus proteome response to different challenges

Stress is a conserved homeostatic regulatory mechanism in vertebrates, to which distinct organs respond differently, but with the common aim of overcoming internal disturbance (Wendelaar Bonga, 1997). This stress response is a complex event influenced by an individual (e.g., species, age, sex, previous experiences, or coping styles) and/or stressor-related factors e.g., intensity and duration (Galhardo et al., 2009). The differences in fish skin mucus proteome profiles under different challenge intensities within each trial were assessed by One-way ANOVA followed by Tukey's HSD test ($p < 0.05$) (Table S4 - [online](#)). The NET trial registered the highest number of differentially abundant proteins (DAPs), with 272 proteins, whereas OC registered the lowest number, i.e., 64 proteins (Table S4 - [online](#)). In the HYP trial, 183 DAPs were found in hypoxia-exposed gilthead seabream skin mucus (Table S4 - [online](#)). A similar proteomic profile was observed in the liver of the same fish by label-free shotgun proteomics, with a higher number of DAPs in the NET-challenged fish, i.e., 349 proteins, compared to OC and HYP fish, with 40 and 46 proteins (Raposo de Magalhães et al., 2022), respectively. The same was found in the plasma proteome, analyzed by 2D-DIGE, with a higher number of DAPs in NET fish (360 proteins), than in those challenged by HYP (34 proteins) and OC (19 proteins). This trend was concomitant with the plasma cortisol levels, the most common physiological stress indicator, found in these fish (Raposo de Magalhães, Schrama, et al., 2020). Recent studies on mucus production and renewal in gilthead seabream found a close rate of

isotope incorporation in the liver, plasma, and skin mucus, after fish were fed a labelled meal (Ibarz et al., 2019).

The significant changes in the skin mucus proteome indicated that net handling was the most impactful challenge for gilthead seabream, most likely due to its repetitive mode. A plausible explanation for the lower impact on the overcrowded fish proteome compared with NET- and HYP-challenged fish might be that fish might have coped with the OC through less intense metabolic reprogramming, suggesting adaptation or desensitization. In fish exposed to hypoxia, a higher number of DAPs were observed in the skin mucus as compared with the remaining tissues (Raposo de Magalhães et al., 2021, 2022; Raposo de Magalhães, Schrama, et al., 2020), which could be related to a faster response in the skin mucus, due to the short-term nature of this challenge. It has been shown that the peripheral response can be more immediate than the metabolic shift occurring in central organs during acute/short-term stress, as in the case of physical injury (H. Guo & Dixon, 2021). In fact, the neuroendocrine response in fish, which is immediately activated following a perceived stressor, is accompanied by a local response in the mucosal surfaces, that is, the nose, skin, gills, and gut, independent of the central organs. These mucosae can react to stressors even if the challenge does not involve a typical immune response e.g., the presence of a pathogen (Yada & Tort, 2016).

4.4.3. Functional analysis of skin mucus DAPs

4.4.3.1. REACTOME pathway analysis

Functional annotation using REACTOME revealed 257 out of 429 unique DAPs (60% of proteins annotated) across all trials, mapping into 16 major categories. The categories “Metabolism” (57 proteins) “Metabolism of proteins” (54), “Immune system” (35) and “Signal transduction” (29) were largely represented when compared to the remaining ones (Figure 4.2; Table S5 - [online](#)). This is expected because teleost skin mucus is a dynamic layer known to display important physiological functions and to contain a wide variety of biologically active molecules that participate in distinct cellular processes. Exogenous factors, such as stressful conditions, can change the mucus viscosity, exudation, and composition, including the level of specific proteins (Reverter et al., 2018). In this case, several pathways associated with protein turnover were dysregulated by the distinct challenging conditions, to different extents, according to their nature (Figure 4.2; Table S5 - [online](#)). These results further indicated that the

regulation of the translational machinery was highly coordinated with amino acid and carbohydrate metabolism, most likely in the control of pools of amino acids and energy during the interplay of protein biosynthesis and degradation in response to each challenge. Moreover, the fish skin mucus was demonstrated to be part of an active mucosal immune system, in this case, the skin-associated lymphoid tissue (SALT), known, as previously described, to respond to stimuli independently of central organs (Salinas & Magadán, 2017). The high number of DAPs (51 proteins) related to the immune system and hemostasis identified in this study is noteworthy, indicating the importance of this tissue in the immune stress response. Proteins involved in protein turnover, different metabolic pathways, and the immune system have also been identified in multiple studies on the skin mucus of gilthead seabream (Cordero et al., 2016; Pérez-Sánchez et al., 2017; Sanahuja & Ibarz, 2015). Additionally, a study has shown that proteins found in the skin mucus can either result from direct expression in epidermal cells or secretion by a secondary circulatory system, which might explain the high diversity of biological functions found in this mucosal tissue (Easy & Ross, 2009).

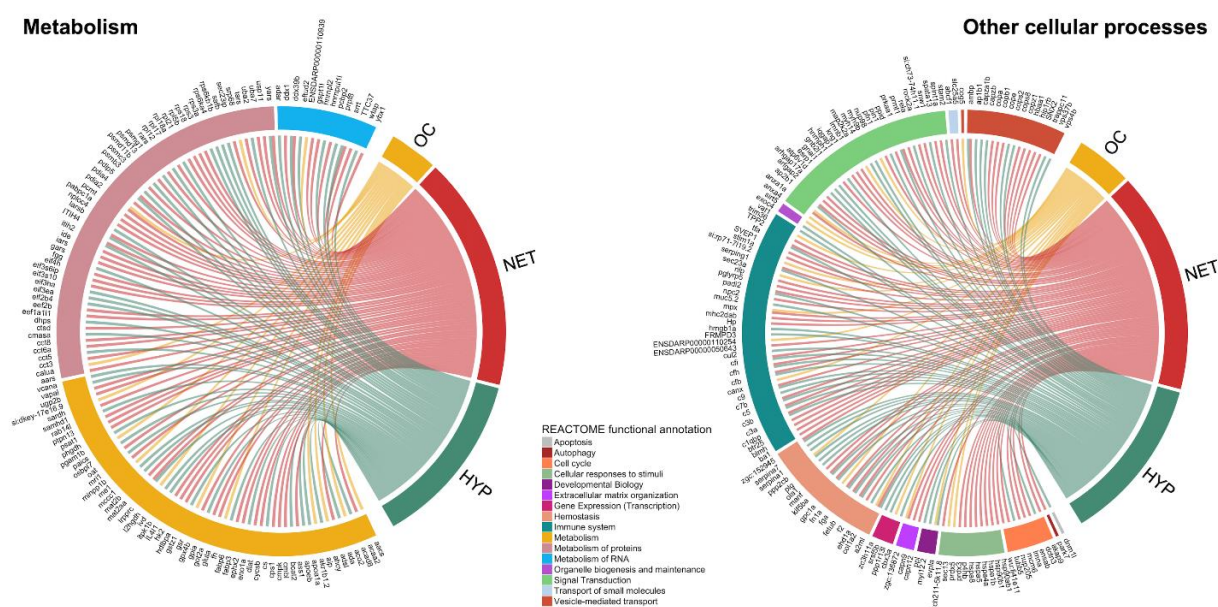


Figure 4.2. Circos plots displaying a comprehensive functional characterization of skin mucus DAPs identified in gilthead seabream by label-free shotgun proteomics. Protein functions were annotated according to REACTOME pathways. DAPs within each fish trial i.e., overcrowding (OC), repetitive net handling (NET) and hypoxia (HYP) were assessed by One-way ANOVA followed by Tukey's test ($p < 0.05$) (see Table S3 - [online](#)). Protein annotation into REACTOME pathways is detailed on Table S4 - [online](#).

4.4.3.2. Stress-responsive protein-protein interaction network

Protein-protein interaction (PPI) network analysis was performed to depict the biological interactions between the DAPs identified in the skin mucus and pop-up candidate proteins as potential stress markers in gilthead seabream adults. The NET PPI network disclosed 958 interactions among 216 proteins (Figure 4.3), whereas 136 proteins generated 454 interactions in the HYP PPI network (Figure S4.2 - [APPENDIX](#)). A lower number of protein interactions was observed in the OC PPI network, with 44 interactions among the 36 proteins (Figure S4.3 - [APPENDIX](#)). The clustering coefficients in NET, HYP and OC PPI networks were 0.296, 0.405 and 0.126, respectively. The coefficients of node betweenness centrality and degree were used to highlight the most critical points in the network by indicating the bottleneck and hub proteins, respectively (Table S6 - [online](#)). These values were further used for comparison with the features selected by the recursive feature elimination method which is discussed in detail in the following sections.

GNB2|1, HSPA5, and F2 were the top three proteins with the highest values of betweenness centrality in the NET network (Figure 4.3; Table S6 - [online](#)). According to the REACTOME annotation (Figure 4.2; Table S5 - [online](#)), these proteins are involved in signal transduction, cellular responses to stress, and hemostasis, respectively. GNB2|1 encodes the protein receptor for activated C kinase 1, a multifaceted scaffolding protein with a wide variety of critical roles, from mRNA translation to cell survival and death. In humans, the aberrant expression of this protein has been associated with numerous pathologies (Gandin et al., 2013). HSPA5 is a heat-shock protein with chaperoning functions that is involved in the UPR during ER stress. F2 is a prothrombin, a key protein in blood coagulation. In the HYP network, RPL18a, CAPZB, and ZGC:86896 were the three proteins with the highest betweenness centrality (Figure S4.2 - [APPENDIX](#); Table S6 - [online](#)). The first is a ribosomal protein involved in translation, whereas CAPZB and ZGC:86896 are actin binding proteins involved in vesicle-mediated transport. The three proteins with the highest betweenness centrality in the OC network were SPNA2, EVPLA, and GSR (Figure S4.3 - [APPENDIX](#); Table S6 - [online](#)). The first two are cytoskeletal proteins involved in cell adhesion and communication, while GSR, the glutathione-disulfide reductase, is a critical protein in oxidative stress.

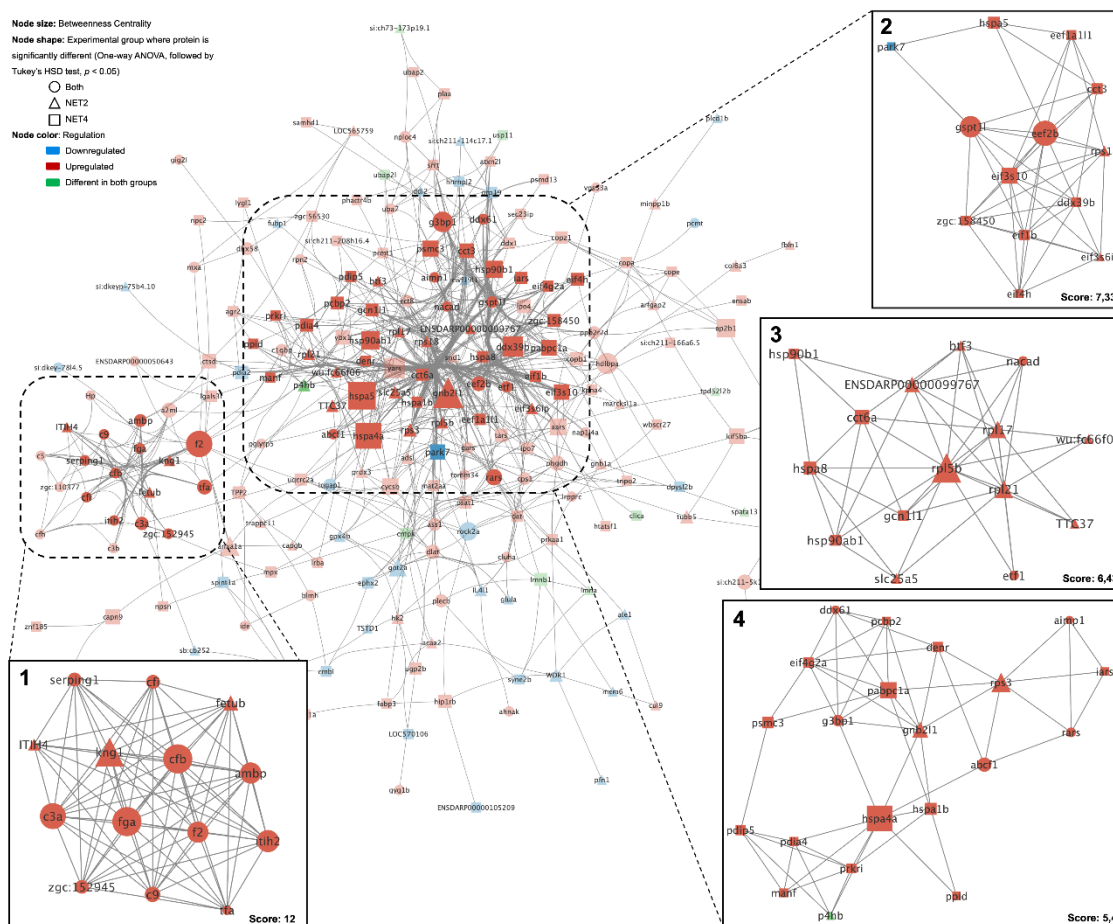


Figure 4.3. PPI network of the DAPs identified in the skin mucus of gilthead seabream, submitted to control and repetitive net handling in two intensities, namely “NET2” and “NET4” challenging conditions (Table S3 - [online](#)). Nodes represent proteins, and edges, the interactions between them. Betweenness centrality is represented by the size of the nodes, while node color and shape indicate protein regulation and significant differences, respectively, according to the figure legend. Four densely interconnected regions/clusters are highlighted in the squared boxes.

4.4.3.3. GO enrichment of proteins highly interconnected in the network

Four densely connected regions (clusters) were detected in the NET network (Figure 4.3), three were identified in the HYP network (Figure S4.2 - [APPENDIX](#)), and no clusters were identified in the OC network (Figure S4.3 - [APPENDIX](#)). GO enrichment analysis (hypergeometric Benjamini & Hochberg FDR correction, $q < 0.05$) of the main clusters in the NET network revealed proteins involved in proteolysis, the complement system and hemostasis (cluster 1), translation (cluster 2), and tRNA aminoacylation and cell redox homeostasis (cluster 4) (Figure 4.4). No enriched GO terms were found for cluster 3. In the case of the clusters in the HYP network, only one cluster was found to be significantly enriched in terms associated with proteolysis, the complement system and hemostasis (Figure S4.4 - [APPENDIX](#)).

The PPI analysis emphasized the major role of the skin mucus in the immune system, although the divergent response at the proteome level between net handling and hypoxia challenges revealed a cluster of proteins associated with the immune system predominantly upregulated in the former case, and downregulated, in the latter case. It can be hypothesized that this difference might be due to the different durations of the challenges (i.e., net handling lasted for 1.5 months, while hypoxia lasted for 48 h) and/or the type of stress imposed. Concomitantly, several proteins involved in the immune system, specifically acute phase proteins (i.e., fibrinogen alpha-chain, complement component C3, haptoglobin, complement factor B, warm-temperature acclimation 65kDa protein, alpha-1-antitrypsin) were upregulated in the plasma of net-handled fish. In contrast, complement C3, a fundamental protein in the complement system of innate immunity in fish (Boshra et al., 2006), was downregulated in the plasma of hypoxia-exposed fish (Raposo de Magalhães, Schrama, et al., 2020). Negative regulation of proteolysis was also enriched in both trials, which is consistent with the high antiprotease activity reported in this tissue (Guardiola et al., 2014). Furthermore, protein biosynthesis appeared to be upregulated in NET-challenged fish, according to the GO enrichment analysis of cluster 2 (Figure 4.4). Protein translation is usually downregulated under stress conditions, as protein synthesis represents a highly energetic biological process in cells (B. Liu & Qian, 2014). However, specific messenger RNAs, such as those encoding stress-related proteins required for cellular protection, can escape this repression (Richter et al., 2010). This is consistent with the liver response of these fish, where protein biosynthesis was also found to be upregulated and was closely associated with ER stress (Raposo de Magalhães et al., 2022).

4.4.4. Correlation analysis between the skin mucus proteome and physiological stress indicators in plasma

A correlation analysis was performed using sparse Partial Least Squares (sPLS) regression between the abundance of proteins identified in the gilthead seabream skin mucus and physiological stress indicators (cortisol, glucose, and lactate) previously found in the plasma of fish from the same trials (Raposo de Magalhães, Schrama, et al., 2020).

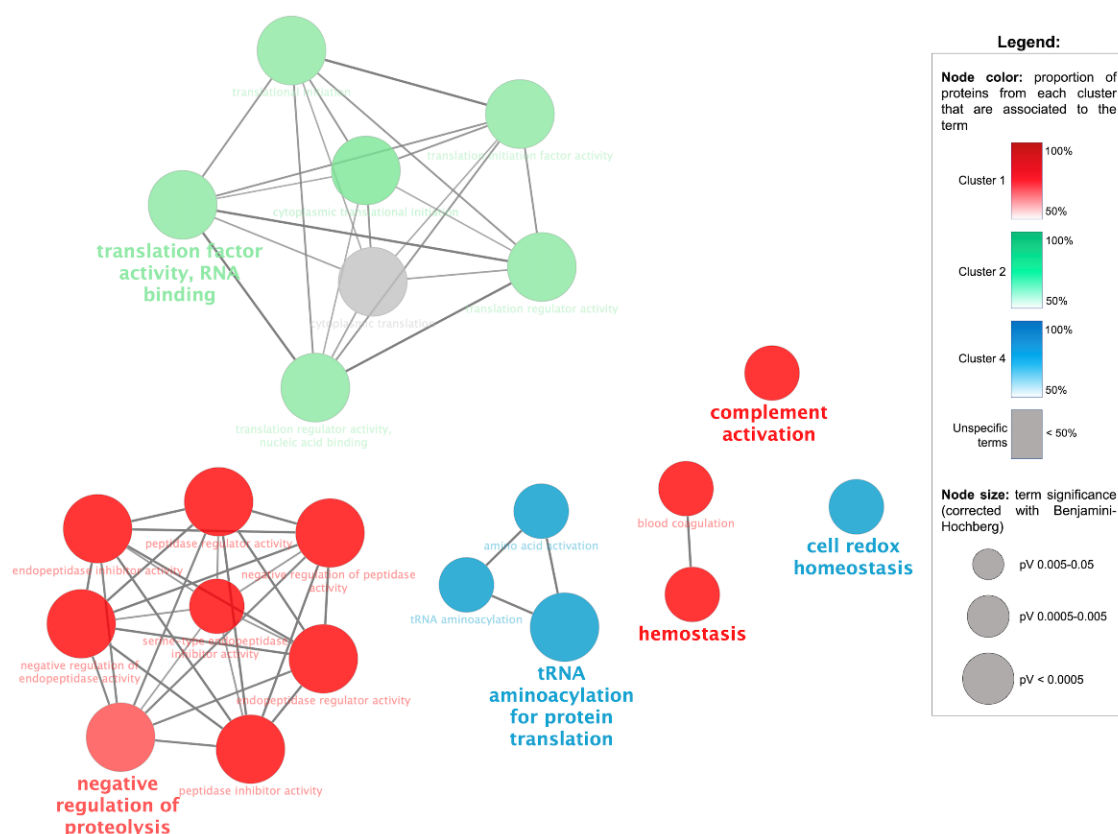


Figure 4.4. Networks of enriched GO terms (hypergeometric Benjamini & Hochberg FDR correction, $q < 0.05$) in the main clusters depicted in the NET PPI network (Figure 4.3). GO enrichment analysis was performed based on the biological process category.

Activation of the HPI axis, following the perception of a stressful stimulus by the fish, results in the release of cortisol into the bloodstream as a primary response. This increase in plasma cortisol levels is usually followed by a rise in the concentration of energetic substrates, such as glucose and lactate, the so-called secondary stress responses. Thus, these metabolites are regularly used in fish research as indicators of an activated stress response (T. Ellis et al., 2012). Hence, this correlation analysis aimed to identify the skin mucus proteins following the same response outline as physiological stress indicators. As a result of the sPLS regression analysis, 50 (OC), 40 (NET), and 38 (HYP) predictor proteins were selected (Table S7 - [online](#)) and those with a significant Pearson's correlation coefficient > 0.75 ($p < 0.05$) in the first component are represented in Figure 4.5. These were used for further comparison with the proteins/features selected by the recursive feature elimination method. The Pearson's correlation coefficient ($p < 0.05$) between the "X" (proteome) and "Y" (plasma physiological indicators) variables was 0.985 ($p = 1.232e^{-06}$), 0.983 ($p = 2.05e^{-06}$), and 0.993 ($p = 7.624e^{-08}$), for OC, NET an HYP trials, respectively, indicating that

sPLS effectively modeled a linear and significant ($p < 0.01$) relationship between the combinations of variables selected in “X” and “Y”. The number of predictor proteins was also in accordance with the statistical differences found for physiological stress indicators (published in (Raposo de Magalhães, Schrama, et al., 2020)). In OC, statistical differences between the control and challenged groups were only found for lactate levels, whereas glucose levels were significantly different in the NET and HYP trials.

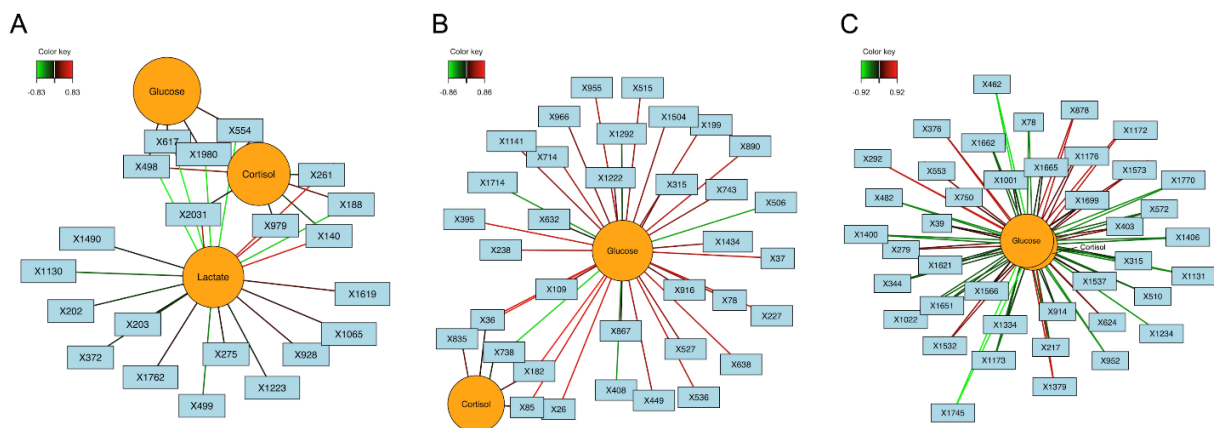


Figure 4.5. Sparse partial least squares regression analysis of the skin mucus proteome and the plasma physiological indicators. Networks indicate predictor proteins selected among OC (A), NET (B) and HYP (C) identified proteins with a correlation coefficient higher than 0.75 with the physiological indicators. Proteins (rectangles) are represented by the Protein ID (Table S2 - [online](#)). Positive correlations are represented by red edges and negative correlation by green edges.

4.4.5. Discovery of candidate stress biomarkers in the gilthead seabream skin mucus

A biomarker is defined as a biologically important signature that unambiguously identifies when a specific physiological condition exists (sensitivity) or when it does not (specificity). Additionally, it should be sensible, quantitative, and reproducible among experiments, and its assessment should be noninvasive (Benninghoff, 2007). It has been recently proposed to use fish skin mucus to find biomarkers for evaluating fish stress under farming conditions (Sanahuja & Ibarz, 2015). Typical stress indicators e.g., cortisol, glucose, lactate, and oxidative stress markers, have been identified in the skin mucus of rainbow trout and meagre exposed to different challenges (De Mercado et al., 2018; Fernández-Alacid et al., 2019). A study involving the functional analysis of 2060 epidermal mucus proteins in gilthead seabream also pointed to the role of this tissue as a potential source of chronic stress biomarkers in fish (Pérez-

Sánchez et al., 2017). Our work further supports that skin mucus is appropriate for screening for biomarkers in *S. aurata* adults in response to NET and OC and suggests the same for short term/acute stressors such as HYP, leveraging for transversal stressor management.

4.4.5.1. Principal component analysis

An unsupervised PCA was performed for each trial, using the DAPs, to inspect the samples' clustering, group separation and highlight the proteins that contributed the most to discriminating between control and challenged groups. The score scatter plots indicate that the first principal component (x-axis) separated control from challenged groups, in all trials, with 23.1, 23.9 and 20.9%, of explained variance for OC, NET, and HYP data, respectively (Figure 4.6). The loading values of the first principal component were extracted (Figure S4.5 - [APPENDIX](#)) and the top 10 variables (proteins) with the highest weights are represented by arrows in the biplots in Figure 4.6. These were further compared with the features selected by the recursive feature elimination method.

4.4.5.2. Selection of predictor proteins by RFE

RFE is a wrapper-type feature selection algorithm commonly used for feature selection in proteomics studies (Lualdi & Fasano, 2019; Suppers et al., 2018). In this study, within each set of identified proteins in the skin mucus of gilthead seabream, a subset of proteins that were the most predictive of a challenged/stressed status was depicted by 10-fold CV repeated three times (Table S8 - [online](#)). Within each fold, proteins were selected on the training set by RFE coupled to a Naïve Bayes classifier. In total, 10, 11, and 17 predictor proteins were selected in ≥ 5 folds plus ≥ 2 repetitions for OC, NET and HYP datasets, respectively. These were then compared with 1) the top 10 proteins with the highest loading values in the first principal component of the PCA biplots (Figure 4.6), 2) the top 20 proteins with the highest values of betweenness centrality in the PPI networks (Table S6 - [online](#)), and 3) the predictor proteins selected by the sPLS analysis (Table S7 - [online](#)). Proteins in common between all the described methods were further used individually as input to logistic regression models that classified challenged fish versus control fish (Table S9 - [online](#)). Two DAPs commonly identified across all trials, i.e., alpha-2-macroglobulin (A2ML) and inter-alpha-trypsin inhibitor heavy chain H3 (zgc:110377), were also used as inputs.

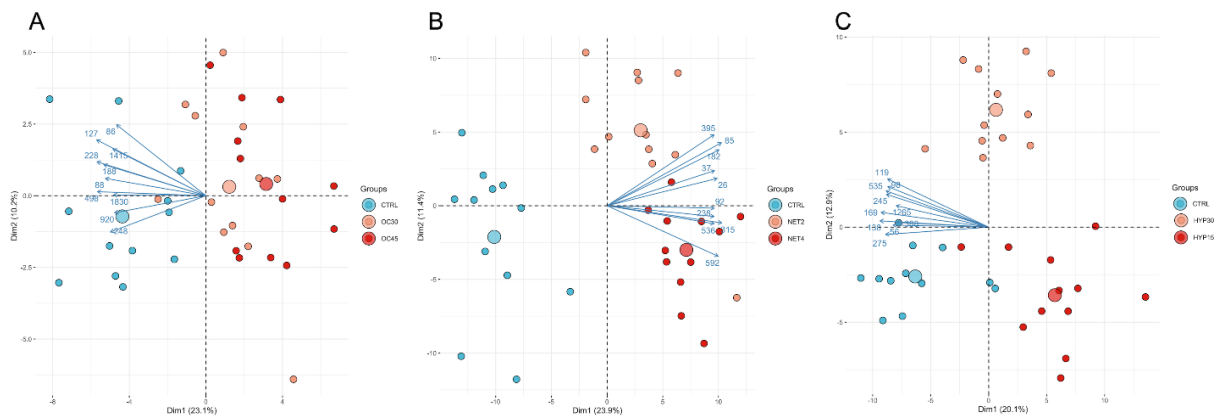


Figure 4.6. PCA biplots of the skin mucus proteomics data of gilthead seabream adults from OC (A), NET (B) and HYP (C) trials. Experimental groups within trials are represented by different colors, as indicated in the figure legend. The largest point, in each group, represents the group mean. Axis' percentages indicate the proportions of explained variance. Arrows represent the top ten features with the highest loading values in the first principal component.

4.4.5.3. Predictive logistic regression model

Based on the protein abundance values, a binary logistic regression (LR) model was used to predict whether a certain sample belonged to a control or challenge-exposed fish (both challenged groups were grouped together as one categorical variable). Each trial was analyzed separately since most of the selected proteins were challenge/stress-specific. Proteins in common across all trials were likewise analyzed separately due to the different baseline levels of protein abundance. For the OC, NET and HYP trials, 10, 12 and 13 predictor proteins were used, respectively (Table 4.1). For each selected protein, an LR model was fitted to the training sets over a 10-fold CV, and externally validated by predicting the outcome on the hold-out samples. The average accuracy of the training and testing sets was calculated over the 10 folds for each protein (Table 4.1). Overall, higher accuracies were obtained in the NET trial, which was consistent with the PCA biplots (Figure 4.6), as NET groups showed better separation over the first two components.

4.4.5.4. Evaluation of model performance through ROC curve analysis

The diagnostic performance of each protein was assessed using ROC curve analysis on the testing set to estimate how well the model could generalize new data (Table S10 - [online](#)). In the OC trial, five out of 10 proteins presented an AUC > 0.8, with sarcosine dehydrogenase (SARDH), programmed cell death 6-interacting protein (PDCD6IP), and mitogen-activated protein kinase 2a (MAP2K2A) presenting the

highest values (Table 4.1). According to the REACTOME annotation, SARDH is involved in metabolism (Figure 4.2; Table S5 - [online](#)), catalyzing the last step of the oxidative degradation of choline to glycine. PDCD6IP is a multifunctional protein that is primarily involved in endocytosis and apoptosis. Finally, MAP2K2A is involved in signal transduction, specifically in the mitogen-activated protein kinase (MAPK) cascade, a central signaling pathway that regulates cell proliferation, apoptosis, and the stress response (Plotnikov et al., 2011). SARDH and MAP2K2A were also selected by the sPLS algorithm as predictor proteins of the variance in plasma cortisol, glucose, and lactate levels (Figure 4.5). In the NET trial, all 12 predictor proteins presented a high predictive power i.e., $AUC > 0.9$ (Table 4.1). Based on the REACTOME annotation analysis, seven out of the 12 proteins were involved in the immune system and hemostasis (Figure 4.2; Table S5- [online](#)), reinforcing this way the importance of skin mucus in the immune defense. The remaining proteins e.g., eukaryotic translation elongation factor 2b (EEF2B) and T-complex protein 1 subunit theta (CCT8), were involved in protein turnover. In fact, EEF2B was the most centric protein in cluster 2 from the PPI network (Figure 4.3), exhibiting the highest betweenness centrality, thus highlighting its importance in the orchestration of protein metabolism. Moreover, nine out of the 12 proteins were selected as predictor proteins for the sPLS model, whereas hemopexin (ZGC:152945), transferrin (TFA), A2ML and EEF2B presented a correlation > 0.75 with plasma cortisol and glucose (Figure 4.5). Likewise, in the HYP trial, two out of 13 proteins showed an $AUC > 0.9$, namely, ribosome binding protein 1b (RRBP1A) and N-myc downstream-regulated gene 1a (NDRG1A), and other 10 proteins showed AUC values > 0.8 (Table 4.1). RNA-binding proteins are key regulators of gene expression and are involved in the assembly of stress granules, i.e., membraneless cell compartments formed in response to distinct stress stimuli and crucial for cell survival (Marcelo et al., 2021). NDRG1A is involved in the cellular stress response, and it is specifically induced under hypoxic conditions. Under low oxygen levels, the hypoxia inducible factor-1 α (HIF-1 α) accumulates in the cytoplasm and translocates into the nucleus, binding to HIF-1 β to form the HIF-1 complex and inducing the expression of NDRG1A by binding to hypoxia response elements (HREs) located in the promoter of its gene (Cangul, 2004; K. C. Park et al., 2020). Notably, NDRG1 can also be upregulated in a HIF-1 α -independent manner, involving the eukaryotic initiation factor 3a (eIF3a) (Lane et al., 2013). Interestingly, NDRG1A and eIF3a were also significantly upregulated in the NET trial (Table S4 - [online](#)).

Furthermore, NDRG1 has been evaluated as a potential biomarker of different human cancers (Cheng et al., 2011; Y. J. Sun et al., 2021). However, to the best of our knowledge, the role of this protein in the fish stress response remains unexplored. The other upregulated protein selected in the HYP trial was protein phosphatase 2 catalytic subunit β (PPP2CB), which was also selected in the OC trial, although downregulated (Table 4.1). Protein phosphatase 2A also appears to be modulated by HIF-1 α (Elgenaidi & Spiers, 2019). In the HYP trial, two of the selected proteins, namely spectrin repeat containing nuclear envelope 2b (SYNE2B) and serpine1 mRNA binding protein 1 (WU:FC66F06) were also highly correlated with the plasma physiological indicators of stress, according to the sPLS analysis (Figure 4.5).

This discovery analysis of a specific set of 28 skin mucus proteins' diagnostic performance demonstrates their discriminating power and usefulness as potential stress-specific biomarkers. Remarkably, A2ML and ZGC:110377 were able to discriminate more than one type of stress, with better performance for NET and HYP fish (AUC > 0.85) (Table 4.1). A2ML is a broad-spectrum proteinase inhibitor, abundant in the plasma of vertebrates and invertebrates, participating in the non-specific humoral response of fish's innate immune system (Funkenstein et al., 2005; Natnan et al., 2021). It has been recently identified as a biomarker of bovine paratuberculosis (H.-E. Park et al., 2021) and liver fibrosis in hepatitis C patients (Ho et al., 2010). Inter-alpha-trypsin inhibitor heavy chain H3 (ZGC:110377) has been studied as a biomarker of human colorectal cancer (X. Jiang et al., 2019).

Table 4.1. Logistic regression and ROC curve analyses of predictor proteins selected by the RFE. Values of accuracy and AUC of the training and testing sets are the mean of 10-fold cross validation. Proteins, represented by STRING annotations, highlighted in blue correspond to downregulated proteins while the ones highlighted in red represented upregulated proteins.

ID ¹	STRING ²	Training set								Testing set							
		Acc. ³	SD	Min	Max	AUC-ROC ⁴	SD	Min	Max	Acc. ³	SD	Min	Max	AUC-ROC ⁴	SD	Min	Max
OC trial																	
920	map2k2a	0.846	0.057	0.76	0.9	0.893	0.049	0.82	0.96	0.752	0.045	0.67	0.8	0.83	0.075	0.72	0.94
372	prdx5	0.846	0.052	0.76	0.9	0.871	0.079	0.73	0.98	0.82	0.089	0.67	0.93	0.818	0.109	0.64	1
498	sardh	0.809	0.086	0.67	0.95	0.878	0.060	0.79	0.98	0.773	0.090	0.67	0.93	0.884	0.094	0.74	1
402	ppp2ca	0.78	0.042	0.71	0.86	0.803	0.050	0.73	0.88	0.706	0.090	0.53	0.8	0.752	0.085	0.64	0.9
1036	anxa1a	0.771	0.080	0.67	0.9	0.835	0.096	0.68	0.99	0.726	0.048	0.67	0.8	0.768	0.134	0.58	1
1552	prpsap2	0.821	0.059	0.67	0.86	0.86	0.037	0.77	0.9	0.745	0.042	0.67	0.8	0.802	0.073	0.72	0.98
127	pdcd6ip	0.829	0.047	0.76	0.9	0.832	0.071	0.76	0.95	0.82	0.089	0.67	0.93	0.842	0.108	0.68	0.98
391	ppp2cb	0.741	0.040	0.67	0.81	0.803	0.060	0.71	0.87	0.693	0.084	0.53	0.8	0.74	0.082	0.64	0.88
532	a2ml	0.752	0.063	0.67	0.86	0.751	0.065	0.64	0.86	0.698	0.064	0.53	0.73	0.65	0.156	0.36	0.86
493	zgc:110377	0.772	0.093	0.62	0.86	0.76	0.088	0.65	0.9	0.74	0.086	0.6	0.87	0.656	0.170	0.4	0.86
NET trial																	
638	c9	0.913	0.037	0.87	0.96	0.948	0.047	0.83	0.99	0.907	0.069	0.77	1	0.997	0.009	0.97	1
85	zgc:152945	0.95	0.053	0.9	1	0.995	0.005	0.99	1	0.958	0.036	0.93	1	0.966	0.046	0.9	1
37	plecb	0.932	0.061	0.86	1	0.964	0.037	0.92	1	0.893	0.077	0.8	1	0.945	0.058	0.84	1
1434	Hp	0.927	0.045	0.86	1	0.967	0.019	0.94	1	0.901	0.063	0.8	1	0.935	0.057	0.81	1
26	eef2b	0.892	0.058	0.86	1	0.966	0.024	0.92	1	0.894	0.031	0.87	0.93	0.938	0.081	0.78	1
238	cct8	0.871	0.058	0.81	1	0.931	0.038	0.86	1	0.82	0.136	0.47	0.93	0.902	0.112	0.6	1
182	a2ml	0.922	0.056	0.86	1	0.974	0.025	0.93	1	0.874	0.073	0.73	1	0.93	0.101	0.7	1
581	gig2l	0.833	0.051	0.76	0.9	0.926	0.033	0.89	0.98	0.846	0.106	0.73	1	0.94	0.047	0.86	1
36	tfa	0.848	0.071	0.76	1	0.949	0.032	0.89	1	0.807	0.086	0.6	0.93	0.913	0.129	0.55	1
463	c5	0.868	0.073	0.81	1	0.94	0.040	0.89	1	0.874	0.106	0.67	1	0.931	0.088	0.75	1
78	c3a	0.856	0.066	0.81	1	0.958	0.023	0.93	1	0.852	0.082	0.73	0.93	0.932	0.081	0.72	0.98

527	zgc:110377	0.838	0.076	0.76	1	0.933	0.039	0.87	1	0.78	0.055	0.67	0.87	0.908	0.072	0.8	1
HYP trial																	
1597	rrbp1a	0.833	0.045	0.76	0.9	0.894	0.057	0.81	0.99	0.793	0.061	0.73	0.87	0.903	0.078	0.74	1
705	ndrg1a	0.848	0.066	0.76	1	0.931	0.042	0.87	1	0.821	0.077	0.67	0.93	0.937	0.073	0.79	1
535	zgc:110377	0.836	0.091	0.67	0.95	0.881	0.081	0.77	0.99	0.787	0.104	0.6	0.93	0.85	0.118	0.68	1
462	syne2b	0.806	0.073	0.7	0.9	0.826	0.062	0.74	0.92	0.786	0.076	0.67	0.93	0.898	0.096	0.74	1
413	ppp2cb	0.761	0.061	0.67	0.86	0.862	0.045	0.8	0.92	0.773	0.077	0.67	0.93	0.874	0.061	0.79	0.98
1265	itih2	0.794	0.045	0.76	0.9	0.867	0.065	0.73	0.96	0.734	0.076	0.6	0.8	0.81	0.077	0.66	0.92
217	wu:fc66f06	0.752	0.070	0.62	0.86	0.811	0.049	0.71	0.86	0.828	0.049	0.73	0.87	0.848	0.062	0.76	0.94
245	habp2	0.864	0.090	0.67	0.95	0.825	0.105	0.69	0.99	0.8	0.077	0.67	0.93	0.811	0.153	0.57	1
275	sb:cb37	0.923	0.055	0.86	1	0.832	0.114	0.71	1	0.911	0.084	0.73	1	0.876	0.110	0.72	1
81	c3a	0.759	0.055	0.71	0.9	0.814	0.089	0.66	0.98	0.746	0.083	0.6	0.87	0.81	0.109	0.6	0.98
138	a2ml	0.904	0.063	0.81	1	0.835	0.110	0.71	1	0.92	0.051	0.87	1	0.886	0.099	0.8	1
119	zgc:152945	0.855	0.090	0.67	0.95	0.823	0.103	0.67	0.96	0.8	0.074	0.73	0.87	0.814	0.145	0.6	1
56	apoa1a	0.795	0.041	0.76	0.86	0.815	0.085	0.7	0.95	0.767	0.092	0.6	0.87	0.784	0.124	0.6	0.96

1 – Protein ID, as in Table S4 - [online](#)

2 - Annotation retrieved from STRING database

3 - Averaged accuracy among 10-folds

4 - Averaged AUC among 10-folds

4.4.6. Study limitations and future perspectives

Screening for biomarkers at the discovery phase can face many challenges due to the complexity of biological samples, heterogeneity of the analytes and analytical methods' constraints. The limitations in the pipeline of biomarker identification multiply when applied to the aquaculture field. After the discovery phase, verification and validation steps are critical in fish research for several reasons: 1) the lack of public databases providing fish omics data for bioinformatic analysis e.g., TCGA and CPTAC databases widely used in cancer biomarkers' studies; this implies that the only possible way to gather new data from independent samples is to establish new fish trials; 2) a limited number of samples/animals (complying with the 3Rs principles of animal research) in each stage of biomarker identification; this may indirectly oblige to repeat and establish new fish experiments with a higher number of animals if enough statistical power has not been previously achieved; 3) sampling is usually invasive or lethal. A possible way to overcome this hindrance is using body fluid samples e.g., fish skin mucus, as proposed in this study. This fluid can be collected in a minimally invasive way and be obtained repeatedly from the same animal (at reasonable time intervals), thus allowing for multiple sampling without sacrificing animals. Moreover, this type of sampling refines (the third R) the way animals are used in research.

In this study, it is important to note that the predictive models generated require further external validation with independent samples because the testing sets created here were derived from data splitting (samples from other experiments should ideally be used for a testing set to be completely independent). New data covariates should be minimized, e.g., same fish species and developmental stage, similar methodology and challenging conditions. Re-using MS data from databases such as PRIDE is a valid way of overcoming this issue, and indirectly increases the sample size, however, in fish research, publicly available skin mucus MS datasets are still scarce.

After the discovery phase has been completed, a targeted proteomics approach (verification step) should be performed to provide some diagnostic value for a predictor protein. Lastly, in the validation step, candidate biomarkers should be evaluated across different groups of fish (e.g., from independent experimental trials), preferentially at different sites/laboratories, and using complementary methodologies, e.g., immunological assays. Larger sample sizes are usually needed in these subsequent phases after the discovery to increase the statistical power. A multi-protein signature can also be used rather than individual proteins to increase biomarkers' sensitivity,

specificity, and diagnostic power (Nakayasu et al., 2021). Future research on biomarkers with interest for the aquaculture industry would need to integrate standardized operating procedures to maintain experimental (pre-analytical variables) and analytical (protocols) variance to a minimum, thus facilitating cross-validation between different research studies/laboratories. The procedures should mimic routine procedures in a fish farm to validate and increase the viability of such research.

4.5. CONCLUSIONS

In summary, in this discovery phase, we propose a set of 28 skin mucus candidate biomarkers that could be further validated for a minimally invasive early diagnostic stress/welfare assessment in gilthead seabream adults. Early diagnosis of the stocked fish through stress/welfare measures, based on minimally invasive stress biomarkers can help to prevent the unintended overload of the fish physiological responses, with adverse effects on growth, reproduction, immunity, and therefore reduce or avoid the use of chemicals to mitigate such effects. By promoting fish welfare, in a “one-health” approach, as beneficial for the environment and for human health, we expect to contribute to improve aquaculture’s sustainability and fish food safety.

4.6. SUPPLEMENTARY MATERIAL

Supplementary figures can be found in the [APPENDIX](#). Supplementary tables are available for this paper at: <https://doi.org/10.1016/j.jprot.2023.104904>

5

The background of the page features a faint, grayscale illustration of two fish swimming. The fish are positioned diagonally, with one above the other, both facing towards the left. The top fish is slightly larger and more detailed than the bottom one. The overall style is minimalist and artistic.

General Discussion, Main Conclusions and Future Perspectives

”

How inappropriate to call this planet "Earth," when it is clearly "Ocean".

— Arthur C. Clarke

There is a fine line between beneficial stress (eustress) and harmful stress (distress), which depends on numerous factors related to the species biology in question and the intrinsic attributes of the stimulus itself. However, there is compelling and irrefutable evidence that many stimuli inherent in routine aquaculture procedures and husbandry conditions pose major challenges to farmed fish. Ultimately, prolonged, or constant exposure to harsh farming conditions that surpass the adaptive capacity of fish can impair welfare and negatively impact multiple aspects of aquaculture sustainability. Considering the current demographic growth rate and climate change, increasing food production while reducing the environmental footprint is of utmost importance. As the fastest-growing food sector, aquaculture bears an enormous responsibility for achieving these objectives, and the commercialization of species that are resilient to changing environments, coupled with the maximization of their welfare, represents the path forward. Gilthead seabream (*Sparus aurata*), an important species in Mediterranean aquaculture and a highly consumed species in Portugal, is well known for its robustness and phenotypic plasticity; however, the limits of its stress tolerance and the underlying molecular mechanisms and main regulators remain elusive. The use of high-throughput technologies, such as omics approaches in fish research, is continuously increasing and has the potential to provide in-depth knowledge of stress adaptation pathways. Bearing this in mind, this PhD thesis sheds light on the underlying mechanisms of the fish stress response and provides the basis for a new toolset to assess farmed fish welfare. Hence, this work presents a comprehensive system-wide characterization of the molecular stress response in gilthead seabream using a multidisciplinary approach that targets the entire flow of information from the gene to the metabolite proposing a set of stressor-specific candidate biomarkers. The main findings of this study, along with future research directions and perspectives, are discussed in this chapter.

5.1. Farmed gilthead seabream can tolerate rearing densities up to 45 kg m⁻³

In summary, the analyses of the different gilthead seabream tissues and body fluids revealed that exposure to stocking densities up to 45 kg m⁻³ for 54 days did not affect fish survival nor growth performance (**Chapter 2**). Moreover, it induced minor or no changes in the plasma (**Chapter 2**) and skin mucus proteome (**Chapter 4**), in the liver proteome, metabolome (**Chapters 3.1, 3.2, and 3.3**), and transcriptome (**Chapter 3.4**), and in the muscle biochemical properties (**Chapter 2**). Muscle pH and *rigor mortis*

remained unchanged (**Chapter 2**), consistent with the unchanged hepatic glycogen levels (**Chapter 3.2**). Regarding the conventional plasma stress markers, cortisol, glucose, and lactate, only the latter exhibited significant changes, showing an increase with the increased rearing density. This variation may be attributed to the potential activation of muscle anaerobic glycolysis in response to faster swimming activity. This hypothesis was reinforced by the lower plasma glucose levels (**Chapter 2**), the up and downregulation of the protein alpha-enolase (ENO1A), which is the enzyme responsible for catalyzing the first step of glycolysis, in the muscle and the liver, respectively (**Chapter 3.2**), as well as by the downregulation of isocitrate dehydrogenase (IDH1), a key enzyme of the TCA cycle, as reported in **Chapter 3.3**. On the other hand, plasma cortisol levels remained unchanged after 54 days of high stocking densities; however, one cannot exclude the possibility of an increase earlier in the trial, followed by a negative feedback regulation of the cortisol itself, as no time course measurements were performed. Chronic negative regulation of the cortisol response has also been demonstrated in other studies due to habituation of the fish to the new condition or exhaustion of the HPI axis, i.e., the interrenal tissue of the fish becomes less sensitive to the action of pituitary hormones (Madaro et al., 2015; Martinez-Porchas et al., 2009). This reinforces the idea that cortisol levels should be cautiously interpreted when used to assess chronic stress and should ideally be complemented with other indicators. When considering the different omics analyses, a considerably less intense global response was observed in fish challenged with high stocking densities compared with the other challenges. No DAPs or DAMs were found in the plasma and liver of the OC-challenged fish, respectively. Concomitantly, the number of dysregulated proteins and protein-protein interactions in the liver (**Chapter 3.3**) and skin mucus proteomes (**Chapter 4**) was much lower. The discriminatory power of skin mucus proteins proposed as candidate stress biomarkers, as indicated by the AUC-ROC values, was also lower (**Chapter 4**). Overall, this work indicates that overcrowded fish coped with the challenge through a less intricate network of cellular reprogramming, suggesting a higher resilience to this condition when compared with the other challenges.

The remarkable resilience of gilthead seabream to this challenge could be due to various genotypic- and/or phenotypic-related reasons or even to the experimental setup itself. For instance, to isolate the effects of overcrowding on the molecular stress response, the O₂ levels were carefully maintained above 5 mg L⁻¹, the same as in the

other experimental groups (except for the hypoxia groups), which could have minimized the impact of overcrowding per se, as observed in previous studies (Araújo-Luna et al., 2018). Alternatively, the higher resistance of the gilthead seabream could stem from adaptive changes in behavior. Recent findings on Nile tilapia demonstrated that an alteration of the social structure from aggression and social hierarchies to shoaling, accompanied by changes in the expression of specific stress-related genes, improved tolerance to high stocking densities (Rodríguez-Barreto et al., 2019). Similarly, a study on gilthead seabream showed that crowding reinforced schooling, highlighting the association between social behavior and stocking densities (Arechavala-Lopez et al., 2020). Further investigations, such as behavioral observations/recordings and genome-wide studies, are required to elucidate the relationship between behavior and increased stress tolerance. Another reason could be the developmental stage of the fish, as in other studies with gilthead seabream juveniles, stocking densities up to 40 kg m⁻³ induced significant changes not only in plasma metabolites but also in the expression of genes related to stress pathways (Martos-Sitcha et al., 2019; Montero et al., 1999; Skrzynska et al., 2018). The distinct sensitivities of adult and juvenile fish to high stocking densities could potentially be attributed to their individual experiences and epigenetic adaptations. Evidence suggests that epigenetic changes play a significant role in stress adaptation in fish, with effects ranging from immediate phenotypic changes to transgenerational transmissions (Moghadam et al., 2015; Petitjean et al., 2019). In this context, the resilience of this species to high rearing densities could also be due to domestication and genetic and epigenetic evolutionary adaptation of farmed populations associated with intensive farming practices that have been utilized since the 1980s (Moretti et al., 1999). However, research investigating the genetic signatures of these adaptations is limited, with only a handful of studies providing insights into the genetic specificity of farmed populations of gilthead seabream. One study found that aquaculture likely plays a significant role in driving genetic differences in this species (Franchini et al., 2012), whereas another study identified genetic drift as a key factor (Cossu et al., 2019). Recently, a study presented the first genome-wide evidence of the genetic basis of domestication in this species, identifying specific SNPs and genes related to stress coping, growth, and resistance to pathogens (Gkagkavouzis et al., 2021).

5.2. Gilthead seabream netted four times a week activated several prosurvival pathways as an adaptation response to cellular stress

The net handling challenge undoubtedly had the greatest impact on the physiology and metabolism of gilthead seabream, which has been extensively discussed in all chapters. Both experimental conditions, NET2 and NET4, induced significant changes in the overall organism, whereas the most intense challenge (NET4) was undeniably the most impactful. Notably, **Chapter 2** highlighted significant changes in plasma metabolites and abundance of plasma proteins related to the innate immune response, with no impact on fish survival nor growth. In **Chapters 3.1** and **3.2**, major changes in liver metabolism are reported, accompanied by a significant reduction in hepatic glycogen stores. **Chapter 3.3** and **3.4** further demonstrated that net handling four times a week induced cellular stress in fish hepatocytes, mainly related to ER stress. Lastly, **Chapter 4** demonstrated the promisor role of skin mucus in the evaluation of the stress response to net handling and proposed a set of proteins as candidate stress biomarkers that exhibited the highest discriminatory power when compared to candidate biomarkers identified for OC and HYP trials.

Despite the significant increase in plasma cortisol levels (**Chapter 2**), net-handled fish also showed the highest biological variability. The intermittent nature of the challenge and its unpredictability could have prevented the possibility of acclimation of the HPI axis, as proposed for OC fish, and could also have helped shape individual responses. Different stress coping styles (SCS) are known to modulate the fish glucocorticoid response, and reactive fish have been demonstrated to have a more sensitive HPI axis than proactive fish (Alfonso et al., 2020; Castanheira et al., 2017), which could explain the high dispersion of values in these measurements. The significant increase in glucose levels following the cortisol trend was attributed to the liver glycogenolysis pathway, which is commonly activated by catecholamines. These results were further corroborated by the significant decrease in hepatic carbohydrate content assessed by FTIR (**Chapter 3.1**), and glycogen levels reported in **Chapter 3.2**. In addition, **Chapter 3.3** demonstrated for the first time in fish hepatocytes evidence of glycogen breakdown at the lysosomal level, instead of the canonical cytosolic pathway, a process that has been extensively described in humans to produce non-phosphorylated glucose that can be used more rapidly (Mandl & Bánhegyi, 2018).

Multimomics analysis of the liver (**Chapters 3.2, 3.3, and 3.4**) indicated that net-handled fish altered their overall metabolism to prioritize stress-responsive pathways

over energy-consuming processes such as gluconeogenesis and amino acid catabolism. Similarly, amino acids, instead of being incorporated into the TCA cycle to produce glucose, were also redirected as building blocks for the synthesis of proteins involved in stress and the immune response. Mitochondrial dysfunction, which is typically associated with stress, has also been observed in another study with gilthead seabream (Bermejo-Nogales et al., 2014). In this work, netting the fish four times a week induced cellular stress in hepatocytes, activating attenuation mechanisms, such as the UPR and ERAD systems in the endoplasmic reticulum, clathrin-mediated endocytosis, autophagy, and ribosomal assembly stress, to prevent proteotoxicity and cell death. Autophagy was found to be an important pathway for restoring cellular homeostasis during stress responses in fish (Z. Zhou et al., 2022), while chaperone-mediated autophagy (CMA), a specific route of autophagy that until recently was only described in mammals and birds (Lescat et al., 2020), was also demonstrated in net-handled fish by the simultaneous upregulation of the protein HSPA8/HSC70 and the gene *lamp2*. **Chapter 3.4** also described, for the first time, evidence of a ribosomal assembly stress response similar to that described in yeast and humans (Albert et al., 2019). The complex regulation of this process can occur at the transcriptional level, of RPGs and rRNA, and at the post-transcriptional and post-translational levels. In fact, RPGs are among the most highly expressed genes in most cell types, and their architecture increases the complexity of ribosome biogenesis (Pelletier et al., 2017). The number of genes coding for these RPs varies greatly between species, owing to processes such as gene duplication (Dharia et al., 2014). For example, a recent study identified 85, 125, 90, 148, 88, 92, and 86 RPGs in zebrafish, common carp, channel catfish, Atlantic salmon, medaka, tilapia, and fugu, respectively (Kuang et al., 2020). Different rounds of whole-genome duplication (WGD) might explain the diversity of RPGs in teleost fish (Glasauer & Neuhauss, 2014; Hoegg et al., 2004). In **Chapter 3.4**, 53 different RPGs were identified in gilthead seabream.

This study showed that after 48 days of exposure to net handling, gilthead seabream regulated different pathways in an attempt to restore cellular homeostasis. However, the effects of these cellular mechanisms on long-term fish performance are not yet fully understood. Recovery from net handling stress may not be equivalent to reversal, and further studies are needed to determine the potential long-term effects of such severe stressors on fish performance.

5.3. Exposure to 15% DO for 48h induced an “energy-conservation state” through cell cycle arrest in gilthead seabream hepatocytes

Exposure of gilthead seabream to low oxygen levels (i.e., 30 and 15% DO) for 48 h induced an overall shutdown of aerobic metabolism, which was reflected in the liver proteome (**Chapters 3.2** and **3.3**). This is a typical response to hypoxic conditions, as inadequate tissue oxygenation inhibits OXPHOS. This is supported by the downregulation of ATP synthase subunit d (ATP5H) in the liver (**Chapter 3.2**), which is the complex responsible for producing ATP from ADP in the presence of a proton gradient across the mitochondrial membrane. This, in turn, depletes the cellular energetic reserves, as observed in the liver metabolomics analysis (**Chapter 3.3**), which in part can be supported by the significant changes observed in the muscle pH and *rigor mortis*, although no ATP measurements were performed in the muscle (**Chapter 2**). Hepatocytes, however, resorted to substrate-level phosphorylation for energy generation, such as conversion from pyruvate to lactate in the cytosol and phosphate transfer from intermediates such as creatine phosphate (PCr) (**Chapter 3.3**). Finally, the RNA-seq analysis in **Chapter 3.4** revealed that the well-known transcription factor HIF is at the crossroads of almost all the observed cellular adaptations to low oxygen and energy availability in the liver, such as DNA replication stress and cell cycle arrest, downregulation of the mTORC1 pathway and consequent inhibition of translation, induction of autophagy, and anaerobic metabolism. Interestingly, shotgun proteomics did not identify HIF1 at the protein level. Skin mucus proteomics analysis (**Chapter 4**) revealed a major shutdown of the overall immune system, which was again concomitant with the overall “energy conservation state. Remarkably, a higher number of DAPs was observed in the skin mucus than in the other tissues. This was attributed to a faster response at the mucosal surfaces than that occurring in the central organs in the case of short-term stressors (H. Guo & Dixon, 2021; Yada & Tort, 2016). To further understand the effect of hypoxia, an experimental trial with a recovery period after the challenge would be necessary to determine whether cell cycle arrest at these concentrations of DO is reversible and whether any permanent effect on immune resistance is induced.

5.4. Skin mucus is a promisor minimally invasive biological matrix to identify both chronic and acute stress biomarkers

Chapter 4 revealed the ability of the gilthead seabream skin mucus to provide an insightful snapshot of the main changes driven by the stress response, including those in other tissues, such as the liver (**Chapter 3.3**) and blood plasma (**Chapter 2**). Skin mucus proteome analysis identified several proteins involved in the innate immune response and hemostasis that were consistent with the immune-related proteins observed in the plasma and liver, along with proteins involved in metabolic and other cellular processes. This finding supports the understanding that skin mucus serves as both an active mucosal immune tissue (SALT) and a disposal fluid for proteins excreted by the epidermal cells and tissue leakage proteins (Easy & Ross, 2009; Salinas & Magadán, 2017).

A discovery-based search for diagnostic biomarkers of a stressed state, integrating data-driven and knowledge-driven approaches, was performed using skin mucus shotgun proteomics datasets. This investigation led to the discovery of 28 candidate biomarkers, each exhibiting specificity to particular stressors. Among these candidates, seven were specific to overcrowding (MAP2K2A, PRDX5, SARDH, PPP2CA, ANXA1A, PRPSAP2, and PDCD6IP), eight were specific to net handling (C9, PLECB, HP, EEF2B, CCT8, GIG2L, TFA, and C5), eight were specific to hypoxia (RRBP1A, NDRG1A, SYNE2B, ITIH2, WU:FC66F06, HABP2, SB:CB37, and APOA1A), three were common to two challenges (ZGC:152945, C3A, and PPP2CB), and two were common to all three challenges (A2ML and ZGC:110377). It is noteworthy, however, that the regulation of the common proteins may differ among trials, as observed by the upregulation of ZGC:152945 and C3A in net-handled fish and the downregulation in hypoxia-exposed fish; PPP2CB is downregulated in overcrowded fish but upregulated in hypoxia-exposed fish, and both A2ML and ZGC:110377 are upregulated in net-handled and overcrowded fish but downregulated in hypoxia-exposed fish. Interestingly, the regulation of common proteins in the OC and NET trials differed from that in the HYP trial, which was attributed to the distinct duration (and intensity) of the challenges.

The following steps in the biomarker identification pipeline include verification and validation. However, in fish studies, there are numerous challenges and limitations related to generating new samples and, consequently, low statistical power. These issues are exacerbated by: (1) the lack of publicly available MS datasets for fish omics

studies, making computational verification of candidate biomarkers impossible and implying that new experimental trials should be conducted to obtain new samples for verification and validation steps. Unfortunately, this compromises the reduction aspect of the three-Rs principle, which promotes the reduction of the number of animals used in research. (2) the lack of standardization in omics protocols for fish studies; thus, experimental (pre-analytical variables) and analytical (protocols) variability becomes a problem. This variability can hinder the reproducibility and robustness of candidate biomarkers across different studies and laboratories. Finally, (3) the use of immunological assays for validation presents various challenges, such as limited multiplexing capabilities, occurrence of cross-reactivity between different fish species, and lack of commercially available fish-specific antibodies (Forné et al., 2010; Haab et al., 2006).

5.5. Directions for upcoming research

5.5.1. Targeting specific biomolecules

This work allowed for the identification of a specific set of features, i.e., genes, proteins or metabolites, whose functions in fish or their response to stress are not well understood. Despite this lack of information, the regulation of these features and their anticipated biological role in other vertebrates suggest an important role in fish response to stress. Therefore, it is crucial to conduct further research on these features, and this section emphasizes their importance.

The insulin growth factor-binding protein was found in **Chapter 3.4** to be significantly upregulated at the mRNA level (*igfbp1a*) in both net-handled and hypoxia-exposed fish. This protein is responsible for regulating the availability of IGF, and therefore, for controlling several downstream pathways related to cell proliferation. In human hepatocytes, it was found to be induced by ER stress (Marchand et al., 2006), whereas studies in mice have linked it to genotoxic stress and cellular senescence (Alessio et al., 2020). A recent study on Atlantic salmon parr concluded that hepatic mRNA levels of IGFBP1 were regulated by cortisol (Breves et al., 2020). A review of teleost IGFBPs compiled the most recent studies reporting upregulation of this protein in fish under stressful conditions (de la Serrana & Macqueen, 2018).

Hepcidin, a protein produced in the liver in response to high circulating iron levels (Hintze & McClung, 2011), was found to be upregulated at the mRNA level (*hamp*) in fish exposed to net handling and hypoxia according to **Chapter 3.4**. This

protein plays a significant role in regulating iron absorption by binding to ferroportin, which is its export channel (Álvarez et al., 2014). In net-handled fish, the gene encoding the transporter protein, *slc40a1*, was also upregulated. Unlike humans, fish possess two functionally distinct hepcidin types, where the *hamp1* gene is more involved in iron metabolism, and the duplicate *hamp2* acts in the immune system as an antimicrobial peptide (Neves et al., 2017). Interestingly, a study of hepcidin protein sequences in gilthead seabream showed the presence of one type I hepcidin and 12 type II hepcidins with antimicrobial potential, demonstrating the highest number within Eupercaria (Serna-Duque et al., 2022). ER stress and UPR have also been found to induce hepcidin expression in mice (Vecchi et al., 2009).

The gene *steap4*, which encodes a metalloreductase involved in iron and copper homeostasis, was also upregulated in response to net handling and hypoxic challenges (**Chapter 3.4**). Similarly, STEAP4 was also upregulated in the hepatic proteome of the same fish in response to all challenges, i.e., overcrowding, net handling, and hypoxia (**Chapter 3.3**). Studies have suggested that this protein plays a fundamental role in the response to inflammatory stress mediated by elevated cytokine levels (Scarl et al., 2017). In fish, it has been demonstrated to be upregulated in response to thermal stress (S. Liu et al., 2013; Logan & Somero, 2010), followed by bacterial infection (Causey et al., 2018). The elevation of HAMP and STEAP4 mRNA and protein levels suggests that iron metabolism might be crucial for regulating the immune system and stress response in this species.

The metabolite itaconate is another biomolecule that deserves further attention in fish stress research, which was upregulated in net-handled fish (**Chapter 3.3**). This metabolite is derived from the decarboxylation of a TCA cycle intermediate and is known to inhibit SDH, GAPDH, and ALDOA (Shi et al., 2022). Concurrently, the mRNA levels of GAPDH and ALDOA were downregulated in net-handled fish (**Chapter 3.4**). Moreover, it alkylates Kelch-like ECH-associated protein 1 (KEAP1), inducing the release of nuclear factor NRF2, an antioxidant regulator, and has an anti-inflammatory effect by decreasing the levels of inflammatory cytokines (R. Li et al., 2020). Although nothing is currently known about its role in fish physiology, studies in humans have described it in macrophages and recently in liver tissue as an important regulatory metabolite of inflammation that modulates innate immunity to limit tissue damage and metabolism (Yi et al., 2020). This finding suggests a potential connection between

itaconate and fish stress response. However, further investigation is required to fully understand its role.

The 2-hydroxyglutarate (2-HG) is a metabolite structurally similar to the 2-oxoglutarate/ α -ketoglutarate (α -KG), an intermediate product of the tricarboxylic acid (TCA), derived from the reduction of its ketone group to a hydroxyl group by the mutant enzyme IDH1 and from “errors” of other enzymes such as MDH and LDHA (Du & Hu, 2021). In **Chapter 3.3**, this metabolite was reported to be upregulated in response to net handling and hypoxia, and the protein responsible for its conversion back to α -KG, that is, L-2-hydroxyglutarate dehydrogenase (L2HGDH), was also found to be upregulated at the protein level in net-handled fish (**Chapter 3.2**) and at the mRNA level in both net-handled and hypoxia-exposed fish (**Chapter 3.4**). 2-HG is considered an oncometabolite linked to several human pathologies, such as organic acidurias (Kranendijk et al., 2012), and has been shown to be induced by hypoxia in cancer cells (Intlekofer et al., 2015; Oldham et al., 2015). The roles of 2-HG and L2HGDH in fish physiology are not yet clear, but their upregulation in response to stress suggests a potentially important role in the fish stress response.

5.5.2. Targeting specific levels of regulation

MicroRNAs (miRNAs) are short non-coding RNA molecules (18-25 nucleotides) that act as post-transcriptional regulators of gene expression through sequence-specific interactions with the 3'-untranslated regions (UTR) of mRNAs, inhibiting translation or inducing the degradation of the transcript (Herkenhoff et al., 2018). This class of RNAs and their functions have recently been studied in farmed fish species; however, they have not yet been described in gilthead seabream. Environmental factors, such as temperature, salinity, chemicals, pH, and DO, are known to affect the expression of different miRNAs (Q. Cao et al., 2023), demonstrating their important role in stress adaptation. Under hypoxic conditions, HIF1 modulates the expression profiles of specific miRNAs in zebrafish (C.-X. Huang et al., 2015). In this study, several miRNAs were identified; however, differences in expression were only detected in hypoxia-exposed fish: miRNA-142a and Let-7a were significantly downregulated, whereas miRNA-29a1 and miRNA-29b1 were upregulated (**Chapter 3.4**). Downregulation of Let-7a has also been reported in the liver of hypoxic female medaka (Lau et al., 2014). More research is required to determine the role of these miRNAs in adaptation to hypoxia.

miRNAs are also known to play pivotal roles in the regulation of epigenetic mechanisms. For instance, miRNA-29b1, which was significantly upregulated in hypoxia-exposed fish, is known to regulate DNA methylation (Z. Zhang et al., 2018). As previously explained, epigenetic marks are environment-sensitive molecular elements involved in several biological processes and can accelerate phenotypic and genetic responses to stress. These epigenetic components can rapidly adjust the phenotype (e.g., DNA methylation) and/or form new phenotypes that can be transmitted to offspring without changing the DNA sequence. These mechanisms are responsible for the phenotypic plasticity of populations (O. Rey et al., 2016). Although research on epigenetic mechanisms in teleosts is still emerging, studies on the gilthead seabream have not yet been conducted (Best et al., 2018). It is essential to investigate the epigenetic marks underpinning fish stress tolerance and their transgenerational inheritance to fully understand the mechanisms involved in stress adaptation.

PTMs are a key mechanism regulating the structure, function, and dynamics of almost all proteins in eukaryotes, thus affecting countless biological processes and regulating many signaling pathways. In **Chapter 2**, 20 proteins were identified across 56 protein spots in the 2D plasma gels, indicating that the same protein was identified at different molecular weights and pIs. As hypothesized, this could be due to different proteoforms or PTMs, which have been demonstrated to be more energetically efficient in maximizing the functionality of a single gene product than *de novo* protein synthesis, in cases where rapid adaptation of the proteome is required (Karve & Cheema, 2011). There are more than 300 PTMs known in eukaryotes, of which phosphorylation, acetylation, and ubiquitination are usually the most common, and some are already being evaluated as biomarkers of certain types of cancers and other diseases (Mnatsakanyan et al., 2018). Moreover, a study in porcine muscle demonstrated that preslaughter handling stress induced PTMs, specifically acetylation, in contractile proteins that regulate *rigor mortis* (T. Zhou et al., 2019). Therefore, it would be interesting to characterize the specific PTMs responsible for the main stress-induced changes in gilthead seabream.

5.5.3. Next steps in biomarker identification

After verification through targeted proteomics and quantification, a smaller set of proteins will be used for antibody production. Subsequently, validation of the identified biomarkers is the final step, which includes immunological assays using

antibodies produced specific for the gilthead seabream species. Furthermore, other validation procedures should ideally be performed to reinforce the robustness of the validated biomarkers, such as for example (1) cross-validation by different laboratories; (2) identification of the validated biomarkers in different developmental stages of the fish and comparison of the response/regulation of the protein; (3) a “dose-response” trial to understand if the diagnostic value of the biomarker increases/decreases with the intensity of the stressor and finally (4) correlation of the biomarkers’ response with parameters of fish performance, such as growth and behavior, and other indicators, such as the OWI and other LABWI indicators (e.g., hematocrit, lysozyme activity, oxidative stress and skin mucus cortisol). This comprehensive validation process will provide valuable information regarding the applications of these biomarkers in aquaculture practices.

5.6. Future perspectives and implications for aquaculture sustainability

The culmination of this doctoral thesis underscores the significance of identifying and validating a biosignature of stress-specific molecular markers. These markers will support future molecular studies on gilthead seabream stress and are expected to further contribute to welfare recommendations and guidelines for this species. The integration of these biomarkers into welfare assessment protocols will augment their effectiveness and provide an essential minimal standard for welfare in sustainability certification schemes. To this end, skin mucus samples collected in aquaculture farms could be analyzed in specialized laboratories, or alternatively, specific devices or biosensors could be developed with these biomarkers for a readily on-site assessment. This development has the potential to significantly enhance the transparency, accountability, and ethical responsibility of the aquaculture industry and promote its long-term sustainability, prioritizing the welfare of farmed fish. The potential impact of these findings will extend beyond the immediate benefits to the aquaculture industry, as it lays a foundation for ethical and environmentally conscious animal husbandry practices in other domains.

REFERENCES

- Abdallah, C., Dumas-Gaudot, E., Renaut, J., & Sergeant, K. (2012). Gel-based and gel-free quantitative proteomics approaches at a glance. *International Journal of Plant Genomics*, 2012. <https://doi.org/10.1155/2012/494572>
- Abdel-Tawwab, M., Monier, M. N., Hoseinifar, S. H., & Faggio, C. (2019). Fish response to hypoxia stress: growth, physiological, and immunological biomarkers. *Fish Physiology and Biochemistry*, 45(3), 997–1013. <https://doi.org/10.1007/s10695-019-00614-9>
- Acerete, L., Reig, L., Alvarez, D., Flos, R., & Tort, L. (2009). Comparison of two stunning/slaughtering methods on stress response and quality indicators of European sea bass (*Dicentrarchus labrax*). *Aquaculture*, 287(1–2), 139–144. <https://doi.org/10.1016/J.AQUACULTURE.2008.10.012>
- Akbarzadeh, A., Houde, A. L. S., Sutherland, B. J. G., Günther, O. P., & Miller, K. M. (2020). Identification of hypoxia-specific biomarkers in salmonids using RNA-sequencing and validation using high-throughput qPCR. *G3: Genes, Genomes, Genetics*, 10(9), 3321–3336. <https://doi.org/10.1534/g3.120.401487>
- Albert, B., Kos-Braun, I. C., Henras, A. K., Dez, C., Rueda, M. P., Zhang, X., Gadai, O., Kos, M., & Shore, D. (2019). A ribosome assembly stress response regulates transcription to maintain proteome homeostasis. *ELife*, 8, 1–24. <https://doi.org/10.7554/eLife.45002>
- Alessio, N., Squillaro, T., Di Bernardo, G., Galano, G., De Rosa, R., Melone, M. A., Peluso, G., & Galderisi, U. (2020). Increase of circulating IGFBP-4 following genotoxic stress and its implication for senescence. *ELife*, 9, 1–20. <https://doi.org/10.7554/eLife.54523>
- Alfaro, A. C., Nguyen, T. V., Venter, L., Ericson, J. A., Sharma, S., Ragg, N. L. C., & Mundy, C. (2021). The Effects of Live Transport on Metabolism and Stress Responses of Abalone (*Haliotis iris*). *Metabolites* 2021, Vol. 11, Page 748, 11(11), 748. <https://doi.org/10.3390/METABO11110748>
- Alfaro, A. C., & Young, T. (2018). Showcasing metabolomic applications in aquaculture: a review. *Reviews in Aquaculture*, 10(1), 135–152. <https://doi.org/10.1111/raq.12152>
- Alfonso, S., Zupa, W., Manfrin, A., Fiocchi, E., Spedicato, M. T., Lembo, G., & Carbonara, P. (2020). Stress coping styles: Is the basal level of stress physiological indicators linked to behaviour of sea bream? *Applied Animal Behaviour Science*, 231(June), 105085. <https://doi.org/10.1016/j.applanim.2020.105085>
- Algers, B., Blokhuis, H. J., Bøtner, A., Broom, D. M., Costa, P., Domingo, M., Greiner, M., Hartung, J., Koenen, F., Müller-Graf, C., Morton, D. B., Osterhaus, A., Pfeiffer, D. U., Raj, M., Roberts, R., Sanaa, M., Salman, M., Sharp, J. M., Vannier, P., & Wierup, M. (2009). SCIENTIFIC OPINION General approach to fish welfare and to the concept of sentience in fish Scientific Opinion of the Panel on Animal Health and Welfare PANEL MEMBERS. *The EFSA Journal*, 954(954), 1–27.
- Algers, B., Blokhuis, H. J., Broom, D. M., Costa, P., Domingo, M., Greiner, M., Guemene, D., Hartung, J., Koenen, F., Müller-graf, C., Morton, D. B., Osterhaus, A., Pfeiffer, D. U., Roberts, R., Sanaa, M., Salman, M., Sharp, J. M., Vannier, P., & Wierup, M. (2008). Scientific Opinion of the Panel on Animal Health and Welfare on a request from the European Commission on animal welfare aspects of husbandry systems for farmed European seabass and Gilthead seabream. *The EFSA Journal*, 844, 1–21. [file:///D:/Uni Backup/Research papers/animal welfare aspects of the panel on animal health and welfare.pdf](file:///D:/Uni%20Backup/Research%20papers/animal%20welfare%20aspects%20of%20the%20panel%20on%20animal%20health%20and%20welfare.pdf)
- Almeida, A. M., Bassols, A., Bendixen, E., Bhide, M., Cecilian, F., Cristobal, S., Eckersall, P. D., Hollung, K., Lisacek, F., Mazzucchelli, G., McLaughlin, M., Miller, I., Nally, J. E., Plowman, J., Renaut, J., Rodrigues, P., Roncada, P., Staric, J., & Turk, R. (2014). Animal board invited review: Advances in proteomics for animal and food sciences. *Animal*, 9(1), 1–17. <https://doi.org/10.1017/S1751731114002602>
- Aluru, N., & Vijayan, M. M. (2007). Hepatic transcriptome response to glucocorticoid receptor activation in rainbow trout. *Physiological Genomics*, 31(3), 483–491. <https://doi.org/10.1152/physiolgenomics.00118.2007>

- Aluru, N., & Vijayan, M. M. (2009). Stress transcriptomics in fish: A role for genomic cortisol signaling. *General and Comparative Endocrinology*, *164*(2–3), 142–150. <https://doi.org/10.1016/j.ygcen.2009.03.020>
- Álvarez, C. A., Guzmán, F., Cárdenas, C., Marshall, S. H., & Mercado, L. (2014). Antimicrobial activity of trout hepcidin. *Fish and Shellfish Immunology*, *41*(1), 93–101. <https://doi.org/10.1016/j.fsi.2014.04.013>
- Alves, R. N., & Agustí, S. (2022). Transcriptional changes in the gilthead seabream (*Sparus aurata*) skin in response to ultraviolet B radiation exposure. *Frontiers in Marine Science*, *9*(September), 1–21. <https://doi.org/10.3389/fmars.2022.966654>
- Alves, R. N., Cordeiro, O., Silva, T. S., Richard, N., de Vareilles, M., Marino, G., Di Marco, P., Rodrigues, P. M., & Conceição, L. E. C. (2010). Metabolic molecular indicators of chronic stress in gilthead seabream (*Sparus aurata*) using comparative proteomics. *Aquaculture*, *299*(1–4), 57–66. <https://doi.org/10.1016/j.aquaculture.2009.11.014>
- Andersen, C. L., Jensen, J. L., & Ørntoft, T. F. (2004). Normalization of Real-Time Quantitative Reverse Transcription-PCR Data: A Model-Based Variance Estimation Approach to Identify Genes Suited for Normalization, Applied to Bladder and Colon Cancer Data Sets. *Cancer Research*, *64*(15), 5245 LP – 5250. <https://doi.org/10.1158/0008-5472.CAN-04-0496>
- Ángeles Esteban, M. (2012). An Overview of the Immunological Defenses in Fish Skin. *ISRN Immunology*, *2012*, 1–29. <https://doi.org/10.5402/2012/853470>
- Ángeles Esteban, M., & Cerezuela, R. (2015). 4 - Fish mucosal immunity: skin. In B. H. Beck & E. Peatman (Eds.), *Mucosal Health in Aquaculture* (pp. 67–92). Academic Press. <https://doi.org/https://doi.org/10.1016/B978-0-12-417186-2.00004-2>
- Aquatic Life Institute. (2021). *Benefits of Aquatic Animal Welfare for Sustainability*. https://drive.google.com/file/d/1Tg_zqntG98FTGK6YFWx_rNsMZIt9WFV/view
- Araújo-Luna, R., Ribeiro, L., Bergheim, A., & Pousão-Ferreira, P. (2018). The impact of different rearing condition on gilthead seabream welfare: Dissolved oxygen levels and stocking densities. *Aquaculture Research*, *49*(12), 3845–3855. <https://doi.org/10.1111/are.13851>
- Arechavala-Lopez, P., Nazzaro-Alvarez, J., Jardí-Pons, A., Reig, L., Carella, F., Carrassón, M., & Roque, A. (2020). Linking stocking densities and feeding strategies with social and individual stress responses on gilthead seabream (*Sparus aurata*). *Physiology and Behavior*, *213*(October 2019), 112723. <https://doi.org/10.1016/j.physbeh.2019.112723>
- Ashley, P. J. (2007). Fish welfare: Current issues in aquaculture. *Applied Animal Behaviour Science*, *104*(3–4), 199–235. <https://doi.org/10.1016/J.APPLANIM.2006.09.001>
- Athar, A., Füllgrabe, A., George, N., Iqbal, H., Huerta, L., Ali, A., Snow, C., Fonseca, N. A., Petryszak, R., Papatheodorou, I., Sarkans, U., & Brazma, A. (2019). ArrayExpress update - From bulk to single-cell expression data. *Nucleic Acids Research*, *47*(D1), D711–D715. <https://doi.org/10.1093/nar/gky964>
- Ayala, M. D., Abdel, I., Santaella, M., Martínez, C., Periago, M. J., Gil, F., Blanco, A., & Albors, O. L. (2010). Muscle tissue structural changes and texture development in sea bream, *Sparus aurata* L., during post-mortem storage. *LWT - Food Science and Technology*, *43*(3), 465–475. <https://doi.org/10.1016/j.lwt.2009.08.023>
- Bader, G. D., & Hogue, C. W. (2003). An automated method for finding molecular complexes in large protein interaction networks. *BMC Bioinformatics*, *4*, 2. <https://doi.org/10.1186/1471-2105-4-2>
- Bagni, M., Civitareale, C., Priori, A., Ballerini, A., Finoia, M., Brambilla, G., & Marino, G. (2007). Pre-slaughter crowding stress and killing procedures affecting quality and welfare in sea bass (*Dicentrarchus labrax*) and sea bream (*Sparus aurata*). *Aquaculture*, *263*, 52–60. <https://doi.org/10.1016/j.aquaculture.2006.07.049>
- Bahuaud, D., Mørkøre, T., Østbye, T.-K., Veiseth-Kent, E., Thomassen, M. S., & Ofstad, R. (2010). Muscle structure responses and lysosomal cathepsins B and L in farmed Atlantic salmon (*Salmo salar* L.) pre- and post-rigor fillets exposed to short and long-term crowding stress. *Food Chemistry*, *118*(3), 602–615. <https://doi.org/10.1016/J.FOODCHEM.2009.05.028>

- Baker, M. R., & Vynne, C. H. (2014). Cortisol profiles in sockeye salmon: Sample bias and baseline values at migration, maturation, spawning, and senescence. *Fisheries Research*, 154, 38–43. <https://doi.org/10.1016/j.fishres.2014.01.015>
- Balcombe, J. (2016). *What a fish knows: the inner lives of our underwater* (Scientific).
- Baldwin, L. (2010). The effects of stocking density on fish welfare. *The Plymouth Student Scientist*, 4(1), 372–383. <http://bcur.org/journals/index.php/TPSS/article/view/300>
- Banh, S., Wiens, L., Sotiri, E., & Treberg, J. R. (2016). Mitochondrial reactive oxygen species production by fish muscle mitochondria: Potential role in acute heat-induced oxidative stress. *Comparative Biochemistry and Physiology Part - B: Biochemistry and Molecular Biology*, 191, 99–107. <https://doi.org/10.1016/j.cbpb.2015.10.001>
- Bantscheff, M., Schirle, M., Sweetman, G., Rick, J., & Kuster, B. (2007). Quantitative mass spectrometry in proteomics: a critical review. *Analytical and Bioanalytical Chemistry*, 389(4), 1017–1031. <https://doi.org/10.1007/s00216-007-1486-6>
- Barreto, M. O., Rey Planellas, S., Yang, Y., Phillips, C., & Descovich, K. (2022). Emerging indicators of fish welfare in aquaculture. *Reviews in Aquaculture*, 14(1), 343–361. <https://doi.org/10.1111/raq.12601>
- Barton, B. A. (2002). Stress in Fishes: A Diversity of Responses with Particular Reference to Changes in Circulating Corticosteroids. *Integrative and Comparative Biology*, 42(3), 517–525. <https://doi.org/10.1093/icb/42.3.517>
- Barton, B. A., Ribas, L., Acerete, L., & Tort, L. (2005). Effects of chronic confinement on physiological responses of juvenile gilthead sea bream, *Sparus aurata* L., to acute handling. *Aquaculture Research*, 36(2), 172–179. <https://doi.org/10.1111/j.1365-2109.2004.01202.x>
- Bassols, A., Turk, R., & Roncada, P. (2014). A proteomics perspective: from animal welfare to food safety. *Current Protein & Peptide Science*, 15(2), 156–168. <https://doi.org/10.2174/1389203715666140221125958>
- Bayne, C. J., & Gerwick, L. (2001). The acute phase response and innate immunity of fish. *Developmental & Comparative Immunology*, 25(8–9), 725–743. [https://doi.org/10.1016/S0145-305X\(01\)00033-7](https://doi.org/10.1016/S0145-305X(01)00033-7)
- Bendixen, E., Danielsen, M., Hollung, K., Gianazza, E., & Miller, I. (2011). Farm animal proteomics — A review. *Journal of Proteomics*, 74(3), 282–293. <https://doi.org/10.1016/j.jprot.2010.11.005>
- Béné, C., Arthur, R., Norbury, H., Allison, E. H., Beveridge, M., Bush, S., Campling, L., Leschen, W., Little, D., Squires, D., Thilsted, S. H., Troell, M., & Williams, M. (2016). Contribution of Fisheries and Aquaculture to Food Security and Poverty Reduction: Assessing the Current Evidence. *World Development*, 79, 177–196. <https://doi.org/10.1016/J.WORLDDEV.2015.11.007>
- Benktander, J., Sundh, H., Sundell, K., Murugan, A. V. M., Venkatakrisnan, V., Padra, J. T., Kolarevic, J., Terjesen, B. F., Gorissen, M., & Lindén, S. K. (2021). Stress impairs skin barrier function and induces α 2-3 linked n-acetylneuraminic acid and core 1 o-glycans on skin mucins in atlantic salmon, *salmo salar*. *International Journal of Molecular Sciences*, 22(3), 1–18. <https://doi.org/10.3390/ijms22031488>
- Benninghoff, A. D. (2007). Toxicoproteomics-The Next Step in the Evolution of Environmental Biomarkers? *Toxicological Sciences*, 95(1), 1–4. <https://doi.org/10.1093/toxsci/kfl157>
- Bergqvist, J., & Gunnarsson, S. (2013). Finfish Aquaculture: Animal Welfare, the Environment, and Ethical Implications. *Journal of Agricultural and Environmental Ethics*, 26(1), 75–99. <https://doi.org/10.1007/s10806-011-9346-y>
- Bermejo-Nogales, A., Nederlof, M., Benedito-Palos, L., Ballester-Lozano, G. F., Folkedal, O., Olsen, R. E., Sitjà-Bobadilla, A., & Pérez-Sánchez, J. (2014). Metabolic and transcriptional responses of gilthead sea bream (*Sparus aurata* L.) to environmental stress: New insights in fish mitochondrial phenotyping. *General and Comparative Endocrinology*, 205, 305–315. <https://doi.org/10.1016/j.ygcen.2014.04.016>
- Berrill, I. K., Kadri, S., Ruohonen, K., Kankainen, M., Damsgård, B., Toften, H., Noble, C., Schneider, O., & Turnbull, J. F. (2009). BENEFISH: A European project to put a cost on fish welfare actions. *Fish Veterinary Journal*, 11(11), 23–28.

- Best, C., Ikert, H., Kostyniuk, D. J., Craig, P. M., Navarro-Martin, L., Marandel, L., & Mennigen, J. A. (2018). Epigenetics in teleost fish: From molecular mechanisms to physiological phenotypes. *Comparative Biochemistry and Physiology Part - B: Biochemistry and Molecular Biology*, 224(September 2017), 210–244. <https://doi.org/10.1016/j.cbpb.2018.01.006>
- Bhattacharya, S. (2015). Reactive Oxygen Species and Cellular Defense System. In V. Rani & U. C. Yadav (Eds.), *Free Radicals in Human Health and Disease*. <https://doi.org/10.1007/978-81-322-2035-0>
- Bindea, G., Mlecnik, B., Hackl, H., Charoentong, P., Tosolini, M., Kirilovsky, A., Fridman, W.-H., Pagès, F., Trajanoski, Z., & Galon, J. (2009). ClueGO: a Cytoscape plug-in to decipher functionally grouped gene ontology and pathway annotation networks. *Bioinformatics*, 25(8), 1091–1093. <https://doi.org/10.1093/BIOINFORMATICS/BTP101>
- Blighe, K., & Lun, A. (2022). PCAtools: PCAtools: Everything Principal Components Analysis. *R Package Version 2.10.0*. <https://github.com/kevinblighe/PCAtools>
- Blighe, K., Rana, S., & Lewis, M. (2021). EnhancedVolcano: Publication-ready volcano plots with enhanced colouring and labeling. *R Package Version 1.6.0*. <https://github.com/kevinblighe/EnhancedVolcano>
- Bohne-Kjersem, A., Skadsheim, A., Goksøyr, A., & Grøsvik, B. E. (2009). Candidate biomarker discovery in plasma of juvenile cod (*Gadus morhua*) exposed to crude North Sea oil, alkyl phenols and polycyclic aromatic hydrocarbons (PAHs). *Marine Environmental Research*, 68(5), 268–277. <https://doi.org/10.1016/j.marenvres.2009.06.016>
- Bonier, F., Martin, P. R., Moore, I. T., & Wingfield, J. C. (2009). Do baseline glucocorticoids predict fitness? *Trends in Ecology & Evolution*, 24(11), 634–642. <https://doi.org/10.1016/J.TREE.2009.04.013>
- Boonstra, R. (2013). Reality as the leading cause of stress: rethinking the impact of chronic stress in nature. *Functional Ecology*, 27(1), 11–23. <https://doi.org/10.1111/1365-2435.12008>
- Boshra, H., Li, J., & Sunyer, J. O. (2006). Recent advances on the complement system of teleost fish. *Fish & Shellfish Immunology*, 20(2), 239–262. <https://doi.org/10.1016/J.FSI.2005.04.004>
- Braakman, I., & Bulleid, N. J. (2011). Protein folding and modification in the mammalian endoplasmic reticulum. *Annual Review of Biochemistry*, 80, 71–99. <https://doi.org/10.1146/annurev-biochem-062209-093836>
- Braithwaite, V. A., & Boulcott, P. (2007). Pain perception, aversion and fear in fish. *Diseases of Aquatic Organisms*, 75, 131–138. <http://www.scopus.com/inward/record.url?eid=2-s2.0-34250373357&partnerID=8YFLogxK>
- Braithwaite, V. A., & Ebbesson, L. O. E. (2014). Pain and stress responses in farmed fish. *Revue Scientifique et Technique (International Office of Epizootics)*, 33(1), 245–253. <http://www.ncbi.nlm.nih.gov/pubmed/25000797>
- Braithwaite, V. A., & Huntingford, F. A. L. B. (2004). Fish and welfare: do fish have the capacity for pain perception and suffering? *Animal Welfare*, 13, S87–S92. <http://eprints.gla.ac.uk/9720/>
- Brambell, R. (1965). *Report of the Technical Committee to Enquire Into the Welfare of Animals kept under Intensive Livestock Husbandry Systems*. https://books.google.pt/books/about/Report_of_the_Technical_Committee_to_Enq.html?id=KcbwPgAACAAJ&redir_esc=y
- Branson, E. J. (2008). *Fish Welfare* (E. J. Branson, Ed.). Blackwell Publishing Ltd. [https://doi.org/10.1016/S0065-2776\(08\)60014-0](https://doi.org/10.1016/S0065-2776(08)60014-0)
- Breves, J. P., Springer-Miller, R. H., Chenoweth, D. A., Paskavitz, A. L., Chang, A. Y. H., Regish, A. M., Einarsdottir, I. E., Björnsson, B. T., & McCormick, S. D. (2020). Cortisol regulates insulin-like growth-factor binding protein (igfbp) gene expression in Atlantic salmon parr. *Molecular and Cellular Endocrinology*, 518(July), 108989. <https://doi.org/10.1016/j.mce.2020.110989>
- Britto, F. A., Dumas, K., Giorgetti-Peraldi, S., Ollendorff, V., & Favier, F. B. (2020). Is REDD1 a metabolic double agent? Lessons from physiology and pathology. *American Journal of*

- Browman, H. I., Cooke, S. J., Cowx, I. G., Derbyshire, S. W. G., Kasumyan, A., Key, B., Rose, J. D., Schwab, A., Skiftesvik, A. B., Stevens, E. D., Watson, C. A., & Arlinghaus, R. (2019). Welfare of aquatic animals: where things are, where they are going, and what it means for research, aquaculture, recreational angling, and commercial fishing. *ICES Journal of Marine Science*, 76(1), 82–92. <https://doi.org/10.1093/ICESJMS/FSY067>
- Brown, C. (2015). Fish intelligence, sentience and ethics. *Animal Cognition*, 18(1), 1–17. <https://doi.org/10.1007/s10071-014-0761-0>
- Brunt, J., Hansen, R., Jamieson, D. J., & Austin, B. (2008). Proteomic analysis of rainbow trout (*Oncorhynchus mykiss*, Walbaum) serum after administration of probiotics in diets. *Veterinary Immunology and Immunopathology*, 121(3–4), 199–205. <https://doi.org/10.1016/j.vetimm.2007.09.010>
- Bshary, R., & Brown, C. (2014). Fish cognition. *Current Biology*, 24(19), R947–R950. <https://doi.org/10.1016/j.cub.2014.08.043>
- Buján, N., Hernández-Haro, C., Monteoliva, L., Gil, C., & Magariños, B. (2015). Comparative proteomic study of *Edwardsiella tarda* strains with different degrees of virulence. *Journal of Proteomics*, 127(B), 310–320. <https://doi.org/10.1016/j.jprot.2015.05.008>
- Cakmak, G., Togan, I., & Severcan, F. (2006). 17 β -Estradiol induced compositional, structural and functional changes in rainbow trout liver, revealed by FT-IR spectroscopy: A comparative study with nonylphenol. *Aquatic Toxicology*, 77(1), 53–63. <https://doi.org/10.1016/j.aquatox.2005.10.015>
- Çakmak, G., Togan, I., Uğuz, C., & Severcan, F. (2003). FT-IR spectroscopic analysis of rainbow trout liver exposed to nonylphenol. *Applied Spectroscopy*, 57(7), 835–841. <https://doi.org/10.1366/000370203322102933>
- Campos, A., & de Almeida, A. (2016). Top-Down Proteomics and Farm Animal and Aquatic Sciences. *Proteomes*, 4(4), 38. <https://doi.org/10.3390/proteomes4040038>
- Canellas, A. L. B., Costa, W. F., Freitas-Silva, J., Lopes, I. R., de Oliveira, B. F. R., & Laport, M. S. (2022). In sickness and in health: Insights into the application of omics in aquaculture settings under a microbiological perspective. *Aquaculture*, 554(December 2021). <https://doi.org/10.1016/j.aquaculture.2022.738132>
- Cangul, H. (2004). Hypoxia upregulates the expression of the NDRG1 gene leading to its overexpression in various human cancers. *BMC Genetics*, 5(1), 1–11. <https://doi.org/10.1186/1471-2156-5-27/FIGURES/6>
- Cao, K.-A. L., & Besse, P. (2008). A Sparse PLS for Variable Selection when Integrating Omics Data. *Article 35 Statistical Applications in Genetics and Molecular Biology Genetics and Molecular Biology*, 7(1), 35. <https://doi.org/10.2202/1544-6115.1390>
- Cao, Q., Zhang, H., Li, T., He, L., Zong, J., Shan, H., & Huang, L. (2023). *Profiling miRNAs of Teleost Fish in Responses to Environmental Stress: A Review*.
- Cappello, T., Brandão, F., Guilherme, S., Santos, M. A., Maisano, M., Mauceri, A., Canário, J., Pacheco, M., & Pereira, P. (2016). Insights into the mechanisms underlying mercury-induced oxidative stress in gills of wild fish (*Liza aurata*) combining 1H NMR metabolomics and conventional biochemical assays. *Science of the Total Environment*, 548–549, 13–24. <https://doi.org/10.1016/j.scitotenv.2016.01.008>
- Carballeira Braña, C. B., Cerbule, K., Senff, P., & Stolz, I. K. (2021). Towards Environmental Sustainability in Marine Finfish Aquaculture. *Frontiers in Marine Science*, 8, 343. <https://doi.org/10.3389/FMARS.2021.666662>
- Carenzi, C., & Verga, M. (2009). Animal welfare: review of the scientific concept and definition. *Italian Journal of Animal Science*, 8(sup1), 21–30. <https://doi.org/10.4081/ijas.2009.s1.21>
- Carlson, M. (2019). org.Dr.eg.db: Genome wide annotation for Zebrafis. *R Package Version 3.8.2*.
- Caron, E., Ghosh, S., Matsuoka, Y., Ashton-Beaucage, D., Therrien, M., Lemieux, S., Perreault, C., Roux, P. P., & Kitano, H. (2010). A comprehensive map of the mTOR signaling network. *Molecular Systems Biology*, 6(453). <https://doi.org/10.1038/msb.2010.108>

- Cassidy, A. A., & Lamarre, S. G. (2019). Activation of oxygen-responsive pathways is associated with altered protein metabolism in Arctic char exposed to hypoxia. *Journal of Experimental Biology*, 222(22). <https://doi.org/10.1242/jeb.203901>
- Castanheira, M. F., Conceição, L. E. C., Millot, S., Rey, S., Bégout, M.-L., Damsgård, B., Kristiansen, T., Höglund, E., Øverli, Ø., & Martins, C. I. M. (2017). Coping styles in farmed fish: consequences for aquaculture. *Reviews in Aquaculture*, 9(1), 23–41. <https://doi.org/10.1111/raq.12100>
- Causey, D. R., N Pohl, M. A., Stead, D. A., M Martin, S. A., Secombes, C. J., & Macqueen, D. J. (2018). High-throughput proteomic profiling of the fish liver following bacterial infection. *BMC Genomics*, 19, 719. <https://doi.org/10.1186/s12864-018-5092-0>
- Cerqueira, M., Millot, S., Castanheira, M. F., Félix, A. S., Silva, T., Oliveira, G. A., Oliveira, C. C., Martins, C. I. M., & Oliveira, R. F. (2017). Cognitive appraisal of environmental stimuli induces emotion-like states in fish. *Scientific Reports*, 7, 13181. <https://doi.org/10.1038/s41598-017-13173-x>
- Cerqueira, M., Schrama, D., Silva, T. S., Colen, R., Engrola, S. A. D., Conceição, L. E. C., Rodrigues, P. M. L., & Farinha, A. P. (2020). How tryptophan levels in plant-based aquafeeds affect fish physiology, metabolism and proteome. *Journal of Proteomics*, 221(April). <https://doi.org/10.1016/j.jprot.2020.103782>
- Ceylan, C., Tanrikul, T., & Özgener, H. (2014). Biophysical evaluation of physiological effects of gilthead sea bream (*Sparus aurata*) farming using FTIR spectroscopy. *Food Chemistry*, 145, 1055–1060. <https://doi.org/10.1016/j.foodchem.2013.08.111>
- Chandhini, S., & Rejish Kumar, V. J. (2019). Transcriptomics in aquaculture: current status and applications. *Reviews in Aquaculture*, 11(4), 1379–1397. <https://doi.org/10.1111/raq.12298>
- Chang, C.-H., Tang, C.-H., Kang, C.-K., Lo, W.-Y., & Lee, T.-H. (2016). Comparison of Integrated Responses to Nonlethal and Lethal Hypothermal Stress in Milkfish (*Chanos chanos*): A Proteomics Study. *PLOS ONE*, 11(9), e0163538. <https://doi.org/10.1371/journal.pone.0163538>
- Charlie-Silva, I., Klein, A., Gomes, J. M. M., Prado, E. J. R., Moraes, A. C., Eto, S. F., Fernandes, D. C., Fagliari, J. J., Junior, J. D. C., Lima, C., Lopes-Ferreira, M., Conceição, K., Manrique, W. G., & Belo, M. A. A. (2019). Acute-phase proteins during inflammatory reaction by bacterial infection: Fish-model. *Scientific Reports*, 9(1), 4776. <https://doi.org/10.1038/s41598-019-41312-z>
- Chen, C., Pore, N., Behrooz, A., Ismail-Beigi, F., & Maity, A. (2001). Regulation of glut1 mRNA by hypoxia-inducible factor-1: Interaction between H-ras and hypoxia. *Journal of Biological Chemistry*, 276(12), 9519–9525. <https://doi.org/10.1074/jbc.M010144200>
- Chen, G., Pang, M., Yu, X., Wang, J., & Tong, J. (2021). Transcriptome sequencing provides insights into the mechanism of hypoxia adaption in bighead carp (*Hypophthalmichthys nobilis*). *Comparative Biochemistry and Physiology - Part D: Genomics and Proteomics*, 40(August), 100891. <https://doi.org/10.1016/j.cbd.2021.100891>
- Chen, G., Zhang, C., Li, C., Wang, C., Xu, Z., & Yan, P. (2011). Haemocyte protein expression profiling of scallop *Chlamys farreri* response to acute viral necrosis virus (AVNV) infection. *Developmental & Comparative Immunology*, 35(11), 1135–1145. <https://doi.org/10.1016/j.dci.2011.03.022>
- Chen, S., Zhou, Y., Chen, Y., & Gu, J. (2018). fastp: an ultra-fast all-in-one FASTQ preprocessor. *Bioinformatics*, 34, i884–i890. <https://doi.org/10.1093/bioinformatics/bty560>
- Chen, X., Wu, Z., Yu, S., Wang, S., & Peng, X. (2010). Beta2-microglobulin is involved in the immune response of large yellow croaker to *Aeromonas hydrophila*: A proteomic based study. *Fish & Shellfish Immunology*, 28(1), 151–158. <https://doi.org/10.1016/J.FSI.2009.10.015>
- Cheng, J., Xie, H. Y., Xu, X., Wu, J., Wei, X., Su, R., Zhang, W., Lv, Z., Zheng Shusen, S., & Zhou, L. (2011). NDRG1 as a biomarker for metastasis, recurrence and of poor prognosis in hepatocellular carcinoma. *Cancer Letters*, 310(1), 35–45. <https://doi.org/10.1016/J.CANLET.2011.06.001>

- Chervoneva, I., Li, Y., Schulz, S., Croker, S., Wilson, C., Waldman, S. A., & Hyslop, T. (2010). Selection of optimal reference genes for normalization in quantitative RT-PCR. *BMC Bioinformatics*, *11*(1), 253. <https://doi.org/10.1186/1471-2105-11-253>
- Choi, S. B., Park, J. B., Song, T. J., & Choi, S. Y. (2011). Molecular mechanism of HIF-1-independent VEGF expression in a hepatocellular carcinoma cell line. *International Journal of Molecular Medicine*, *28*(3), 449–454. <https://doi.org/10.3892/ijmm.2011.719>
- Chongsatja, P., Bourchookarn, A., Lo, C. F., Thongboonkerd, V., & Krittanai, C. (2007). Proteomic analysis of differentially expressed proteins in *Penaeus vannamei* hemocytes upon Taura syndrome virus infection. *Proteomics*, *7*(19), 3592–3601. <https://doi.org/10.1002/pmic.200700281>
- Chun, Y., & Kim, J. (2021). AMPK–mTOR Signaling and Cellular Adaptations in Hypoxia. *International Journal of Molecular Sciences 2021*, Vol. 22, Page 9765, *22*(18), 9765. <https://doi.org/10.3390/IJMS22189765>
- Coccia, E., Imperatore, R., Orso, G., Melck, D., Varricchio, E., Volpe, M. G., & Paolucci, M. (2019). Explants of *Oncorhynchus mykiss* intestine to detect bioactive molecules uptake and metabolic effects: Applications in aquaculture. *Aquaculture*, *506*(November 2018), 193–204. <https://doi.org/10.1016/j.aquaculture.2019.03.041>
- Colás-Ruiz, N. R., Courant, F., Gomez, E., Lara-Martín, P. A., & Hampel, M. (2023). Transcriptomic and metabolomic integration to assess the response of gilthead sea bream (*Sparus aurata*) exposed to the most used insect repellent: DEET. *Environmental Pollution*, *316*(September 2022). <https://doi.org/10.1016/j.envpol.2022.120678>
- Colás-Ruiz, N. R., Ramirez, G., Courant, F., Gomez, E., Hampel, M., & Lara-Martín, P. A. (2022). Multi-omic approach to evaluate the response of gilt-head sea bream (*Sparus aurata*) exposed to the UV filter sulisobenzone. *Science of The Total Environment*, *803*, 150080. <https://doi.org/10.1016/J.SCITOTENV.2021.150080>
- Colli-Dula, R. C., Fang, X., Moraga-Amador, D., Albornoz-Abud, N., Zamora-Bustillos, R., Conesa, A., Zapata-Perez, O., Moreno, D., & Hernandez-Nuñez, E. (2018). Transcriptome analysis reveals novel insights into the response of low-dose benzo(a)pyrene exposure in male tilapia. *Aquatic Toxicology*, *201*(April), 162–173. <https://doi.org/10.1016/j.aquatox.2018.06.005>
- Conceição, L. E. C., Aragão, C., Dias, J., Costas, B., Terova, G., Martins, C., & Tort, L. (2012). Dietary nitrogen and fish welfare. *Fish Physiology and Biochemistry*, *38*(1), 119–141. <https://doi.org/10.1007/s10695-011-9592-y>
- Concha, M. I., Molina, S., Oyarzún, C., Villanueva, J., & Amthauer, R. (2003). Local expression of apolipoprotein A-I gene and a possible role for HDL in primary defence in the carp skin. *Fish & Shellfish Immunology*, *14*(3), 259–273. <https://doi.org/10.1006/FSIM.2002.0435>
- Cone, R. A. (2009). Barrier properties of mucus. *Advanced Drug Delivery Reviews*, *61*(2), 75–85. <https://doi.org/10.1016/j.addr.2008.09.008>
- Conesa, A., Götz, S., García-Gómez, J. M., Terol, J., Talón, M., & Robles, M. (2005). Blast2GO: A universal tool for annotation, visualization and analysis in functional genomics research. *Bioinformatics*, *21*(18), 3674–3676. <https://doi.org/10.1093/bioinformatics/bti610>
- CONSENSUS. (2009). Towards sustainable aquaculture in Europe. *An Overview of Sustainability in European Aquaculture*. <http://eprints.cmfri.org.in/8533/>
- Conte, F. S. (2004). Stress and the welfare of cultured fish. *Applied Animal Behaviour Science*, *86*(3–4), 205–223. <https://doi.org/10.1016/j.applanim.2004.02.003>
- Corazzari, M., Gagliardi, M., Fimia, G. M., & Piacentini, M. (2017). Endoplasmic reticulum stress, unfolded protein response, and cancer cell fate. *Frontiers in Oncology*, *7*(APR), 1–11. <https://doi.org/10.3389/fonc.2017.00078>
- Cordeiro, O. D., Silva, T. S., Alves, R. N., Costas, B., Wulff, T., Richard, N., de Vareilles, M., Conceição, L. E. C., & Rodrigues, P. M. (2012a). Changes in Liver Proteome Expression of Senegalese Sole (*Solea senegalensis*) in Response to Repeated Handling Stress. *Marine Biotechnology*, *14*(6), 714–729. <https://doi.org/10.1007/s10126-012-9437-4>
- Cordeiro, O. D., Silva, T. S., Alves, R. N., Costas, B., Wulff, T., Richard, N., de Vareilles, M., Conceição, L. E. C., & Rodrigues, P. M. (2012b). Changes in Liver Proteome Expression

- of Senegalese Sole (*Solea senegalensis*) in Response to Repeated Handling Stress. *Marine Biotechnology*, 14(6), 714–729. <https://doi.org/10.1007/s10126-012-9437-4>
- Cordero, H., Brinchmann, M. F., Cuesta, A., & Esteban, M. A. (2017). Chronic wounds alter the proteome profile in skin mucus of farmed gilthead seabream. *BMC Genomics*, 18(1), 939. <https://doi.org/10.1186/s12864-017-4349-3>
- Cordero, H., Morcillo, P., Cuesta, A., Brinchmann, M. F., & Esteban, M. A. (2016). Differential proteome profile of skin mucus of gilthead seabream (*Sparus aurata*) after probiotic intake and/or overcrowding stress. *Journal of Proteomics*, 132, 41–50. <https://doi.org/10.1016/J.JPROT.2015.11.017>
- Corte, L., Rellini, P., Roscini, L., Fatichenti, F., & Cardinali, G. (2010). Development of a novel, FTIR (Fourier transform infrared spectroscopy) based, yeast bioassay for toxicity testing and stress response study. *Analytica Chimica Acta*, 659(1–2), 258–265. <https://doi.org/10.1016/j.aca.2009.11.035>
- Cossu, P., Scarpa, F., Sanna, D., Lai, T., Dedola, G. L., Curini-Galletti, M., Mura, L., Fois, N., & Casu, M. (2019). Influence of genetic drift on patterns of genetic variation: The footprint of aquaculture practices in *Sparus aurata* (Teleostei: Sparidae). *Molecular Ecology*, 28(12), 3012–3024. <https://doi.org/10.1111/mec.15134>
- Cowan, M. L., & Vera, J. (2008). Proteomics: Advances in Biomarker Discovery. *Expert Review of Proteomics*, 5(1), 21–23. <https://doi.org/10.1586/14789450.5.1.21>
- Cray, C., Zaias, J., & Altman, N. H. (2009). Acute phase response in animals: a review. *Comparative Medicine*, 59(6), 517–526. <http://www.ncbi.nlm.nih.gov/pubmed/20034426>
- Crollius, H. R., & Weissenbach, J. (2005). Fish genomics and biology. *Genome Research*, 15, 1675–1682. <https://doi.org/10.1101/gr.3735805>
- Cuervo, A. M. (2004). Autophagy: Many paths to the same end. *Molecular and Cellular Biochemistry*, 263(1), 55–72. <https://doi.org/10.1023/B:MCBI.0000041848.57020.57>
- Dai, Q., Cheng, J. H., Sun, D. W., & Zeng, X. A. (2015). Advances in feature selection methods for hyperspectral image processing in food industry applications: A review. *Critical Reviews in Food Science and Nutrition*, 55(10), 1368–1382. <https://doi.org/10.1080/10408398.2013.871692>
- Dai, Y. F., Shen, Y. bang, Wang, S. T., Zhang, J. H., Su, Y. H., Bao, S. C., Xu, X. Y., & Li, J. Le. (2021). RNA-Seq Transcriptome Analysis of the Liver and Brain of the Black Carp (*Mylopharyngodon piceus*) During Fasting. *Marine Biotechnology*, 23(3), 389–401. <https://doi.org/10.1007/s10126-021-10032-9>
- Dale, K., Yadetie, F., Müller, M. B., Pampanin, D. M., Gilabert, A., Zhang, X., Tairova, Z., Haarr, A., Lille-Langøy, R., Lyche, J. L., Porte, C., Karlsen, O. A., & Goksøyr, A. (2020). Proteomics and lipidomics analyses reveal modulation of lipid metabolism by perfluoroalkyl substances in liver of Atlantic cod (*Gadus morhua*). *Aquatic Toxicology*, 227, 105590. <https://doi.org/10.1016/J.AQUATOX.2020.105590>
- Das, C., Thraya, M., & Vijayan, M. M. (2018). Nongenomic cortisol signaling in fish. *General and Comparative Endocrinology*, 265, 121–127. <https://doi.org/10.1016/J.YGCEN.2018.04.019>
- Das, P., Roychowdhury, A., Das, S., Roychoudhury, S., & Tripathy, S. (2020). sigFeature: Novel Significant Feature Selection Method for Classification of Gene Expression Data Using Support Vector Machine and t Statistic. *Frontiers in Genetics*, 11(April), 1–12. <https://doi.org/10.3389/fgene.2020.00247>
- Dash, S., Das, S. K., Samal, J., & Thatoi, H. N. (2018). Epidermal mucus, a major determinant in fish health: a review. *Iranian Journal of Veterinary Research*, 19(2), 72. <https://pmc/articles/PMC6056142/>
- Davis Jr, K. B., & McEntire, M. E. (2006). Comparison of the cortisol and glucose stress response to acute confinement and resting insulin-like growth factor-I concentrations among white bass, striped bass and sunshine bass. *Aquaculture America Book of Abstracts*, 79. <https://www.ars.usda.gov/research/publications/publication/?seqNo115=183961>
- Dawkins, M. S. (1998). Evolution and animal welfare. *Quarterly Review of Biology*, 73(3), 305–328. <https://doi.org/10.1086/420307>

- de la Serrana, D. G., & Macqueen, D. J. (2018). Insulin-like growth factor-binding proteins of teleost fishes. *Frontiers in Endocrinology*, 9(MAR), 1–12. <https://doi.org/10.3389/fendo.2018.00080>
- de Magalhães, C. R., Carrilho, R., Schrama, D., Cerqueira, M., Rosa, A. M., & Rodrigues, P. M. (2020). Mid-infrared spectroscopic screening of metabolic alterations in stress - exposed gilthead seabream (*Sparus aurata*). *Scientific Reports*, 10, 16343. <https://doi.org/10.1038/s41598-020-73338-z>
- De Mercado, E., Larrán, A. M., Pinedo, J., & Tomás-Almenar, C. (2018). Skin mucous: A new approach to assess stress in rainbow trout. *Aquaculture*, 484, 90–97. <https://doi.org/10.1016/J.AQUACULTURE.2017.10.031>
- de Vareilles, M., Richard, N., Gavaia, P. J., Silva, T. S., Cordeiro, O., Guerreiro, I., Yúfera, M., Batista, I., Pires, C., Pousão-Ferreira, P., Rodrigues, P. M., Rønnestad, I., Fladmark, K. E., & Conceição, L. E. C. (2012). Impact of dietary protein hydrolysates on skeleton quality and proteome in *Diplodus sargus* larvae. *Journal of Applied Ichthyology*, 28(3), 477–487. <https://doi.org/10.1111/J.1439-0426.2012.01986.X>
- Delbarre-Ladrat, C., Chéret, R., Taylor, R., & Verrez-Bagnis, V. (2006). Trends in postmortem aging in fish: Understanding of proteolysis and disorganization of the myofibrillar structure. *Critical Reviews in Food Science and Nutrition*, 46(5), 409–421. <https://doi.org/10.1080/10408390591000929>
- Deutsch, E. W., Bandeira, N., Sharma, V., Perez-Riverol, Y., Carver, J. J., Kundu, D. J., García-Seisdedos, D., Jarnuczak, A. F., Hewapathirana, S., Pullman, B. S., Wertz, J., Sun, Z., Kawano, S., Okuda, S., Watanabe, Y., Hermjakob, H., Maclean, B., Maccoss, M. J., Zhu, Y., ... Vizcaíno, J. A. (2020). The ProteomeXchange consortium in 2020: enabling 'big data' approaches in proteomics. *Nucleic Acids Research*, 48(D1), D1145–D1152. <https://doi.org/10.1093/NAR/GKZ984>
- Dharia, A. P., Obla, A., Gajdosik, M. D., Simon, A., & Nelson, C. E. (2014). Tempo and Mode of Gene Duplication in Mammalian Ribosomal Protein Evolution. *PLoS ONE*, 9(11), 111721. <https://doi.org/10.1371/JOURNAL.PONE.0111721>
- Di Girolamo, F., D'Amato, A., Lante, I., Signore, F., Muraca, M., & Putignani, L. (2014). Farm Animal Serum Proteomics and Impact on Human Health. *International Journal of Molecular Sciences*, 15(9), 15396–15411. <https://doi.org/10.3390/ijms150915396>
- Diaz-Rosales, P., Pereiro, P., Figueras, A., Novoa, B., & Dios, S. (2014). The warm temperature acclimation protein (Wap65) has an important role in the inflammatory response of turbot (*Scophthalmus maximus*). *Fish & Shellfish Immunology*, 41(1), 80–92. <https://doi.org/10.1016/J.FSI.2014.04.012>
- Diem, M. (1994). *Modern Vibrational Spectroscopy*. John Wiley & Sons. <http://linkinghub.elsevier.com/retrieve/pii/0584853994800731>
- Dietrich, M. A., Hliwa, P., Adamek, M., Steinhagen, D., Karol, H., & Ciereszko, A. (2018). Acclimation to cold and warm temperatures is associated with differential expression of male carp blood proteins involved in acute phase and stress responses, and lipid metabolism. *Fish & Shellfish Immunology*, 76, 305–315. <https://doi.org/10.1016/J.FSI.2018.03.018>
- Diggle, C. P., Shires, M., Leitch, D., Brooke, D., Carr, I. M., Markham, A. F., Hayward, B. E., Asipu, A., & Bonthron, D. T. (2009). Ketohexokinase: Expression and localization of the principal fructose-metabolizing enzyme. *Journal of Histochemistry and Cytochemistry*, 57(8), 763–774. <https://doi.org/10.1369/jhc.2009.953190>
- Dobin, A., Davis, C. A., Schlesinger, F., Drenkow, J., Zaleski, C., Jha, S., Batut, P., Chaisson, M., & Gingeras, T. R. (2013). *Sequence analysis STAR: ultrafast universal RNA-seq aligner*. 29(1), 15–21. <https://doi.org/10.1093/bioinformatics/bts635>
- Douxfiis, J., Deprez, M., Mandiki, S. N. M., Milla, S., Henrotte, E., Mathieu, C., Silvestre, F., Vandecan, M., Rougeot, C., Mélard, C., Dieu, M., Raes, M., & Kestemont, P. (2012). Physiological and proteomic responses to single and repeated hypoxia in juvenile Eurasian perch under domestication – Clues to physiological acclimation and humoral immune modulations. *Fish & Shellfish Immunology*, 33(5), 1112–1122. <https://doi.org/10.1016/j.fsi.2012.08.013>

- Druker, J., Wilson, J. W., Child, F., Shakir, D., Fasanya, T., & Rocha, S. (2021). Role of hypoxia in the control of the cell cycle. *International Journal of Molecular Sciences*, 22(9). <https://doi.org/10.3390/ijms22094874>
- Du, X., & Hu, H. (2021). The Roles of 2-Hydroxyglutarate. *Frontiers in Cell and Developmental Biology*, 9(March), 1–13. <https://doi.org/10.3389/fcell.2021.651317>
- Duan, K. B., Rajapakse, J. C., Wang, H., & Azuaje, F. (2005). Multiple SVM-RFE for gene selection in cancer classification with expression data. *IEEE Transactions on Nanobioscience*, 4(3), 228–233. <https://doi.org/10.1109/TNB.2005.853657>
- Dunn, W. B., & Ellis, David. I. (2005). Metabolomics: Current analytical platforms and methodologies. *TrAC Trends in Analytical Chemistry*, 24(4), 285–294. <https://doi.org/10.1016/J.TRAC.2004.11.021>
- Düvel, K., Yecies, J. L., Menon, S., Raman, P., Lipovsky, A. I., Souza, A. L., Triantafellow, E., Ma, Q., Gorski, R., Cleaver, S., vander Heiden, M. G., MacKeigan, J. P., Finan, P. M., Clish, C. B., Murphy, L. O., & Manning, B. D. (2010). Activation of a metabolic gene regulatory network downstream of mTOR complex 1. *Molecular Cell*, 39(2), 171–183. <https://doi.org/10.1016/j.molcel.2010.06.022>
- Easy, R. H., & Ross, N. W. (2009). Changes in Atlantic salmon (*Salmo salar*) epidermal mucus protein composition profiles following infection with sea lice (*Lepeophtheirus salmonis*). *Comparative Biochemistry and Physiology. Part D, Genomics & Proteomics*, 4(3), 159–167. <https://doi.org/10.1016/J.CBD.2009.02.001>
- Easy, R. H., & Ross, N. W. (2010). Changes in Atlantic salmon *Salmo salar* mucus components following short- and long-term handling stress. *Journal of Fish Biology*, 77(7), 1616–1631. <https://doi.org/10.1111/j.1095-8649.2010.02796.x>
- EC. (2012). Communication from the Commission to the European Parliament, the Council, the European Economic and Social Committee and the Committee of the Regions: Blue Growth—opportunities for marine and maritime sustainable growth. In *COM/2012/494/Final*. http://ec.europa.eu/maritimeaffairs/policy/blue_growth/
- EC. (2021). Communication from the commission to the european parliament, the council, the european economic and social committee and the committee of the regions empty "Strategic guidelines for a more sustainable and competitive EU aquaculture for the period 2021 to. In *COM/2021/236/Final*.
- Eckersall, P. D., Almeida, A. M. de, & Miller, I. (2012). Proteomics, a new tool for farm animal science. *Journal of Proteomics*, 75(14), 4187–4189. <https://doi.org/10.1016/J.JPROT.2012.05.014>
- Einarsdottir, I. E., Nilssen, K. J., & Iversen, M. (2000). Effects of rearing stress on Atlantic salmon (*Salmo salar* L.) antibody response to a non-pathogenic antigen. *Aquaculture Research*, 31(12), 923–930. <https://doi.org/10.1046/j.1365-2109.2000.00506.x>
- Eissa, N., Wang, H.-P., Yao, H., Shen, Z.-G., Shaheen, A. A., & Abou-ElGheit, E. N. (2017). Expression of Hsp70, Igf1, and Three Oxidative Stress Biomarkers in Response to Handling and Salt Treatment at Different Water Temperatures in Yellow Perch, *Perca flavescens*. *Frontiers in Physiology*, 8, 683. <https://doi.org/10.3389/fphys.2017.00683>
- Elgenaidi, I. S., & Spiers, J. P. (2019). Regulation of the phosphoprotein phosphatase 2A system and its modulation during oxidative stress: A potential therapeutic target? *Pharmacology and Therapeutics*, 198, 68–89. <https://doi.org/10.1016/j.pharmthera.2019.02.011>
- Ellis, D. I., Dunn, W. B., Griffin, J. L., Allwood, J. W., & Goodacre, R. (2007). Metabolic fingerprinting as a diagnostic tool. *Pharmacogenomics*, 8(9), 1243–1266. <https://doi.org/10.2217/14622416.8.9.1243>
- Ellis, D. I., & Goodacre, R. (2006). Metabolic fingerprinting in disease diagnosis: Biomedical applications of infrared and Raman spectroscopy. *Analyst*, 131(8), 875–885. <https://doi.org/10.1039/b602376m>
- Ellis, T., North, B., Scott, A. P., Bromage, N. R., Porter, M., & Gadd, D. (2002). The relationships between stocking density and welfare in farmed rainbow trout. *Journal of Fish Biology*, 61(3), 493–531. <https://doi.org/10.1111/j.1095-8649.2002.tb00893.x>

- Ellis, T., Yildiz, H. Y., López-Olmeda, J., Spedicato, M. T., Tort, L., Øverli, Ø., & Martins, C. I. M. (2012). Cortisol and finfish welfare. *Fish Physiology and Biochemistry*, 38(1), 163–188. <https://doi.org/10.1007/s10695-011-9568-y>
- Ellison, A. R., Uren Webster, T. M., Rodriguez-Barreto, D., de Leaniz, C. G., Consuegra, S., Orozco-terWengel, P., & Cable, J. (2020). Comparative transcriptomics reveal conserved impacts of rearing density on immune response of two important aquaculture species. *Fish and Shellfish Immunology*, 104(March), 192–201. <https://doi.org/10.1016/j.fsi.2020.05.043>
- Enes, P., Panserat, S., Kaushik, S., & Oliva-Teles, A. (2009). Nutritional regulation of hepatic glucose metabolism in fish. *Fish Physiology and Biochemistry*, 35(3), 519–539. <https://doi.org/10.1007/s10695-008-9259-5>
- Eriksen, H. R., Murison, R., Pensaard, A. M., & Ursin, H. (2005). Cognitive activation theory of stress (CATS): From fish brains to the Olympics. *Psychoneuroendocrinology*, 30, 933–938. <http://www.sciencedirect.com/science/article/pii/S0306453005001058>
- Erikson, U. (2001). Rigor measurements. In S. C. Kestin & P. D. Warriss (Eds.), *Farmed fish quality* (pp. 283–297). Blackwell Science Inc.
- Eslamloo, K., Akhavan, S. R., Fallah, F. J., & Henry, M. A. (2014). Variations of physiological and innate immunological responses in goldfish (*Carassius auratus*) subjected to recurrent acute stress. *Fish and Shellfish Immunology*, 37(1), 147–153. <https://doi.org/10.1016/j.fsi.2014.01.014>
- European Parliament. (2010). Directive 2010/63/EU of the European parliament and of the Council of 22 September 2010 on the protection of animals used for scientific purposes. *Official Journal of the European Union*, June, 1–61. <http://eur-lex.europa.eu/legal-content/EN/TXT/HTML/?uri=CELEX:32010L0063&from=EN>
- Evans, T. G., & Kültz, D. (2020). The cellular stress response in fish exposed to salinity fluctuations. *Journal of Experimental Zoology Part A: Ecological and Integrative Physiology*, 333(6), 421–435. <https://doi.org/10.1002/JEZ.2350>
- Ewels, P., Ns Magnusson, M., Lundin, S., & Aller, M. K. (2016). Data and text mining MultiQC: summarize analysis results for multiple tools and samples in a single report. *Bioinformatics*, 32(19), 3047–3048. <https://doi.org/10.1093/bioinformatics/btw354>
- Fabbri, E., & Moon, T. W. (2016). Adrenergic signaling in teleost fish liver, a challenging path. *Comparative Biochemistry and Physiology Part B: Biochemistry and Molecular Biology*, 199, 74–86. <https://doi.org/10.1016/J.CBPB.2015.10.002>
- Fabregat, A., Sidiropoulos, K., Viteri, G., Forner, O., Marin-Garcia, P., Arnau, V., D'Eustachio, P., Stein, L., & Hermjakob, H. (2017). Reactome pathway analysis: A high-performance in-memory approach. *BMC Bioinformatics*, 18(1), 1–9. <https://doi.org/10.1186/S12859-017-1559-2/TABLES/1>
- Fanouraki, E., Mylonas, C. C., Papandroulakis, N., & Pavlidis, M. (2011). Species specificity in the magnitude and duration of the acute stress response in Mediterranean marine fish in culture. *General and Comparative Endocrinology*, 173(2), 313–322. <https://doi.org/10.1016/J.YGCEN.2011.06.004>
- FAO. (1995). *Code of Conduct for Responsible Fisheries*. <https://doi.org/10.5040/9781509955572.0062>
- FAO. (2011). *Technical Guidelines on Aquaculture Certification*.
- FAO. (2018). *Transforming Food and Agriculture To Achieve the SDGs*.
- FAO. (2020). *The State of World Fisheries and Aquaculture 2020. Sustainability in action*.
- FAO. (2022). *The State of World Fisheries and Aquaculture (SOFIA) 2022. Towards blue transformation*. https://www.fao.org/3/ca9229en/online/ca9229en.html#chapter-1_1
- Farinha, A. P., Schrama, D., Silva, T., Conceição, L. E. C., Colen, R., Engrola, S., Rodrigues, P., & Cerqueira, M. (2021). Evaluating the impact of methionine-enriched diets in the liver of European seabass through label-free shotgun proteomics. *Journal of Proteomics*, 232, 104047. <https://doi.org/10.1016/J.JPROT.2020.104047>
- Fast, M. D., Hosoya, S., Johnson, S. C., & Afonso, L. O. B. (2008). Cortisol response and immune-related effects of Atlantic salmon (*Salmo salar* Linnaeus) subjected to short- and

- long-term stress. *Fish & Shellfish Immunology*, 24(2), 194–204. <https://doi.org/10.1016/J.FSI.2007.10.009>
- Faught, E., & Vijayan, M. M. (2016). Mechanisms of cortisol action in fish hepatocytes. *Comparative Biochemistry and Physiology Part B: Biochemistry and Molecular Biology*, 199, 136–145. <https://doi.org/10.1016/J.CBPB.2016.06.012>
- Faustino, A. I., Oliveira, G. A., & Oliveira, R. F. (2015). Linking appraisal to behavioral flexibility in animals: implications for stress research. *Frontiers in Behavioral Neuroscience*, 9, 104. <https://doi.org/10.3389/fnbeh.2015.00104>
- Federation of European Aquaculture Producers. (2008). *FEAP Code of Conduct*.
- Federation of European Aquaculture Producers. (2022). *FEAP Annual Report 2022*.
- Fengou, L. C., Lianou, A., Tsakanikas, P., Gkana, E. N., Panagou, E. Z., & Nychas, G. J. E. (2019). Evaluation of Fourier transform infrared spectroscopy and multispectral imaging as means of estimating the microbiological spoilage of farmed sea bream. *Food Microbiology*, 79(February 2018), 27–34. <https://doi.org/10.1016/j.fm.2018.10.020>
- Fernández-Alacid, L., Sanahuja, I., Ordóñez-Grande, B., Sánchez-Nuño, S., Herrera, M., & Ibarz, A. (2019). Skin mucus metabolites and cortisol in meagre fed acute stress-attenuating diets: Correlations between plasma and mucus. *Aquaculture*, 499, 185–194. <https://doi.org/10.1016/j.aquaculture.2018.09.039>
- Fernández-Alacid, L., Sanahuja, I., Ordóñez-Grande, B., Sánchez-Nuño, S., Viscor, G., Gisbert, E., Herrera, M., & Ibarz, A. (2018). Skin mucus metabolites in response to physiological challenges: A valuable non-invasive method to study teleost marine species. *Science of The Total Environment*, 644, 1323–1335. <https://doi.org/10.1016/J.SCITOTENV.2018.07.083>
- Fernández-Montero, A., Torrecillas, S., Tort, L., Ginés, R., Acosta, F., Izquierdo, M. S., & Montero, D. (2020). Stress response and skin mucus production of greater amberjack (*Seriola dumerili*) under different rearing conditions. *Aquaculture*, 520, 735005. <https://doi.org/10.1016/j.aquaculture.2020.735005>
- Filzmoser, P., Fritz, H., & Kalcher, K. (2018). pcaPP: Robust PCA by Projection Pursuit. *R Package Version 1.9-73*.
- Filzmoser, P., Maronna, R., & Werner, M. (2008). Outlier identification in high dimensions. *Computational Statistics and Data Analysis*, 52(3), 1694–1711. <https://doi.org/10.1016/j.csda.2007.05.018>
- Filzmoser, P., & Varmuza, K. (2017). chemometrics: Multivariate Statistical Analysis in Chemometrics. *R Package Version 1.4.2*.
- Forbes, J. L. I., Kostyniuk, D. J., Mennigen, J. A., & Weber, J.-M. (2019). Glucagon regulation of carbohydrate metabolism in rainbow trout: in vivo glucose fluxes and gene expression. *The Journal of Experimental Biology*, 222(24), jeb211730. <https://doi.org/10.1242/jeb.211730>
- Forné, I., Abián, J., & Cerdà, J. (2010). Fish proteome analysis: Model organisms and non-sequenced species. *Proteomics*, 10(4), 858–872. <https://doi.org/10.1002/pmic.200900609>
- Franchini, P., Sola, L., Crosetti, D., Milana, V., & Rossi, A. R. (2012). Low levels of population genetic structure in the gilthead sea bream, *Sparus aurata*, along the coast of Italy. *ICES Journal of Marine Science*, 69(1), 41–50. <https://doi.org/10.1093/icesjms/fsr175>
- Franco-Martinez, L., Brandts, I., Reyes-López, F., Tort, L., Tvarijonaviciute, A., & Teles, M. (2022). Skin Mucus as a Relevant Low-Invasive Biological Matrix for the Measurement of an Acute Stress Response in Rainbow Trout (*Oncorhynchus mykiss*). *Water (Switzerland)*, 14(11). <https://doi.org/10.3390/w14111754>
- Franks, B., Ewell, C., & Jacquet, J. (2021). Animal welfare risks of global aquaculture. *Science Advances*, 7(14), eabg0677. <https://doi.org/10.1126/SCIADV.ABG0677>
- Fry, J. P., Mailloux, N. A., Love, D. C., Milli, M. C., & Cao, L. (2018). Feed conversion efficiency in aquaculture: Do we measure it correctly? *Environmental Research Letters*, 13(2). <https://doi.org/10.1088/1748-9326/aaa273>
- FSBI. (2002). Fish Welfare, Briefing Paper 2. In *Fisheries Society of the British Isles*.

- Fuest, M., Willim, K., Macnelly, S., Fellner, N., Resch, G. P., Blum, H. E., & Hasselblatt, P. (2012). The transcription factor c-Jun protects against sustained hepatic endoplasmic reticulum stress thereby promoting hepatocyte survival. *Hepatology*, *55*(2), 408–418. <https://doi.org/10.1002/hep.24699>
- Fulda, S., Gorman, A. M., Hori, O., & Samali, A. (2010). Cellular Stress Responses: Cell Survival and Cell Death. *International Journal of Cell Biology*, *2010*. <https://doi.org/10.1155/2010/214074>
- Funkenstein, B., Rebhan, Y., Dyman, A., & Radaelli, G. (2005). α 2-Macroglobulin in the marine fish *Sparus aurata*. *Comparative Biochemistry and Physiology Part A: Molecular & Integrative Physiology*, *141*(4), 440–449. <https://doi.org/10.1016/j.cbpb.2005.06.010>
- Furuhashi, M., Ishimura, S., Ota, H., & Miura, T. (2011). Lipid Chaperones and Metabolic Inflammation. *International Journal of Inflammation*, *2011*, 1–12. <https://doi.org/10.4061/2011/642612>
- Gabay, C., & Kushner, I. (1999). Acute-Phase Proteins and Other Systemic Responses to Inflammation. *New England Journal of Medicine*, *340*(6), 448–454. <https://doi.org/10.1056/NEJM199902113400607>
- Galhardo, L., & Oliveira, R. F. (2009). Psychological Stress and Welfare in Fish. *Annual Review of Biomedical Sciences*, *11*, 1–20. <https://doi.org/10.5016/1806-8774.2009v11p1>
- Galhardo, L., Oliveira, R. F., & Galhardo Oliveira, R.F.; L. (2009). Psychological Stress and Welfare in Fish. *Annual Review of Biomedical Sciences*, *11*, 1–20. [https://repositorio.ispa.pt/bitstream/10400.12/1251/1/ARBS 11 1-20.pdf](https://repositorio.ispa.pt/bitstream/10400.12/1251/1/ARBS%2011%201-20.pdf)
- Gandar, A., Laffaille, P., Marty-Gasset, N., Viala, D., Molette, C., & Jean, S. (2017). Proteome response of fish under multiple stress exposure: Effects of pesticide mixtures and temperature increase. *Aquatic Toxicology*, *184*, 61–77. <https://doi.org/10.1016/j.aquatox.2017.01.004>
- Gandin, V., Senft, D., Topisirovic, I., & Ronai, Z. A. (2013). RACK1 Function in Cell Motility and Protein Synthesis. *Genes and Cancer*, *4*(9–10), 369–377. <https://doi.org/10.1177/1947601913486348>
- Ge, H., Lin, K., Zhou, C., Lin, Q., Zhang, Z., Wu, J., Zheng, L., Yang, Q., Wu, S., Chen, W., & Wang, Y. (2020). A multi-omic analysis of orange-spotted grouper larvae infected with nervous necrosis virus identifies increased adhesion molecules and collagen synthesis in the persistent state. *Fish & Shellfish Immunology*, *98*, 595–604. <https://doi.org/10.1016/J.FSI.2020.01.056>
- Georges, A., Dhote, V., Kuhn, L., Hellen, C. U. T., Pestova, T. v, Frank, J., & Hashem, Y. (2015). Structure of mammalian eIF3 in the context of the 43S preinitiation complex. *Nature*, *525*, 491–495. <https://doi.org/10.1038/nature14891>
- German, J. B., Hammock, B. D., & Watkins, S. M. (2005). Metabolomics: building on a century of biochemistry to guide human health. *Metabolomics*, *1*(1), 3–9. <https://doi.org/10.1007/s11306-005-1102-8>
- Gesto, M., Lopez-Patino, M. A., Hernandez, J., Soengas, J. L., & Miguez, J. M. (2013). The response of brain serotonergic and dopaminergic systems to an acute stressor in rainbow trout: a time course study. *Journal of Experimental Biology*, *216*(23), 4435–4442. <https://doi.org/10.1242/jeb.091751>
- Gesto, M., Soengas, J. L., & Miguez, J. M. (2008). Acute and prolonged stress responses of brain monoaminergic activity and plasma cortisol levels in rainbow trout are modified by PAHs (naphthalene, b-naphthoflavone and benzo(a)pyrene) treatment. *Aquatic Toxicology*, *86*, 341–351.
- Gevaert, Kris., & Vandekerckhove, J el. (2011). *Gel-free proteomics : methods and protocols* (K. Gevaert & J. Vandekerckhove, Eds.). Springer.
- Ghisaura, S., Anedda, R., Pagnozzi, D., Biosa, G., Spada, S., Bonaglini, E., Cappuccinelli, R., Roggio, T., Uzzau, S., & Addis, M. F. (2014). Impact of three commercial feed formulations on farmed gilthead sea bream (*Sparus aurata*, L.) metabolism as inferred from liver and blood serum proteomic. *Proteome Science*, *12*(1). <https://doi.org/10.1186/s12953-014-0044-3>

- Ghisaura, S., Pagnozzi, D., Melis, R., Biosa, G., Slawski, H., Uzzau, S., Anedda, R., & Addis, M. F. (2019). Liver proteomics of gilthead sea bream (*Sparus aurata*) exposed to cold stress. *Journal of Thermal Biology*, 82(February), 234–241. <https://doi.org/10.1016/j.jtherbio.2019.04.005>
- Ghomlaghi, M., Hart, A., Hoang, N., Shin, S., & Nguyen, L. K. (2021). Feedback, crosstalk and competition: Ingredients for emergent non-linear behaviour in the pi3k/mtor signalling network. *International Journal of Molecular Sciences*, 22(13). <https://doi.org/10.3390/ijms22136944>
- Gil-Solsona, R., Nácher-Mestre, J., Lacalle-Bergeron, L., Sancho, J. V., Calduch-Giner, J. A., Hernández, F., & Pérez-Sánchez, J. (2017). Untargeted metabolomics approach for unraveling robust biomarkers of nutritional status in fasted gilthead sea bream (*Sparus aurata*). *PeerJ*, 5, e2920. <https://doi.org/10.7717/peerj.2920>
- Gizak, A., Sok, A. J., Lipinska, A., Zarzycki, M., Rakus, D., & Dzugaj, A. (2012). A comparative study on the sensitivity of *Cyprinus carpio* muscle and liver FBPase toward AMP and calcium. *Comparative Biochemistry and Physiology - B Biochemistry and Molecular Biology*, 162(1–3), 51–55. <https://doi.org/10.1016/j.cbpb.2012.03.001>
- Gkagkavouzis, K., Papakostas, S., Maroso, F., Karaïskou, N., Carr, A., Nielsen, E. E., Bargelloni, L., & Triantafyllidis, A. (2021). Investigating genetic diversity and genomic signatures of hatchery-induced evolution in gilthead seabream (*Sparus aurata*) populations. *Diversity*, 13(11). <https://doi.org/10.3390/d13110563>
- Glasauer, S. M. K., & Neuhauss, S. C. F. (2014). Whole-genome duplication in teleost fishes and its evolutionary consequences. *Molecular Genetics and Genomics*, 289(6), 1045–1060. <https://doi.org/10.1007/s00438-014-0889-2>
- Gloaguen, Y., Morton, F., Daly, R., Gurden, R., Rogers, S., Wandy, J., Wilson, D., Barrett, M., & Burgess, K. (2017). PiMP my metabolome: an integrated, web-based tool for LC-MS metabolomics data. *Bioinformatics*, 33(24), 4007–4009. <https://doi.org/10.1093/BIOINFORMATICS/BTX499>
- Gnanasundram, S. V., & Fåhræus, R. (2018). Translation Stress Regulates Ribosome Synthesis and Cell Proliferation. *International Journal of Molecular Sciences*, 19, 3757. <https://doi.org/10.3390/ijms19123757>
- Gomez, D., Sunyer, J. O., & Salinas, I. (2013). The mucosal immune system of fish: The evolution of tolerating commensals while fighting pathogens. In *Fish and Shellfish Immunology* (Vol. 35, Issue 6, pp. 1729–1739). Academic Press. <https://doi.org/10.1016/j.fsi.2013.09.032>
- Gracey, A. Y., Lee, T. H., Higashi, R. M., & Fan, T. (2011). Hypoxia-induced mobilization of stored triglycerides in the euryoxic goby *Gillichthys mirabilis*. *Journal of Experimental Biology*, 214(18), 3005–3012. <https://doi.org/10.1242/jeb.059907>
- Greenbaum, D., Colangelo, C., Williams, K., & Gerstein, M. (2003). Comparing protein abundance and mRNA expression levels on a genomic scale. *Genome Biology*, 4(9), 117. <https://doi.org/10.1186/gb-2003-4-9-117>
- Grek, C., & Townsend, D. M. (2013). Protein Disulfide Isomerase Superfamily in Disease and the Regulation of Apoptosis. *Endoplasmic Reticulum Stress in Diseases*, 1(1), 4–17. <https://doi.org/10.2478/ersc-2013-0001>
- Grigorakis, K. (2009). Ethical Issues in Aquaculture Production. *Journal of Agricultural and Environmental Ethics*, 23, 345–370. <https://doi.org/10.1007/s10806-009-9210-5> LB - Grigorakis2009
- Gu, Z., Eils, R., & Schlesner, M. (2016). Complex heatmaps reveal patterns and correlations in multidimensional genomic data. *Bioinformatics*, 32(18), 2847–2849. <https://doi.org/10.1093/BIOINFORMATICS/BTW313>
- Gu, Z., Gu, L., Eils, R., Schlesner, M., & Brors, B. (2014). circlize implements and enhances circular visualization in R. *Bioinformatics*, 30(19), 2811–2812. <https://doi.org/10.1093/BIOINFORMATICS/BTU393>
- Guardiola, F. A., Cuesta, A., Arizcun, M., Meseguer, J., & Esteban, M. A. (2014). Comparative skin mucus and serum humoral defence mechanisms in the teleost gilthead seabream

- (*Sparus aurata*). *Fish and Shellfish Immunology*, 36(2), 545–551. <https://doi.org/10.1016/j.fsi.2014.01.001>
- Guardiola, F. A., Cuesta, A., & Esteban, M. Á. (2016). Using skin mucus to evaluate stress in gilthead seabream (*Sparus aurata* L.). *Fish & Shellfish Immunology*, 59, 323–330. <https://doi.org/10.1016/J.FSI.2016.11.005>
- Guillén, M. D., Carton, I., Goicoechea, E., & Uriarte, P. S. (2008). Characterization of cod liver oil by spectroscopic techniques. New approaches for the determination of compositional parameters, acyl groups, and cholesterol from 1H nuclear magnetic resonance and fourier transform infrared spectral data. *Journal of Agricultural and Food Chemistry*, 56(19), 9072–9079. <https://doi.org/10.1021/jf801834j>
- Guo, C., Huang, X. yan, Yang, M. jun, Wang, S., Ren, S. tong, Li, H., & Peng, X. xian. (2014). GC/MS-based metabolomics approach to identify biomarkers differentiating survivals from death in crucian carps infected by *Edwardsiella tarda*. *Fish and Shellfish Immunology*, 39(2), 215–222. <https://doi.org/10.1016/j.fsi.2014.04.017>
- Guo, H., & Dixon, B. (2021). Understanding acute stress-mediated immunity in teleost fish. *Fish and Shellfish Immunology Reports*, 2, 100010. <https://doi.org/10.1016/J.FSIREP.2021.100010>
- Gutierrez Rabadan, C., Spreadbury, C., Consuegra, S., & Garcia de Leaniz, C. (2021). Development, validation and testing of an Operational Welfare Score Index for farmed lumpfish *Cyclopterus lumpus* L. *Aquaculture*, 531(April 2020), 735777. <https://doi.org/10.1016/j.aquaculture.2020.735777>
- Guyon, I., Weston, J., Barnhill, S., & Vapnik, V. (2002). Gene Selection for Cancer Classification using Support Vector Machines. *Machine Learning*, 46, 389–422. <https://doi.org/10.1023/A:1012487302797>
- Haab, B. B., Paulovich, A. G., Anderson, N. L., Clark, A. M., Downing, G. J., Hermjakob, H., Labaer, J., & Uhlen, M. (2006). A reagent resource to identify proteins and peptides of interest for the cancer community: a workshop report. *Molecular & Cellular Proteomics : MCP*, 5(10), 1996–2007. <https://doi.org/10.1074/mcp.T600020-MCP200>
- Haider, S., & Pal, R. (2013). Integrated Analysis of Transcriptomic and Proteomic Data. *Current Genomics*, 14(2), 91–110. <http://www.ingentaconnect.com/content/ben/cg/2013/00000014/00000002/art00003>
- Han, J. M., Jeong, S. J., Park, M. C., Kim, G., Kwon, N. H., Kim, H. K., Ha, S. H., Ryu, S. H., & Kim, S. (2012). Leucyl-tRNA Synthetase Is an Intracellular Leucine Sensor for the mTORC1-Signaling Pathway. *Cell*, 149(2), 410–424. <https://doi.org/10.1016/J.CELL.2012.02.044>
- Han, S. L., Wang, J., Li, L. Y., Lu, D. L., Chen, L. Q., Zhang, M. L., & Du, Z. Y. (2020). The regulation of rapamycin on nutrient metabolism in Nile tilapia fed with high-energy diet. *Aquaculture*, 520, 734975. <https://doi.org/10.1016/J.AQUACULTURE.2020.734975>
- Harrell, F. (2019). Hmisc: Harrell Miscellaneous. *R Package Version 4.2-0*.
- Haug, K., Cochrane, K., Nainala, V. C., Williams, M., Chang, J., Jayaseelan, K. V., & O'Donovan, C. (2020). MetaboLights: a resource evolving in response to the needs of its scientific community. *Nucleic Acids Research*, 48(D1), D440–D444. <https://doi.org/10.1093/NAR/GKZ1019>
- He, Y., Yu, H., Zhang, Z., Zhang, J., Kang, S., & Zhang, X. (2022). Effects of chronic hypoxia on growth performance, antioxidant capacity and protein turnover of largemouth bass (*Micropterus salmoides*). *Aquaculture*, 561(January). <https://doi.org/10.1016/j.aquaculture.2022.738673>
- Heberle, A. M., Prentzell, M. T., van Eunen, K., Bakker, B. M., Grellscheid, S. N., & Thedieck, K. (2015). Molecular mechanisms of mTOR regulation by stress. *Molecular & Cellular Oncology*, 2(2). <https://doi.org/10.4161/23723548.2014.970489>
- Herkenhoff, M. E., Oliveira, A. C., Nachtigall, P. G., Costa, J. M., Campos, V. F., Hilsdorf, A. W. S., & Pinhal, D. (2018). Fishing into the MicroRNA transcriptome. *Frontiers in Genetics*, 9(MAR), 1–15. <https://doi.org/10.3389/fgene.2018.00088>
- Hernández-Pérez, J., Naderi, F., Chivite, M., Soengas, J. L., Míguez, J. M., & López-Patiño, M. A. (2019). Influence of stress on liver circadian physiology. A Study in Rainbow Trout,

- Oncorhynchus mykiss, as Fish Model. *Frontiers in Physiology*, 10(MAY), 611. <https://doi.org/10.3389/fphys.2019.00611>
- Hintze, K. J., & McClung, J. P. (2011). Hcpidin: A critical regulator of iron metabolism during hypoxia. *Advances in Hematology*, 2011. <https://doi.org/10.1155/2011/510304>
- Ho, A.-S., Cheng, C.-C., Lee, S.-C., Liu, M.-L., Lee, J.-Y., Wang, W.-M., & Wang, C.-C. (2010). Novel biomarkers predict liver fibrosis in hepatitis C patients: alpha 2 macroglobulin, vitamin D binding protein and apolipoprotein AI. *Journal of Biomedical Science* 2010 17:1, 17(1), 1–7. <https://doi.org/10.1186/1423-0127-17-58>
- Hoegg, S., Brinkmann, H., Taylor, J. S., & Meyer, A. (2004). Phylogenetic Timing of the Fish-Specific Genome Duplication Correlates with the Diversification of Teleost Fish. *J Mol Evol*, 59, 190–203. <https://doi.org/10.1007/s00239-004-2613-z>
- Hook, S. E., Mondon, J., Revill, A. T., Greenfield, P. A., Smith, R. A., Turner, R. D. R., Corbett, P. A., & Warne, M. S. J. (2018). Transcriptomic, lipid, and histological profiles suggest changes in health in fish from a pesticide hot spot. *Marine Environmental Research*, 140(April), 299–321. <https://doi.org/10.1016/j.marenvres.2018.06.020>
- Horgan, R. P., & Kenny, L. C. (2011). ‘Omic’ technologies: genomics, transcriptomics, proteomics and metabolomics. *The Obstetrician & Gynaecologist*, 13(3), 189–195. <https://doi.org/10.1576/toag.13.3.189.27672>
- Hough, C. (2022). Regional review on status and trends in aquaculture development in Europe - 2020. In *Fisheries and Aquaculture Circular No. 1232/1*. FAO. https://books.google.co.uk/books?hl=en&lr=&id=V8JfEAAAQBAJ&oi=fnd&pg=PR3&dq=ras+system+aquaculture+trends&ots=KTC3rsQq9b&sig=839A8J8KYEb8meugMNJHEK hJLwM&redir_esc=y#v=onepage&q=ras system aquaculture trends&f=false
- Houslay, T. M., Earley, R. L., Young, A. J., & Wilson, A. J. (2019). Habituation and individual variation in the endocrine stress response in the Trinidadian guppy (*Poecilia reticulata*). *General and Comparative Endocrinology*, 270, 113–122. <https://doi.org/10.1016/J.YGCEN.2018.10.013>
- Howe, K., Clark, M. D., Torroja, C. F., Torrance, J., Berthelot, C., Muffato, M., Collins, J. E., Humphray, S., McLaren, K., Matthews, L., McLaren, S., Sealy, I., Caccamo, M., Churcher, C., Scott, C., Barrett, J. C., Koch, R., Rauch, G.-J., White, S., ... Stemple, D. L. (2013). The zebrafish reference genome sequence and its relationship to the human genome. *Nature*, 496(7446), 498–503. <https://doi.org/10.1038/nature12111>
- Hu, G., Gu, W., Sun, P., Bai, Q., & Wang, B. (2016). Transcriptome analyses reveal lipid metabolic process in liver related to the difference of carcass fat content in rainbow trout (*Oncorhynchus mykiss*). *International Journal of Genomics*, 2016. <https://doi.org/10.1155/2016/7281585>
- Huang, C.-X., Chen, N., Wu, X.-J., Huang, C.-H., He, Y., Tang, R., Wang, W.-M., & Wang, H.-L. (2015). The zebrafish miR-462/miR-731 cluster is induced under hypoxic stress via hypoxia-inducible factor 1 α and functions in cellular adaptations. *The FASEB Journal*, 29(12), 4901–4913. <https://doi.org/https://doi.org/10.1096/fj.14-267104>
- Huang, J., Li, Y., Liu, Z., Kang, Y., & Wang, J. (2018). Transcriptomic responses to heat stress in rainbow trout *Oncorhynchus mykiss* head kidney. *Fish and Shellfish Immunology*, 82(August), 32–40. <https://doi.org/10.1016/j.fsi.2018.08.002>
- Huang, J. S., Guo, Z. X., Zhang, J. D., Wang, W. Z., Wang, Z. L., Xie, R. T., Amenyogbe, E., & Chen, G. (2022). Transcriptomic analysis of juvenile cobia in response to hypoxic stress. *Aquaculture International*, 0123456789. <https://doi.org/10.1007/s10499-022-01007-1>
- Huang, T., Wang, J., Yu, W., & He, Z. (2012). Protein inference: A review. *Briefings in Bioinformatics*, 13(5), 586–614. <https://doi.org/10.1093/bib/bbs004>
- Hubbi, M. E., Kshitiz, Gilkes, D. M., Rey, S., Wong, C. C., Luo, W., Kim, D. H., Dang, C. v., Levchenko, A., & Semenza, G. L. (2013). A nontranscriptional role for HIF-1 α as a direct inhibitor of DNA replication. *Science Signaling*, 6(262). <https://doi.org/10.1126/scisignal.2003417>

- Hughes, C. S., Moggridge, S., Müller, T., Sorensen, P. H., Morin, G. B., & Krijgsveld, J. (2018). Single-pot, solid-phase-enhanced sample preparation for proteomics experiments. *Nature Protocols* 2018 14:1, 14(1), 68–85. <https://doi.org/10.1038/s41596-018-0082-x>
- Huntingford, F. (2008). Animal Welfare in Aquaculture. In K. Culver & D. Castle (Eds.), *Aquaculture, Innovation and Social Transformation* (pp. 21–33). Springer Netherlands. https://doi.org/10.1007/978-1-4020-8835-3_2 LB - Huntingford2008
- Huntingford, F. A., Adams, C., Braithwaite, V. A., Kadri, S., Pottinger, T. G., Sandøe, P., & Turnbull, J. F. (2006). Current issues in fish welfare. *Journal of Fish Biology*, 68(2), 332–372. <https://doi.org/10.1111/j.0022-1112.2006.001046.x>
- Huntingford, F. A., Adams, C., Braithwaite, V. A., Kadri, S., Pottinger, T. G., Sandoe, P., & Turnbull, J. F. (2006). Current issues in fish welfare. *Journal of Fish Biology*, 68(2), 332–372. <https://doi.org/10.1111/j.0022-1112.2006.001046.x>
- Iadevaia, V., Liu, R., & Proud, C. G. (2014). mTORC1 signaling controls multiple steps in ribosome biogenesis. *Seminars in Cell and Developmental Biology*, 36, 113–120. <https://doi.org/10.1016/j.semcd.2014.08.004>
- Ibarz, A., Martín-Pérez, M., Blasco, J., Bellido, D., De Oliveira, E., & Fernández-Borràs, J. (2010). Gilthead sea bream liver proteome altered at low temperatures by oxidative stress. *Proteomics*, 10(5), 963–975. <https://doi.org/10.1002/pmic.200900528>
- Ibarz, A., Ordóñez-Grande, B., Sanahuja, I., Sánchez-Nunõ, S., Fernández-Borràs, J., Blasco, J., & Fernández-Alacid, L. (2019). Using stable isotope analysis to study skin mucus exudation and renewal in fish. *Journal of Experimental Biology*, 222(8). <https://doi.org/10.1242/jeb.195925>
- Ikonen, E. (2008). Cellular cholesterol trafficking and compartmentalization. *Nature Reviews Molecular Cell Biology*, 9, 125–138.
- INE, & DGRM. (2021). *Estatísticas da Pesca - 2021*.
- Intlekofer, A. M., DeMatteo, R. G., Venneti, S., Finley, L. W. S., Lu, C., Judkins, A. R., Rustenburg, A. S., Grinaway, P. B., Chodera, J. D., Cross, J. R., & Thompson, C. B. (2015). Hypoxia Induces Production of L-2-Hydroxyglutarate. *Cell Metabolism*, 22(2), 304–311. <https://doi.org/10.1016/j.cmet.2015.06.023>
- Iversen, M., Finstad, B., McKinley, R. S., Eliassen, R. A., Carlsen, K. T., & Evjen, T. (2005). Stress responses in Atlantic salmon (*Salmo salar* L.) smolts during commercial well boat transports, and effects on survival after transfer to sea. *Aquaculture*, 243(1–4), 373–382. <https://doi.org/10.1016/J.AQUACULTURE.2004.10.019>
- Iwama, G. K. (2007). The welfare of fish. *Diseases of Aquatic Organisms*, 75(2), 155–158. <https://doi.org/10.3354/dao075155>
- Iwama, G. K., Afonso, L. O. B., Todgham, A., Ackerman, P., & Nakano, K. (2004). Are hsp90 suitable for indicating stressed states in fish? *Journal of Experimental Biology*, 207(1), 15–19. <https://doi.org/10.1242/jeb.00707>
- Iwama, G. K., Afonso, L. O. B., & Vijayan, M. M. (2004). *Stress in fish*.
- Iwama, G. K., Afonso, L. O. B., & Vijayan, M. M. (2006). Stress in fish. In D. H. Evans & J. B. Claiborne (Eds.), *Physiology of fishes* (3rd ed., pp. 320–342). CRC, Taylor & Francis. <http://dro.deakin.edu.au/view/DU:30060723>
- Jennings, S., Stentiford, G. D., Leocadio, A. M., Jeffery, K. R., Metcalfe, J. D., Katsiadaki, I., Auchterlonie, N. A., Mangi, S. C., Pinnegar, J. K., Ellis, T., Peeler, E. J., Luisetti, T., Baker-Austin, C., Brown, M., Catchpole, T. L., Clyne, F. J., Dye, S. R., Edmonds, N. J., Hyder, K., ... Verner-Jeffreys, D. W. (2016). Aquatic food security: insights into challenges and solutions from an analysis of interactions between fisheries, aquaculture, food safety, human health, fish and human welfare, economy and environment. *Fish and Fisheries*, 17(4), 893–938. <https://doi.org/10.1111/FAF.12152>
- Ji, C., & Kaplowitz, N. (2006). ER stress: Can the liver cope? *Journal of Hepatology*, 45, 321–333. <https://doi.org/10.1016/j.jhep.2006.06.004>
- Ji, C., Wu, H., Wei, L., Zhao, J., Wang, Q., & Lu, H. (2013). Responses of *Mytilus galloprovincialis* to bacterial challenges by metabolomics and proteomics. *Fish & Shellfish Immunology*, 35(2), 489–498. <https://doi.org/10.1016/j.fsi.2013.05.009>

- Jia, E., Jiang, W., Liu, W., Jiang, G., Li, X., Chi, C., & Zhang, D. (2022). Crowding stress-related protein markers: New candidates for assessing welfare of largemouth bass reared in an in-pond raceway system. *Aquaculture*, 550(December 2021), 737821. <https://doi.org/10.1016/j.aquaculture.2021.737821>
- Jia, R., Du, J., Cao, L., Feng, W., He, Q., Xu, P., & Yin, G. (2020). Chronic exposure of hydrogen peroxide alters redox state, apoptosis and endoplasmic reticulum stress in common carp (*Cyprinus carpio*). *Aquatic Toxicology*, 229, 105657. <https://doi.org/10.1016/J.AQUATOX.2020.105657>
- Jia, R., Liu, B. L., Feng, W. R., Han, C., Huang, B., & Lei, J. L. (2016). Stress and immune responses in skin of turbot (*Scophthalmus maximus*) under different stocking densities. *Fish & Shellfish Immunology*, 55, 131–139. <https://doi.org/10.1016/J.FSI.2016.05.032>
- Jiang, B. H., Rue, E., Wang, G. L., Roe, R., & Semenza, G. L. (1996). Dimerization, DNA binding, and transactivation properties of hypoxia-inducible factor 1. *Journal of Biological Chemistry*, 271(30), 17771–17778. <https://doi.org/10.1074/jbc.271.30.17771>
- Jiang, H., Li, F., Xie, Y., Huang, B., Zhang, J. J., Zhang, J. J., Zhang, C., Li, S., & Xiang, J. (2009). Comparative proteomic profiles of the hepatopancreas in *Fenneropenaeus chinensis* response to hypoxic stress. *Proteomics*, 9(12), 3353–3367. <https://doi.org/10.1002/pmic.200800518>
- Jiang, X., Bai, X. Y., Li, B., Li, Y., Xia, K., Wang, M., Li, S., & Wu, H. (2019). Plasma Inter-Alpha-Trypsin Inhibitor Heavy Chains H3 and H4 Serve as Novel Diagnostic Biomarkers in Human Colorectal Cancer. *Disease Markers*, 2019, 5069614. <https://doi.org/10.1155/2019/5069614>
- Jiao, S., Nie, M., Song, H., Xu, D., & You, F. (2020). Physiological responses to cold and starvation stresses in the liver of yellow drum (*Nibea albiflora*) revealed by LC-MS metabolomics. *Science of The Total Environment*, 715, 136940. <https://doi.org/10.1016/J.SCITOTENV.2020.136940>
- Jibb, L. A., & Richards, J. G. (2008). AMP-activated protein kinase activity during metabolic rate depression in the hypoxic goldfish, *Carassius auratus*. *Journal of Experimental Biology*, 211(19), 3111–3122. <https://doi.org/10.1242/JEB.019117>
- Johnson, S. S., Zhang, C., Fromm, J., Willis, I. M., & Johnson, D. L. (2007). Mammalian Maf1 Is a Negative Regulator of Transcription by All Three Nuclear RNA Polymerases. *Molecular Cell*, 26(3), 367–379. <https://doi.org/10.1016/j.molcel.2007.03.021>
- Johnston, I. A., Bower, N. I., & Macqueen, D. J. (2011). Growth and the regulation of myotomal muscle mass in teleost fish. *Journal of Experimental Biology*, 214(10), 1617–1628. <https://doi.org/10.1242/jeb.038620>
- Jolliffe, I. T. (1986). *Principal components analysis* (Springer S). Springer-Verlag.
- Jung, K. (2016). *Statistical Analysis in Proteomics* (K. Jung, Ed.). Humana Press. <https://doi.org/10.1007/978-1-4939-3106-4>
- Kajimura, S., Aida, K., & Duan, C. (2005). Insulin-like growth factor-binding protein-1 (IGFBP-1) mediates hypoxia-induced embryonic growth and developmental retardation. *Proceedings of the National Academy of Sciences of the United States of America*, 102(4), 1240–1245. <https://doi.org/10.1073/pnas.0407443102>
- Kajimura, S., Aida, K., & Duan, C. (2006). Understanding Hypoxia-Induced Gene Expression in Early Development: In Vitro and In Vivo Analysis of Hypoxia-Inducible Factor 1-Regulated Zebra Fish Insulin-Like Growth Factor Binding Protein 1 Gene Expression. *Molecular and Cellular Biology*, 26(3), 1142–1155. <https://doi.org/10.1128/mcb.26.3.1142-1155.2006>
- Kales, S. C., Bols, N. C., & Dixon, B. (2007). Calreticulin in rainbow trout: A limited response to Endoplasmic Reticulum (ER) stress. *Comparative Biochemistry and Physiology - B Biochemistry and Molecular Biology*, 147(4), 607–615. <https://doi.org/10.1016/j.cbpb.2007.04.002>
- Kang, J., Brajanovski, N., Chan, K. T., Xuan, J., Pearson, R. B., & Sanij, E. (2021). Ribosomal proteins and human diseases: molecular mechanisms and targeted therapy. *Signal Transduction and Targeted Therapy*, 6(1). <https://doi.org/10.1038/s41392-021-00728-8>

- Karakach, T. K., Huenupi, E. C., Soo, E. C., Walter, J. A., & Afonso, L. O. B. (2009). ¹H-NMR and mass spectrometric characterization of the metabolic response of juvenile Atlantic salmon (*Salmo salar*) to long-term handling stress. *Metabolomics*, *5*(1), 123–137. <https://doi.org/10.1007/s11306-008-0144-0>
- Karlsen, O. A., Bjørneklett, S., Berg, K., Brattås, M., Bohne-Kjersem, A., Grøsvik, B. E., & Goksøyr, A. (2011). Integrative Environmental Genomics of Cod (*Gadus morhua*): The Proteomics Approach. *Journal of Toxicology and Environmental Health, Part A*, *74*(7–9), 494–507. <https://doi.org/10.1080/15287394.2011.550559>
- Karve, T. M., & Cheema, A. K. (2011). Small Changes Huge Impact: The Role of Protein Posttranslational Modifications in Cellular Homeostasis and Disease. *Journal of Amino Acids*, *2011*, 13. <https://doi.org/10.4061/2011/207691>
- Kassambara, A., & Mundt, F. (2020). factoextra: Extract and Visualize the Results of Multivariate Data Analyses. *R Package Version 1.0.7*. <https://cran.r-project.org/package=factoextra>
- Keeble, B. R. (1988). The Brundtland Report: “Our Common Future.” *Medicine and War*, *4*(1), 17–25. <https://doi.org/10.1080/07488008808408783>
- Keeling, L., Tunón, H., Olmos Antillón, G., Berg, C., Jones, M., Stuardo, L., Swanson, J., Wallenbeck, A., Winckler, C., & Blokhuis, H. (2019). Animal Welfare and the United Nations Sustainable Development Goals. *Frontiers in Veterinary Science*, *6*, 336. <https://doi.org/10.3389/FVETS.2019.00336>
- Keisham, S. S., Mahesh, S. M., & Supriya, T. (2014). Chapter 6 - Vibrational Spectroscopy for Structural Characterization of Bioactive Compounds. In T. Rocha-Santos & A. C. Duarte (Eds.), *Analysis of Marine Samples in Search of Bioactive Compounds* (pp. 115–148). Elsevier.
- Keller, A., Nesvizhskii, A. I., Kolker, E., & Aebersold, R. (2002). Empirical Statistical Model To Estimate the Accuracy of Peptide Identifications Made by MS/MS and Database Search. *Analytical Chemistry*, *74*(20), 5383–5392. <https://doi.org/10.1021/AC025747H>
- Khansari, A. R., Balasch, J. C., Vallejos-Vidal, E., Parra, D., Reyes-López, F. E., & Tort, L. (2018). Comparative immune- and stress-related transcript response induced by air exposure and *Vibrio anguillarum* bacterin in rainbow trout (*Oncorhynchus mykiss*) and gilthead seabream (*Sparus aurata*) mucosal surfaces. *Frontiers in Immunology*, *9*(MAY), 1–12. <https://doi.org/10.3389/fimmu.2018.00856>
- Kierans, S. J., & Taylor, C. T. (2021). Regulation of glycolysis by the hypoxia-inducible factor (HIF): implications for cellular physiology. *The Journal of Physiology*, *599*(1), 23–37. <https://doi.org/10.1113/JP280572>
- Kim, J. W., Tchernyshyov, I., Semenza, G. L., & Dang, C. v. (2006). HIF-1-mediated expression of pyruvate dehydrogenase kinase: A metabolic switch required for cellular adaptation to hypoxia. *Cell Metabolism*, *3*(3), 177–185. <https://doi.org/10.1016/j.cmet.2006.02.002>
- Kinoshita, S., Itoi, S., & Watabe, S. (2001). cDNA cloning and characterization of the warm-temperature-acclimation-associated protein Wap65 from carp, *Cyprinus carpio*. *Fish Physiology and Biochemistry*, *24*(2), 125–134. <https://doi.org/10.1023/A:1011939321298>
- Koakoski, G., Oliveira, T. A., da Rosa, J. G. S., Fagundes, M., Kreutz, L. C., & Barcellos, L. J. G. (2012). Divergent time course of cortisol response to stress in fish of different ages. *Physiology and Behavior*, *106*(2), 129–132. <https://doi.org/10.1016/j.physbeh.2012.01.013>
- Kocaturk, N. M., & Gozuacik, D. (2018). Crosstalk between mammalian autophagy and the ubiquitin-proteasome system. *Frontiers in Cell and Developmental Biology*, *6*(OCT), 128. <https://doi.org/10.3389/FCCELL.2018.00128/BIBTEX>
- Köhler, A., Wahl, E., & Söffker, K. (2002). Functional and morphological changes of lysosomes as prognostic biomarkers of toxic liver injury in a marine flatfish (*Platichthys flesus* (L.)). *Environmental Toxicology and Chemistry*, *21*(11), 2434–2444. <https://doi.org/10.1002/ETC.5620211124>
- Koolhaas, J. M., Bartolomucci, A., Buwalda, B., de Boer, S. F., Flügge, G., Korte, S. M., Meerlo, P., Murison, R., Olivier, B., Palanza, P., Richter-Levin, G., Sgoifo, A., Steimer, T., Stiedl,

- O., van Dijk, G., Wöhr, M., & Fuchs, E. (2011). Stress revisited: A critical evaluation of the stress concept. *Neuroscience & Biobehavioral Reviews*, 35(5), 1291–1301. <https://doi.org/10.1016/j.neubiorev.2011.02.003>
- Korte, S. M., Olivier, B., & Koolhaas, J. M. (2007). A new animal welfare concept based on allostasis. *Physiology & Behavior*, 92(3), 422–428. <https://doi.org/10.1016/J.PHYSBEH.2006.10.018>
- Kozera, B., & Rapacz, M. (2013). Reference genes in real-time PCR. *Journal of Applied Genetics*, 54(4), 391–406. <https://doi.org/10.1007/s13353-013-0173-x>
- Kranendijk, M., Struys, E. A., Salomons, G. S., Van Der Knaap, M. S., & Jakobs, C. (2012). Progress in understanding 2-hydroxyglutaric acidurias. *Journal of Inherited Metabolic Disease*, 35(4), 571–587. <https://doi.org/10.1007/s10545-012-9462-5>
- Krasnov, A., Koskinen, H., Pehkonen, P., Rexroad, C. E., Afanasyev, S., & Mölsä, H. (2005). Gene expression in the brain and kidney of rainbow trout in response to handling stress. *BMC Genomics*, 6, 3. <https://doi.org/10.1186/1471-2164-6-3>
- Krasny, L., & Huang, P. H. (2021). Data-independent acquisition mass spectrometry (DIA-MS) for proteomic applications in oncology. *Molecular Omics*, 17(1), 29–42. <https://doi.org/10.1039/d0mo00072h>
- Krassowski, M., Das, V., Sahu, S. K., & Misra, B. B. (2020). State of the Field in Multi-Omics Research: From Computational Needs to Data Mining and Sharing. *Frontiers in Genetics*, 11(December), 1–17. <https://doi.org/10.3389/fgene.2020.610798>
- Kuang, G., Tao, W., Zheng, S., Wang, X., & Wang, D. (2020). Genome-Wide Identification, Evolution and Expression of the Complete Set of Cytoplasmic Ribosomal Protein Genes in Nile Tilapia. *International Journal of Molecular Sciences*, 21, 1230.
- Kuhn, M. (2020). caret: Classification and Regression Training. *R Package Version 6.0-86*.
- Kuhn, M., von Mering, C., Campillos, M., Jensen, L. J., & Bork, P. (2008). STITCH: interaction networks of chemicals and proteins. *Nucleic Acids Research*, 36(Database issue), D684. <https://doi.org/10.1093/NAR/GKM795>
- Kuhn, M., & Wickham, H. (2022). recipes: Preprocessing and Feature Engineering Steps for Modeling. *R Package Version 1.0.3*.
- Kulczykowska, E. (2019). Stress response system in the fish skin—welfare measures revisited. *Frontiers in Physiology*, 10, 72. <https://doi.org/10.3389/fphys.2019.00072>
- Kumar, V. B., Jiang, I.-F., Yang, H.-H., & Weng, C.-F. (2009). Effects of serum on phagocytic activity and proteomic analysis of tilapia (*Oreochromis mossambicus*) serum after acute osmotic stress. *Fish & Shellfish Immunology*, 26(5), 760–767. <https://doi.org/10.1016/j.fsi.2009.03.005>
- Kumareswaran, R., Ludkovski, O., Meng, A., Sykes, J., Pintilie, M., & Bristow, R. G. (2012). Chronic hypoxia compromises repair of DNA double-strand breaks to drive genetic instability. *Journal of Cell Science*, 125(1), 189–199. <https://doi.org/10.1242/jcs.092262>
- Lai, X. xing, Zhang, C. ping, Wu, Y. xin, Yang, Y., Zhang, M. qing, Qin, W. jian, Wang, R. xuan, & Shu, H. (2022). Comparative transcriptome analysis reveals physiological responses in liver tissues of *Epinephelus coioides* under acute hypoxia stress. *Comparative Biochemistry and Physiology - Part D: Genomics and Proteomics*, 43(May), 101005. <https://doi.org/10.1016/j.cbd.2022.101005>
- Lakpa, K. L., Khan, N., Afghah, Z., Chen, X., & Geiger, J. D. (2021). Lysosomal stress response (LSR): Physiological importance and pathological relevance. *Journal of Neuroimmune Pharmacology: The Official Journal of the Society on NeuroImmune Pharmacology*, 16(2), 219. <https://doi.org/10.1007/S11481-021-09990-7>
- Lane, D. J. R., Saletta, F., Rahmanto, Y. S., Kovacevic, Z., & Richardson, D. R. (2013). N-myc Downstream Regulated 1 (NDRG1) Is Regulated by Eukaryotic Initiation Factor 3a (eIF3a) during Cellular Stress Caused by Iron Depletion. *PLoS ONE*, 8(2), 1–15. <https://doi.org/10.1371/journal.pone.0057273>
- Laplante, M., & Sabatini, D. M. (2012). mTOR signaling in growth control and disease. *Cell*, 149(2), 274. <https://doi.org/10.1016/J.CELL.2012.03.017>
- Lardon, I., Eyckmans, M., Vu, T. N., Laukens, K., De Boeck, G., & Dommissie, R. (2013). 1H-NMR study of the metabolome of a moderately hypoxia-tolerant fish, the common carp

- (Cyprinus carpio). *Metabolomics*, 9(6), 1216–1227. <https://doi.org/10.1007/S11306-013-0540-Y/TABLES/3>
- Lau, K., Lai, K. P., Bao, J. Y. J., Zhang, N., Tse, A., Tong, A., Li, J. W., Lok, S., Kong, R. Y. C., Lui, W. Y., Wong, A., & Wu, R. S. S. (2014). Identification and expression profiling of MicroRNAs in the brain, liver and gonads of marine medaka (*Oryzias melastigma*) and in response to hypoxia. *PLoS ONE*, 9(10), 7–8. <https://doi.org/10.1371/journal.pone.0110698>
- Lawrence, R. E., & Zoncu, R. (2019). The lysosome as a cellular centre for signalling, metabolism and quality control. *Nature Cell Biology* 2019 21:2, 21(2), 133–142. <https://doi.org/10.1038/s41556-018-0244-7>
- Lazado, C. C., Timmerhaus, G., Breiland, M. W., Pittman, K., & Hytterød, S. (2021). Multiomics provide insights into the key molecules and pathways involved in the physiological adaptation of atlantic salmon (*Salmo salar*) to chemotherapeutic-induced oxidative stress. *Antioxidants*, 10(12). <https://doi.org/10.3390/antiox10121931>
- Lazarus, R. S. (1999). Stress and emotion: A new synthesis. In *Stress and emotion: A new synthesis*. Springer Publishing Co.
- Leek, J. T., Johnson, W. E., Parker, H. S., Jaffe, A. E., & Storey, J. D. (2012). The SVA package for removing batch effects and other unwanted variation in high-throughput experiments. *Bioinformatics*, 28(6), 882–883. <https://doi.org/10.1093/bioinformatics/bts034>
- Lescat, L., Herpin, A., Mourot, B., Véron, V., Guiguen, Y., Bobe, J., & Seilliez, I. (2018). CMA restricted to mammals and birds: myth or reality? *Autophagy*, 14(7), 1267–1270. <https://doi.org/10.1080/15548627.2018.1460021>
- Lescat, L., Véron, V., Mourot, B., Péron, S., Chenais, N., Dias, K., Riera-Heredia, N., Beaumatin, F., Pinel, K., Priault, M., Panserat, S., Salin, B., Guiguen, Y., Bobe, J., Herpin, A., & Seilliez, I. (2020). Chaperone-Mediated Autophagy in the Light of Evolution: Insight from Fish. *Molecular Biology and Evolution*, 37(10), 2887–2899. <https://doi.org/10.1093/MOLBEV/MSAA127>
- Leveelahti, L., Leskinen, P., Leder, E. H., Waser, W., & Nikinmaa, M. (2011). Responses of threespine stickleback (*Gasterosteus aculeatus*, L) transcriptome to hypoxia. *Comparative Biochemistry and Physiology - Part D: Genomics and Proteomics*, 6(4), 370–381. <https://doi.org/10.1016/j.cbd.2011.08.001>
- Li, C., Gao, C., Fu, Q., Su, B., & Chen, J. (2017). Identification and expression analysis of fetuin B (FETUB) in turbot (*Scophthalmus maximus* L.) mucosal barriers following bacterial challenge. *Fish & Shellfish Immunology*, 68, 386–394. <https://doi.org/10.1016/J.FSI.2017.07.032>
- Li, H., Handsaker, B., Wysoker, A., Fennell, T., Ruan, J., Homer, N., Marth, G., Abecasis, G., Durbin, R., Project, G., & Subgroup, D. P. (2009). The Sequence Alignment/Map format and SAMtools. *BIOINFORMATICS APPLICATIONS NOTE*, 25(16), 2078–2079. <https://doi.org/10.1093/bioinformatics/btp352>
- Li, J. N., Zhao, Y. T., Cao, S. L., Wang, H., & Zhang, J. J. (2020). Integrated transcriptomic and proteomic analyses of grass carp intestines after vaccination with a double-targeted DNA vaccine of *Vibrio mimicus*. *Fish & Shellfish Immunology*, 98, 641–652. <https://doi.org/10.1016/J.FSI.2019.10.045>
- Li, J., Zhang, G., Yin, D., Li, Y., Zhang, Y., Cheng, J., Zhang, K., Ji, J., Wang, T., Jia, Y., & Yin, S. (2022). Integrated Application of Multiomics Strategies Provides Insights Into the Environmental Hypoxia Response in *Pelteobagrus vachelli* Muscle. *Molecular and Cellular Proteomics*, 21(3), 100196. <https://doi.org/10.1016/j.mcpro.2022.100196>
- Li, M., Wang, X., Qi, C., Li, E., Du, Z., Qin, J. G., & Chen, L. (2018). Metabolic response of Nile tilapia (*Oreochromis niloticus*) to acute and chronic hypoxia stress. *Aquaculture*, 495(January), 187–195. <https://doi.org/10.1016/j.aquaculture.2018.05.031>
- Li, R., Zhang, P., Wang, Y., & Tao, K. (2020). Itaconate: A Metabolite Regulates Inflammation Response and Oxidative Stress. In *Oxidative Medicine and Cellular Longevity* (Vol. 2020). Hindawi Limited. <https://doi.org/10.1155/2020/5404780>
- Li, Y., Wang, Y., Kim, E., Beemiller, P., Wang, C. Y., Swanson, J., You, M., & Guan, K. L. (2007). Bnip3 mediates the hypoxia-induced inhibition on mammalian target of rapamycin

- by interacting with Rheb. *Journal of Biological Chemistry*, 282(49), 35803–35813. <https://doi.org/10.1074/jbc.M705231200>
- Lieke, T., Meinelt, T., Hoseinifar, S. H., Pan, B., Straus, D. L., & Steinberg, C. E. W. (2020). Sustainable aquaculture requires environmental-friendly treatment strategies for fish diseases. *Reviews in Aquaculture*, 12(2), 943–965. <https://doi.org/10.1111/RAQ.12365>
- Liu, B., & Qian, S.-B. (2014). Translational reprogramming in stress response. *Wiley Interdisciplinary Reviews. RNA*, 5(3), 301. <https://doi.org/10.1002/WRNA.1212>
- Liu, L., Li, C., Su, B., Beck, B. H., & Peatman, E. (2013). Short-Term Feed Deprivation Alters Immune Status of Surface Mucosa in Channel Catfish (*Ictalurus punctatus*). *PLoS ONE*, 8(9), 1–10. <https://doi.org/10.1371/journal.pone.0074581>
- Liu, L., Li, Y., Li, S., Hu, N., He, Y., Pong, R., Lin, D., Lu, L., & Law, M. (2012). Comparison of next-generation sequencing systems. *Journal of Biomedicine and Biotechnology*, 2012. <https://doi.org/10.1155/2012/251364>
- Liu, S., Gao, G., Palti, Y., Cleveland, B. M., Weber, G. M., & Rexroad, C. E. (2014). RNA-seq Analysis of Early Hepatic Response to Handling and Confinement Stress in Rainbow Trout. *PLOS ONE*, 9(2), e88492. <https://doi.org/10.1371/journal.pone.0088492>
- Liu, S., Wang, X., Sun, F., Zhang, J., Feng, J., Liu, H., Rajendran, K. V., Sun, L., Zhang, Y., Jiang, Y., Peatman, E., Kaltenboeck, L., Kucuktas, H., & Liu, Z. (2013). RNA-Seq reveals expression signatures of genes involved in oxygen transport, protein synthesis, folding, and degradation in response to heat stress in catfish. *Physiological Genomics*, 45(12), 462–476. <https://doi.org/10.1152/physiolgenomics.00026.2013>
- Liu, Y., Yao, M., Li, S., Wei, X., Ding, L., Han, S., Wang, P., Lv, B., Chen, Z., & Sun, Y. (2022). Integrated application of multi-omics approach and biochemical assays provides insights into physiological responses to saline-alkaline stress in the gills of crucian carp (*Carassius auratus*). *Science of the Total Environment*, 822, 153622. <https://doi.org/10.1016/j.scitotenv.2022.153622>
- Logan, C. A., & Somero, G. N. (2010). Transcriptional responses to thermal acclimation in the eurythermal fish *Gillichthys mirabilis* (Cooper 1864). *American Journal of Physiology - Regulatory Integrative and Comparative Physiology*, 299(3), 843–852. <https://doi.org/10.1152/ajpregu.00306.2010>
- Long, M., Zhao, J., Li, T., Tafalla, C., Zhang, Q., Wang, X., Gong, X., Shen, Z., & Li, A. (2015). Transcriptomic and proteomic analyses of splenic immune mechanisms of rainbow trout (*Oncorhynchus mykiss*) infected by *Aeromonas salmonicida* subsp. *salmonicida*. *Journal of Proteomics*, 122, 41–54. <https://doi.org/10.1016/J.JPROT.2015.03.031>
- López-Hernández, T., Haucke, V., & Maritzen, T. (2020). Endocytosis in the adaptation to cellular stress. *Cell Stress*, 4(10), 230. <https://doi.org/10.15698/CST2020.10.232>
- López-Patiño, M. A., Hernández-Pérez, J., Gesto, M., Librán-Pérez, M., Míguez, J. M., & Soengas, J. L. (2014). Short-term time course of liver metabolic response to acute handling stress in rainbow trout, *Oncorhynchus mykiss*. *Comparative Biochemistry and Physiology Part A: Molecular & Integrative Physiology*, 168, 40–49. <https://doi.org/10.1016/J.CBPA.2013.10.027>
- Love, M. I., Huber, W., & Anders, S. (2014). Moderated estimation of fold change and dispersion for RNA-seq data with DESeq2. *Genome Biology*, 15(12), 1–21. <https://doi.org/10.1186/S13059-014-0550-8/FIGURES/9>
- Lü, A., Hu, X., Wang, Y., Shen, X., Li, X., Zhu, A., Tian, J., Ming, Q., & Feng, Z. (2014). iTRAQ analysis of gill proteins from the zebrafish (*Danio rerio*) infected with *Aeromonas hydrophila*. *Fish & Shellfish Immunology*, 36(1), 229–239. <https://doi.org/10.1016/j.fsi.2013.11.007>
- Lualdi, M., & Fasano, M. (2019). Statistical analysis of proteomics data: A review on feature selection. *Journal of Proteomics*, 198(December 2018), 18–26. <https://doi.org/10.1016/j.jprot.2018.12.004>
- Lunardon, N., Menardi, G., & Torelli, N. (2022). ROSE: Random Over-Sampling Examples. *R Package Version 0.0-4*.

- Lund, V., Mejdell, C. M., Röcklinsberg, H., Anthony, R., & Håstein, T. (2007). Expanding the moral circle: farmed fish as objects of moral concern. *Diseases of Aquatic Organisms*, 75(2), 109–118. <https://doi.org/10.3354/dao075109>
- Madaro, A., Fernö, A., Kristiansen, T. S., Olsen, R. E., Gorissen, M., Flik, G., & Nilsson, J. (2016). Effect of predictability on the stress response to chasing in Atlantic salmon (*Salmo salar* L.) parr. *Physiology & Behavior*, 153, 1–6. <https://doi.org/10.1016/J.PHYSBEH.2015.10.002>
- Madaro, A., Olsen, R. E., Kristiansen, T. S., Ebbesson, L. O., Nilsen, T. O., Flik, G., & Gorissen, M. (2015). Stress in Atlantic salmon: response to unpredictable chronic stress. *J Exp Biol*, 218, 2538–2550. <https://doi.org/10.1242/jeb.120535>
- Madison, B. N., Tavakoli, S., Kramer, S., & Bernier, N. J. (2015). Chronic cortisol and the regulation of food intake and the endocrine growth axis in rainbow trout. *The Journal of Endocrinology*, 226(2), 103–119. <https://doi.org/10.1530/JOE-15-0186>
- Maere, S., Heymans, K., & Kuiper, M. (2005). BiNGO: A Cytoscape plugin to assess overrepresentation of Gene Ontology categories in Biological Networks. *Bioinformatics*, 21(16), 3448–3449. <https://doi.org/10.1093/bioinformatics/bti551>
- Magnadóttir, B., & Lange, S. (2004). Is Apolipoprotein A-I a regulating protein for the complement system of cod (*Gadus morhua* L.)? *Fish & Shellfish Immunology*, 16(2), 265–269. [https://doi.org/10.1016/S1050-4648\(03\)00061-5](https://doi.org/10.1016/S1050-4648(03)00061-5)
- Mahanty, A., Purohit, G. K., Banerjee, S., Karunakaran, D., Mohanty, S., & Mohanty, B. P. (2016). Proteomic changes in the liver of *Channa striatus* in response to high temperature stress. *Electrophoresis*, 37(12), 1704–1717. <https://doi.org/10.1002/elps.201500393>
- Mahfouz, M. E., Hegazi, M. M., El-Magd, M. A., & Kasem, E. A. (2015). Metabolic and molecular responses in Nile tilapia, *Oreochromis niloticus* during short and prolonged hypoxia. *Marine and Freshwater Behaviour and Physiology*, 48(5), 319–340. <https://doi.org/10.1080/10236244.2015.1055915>
- Malécot, M., Marie, A., Puiseux-Dao, S., & Edery, M. (2011). ITRAQ-based proteomic study of the effects of microcystin-LR on medaka fish liver. *Proteomics*, 11(10), 2071–2078. <https://doi.org/10.1002/pmic.201000512>
- Mandic, M., Best, C., & Perry, S. F. (2020). Loss of hypoxia-inducible factor 1 α affects hypoxia tolerance in larval and adult zebrafish (*Danio rerio*). *Proceedings of the Royal Society B: Biological Sciences*, 287(1927). <https://doi.org/10.1098/rspb.2020.0798>
- Mandl, J., & Bánhegyi, G. (2018). The ER – Glycogen Particle – Phagophore Triangle: A Hub Connecting Glycogenolysis and Glycophagy? *Pathology and Oncology Research*, 24(4), 821–826. <https://doi.org/10.1007/S12253-018-0446-0/FIGURES/1>
- Marcelo, A., Koppenol, R., de Almeida, L. P., Matos, C. A., & Nóbrega, C. (2021). Stress granules, RNA-binding proteins and polyglutamine diseases: too much aggregation? *Cell Death & Disease* 2021 12:6, 12(6), 1–17. <https://doi.org/10.1038/s41419-021-03873-8>
- Marchand, A., Tomkiewicz, C., Magne, L., Barouki, R., & Garlatti, M. (2006). Endoplasmic reticulum stress induction of insulin-like growth factor-binding protein-1 involves ATF4. *Journal of Biological Chemistry*, 281(28), 19124–19133. <https://doi.org/10.1074/jbc.M602157200>
- Marco-Ramell, A., de Almeida, A. M., Cristobal, S., Rodrigues, P., Roncada, P., & Bassols, A. (2016). Proteomics and the search for welfare and stress biomarkers in animal production in the one-health context. *Molecular BioSystems*, 12(7), 2024–2035. <https://doi.org/10.1039/C5MB00788G>
- Marques, I. J., Leito, J. T. D., Spaink, H. P., Testerink, J., Jaspers, R. T., Witte, F., van den Berg, S., & Bagowski, C. P. (2008). Transcriptome analysis of the response to chronic constant hypoxia in zebrafish hearts. *Journal of Comparative Physiology B: Biochemical, Systemic, and Environmental Physiology*, 178(1), 77–92. <https://doi.org/10.1007/s00360-007-0201-4>
- Martinez-Porchas, M., Martinez-Cordova, L. R., & Ramos-Enriquez, R. (2009). Cortisol and Glucose: Reliable indicators of fish stress? *Pan-American Journal of Aquatic Sciences*, 4(2), 158–178. [http://www.panamjas.org/pdf_artigos/PANAMJAS_4\(2\)_158-178.pdf](http://www.panamjas.org/pdf_artigos/PANAMJAS_4(2)_158-178.pdf)

- Martins, C. I. M., Silva, P. I. M., Conceição, L. E. C., Costas, B., Höglund, E., Øverli, Ø., & Schrama, J. W. (2011). Linking Fearfulness and Coping Styles in Fish. *PLoS ONE*, *6*, e28084. <https://doi.org/10.1371/journal.pone.0028084>
- Martos-Sitcha, J. A., Mancera, J. M., Calduch-Giner, J. A., Yúfera, M., Martínez-Rodríguez, G., & Pérez-Sánchez, J. (2016). Unraveling the Tissue-Specific Gene Signatures of Gilthead Sea Bream (*Sparus aurata* L.) after Hyper- and Hypo-Osmotic Challenges. *PLOS ONE*, *11*(2), e0148113. <https://doi.org/10.1371/JOURNAL.PONE.0148113>
- Martos-Sitcha, J. A., Simó-Mirabet, P., de las Heras, V., Calduch-Giner, J. À., & Pérez-Sánchez, J. (2019). Tissue-Specific Orchestration of Gilthead Sea Bream Resilience to Hypoxia and High Stocking Density. *Frontiers in Physiology*, *10*, 840. <https://doi.org/10.3389/FPHYS.2019.00840>
- Matos, E., Dias, J., Dinis, M. T., & Silva, T. S. (2017). Sustainability vs. Quality in gilthead seabream (*Sparus aurata* L.) farming: are trade-offs inevitable? *Reviews in Aquaculture*, *9*(4), 388–409. <https://doi.org/10.1111/raq.12144>
- Matos, E., Gonçalves, A., Nunes, M. L., Dinis, M. T., & Dias, J. (2010). Effect of harvesting stress and slaughter conditions on selected flesh quality criteria of gilthead seabream (*Sparus aurata*). *Aquaculture*, *305*, 66–72. <https://doi.org/10.1016/j.aquaculture.2010.04.020>
- Matos, E., Silva, T. S., Wulff, T., Valente, L. M. P., Sousa, V., Sampaio, E., Gonçalves, A., Silva, J. M. G., Guedes de Pinho, P., Dinis, M. T., Rodrigues, P. M., & Dias, J. (2013). Influence of supplemental maslinic acid (olive-derived triterpene) on the post-mortem muscle properties and quality traits of gilthead seabream. *Aquaculture*, *396–399*, 146–155. <https://doi.org/10.1016/j.aquaculture.2013.02.044>
- Matouke, M. M. (2019). FTIR study of the binary effect of titanium dioxide nanoparticles (nTiO₂) and copper (Cu²⁺) on the biochemical constituents of liver tissues of catfish (*Clarias gariepinus*). *Toxicology Reports*, *6*(October), 1061–1070. <https://doi.org/10.1016/j.toxrep.2019.10.002>
- McCulloch, S. P. (2013). A Critique of FAWC's Five Freedoms as a Framework for the Analysis of Animal Welfare. *Journal of Agricultural and Environmental Ethics*, *26*(5), 959–975. <https://doi.org/10.1007/s10806-012-9434-7>
- McDermott, J. E., Wang, J., Mitchell, H., Webb-Robertson, B. J., Hafen, R., Ramey, J., & Rodland, K. D. (2013). Challenges in biomarker discovery: Combining expert insights with statistical analysis of complex omics data. *Expert Opinion on Medical Diagnostics*, *7*(1), 37–51. <https://doi.org/10.1517/17530059.2012.718329>
- McEwen, B. S., & Wingfield, J. C. (2003). The concept of allostasis in biology and biomedicine. *Hormones and Behavior*, *43*, 2–15. [https://doi.org/http://dx.doi.org/10.1016/S0018-506X\(02\)00024-7](https://doi.org/http://dx.doi.org/10.1016/S0018-506X(02)00024-7)
- McEwen, B. S., & Wingfield, J. C. (2010). What is in a name? Integrating homeostasis, allostasis and stress. *Hormonal Behaviour*, *57*(2), 105–111.
- Mejdell, C., Lund, V., & Håstein, T. (2007). Fish welfare in aquaculture. *Journal of Commonwealth Veterinary Association, Anniversary Celebrations*, *23*, 21–26.
- Melis, R., Sanna, R., Braca, A., Bonaglini, E., Cappuccinelli, R., Slawski, H., Roggio, T., Uzzau, S., & Anedda, R. (2017). Molecular details on gilthead sea bream (*Sparus aurata*) sensitivity to low water temperatures from 1H NMR metabolomics. *Comparative Biochemistry and Physiology -Part A: Molecular and Integrative Physiology*, *204*, 129–136. <https://doi.org/10.1016/j.cbpa.2016.11.010>
- Mellor, D. J., & Stafford, K. J. (2001). Integrating practical, regulatory and ethical strategies for enhancing farm animal welfare. *Australian Veterinary Journal*, *79*, 762–768.
- Metzger, D. C. H., Hemmer-Hansen, J., & Schulte, P. M. (2016). Conserved structure and expression of hsp70 paralogs in teleost fishes. *Comparative Biochemistry and Physiology Part D: Genomics and Proteomics*, *18*, 10–20. <https://doi.org/10.1016/j.cbd.2016.01.007>
- Millán-Cubillo, A. F., Martos-Sitcha, J. A., Ruiz-Jarabo, I., Cárdenas, S., & Mancera, J. M. (2016). Low stocking density negatively affects growth, metabolism and stress pathways in juvenile specimens of meagre (*Argyrosomus regius*, Asso 1801). *Aquaculture*, *451*, 87–92. <https://doi.org/10.1016/J.AQUACULTURE.2015.08.034>

- Milligan, C. L., & Girard, S. S. (1993). Lactate metabolism in rainbow trout. *J. Exp. Biol*, *180*, 175–193. <http://jeb.biologists.org/content/jexbio/180/1/175.full.pdf>
- Millot, S., Cerqueira, M., Castanheira, M.-F., Øverli, Ø., Oliveira, R. F., & Martins, C. I. M. (2014). Behavioural Stress Responses Predict Environmental Perception in European Sea Bass (*Dicentrarchus labrax*). *PLoS ONE*, *9*(9), e108800. <https://doi.org/10.1371/journal.pone.0108800>
- Minden, J. S. (2012). DIGE: Past and Future. In *Methods in molecular biology (Clifton, N.J.)* (Vol. 854, pp. 3–8). https://doi.org/10.1007/978-1-61779-573-2_1
- Mininni, A. N., Milan, M., Ferrareso, S., Petochi, T., Di Marco, P., Marino, G., Livi, S., Romualdi, C., Bargelloni, L., & Patarnello, T. (2014). Liver transcriptome analysis in gilthead sea bream upon exposure to low temperature. *BMC Genomics*, *15*(1), 1–12. <https://doi.org/10.1186/1471-2164-15-765>
- Mnatsakanyan, R., Shema, G., Basik, M., Batist, G., Borchers, C. H., Sickmann, A., & Zahedi, R. P. (2018). Detecting post-translational modification signatures as potential biomarkers in clinical mass spectrometry. *Expert Review of Proteomics*, *15*(6), 515–535. <https://doi.org/10.1080/14789450.2018.1483340>
- Moghadam, H., Mørkøre, T., & Robinson, N. (2015). Epigenetics-potential for programming fish for aquaculture? *Journal of Marine Science and Engineering*, *3*(2), 175–192. <https://doi.org/10.3390/jmse3020175>
- Mommsen, T. P., Vijayan, M. M., & Moon, T. W. (1999). Cortisol in teleosts: dynamics, mechanisms of action, and metabolic regulation. *Reviews in Fish Biology and Fisheries*, *9*, 211–268. <https://doi.org/10.1023/a:1008924418720> LB - ref1
- Momoda, T. S., Schwindt, A. R., Feist, G. W., Gerwick, L., Bayne, C. J., & Schreck, C. B. (2007). Gene expression in the liver of rainbow trout, *Oncorhynchus mykiss*, during the stress response. *Comparative Biochemistry and Physiology - Part D: Genomics and Proteomics*, *2*(4), 303–315. <https://doi.org/10.1016/j.cbd.2007.06.002>
- Montero, D., Izquierdo, M. S., Tort, L., Robaina, L., & Vergara, J. M. (1999). High stocking density produces crowding stress altering some physiological and biochemical parameters in gilthead seabream, *Sparus aurata*, juveniles. *Fish Physiology and Biochemistry*, *20*(1), 53–60. <https://doi.org/10.1023/A:1007719928905>
- Moon, T. W. (2004). Hormones and fish hepatocyte metabolism: “the good, the bad and the ugly!” *Comparative Biochemistry and Physiology Part B: Biochemistry and Molecular Biology*, *139*(3), 335–345. <https://doi.org/10.1016/J.CBPC.2004.06.003>
- Moreira, M., Schrama, D., Soares, F., Wulff, T., Pousão-Ferreira, P., & Rodrigues, P. (2017). Physiological responses of reared sea bream (*Sparus aurata* Linnaeus, 1758) to an *Amyloodinium ocellatum* outbreak. *Journal of Fish Diseases*, *40*(11), 1545–1560. <https://doi.org/10.1111/JFD.12623>
- Moretti, A., Fernandez-Criado, M. P., Cittolin, G., & Guidastri, R. (1999). *Manual on hatchery production of seabass and gilthead seabream. Volume 1*. FAO. <https://doi.org/10.18356/fa70fd58-en>
- Morro, B., Broughton, R., Balseiro, P., Handeland, S. O., Mackenzie, S., Doherty, M. K., Whitfield, P. D., Shimizu, M., Gorissen, M., Sveier, H., & Albalat, A. (2021). Endoplasmic reticulum stress as a key mechanism in stunted growth of seawater rainbow trout (*Oncorhynchus mykiss*). *BMC Genomics* *2021* *22*:1, *22*(1), 1–15. <https://doi.org/10.1186/S12864-021-08153-5>
- Morzel, M., Chambon, C., Lefèvre, F., Paboeuf, G., & Laville, E. (2006). Modifications of trout (*Oncorhynchus mykiss*) muscle proteins by preslaughter activity. *Journal of Agricultural and Food Chemistry*, *54*(8), 2997–3001. <https://doi.org/10.1021/jf0528759>
- Mucherino, A., Papajorgji, P. J., & Pardalos, P. M. (2009). Chapter 4 - K-Nearest Neighbor Classification. In *Data Mining in Agriculture, Springer Optimization and Its Applications* (Vol. 34). Springer. <https://doi.org/10.1007/978-0-387-88615-2>
- Mushtaq, M. Y., Marçal, R. M., Champagne, D. L., Van Der Kooy, F., Verpoorte, R., & Choi, Y. H. (2014). Effect of acute stresses on zebra fish (*danio rerio*) metabolome measured by nmr-based metabolomics. *Planta Medica*, *80*(14), 1227–1233. <https://doi.org/10.1055/s-0034-1382878>

- Musrati, R. A., Kollárová, M., Mernik, N., & Mikulášová, D. (1998). Malate Dehydrogenase: Distribution, Function and Properties. *General Physiology and Biophysics*, 17(3), 193–210.
- Mustafa, S. A., Kariieb, S. S., Davies, S. J., & Jha, A. N. (2015). Assessment of oxidative damage to DNA, transcriptional expression of key genes, lipid peroxidation and histopathological changes in carp *Cyprinus carpio* L. following exposure to chronic hypoxic and subsequent recovery in normoxic conditions. *Mutagenesis*, 30(1), 107–116. <https://doi.org/10.1093/mutage/geu048>
- Naderi, M., Keyvanshokoh, S., Ghaedi, A., & Salati, A. P. (2018). Effect of acute crowding stress on rainbow trout (*Oncorhynchus mykiss*): A proteomics study. *Aquaculture*, 495, 106–114. <https://doi.org/10.1016/J.AQUACULTURE.2018.05.038>
- Naderi, M., Keyvanshokoh, S., Salati, A. P., & Ghaedi, A. (2017). Effects of chronic high stocking density on liver proteome of rainbow trout (*Oncorhynchus mykiss*). *Fish Physiology and Biochemistry*, 43(5), 1373–1385. <https://doi.org/10.1007/s10695-017-0378-8>
- Nakano, T., Afonso, L. O. B., Beckman, B. R., Iwama, G. K., & Devlin, R. H. (2013). Acute Physiological Stress Down-Regulates mRNA Expressions of Growth-Related Genes in Coho Salmon. *PLoS ONE*, 8(8), e71421. <https://doi.org/10.1371/journal.pone.0071421>
- Nakayasu, E. S., Gritsenko, M., Piehowski, P. D., Gao, Y., Orton, D. J., Schepmoes, A. A., Fillmore, T. L., Frohnert, B. I., Rewers, M., Krischer, J. P., Ansong, C., Suchy-Dicey, A. M., Evans-Molina, C., Qian, W.-J., Webb-Robertson, B.-J. M., & Metz, T. O. (2021). Tutorial: best practices and considerations for mass-spectrometry-based protein biomarker discovery and validation. *Nature Protocols* 2021 16:8, 16(8), 3737–3760. <https://doi.org/10.1038/s41596-021-00566-6>
- Narla, A., Hurst, S. N., & Ebert, B. L. (2011). Ribosome defects in disorders of erythropoiesis. *Int J Hematol*, 93, 144–149. <https://doi.org/10.1007/s12185-011-0776-0>
- Natnan, M. E., Low, C.-F., Chong, C.-M., Bunawan, H., & Baharum, S. N. (2021). Integration of Omics Tools for Understanding the Fish Immune Response Due to Microbial Challenge. *Frontiers in Marine Science*, 0, 751. <https://doi.org/10.3389/FMARS.2021.668771>
- Naya-Català, F., Martos-Sitcha, J. A., de las Heras, V., Simó-Mirabet, P., Caldach-Giner, J. À., & Pérez-Sánchez, J. (2021). Targeting the Mild-Hypoxia Driving Force for Metabolic and. *Biology*, 10, 416.
- Nesvizhskii, A. I., Keller, A., Kolker, E., & Aebersold, R. (2003). A Statistical Model for Identifying Proteins by Tandem Mass Spectrometry. *Analytical Chemistry*, 75(17), 4646–4658. <https://doi.org/10.1021/AC0341261>
- Neves, J. V., Ramos, M. F., Moreira, A. C., Silva, T., Gomes, M. S., & Rodrigues, P. N. S. (2017). Hamp1 but not Hamp2 regulates ferroportin in fish with two functionally distinct hepcidin types. *Scientific Reports*, 7(1), 1–14. <https://doi.org/10.1038/s41598-017-14933-5>
- Ng, N., Purshouse, K., Foskolou, I. P., Olcina, M. M., & Hammond, E. M. (2018). Challenges to DNA replication in hypoxic conditions. *FEBS Journal*, 285(9), 1563–1571. <https://doi.org/10.1111/febs.14377>
- Ni, X., Wang, N., Liu, Y., & Lu, C. (2010). Immunoproteomics of extracellular proteins of the *Aeromonas hydrophila* China vaccine strain J-1 reveal a highly immunoreactive outer membrane protein. *FEMS Immunology & Medical Microbiology*, 58(3), 363–373. <https://doi.org/10.1111/j.1574-695X.2009.00646.x>
- Nicklin, P., Bergman, P., Zhang, B., Triantafellow, E., Wang, H., Nyfeler, B., Yang, H., Hild, M., Kung, C., Wilson, C., Myer, V. E., MacKeigan, J. P., Porter, J. A., Wang, Y. K., Cantley, L. C., Finan, P. M., & Murphy, L. O. (2009). Bidirectional Transport of Amino Acids Regulates mTOR and Autophagy. *Cell*, 136(3), 521–534. <https://doi.org/10.1016/J.CELL.2008.11.044>
- Nissa, M. U., Pinto, N., Parkar, H., Goswami, M., & Srivastava, S. (2021). Proteomics in fisheries and aquaculture: An approach for food security. *Food Control*, 127(April), 108125. <https://doi.org/10.1016/j.foodcont.2021.108125>

- Noble, C., Gismervik, K., Iversen, M. H., Kolarevic, J., Nilsson, J., Stien, L. H., & Turnbull, J. F. (2018). *Welfare Indicators for farmed Atlantic salmon: tools for assessing fish welfare* (C. Noble, K. Gismervik, M. H. Iversen, J. Kolarevic, J. Nilsson, L. H. Stien, & J. F. Turnbull, Eds.). www.nofima.no/fishwell/english
- Ntantali, O., Malandrakis, E. E., Abbink, W., Golomazou, E., Karapanagiotidis, I. T., Miliou, H., & Panagiotaki, P. (2020). Whole brain transcriptomics of intermittently fed individuals of the marine teleost *Sparus aurata*. *Comparative Biochemistry and Physiology - Part D: Genomics and Proteomics*, *36*(August), 100737. <https://doi.org/10.1016/j.cbd.2020.100737>
- Nuez-Ortín, W. G., Carter, C. G., Nichols, P. D., Cooke, I. R., & Wilson, R. (2018). Liver proteome response of pre-harvest Atlantic salmon following exposure to elevated temperature. *BMC Genomics*, *19*(1), 133. <https://doi.org/10.1186/s12864-018-4517-0>
- Obeid, R. (2013). The metabolic burden of methyl donor deficiency with focus on the betaine homocysteine methyltransferase pathway. *Nutrients*, *5*(9), 3481–3495. <https://doi.org/10.3390/nu5093481>
- Ogata, M., Hino, S., Saito, A., Morikawa, K., Kondo, S., Kanemoto, S., Murakami, T., Taniguchi, M., Tanii, I., Yoshinaga, K., Shiosaka, S., Hammarback, J. A., Urano, F., & Imaizumi, K. (2006). Autophagy Is Activated for Cell Survival after Endoplasmic Reticulum Stress. *Molecular and Cellular Biology*, *26*(24), 9220–9231. <https://doi.org/10.1128/mcb.01453-06>
- Okonechnikov, K., Conesa, A., & García-Alcalde, F. (2016). Qualimap 2: advanced multi-sample quality control for high-throughput sequencing data. *Bioinformatics*, *32*(2), 292–294. <https://doi.org/10.1093/bioinformatics/btv566>
- Oldham, W. M., Clish, C. B., Yang, Y., & Loscalzo, J. (2015). Hypoxia-Mediated Increases in l-2-hydroxyglutarate Coordinate the Metabolic Response to Reductive Stress. *Cell Metabolism*, *22*(2), 291–303. <https://doi.org/10.1016/j.cmet.2015.06.021>
- Olivares-Rubio, H. F., & Vega-López, A. (2016). Fatty acid metabolism in fish species as a biomarker for environmental monitoring. *Environmental Pollution*, *218*, 297–312. <https://doi.org/10.1016/J.ENVPOL.2016.07.005>
- Olsvik, P. A., Kristensen, T., Waagbø, R., Tollefsen, K. E., Rosseland, B. O., & Toften, H. (2006). Effects of hypo- and hyperoxia on transcription levels of five stress genes and the glutathione system in liver of Atlantic cod *Gadus morhua*. *Journal of Experimental Biology*, *209*(15), 2893–2901. <https://doi.org/10.1242/jeb.02320>
- Omlin, T., & Weber, J. (2010). Hypoxia stimulates lactate disposal in rainbow trout. *The Journal of Experimental Biology*, *213*, 3802–3809. <https://doi.org/10.1242/jeb.048512>
- Ordóñez-Grande, B., Guerreiro, P. M., Sanahuja, I., Fernández-Alacid, L., & Ibarz, A. (2021). Environmental salinity modifies mucus exudation and energy use in european sea bass juveniles. *Animals*, *11*(6), 1–20. <https://doi.org/10.3390/ani11061580>
- Oskoueian, E., Mullen, W., & Albalat, A. (2016). Proteomic Applications for Farm Animal Management. In *Agricultural Proteomics Volume 1* (pp. 157–173). Springer International Publishing. https://doi.org/10.1007/978-3-319-43275-5_9
- Pakos-Zebrucka, K., Koryga, I., Mnich, K., Ljubic, M., Samali, A., & Gorman, A. M. (2016). The integrated stress response. *EMBO Reports*, *17*(10), 1374–1395. <https://doi.org/10.15252/EMBR.201642195>
- Palaniappan, P. R., Nishanth, T., & Renju, V. B. (2010). Bioconcentration of zinc and its effect on the biochemical constituents of the gill tissues of *Labeo rohita*: An FT-IR study. *Infrared Physics and Technology*, *53*(2), 103–111. <https://doi.org/10.1016/j.infrared.2009.10.003>
- Pang, Z., Chong, J., Zhou, G., De Lima Morais, D. A., Chang, L., Barrette, M., Gauthier, C., Jacques, P. É., Li, S., & Xia, J. (2021). MetaboAnalyst 5.0: narrowing the gap between raw spectra and functional insights. *Nucleic Acids Research*, *49*(W1), W388–W396. <https://doi.org/10.1093/NAR/GKAB382>
- Pankhurst, N. W. (2011). The endocrinology of stress in fish: An environmental perspective. *General and Comparative Endocrinology*, *170*(2), 265–275. <https://doi.org/10.1016/J.YGCEN.2010.07.017>

- Park, H.-E., Park, J.-S., Park, H.-T., Choi, J.-G., Shin, J.-I., Jung, M., Kang, H.-L., Baik, S.-C., Lee, W.-K., Kim, D., Yoo, H. S., & Shin, M.-K. (2021). Alpha-2-Macroglobulin as a New Promising Biomarker Improving the Diagnostic Sensitivity of Bovine Paratuberculosis. *Frontiers in Veterinary Science*, 8, 637716. <https://doi.org/10.3389/FVETS.2021.637716>
- Park, K. C., Paluncic, J., Kovacevic, Z., & Richardson, D. R. (2020). Pharmacological targeting and the diverse functions of the metastasis suppressor, NDRG1, in cancer. *Free Radical Biology and Medicine*, 157, 154–175. <https://doi.org/10.1016/J.FREERADBIOMED.2019.05.020>
- Pauletto, M., Manousaki, T., Ferrareso, S., Babbucci, M., Tsakogiannis, A., Louro, B., Vitulo, N., Quoc, V. H., Carraro, R., Bertotto, D., Franch, R., Maroso, F., Aslam, M. L., Sonesson, A. K., Simionati, B., Malacrida, G., Cestaro, A., Caberlotto, S., Sarropoulou, E., ... Bargelloni, L. (2018). Genomic analysis of *Sparus aurata* reveals the evolutionary dynamics of sex-biased genes in a sequential hermaphrodite fish. *Communications Biology*, 1(1). <https://doi.org/10.1038/s42003-018-0122-7>
- Pavlidis, M. A., & Mylonas, C. C. (2011). *Sparidae: Biology and Aquaculture of Gilthead Sea Bream and Other Species* (M. A. Pavlidis & C. C. Mylonas, Eds.). John Wiley & Sons. <https://books.google.pt/books?id=evzGtJScg8UC>
- Pavlidis, M., Angellotti, L., Papandroulakis, N., & Divanach, P. (2003). Evaluation of transportation procedures on water quality and fry performance in red porgy (*Pagrus pagrus*) fry. *Aquaculture*, 218(1–4), 187–202. [https://doi.org/10.1016/S0044-8486\(02\)00314-9](https://doi.org/10.1016/S0044-8486(02)00314-9)
- Pedrazzani, A. S., Tavares, C. P. dos S., Quintiliano, M., Cozer, N., & Ostrensky, A. (2022). New indices for the diagnosis of fish welfare and their application to the grass carp (*Ctenopharyngodon idella*) reared in earthen ponds. *Aquaculture Research*, 53(17), 5825–5845. <https://doi.org/10.1111/are.16105>
- Pédrón, N., Artigaud, S., Infante, J.-L. Z., Le Bayon, N., Charrier, G., Pichereau, V., & Laroche, J. (2017). Proteomic responses of European flounder to temperature and hypoxia as interacting stressors: Differential sensitivities of populations. *Science of The Total Environment*, 586, 890–899. <https://doi.org/10.1016/j.scitotenv.2017.02.068>
- Pelletier, J., Thomas, G., & Volarevic, S. (2017). Ribosome biogenesis in cancer: new players and therapeutic avenues. *Nature Publishing Group*, 18, 51–63. <https://doi.org/10.1038/nrc.2017.104>
- Perez-Riverol, Y., Csordas, A., Bai, J., Bernal-Llinares, M., Hewapathirana, S., Kundu, D. J., Inuganti, A., Griss, J., Mayer, G., Eisenacher, M., Pérez, E., Uszkoreit, J., Pfeuffer, J., Sachsenberg, T., Yilmaz, Ş., Tiwary, S., Cox, J., Audain, E., Walzer, M., ... Vizcaíno, J. A. (2019). The PRIDE database and related tools and resources in 2019: improving support for quantification data. *Nucleic Acids Research*, 47(D1), D442–D450. <https://doi.org/10.1093/NAR/GKY1106>
- Pérez-Sánchez, J., Naya-Català, F., Soriano, B., Piazzon, M. C., Hafez, A., Gabaldón, T., Llorens, C., Sitjà-Bobadilla, A., & Calduch-Giner, J. A. (2019). Genome Sequencing and Transcriptome Analysis Reveal Recent Species-Specific Gene Duplications in the Plastic Gilthead Sea Bream (*Sparus aurata*). *Frontiers in Marine Science*, 6(December), 1–18. <https://doi.org/10.3389/fmars.2019.00760>
- Pérez-Sánchez, J., Terova, G., Simó-Mirabet, P., Rimoldi, S., Folkedal, O., Calduch-Giner, J. A., Olsen, R. E., & Sitjà-Bobadilla, A. (2017). Skin Mucus of Gilthead Sea Bream (*Sparus aurata* L.). Protein Mapping and Regulation in Chronically Stressed Fish. *Frontiers in Physiology*, 8(34). <https://doi.org/10.3389/fphys.2017.00034>
- Perteau, M., & Perteau, G. (2020). GFF Utilities: GffRead and GffCompare. *F1000Research*, 9, 304. <https://doi.org/10.12688/F1000RESEARCH.23297.1>
- Perteau, M., Perteau, G. M., Antonescu, C. M., Chang, T.-C., Mendell, J. T., Salzberg, S. L., & Biotechnol, N. (2015). StringTie enables improved reconstruction of a transcriptome from RNA-seq reads HHS Public Access Author manuscript. *Nat Biotechnol*, 33(3), 290–295. <https://doi.org/10.1038/nbt.3122>

- Peterson, T. S. (2015). 3 - Overview of mucosal structure and function in teleost fishes. In B. H. Beck & E. Peatman (Eds.), *Mucosal Health in Aquaculture* (pp. 55–65). Academic Press. <https://doi.org/https://doi.org/10.1016/B978-0-12-417186-2.00003-0>
- Petibon, C., Ghulam, M. M., Catala, M., & Elela, S. A. (2021). Regulation of ribosomal protein genes : An ordered anarchy. *WIREs RNA*, *12*, e1632. <https://doi.org/10.1002/wrna.1632>
- Petitjean, Q., Jean, S., Gandar, A., Côte, J., Laffaille, P., & Jacquin, L. (2019). Stress responses in fish: From molecular to evolutionary processes. *Science of The Total Environment*, *684*, 371–380. <https://doi.org/10.1016/J.SCITOTENV.2019.05.357>
- Pfaffl, M. W., Tichopad, A., Prgomet, C., & Neuvians, T. P. (2004). Determination of stable housekeeping genes, differentially regulated target genes and sample integrity: BestKeeper - Excel-based tool using pair-wise correlations. *Biotechnology Letters*, *26*(6), 509–515. <https://doi.org/10.1023/B:BILE.0000019559.84305.47>
- Philip, A. M., & Vijayan, M. M. (2015). Stress-Immune-Growth Interactions: Cortisol Modulates Suppressors of Cytokine Signaling and JAK/STAT Pathway in Rainbow Trout Liver. *PLOS ONE*, *10*(6), e0129299. <https://doi.org/10.1371/journal.pone.0129299>
- Piazzon, M. C., Mladineo, I., Naya-Català, F., Dirks, R. P., Jong-Raadsen, S., Vrbatović, A., Hrabar, J., Pérez-Sánchez, J., & Sitjà-Bobadilla, A. (2019). Acting locally - Affecting globally: RNA sequencing of gilthead sea bream with a mild Sparicotyle chrysophrii infection reveals effects on apoptosis, immune and hypoxia related genes. *BMC Genomics*, *20*(1), 1–16. <https://doi.org/10.1186/s12864-019-5581-9>
- Piñeiro, M., Piñeiro, C., Carpintero, R., Morales, J., Campbell, F. M., Eckersall, P. D., Toussaint, M. J. M., & Lampreave, F. (2007). Characterisation of the pig acute phase protein response to road transport. *The Veterinary Journal*, *173*(3), 669–674. <https://doi.org/10.1016/J.TVJL.2006.02.006>
- Pires, I. M., Bencokova, Z., Milani, M., Folkes, L. K., Li, J. A., Stratford, M. R., Harris, A. L., & Hammond, E. M. (2010). Effects of acute versus chronic hypoxia on DNA damage responses and genomic instability. *Cancer Research*, *70*(3), 925–935. <https://doi.org/10.1158/0008-5472.CAN-09-2715>
- Plotnikov, A., Zehorai, E., Procaccia, S., & Seger, R. (2011). The MAPK cascades: Signaling components, nuclear roles and mechanisms of nuclear translocation. *Biochimica et Biophysica Acta (BBA) - Molecular Cell Research*, *1813*(9), 1619–1633. <https://doi.org/10.1016/J.BBAMCR.2010.12.012>
- Poirier, Y., Antonenkov, V. D., Glumoff, T., & Hiltunen, J. K. (2006). Peroxisomal β -oxidation- A metabolic pathway with multiple functions. *Biochimica et Biophysica Acta - Molecular Cell Research*, *1763*(12), 1413–1426. <https://doi.org/10.1016/j.bbamcr.2006.08.034>
- Polakof, S., Panerat, S., Soengas, J. L., & Moon, T. W. (2012). Glucose metabolism in fish: a review. *Journal of Comparative Physiology. B, Biochemical, Systemic, and Environmental Physiology*, *182*(8), 1015–1045. <https://doi.org/10.1007/s00360-012-0658-7>
- Poli, B. M., Parisi, G., Scappini, F., & Zampacavallo, G. (2005). Fish welfare and quality as affected by pre-slaughter and slaughter management. *Aquaculture International*, *13*, 29–49. <https://link.springer.com/content/pdf/10.1007%2Fs10499-004-9035-1.pdf>
- Porcheron, G., Garénaux, A., Proulx, J., Sabri, M., & Dozois, C. M. (2013). Iron, copper, zinc, and manganese transport and regulation in pathogenic Enterobacteria: correlations between strains, site of infection and the relative importance of the different metal transport systems for virulence. *Frontiers in Cellular and Infection Microbiology*, *3*, 90. <https://doi.org/10.3389/fcimb.2013.00090>
- Portenier, I., Waltimo, T., Ørstavik, D., & Haapasalo, M. (2005). The susceptibility of starved, stationary phase, and growing cells of *Enterococcus faecalis* to endodontic medicaments. *Journal of Endodontics*, *31*(5), 380–386. <https://doi.org/10.1097/01.don.0000145421.84121.c8>
- Pottinger, T. G. (2008). The Stress Response in Fish-Mechanisms, Effects and Measurement. In E. J. Branson (Ed.), *Fish Welfare* (pp. 32–48). Blackwell Publishing Ltd. <https://doi.org/10.1002/9780470697610.ch3>

- Prunet, P., Øverli, @bullet Ø, Douxfils, @bullet J, Bernardini, @bullet G, Kestemont, @bullet P, Baron, @bullet D, Øverli, Ø., Douxfils, J., Kestemont, Á. P., Bernardini, G., Baron, D., Kestemont, P., Baron, D., Øverli, O., Douxfils, J., Bernardini, G., Kestemont, P., & Baron, D. (2012). Fish welfare and genomics. *Fish Physiology and Biochemistry*, 38(1), 43–60. <https://doi.org/10.1007/s10695-011-9522-z>
- Qian, B., Xue, L., & Huang, H. (2016). Liver transcriptome analysis of the large yellow croaker (*Larimichthys crocea*) during fasting by using RNA-seq. *PLoS ONE*, 11(3). <https://doi.org/10.1371/journal.pone.0150240>
- Qian, X., Ba, Y., Zhuang, Q., & Zhong, G. (2014). RNA-seq technology and its application in fish transcriptomics. *OMICS A Journal of Integrative Biology*, 18(2), 98–110. <https://doi.org/10.1089/omi.2013.0110>
- Quan, J., Kang, Y., Li, L., Zhao, G., Sun, J., & Liu, Z. (2021). Proteome analysis of rainbow trout (*Oncorhynchus mykiss*) liver responses to chronic heat stress using DIA/SWATH. *Journal of Proteomics*, 233, 104079. <https://doi.org/10.1016/J.JPROT.2020.104079>
- R Core Team. (2022). *R: A Language and Environment for Statistical Computing*. R Foundation for Statistical Computing. <https://www.r-project.org/>.
- Rahman, M. S., & Thomas, P. (2011). Characterization of three IGF1P mRNAs in Atlantic croaker and their regulation during hypoxic stress: Potential mechanisms of their upregulation by hypoxia. *American Journal of Physiology - Endocrinology and Metabolism*, 301(4). <https://doi.org/10.1152/ajpendo.00168.2011>
- Rajan, B., Lokesh, J., Kiron, V., & Brinchmann, M. F. (2013). Differentially expressed proteins in the skin mucus of Atlantic cod (*Gadus morhua*) upon natural infection with *Vibrio anguillarum*. *BMC Veterinary Research*, 9(1), 103. <https://doi.org/10.1186/1746-6148-9-103>
- Raposo de Magalhães, C., Cerqueira, M., Schrama, D., Moreira, M., Boonanuntanasarn, S., & Rodrigues, P. M. L. (2020). A Proteomics and other Omics approach in the context of farmed fish welfare and biomarker discovery. *Reviews in Aquaculture*, 12(1), 122–144.
- Raposo de Magalhães, C., Farinha, A. P., Blackburn, G., Whitfield, P. D., Carrilho, R., Schrama, D., Cerqueira, M., & Rodrigues, P. M. (2022). Gilthead Seabream Liver Integrative Proteomics and Metabolomics Analysis Reveals Regulation by Different Prosurvival Pathways in the Metabolic Adaptation to Stress. *International Journal of Molecular Sciences*, 23, 15395. <https://doi.org/10.3390/ijms232315395>
- Raposo de Magalhães, C., Schrama, D., Farinha, A. P., Revets, D., Kuehn, A., Planchon, S., Rodrigues, P. M., & Cerqueira, M. (2020). Protein changes as robust signatures of fish chronic stress: A proteomics approach to fish welfare research. *BMC Genomics*, 21, 309. <https://doi.org/10.1186/s12864-020-6728-4>
- Raposo de Magalhães, C., Schrama, D., Nakharuthai, C., Boonanuntanasarn, S., Revets, D., Planchon, S., Kuehn, A., Cerqueira, M., Carrilho, R., Farinha, A. P., & Rodrigues, P. M. (2021). Metabolic Plasticity of Gilthead Seabream Under Different Stressors: Analysis of the Stress Responsive Hepatic Proteome and Gene Expression. *Frontiers in Marine Science*, 8(May), 1–19. <https://doi.org/10.3389/fmars.2021.676189>
- Raudvere, U., Kolberg, L., Kuzmin, I., Arak, T., Adler, P., Peterson, H., & Vilo, J. (2019). G:Profiler: A web server for functional enrichment analysis and conversions of gene lists (2019 update). *Nucleic Acids Research*, 47(W1), W191–W198. <https://doi.org/10.1093/nar/gkz369>
- Rebl, A., & Goldammer, T. (2018). Under control: The innate immunity of fish from the inhibitors' perspective. *Fish & Shellfish Immunology*, 77, 328–349. <https://doi.org/10.1016/J.FSI.2018.04.016>
- Ren, Y., Tian, Y., Mao, X., Wen, H., Qi, X., Li, J., Li, J., & Li, Y. (2022). Acute hypoxia changes the gene expression profiles and alternative splicing landscape in gills of spotted sea bass (*Lateolabrax maculatus*). *Frontiers in Marine Science*, 9(October), 1–17. <https://doi.org/10.3389/fmars.2022.1024218>
- Reverter, M., Tapissier-Bontemps, N., Lecchini, D., Banaigs, B., & Sasal, P. (2018). Biological and ecological roles of external fish mucus: A review. *Fishes*, 3(4), 1–19. <https://doi.org/10.3390/fishes3040041>

- Rey, O., Danchin, E., Mirouze, M., Loot, C., & Blanchet, S. (2016). Adaptation to Global Change: A Transposable Element-Epigenetics Perspective. *Trends in Ecology and Evolution*, 31(7), 514–526. <https://doi.org/10.1016/j.tree.2016.03.013>
- Rey, S., Huntingford, F. A., Boltaña, S., Vargas, R., Knowles, T. G., & Mackenzie, S. (2015). Fish can show emotional fever: stress-induced hyperthermia in zebrafish. *Proceedings of the Royal Society of London B: Biological Sciences*, 282, 20152266. <http://rspb.royalsocietypublishing.org/content/282/1819/20152266.abstract>
- Reyes-lópez, F. E., Ibarz, A., Ordóñez-grande, B., Vallejos-vidal, E., Sánchez-nuño, S., Firmino, J. P., Pavez, L., Polo, J., & Tort, L. (2021). Skin Multi-Omics-Based Interactome Analysis: Integrating the Tissue and Mucus Exuded Layer for a Comprehensive Understanding of the Teleost Mucosa Functionality as Model of Study. *Frontiers in Immunology*, 11, 613824. <https://doi.org/10.3389/fimmu.2020.613824>
- Richard, N., Silva, T. S., Wulff, T., Schrama, D., Dias, J. P., Rodrigues, P. M. L., & Conceição, L. E. C. (2016). Nutritional mitigation of winter thermal stress in gilthead seabream: Associated metabolic pathways and potential indicators of nutritional state. *Journal of Proteomics*, 142, 1–14. <https://doi.org/10.1016/j.jprot.2016.04.037>
- Richards, J. G. (2009). Chapter 10 Metabolic and Molecular Responses of Fish to Hypoxia. In *Fish Physiology* (1st ed., Vol. 27, Issue C). Elsevier Inc. [https://doi.org/10.1016/S1546-5098\(08\)00010-1](https://doi.org/10.1016/S1546-5098(08)00010-1)
- Richter, K., Haslbeck, M., & Buchner, J. (2010). The Heat Shock Response: Life on the Verge of Death. *Molecular Cell*, 40(2), 253–266. <https://doi.org/10.1016/J.MOLCEL.2010.10.006>
- Riera-Ferrer, E., Piazzon, M. C., Del Pozo, R., Palenzuela, O., Estensoro, I., & Sitjà-Bobadilla, A. (2022). A bloody interaction: plasma proteomics reveals gilthead sea bream (*Sparus aurata*) impairment caused by *Sparicotyle chrysophrii*. *Parasites and Vectors*, 15(1), 1–16. <https://doi.org/10.1186/s13071-022-05441-1>
- Risius, A., Janssen, M., & Hamm, U. (2017). Consumer preferences for sustainable aquaculture products: Evidence from in-depth interviews, think aloud protocols and choice experiments. *Appetite*, 113, 246–254. <https://doi.org/10.1016/j.appet.2017.02.021>
- Roberts, R. J., Agius, C., Saliba, C., Bossier, P., & Sung, Y. Y. (2010). Heat shock proteins (chaperones) in fish and shellfish and their potential role in relation to fish health: A review. *Journal of Fish Diseases*, 33(10), 789–801. <https://doi.org/10.1111/j.1365-2761.2010.01183.x>
- Robin, X., Turck, N., Hainard, A., Tiberti, N., Lisacek, F., Sanchez, J.-C., & Müller, M. (2011). pROC: an open-source package for R and S+ to analyze and compare ROC curves. *BMC Bioinformatics* 2011 12:1, 12, 77. <https://doi.org/10.1186/1471-2105-12-77>
- Robinson, J. T., Thorvaldsdóttir, H., Winckler, W., Guttman, M., Lander, E. S., Getz, G., & Mesirov, J. P. (2011). Integrative Genomics Viewer. *Nat Biotechnol*, 29(1), 24–26. <https://doi.org/10.1038/nbt.1754>
- Rodrigues, P. M., Silva, T. S., Dias, J., & Jessen, F. (2012). PROTEOMICS in aquaculture: Applications and trends. *Journal of Proteomics*, 75(14), 4325–4345. <https://doi.org/10.1016/j.jprot.2012.03.042>
- Rodriguez-Barreto, D., Rey, O., Uren-Webster, T. M., Castaldo, G., Consuegra, S., & Garcia de Leaniz, C. (2019). Transcriptomic response to aquaculture intensification in Nile tilapia. *Evolutionary Applications*, 12(9), 1757–1771. <https://doi.org/10.1111/eva.12830>
- Rodriguez-Casado, A., Carmona, P., Moreno, P., Sánchez-González, I., Macagnano, A., Natale, C. Di, & Careche, M. (2007). Structural changes in sardine (*Sardina pilchardus*) muscle during iced storage: Investigation by DRIFT spectroscopy. *Food Chemistry*, 103(3), 1024–1030. <https://doi.org/10.1016/j.foodchem.2006.09.054>
- Roh, H., Kim, A., Kim, N., Lee, Y., & Kim, D. H. (2020). Multi-omics analysis provides novel insight into immuno-physiological pathways and development of thermal resistance in rainbow trout exposed to acute thermal stress. *International Journal of Molecular Sciences*, 21(23), 1–21. <https://doi.org/10.3390/ijms21239198>

- Rohart, F., Gautier, B., Singh, A., & Lê Cao, K. A. (2017). mixOmics: An R package for 'omics feature selection and multiple data integration. *PLOS Computational Biology*, *13*(11), e1005752. <https://doi.org/10.1371/JOURNAL.PCBI.1005752>
- Rollin, B. E. (1989). *The Unheeded Cry: Animal Consciousness, Animal Pain, and Science*. Oxford University Press.
- Rose, J. D., Arlinghaus, R., Cooke, S. J., Diggles, B. K., Sawynok, W., Stevens, E. D., & Wynne, C. D. L. (2012). Can fish really feel pain? *Fish and Fisheries*, *15*, 97–133. <https://doi.org/10.1111/faf.12010>
- Rotllant, J., Arends, R. J., Mancera, J. M., Flik, G., Wendelaar Bonga, S. E., & Tort, L. (2000). Inhibition of HPI axis response to stress in gilthead sea bream (*Sparus aurata*) with physiological plasma levels of cortisol. In *Fish Physiology and Biochemistry* (Vol. 23). <https://link.springer.com/content/pdf/10.1023%2FA%3A1007848128968.pdf>
- Roy, S., Kumar, V., Kumar, V., & Behera, B. K. (2016). Acute Phase Proteins and their Potential Role as an Indicator for Fish Health and in Diagnosis of Fish Diseases. *Protein & Peptide Letters*, *24*(1), 78–89. <https://doi.org/10.2174/0929866524666161121142221>
- Ruane, N. M., Carballo, E. C., & Komen, J. (2002). Increased stocking density influences the acute physiological stress response of common carp *Cyprinus carpio* (L.). *Aquaculture Research*, *33*(10), 777–784. <https://doi.org/10.1046/j.1365-2109.2002.00717.x>
- Rüetschi, U., Cerone, R., Pérez-Cerda, C., Schiaffino, M. C., Standing, S., Ugarte, M., & Holme, E. (2000). Mutations in the 4-hydroxyphenylpyruvate dioxygenase gene (HPD) in patients with tyrosinemia type III. *Human Genetics*, *106*(6), 654–662. <https://doi.org/10.1007/s004390050039>
- Russel, S., Hayes, M., Simko, E., & Lumsden, J. (2006). Plasma proteomic analysis of the acute phase response of rainbow trout (*Oncorhynchus mykiss*) to intraperitoneal inflammation and LPS injection. *Developmental & Comparative Immunology*, *30*(4), 393–406. <https://doi.org/10.1016/j.dci.2005.06.002>
- Saera-Vila, A., Calduch-Giner, J. A., Prunet, P., & Pérez-Sánchez, J. (2009). Dynamics of liver GH/IGF axis and selected stress markers in juvenile gilthead sea bream (*Sparus aurata*) exposed to acute confinement. Differential stress response of growth hormone receptors. *Comparative Biochemistry and Physiology - A Molecular and Integrative Physiology*, *154*(2), 197–203. <https://doi.org/10.1016/j.cbpa.2009.06.004>
- Sáez-Arteaga, A., Wu, Y., Silva-Marrero, J. I., Rashidpour, A., Almajano, M. P., Fernández, F., Baanante, I. V., & Metón, I. (2022). Gene markers of dietary macronutrient composition and growth in the skeletal muscle of gilthead sea bream (*Sparus aurata*). *Aquaculture*, *555*, 738221. <https://doi.org/10.1016/J.AQUACULTURE.2022.738221>
- Saftig, P., & Puertollano, R. (2021). How Lysosomes Sense, Integrate, and Cope with Stress. *Trends in Biochemical Sciences*, *46*(2), 97–112. <https://doi.org/10.1016/J.TIBS.2020.09.004>
- Salinas, I. (2015). The mucosal immune system of teleost fish. *Biology*, *4*(3), 525–539. <https://doi.org/10.3390/biology4030525>
- Salinas, I., & Magadán, S. (2017). Omics in fish mucosal immunity. *Developmental and Comparative Immunology*, *75*, 99–108. <https://doi.org/10.1016/J.DCI.2017.02.010>
- Salmerón, C., Navarro, I., Johnston, I. A., Gutiérrez, J., & Capilla, E. (2015). Characterisation and expression analysis of cathepsins and ubiquitin-proteasome genes in gilthead sea bream (*Sparus aurata*) skeletal muscle. *BMC Research Notes*, *8*(1), 1–15. <https://doi.org/10.1186/S13104-015-1121-0/FIGURES/6>
- Samaras, A., Espírito Santo, C., Papandroulakis, N., Mitrizakis, N., Pavlidis, M., Höglund, E., Pelgrim, T. N. M., Zethof, J., Spanings, F. A. T., Vindas, M. A., Ebbesson, L. O. E., Flik, G., & Gorissen, M. (2018). Allostatic Load and Stress Physiology in European Seabass (*Dicentrarchus labrax* L.) and Gilthead Seabream (*Sparus aurata* L.). *Frontiers in Endocrinology*, *9*, 451. <https://doi.org/10.3389/fendo.2018.00451>
- San, L., Liu, B., Liu, B., Guo, H., Guo, L., Zhang, N., Zhu, K., Jiang, S., & Zhang, D. (2021). Transcriptome Analysis of Gills Provides Insights Into Translation Changes Under Hypoxic Stress and Reoxygenation in Golden Pompano, *Trachinotus ovatus* (Linnaeus

- 1758). *Frontiers in Marine Science*, 8(December), 1–14. <https://doi.org/10.3389/fmars.2021.763622>
- Sanahuja, I., & Ibarz, A. (2015). Skin mucus proteome of gilthead sea bream: A non-invasive method to screen for welfare indicators. *Fish and Shellfish Immunology*, 46(2), 426–435. <https://doi.org/10.1016/j.fsi.2015.05.056>
- Sánchez-Alonso, I., Carmona, P., & Careche, M. (2012). Vibrational spectroscopic analysis of hake (*Merluccius merluccius* L.) lipids during frozen storage. *Food Chemistry*, 132(1), 160–167. <https://doi.org/10.1016/j.foodchem.2011.10.047>
- Sangiao-Alvarellos, S., Guzmán, J. M., Láiz-Carrión, R., Míguez, J. M., Martín Del Río, M. P., Mancera, J. M., & Soengas, J. L. (2005). Interactive effects of high stocking density and food deprivation on carbohydrate metabolism in several tissues of gilthead sea bream (*Sparus aurata*). *Journal of Experimental Zoology Part A: Comparative Experimental Biology*, 303A(9), 761–775. <https://doi.org/10.1002/jez.a.203>
- Santoso, H. B., Suhartono, E., Yunita, R., & Biyatmoko, D. (2020). Epidermal mucus as a potential biological matrix for fish health analysis. *Egyptian Journal of Aquatic Biology and Fisheries*, 24(6), 361–382. <https://doi.org/10.21608/EJABF.2020.114402>
- Sapolsky, R. M., Romero, L. M., & Munck, A. U. (2000). How do glucocorticoids influence stress responses? Integrating permissive, suppressive, stimulatory, and preparative actions. *Endocrine Reviews*, 21(1), 55–89. <https://doi.org/10.1210/er.21.1.55>
- Saraiva, C., Vasconcelos, H., & de Almeida, J. M. M. M. (2017). A chemometrics approach applied to Fourier transform infrared spectroscopy (FTIR) for monitoring the spoilage of fresh salmon (*Salmo salar*) stored under modified atmospheres. *International Journal of Food Microbiology*, 241, 331–339. <https://doi.org/10.1016/j.ijfoodmicro.2016.10.038>
- Saraiva, J. L., Arechavala-Lopez, P., Castanheira, M. F., Volstorf, J., & Heinzpeter Studer, B. (2019). A Global Assessment of Welfare in Farmed Fishes: The FishEthoBase. *Fishes*, 4(2), 30. <https://doi.org/10.3390/fishes4020030>
- Sathiyaa, R., & Vijayan, M. M. (2003). Autoregulation of glucocorticoid receptor by cortisol in rainbow trout hepatocytes. *American Journal of Physiology - Cell Physiology*, 284(6 53-6), 1508–1515. <https://doi.org/10.1152/ajpcell.00448.2002>
- Saxton, R. A., & Sabatini, D. M. (2017). mTOR Signaling in Growth, Metabolism, and Disease. *Cell*, 168(6), 960–976. <https://doi.org/10.1016/j.cell.2017.02.004>
- Scarl, R. T., Lawrence, C. M., Gordon, H. M., & Nunemaker, C. S. (2017). STEAP4: Its emerging role in metabolism and homeostasis of cellular iron and copper. *Journal of Endocrinology*, 234(3), R123–R134. <https://doi.org/10.1530/JOE-16-0594>
- Scheltema, R. A., Jankevics, A., Jansen, R. C., Swertz, M. A., & Breitling, R. (2011). PeakML/mzMatch: A file format, Java library, R library, and tool-chain for mass spectrometry data analysis. *Analytical Chemistry*, 83(7), 2786–2793. https://doi.org/10.1021/AC2000994/ASSET/IMAGES/MEDIUM/AC-2011-000994_0001.GIF
- Schiener, M., Hilger, C., Eberlein, B., Pascal, M., Kuehn, A., Revets, D., Planchon, S., Pietsch, G., Serrano, P., Moreno-Aguilar, C., De La Roca, F., Biedermann, T., Darsow, U., Schmidt-Weber, C. B., Ollert, M., & Blank, S. (2018). The high molecular weight dipeptidyl peptidase IV Pol d 3 is a major allergen of *Polistes dominula* venom. *Scientific Reports*, 8(1), 1–10. <https://doi.org/10.1038/s41598-018-19666-7>
- Schrama, D., Richard, N., Silva, T. S., Figueiredo, F. A., Conceição, L. E. C., Burchmore, R., Eckersall, D., & Rodrigues, P. M. L. (2017). Enhanced dietary formulation to mitigate winter thermal stress in gilthead sea bream (*Sparus aurata*): a 2D-DIGE plasma proteome study. *Fish Physiology and Biochemistry*, 43(2), 603–617. <https://doi.org/10.1007/s10695-016-0315-2>
- Schreck, C. B. (2010). Stress and fish reproduction: The roles of allostasis and hormesis. *General and Comparative Endocrinology*, 165(3), 549–556. <https://doi.org/10.1016/J.YGCEN.2009.07.004>
- Schreck, C. B., & Tort, L. (2016). The Concept of Stress in Fish. *Fish Physiology*, 35, 1–34. <https://doi.org/10.1016/B978-0-12-802728-8.00001-1>

- Schreck, C. B., Tort, L., Farrell, A. P., & Brauner, C. J. (2016). *Biology of Stress in Fish*. Academic Press - Elsevier. <https://linkinghub.elsevier.com/retrieve/pii/B9780128027288000163>
- Schulze, W. X., & Usadel, B. (2010). Quantitation in Mass-Spectrometry-Based Proteomics. *Annual Review of Plant Biology*, *61*(1), 491–516. <https://doi.org/10.1146/annurev-arplant-042809-112132>
- Segner, H., Sundh, H., Buchmann, K., Douxfils, J., Sundell, K. S., Mathieu, C., Ruane, N., Jutfelt, F., Toften, H., & Vaughan, L. (2012). Health of farmed fish: Its relation to fish welfare and its utility as welfare indicator. *Fish Physiology and Biochemistry*, *38*(1), 85–105. <https://doi.org/10.1007/s10695-011-9517-9>
- Séité, S., Mourier, A., Camougrand, N., Salin, B., Figueiredo-Silva, A. C., Fontagné-Dicharry, S., Panserat, S., & Seilliez, I. (2018). Dietary methionine deficiency affects oxidative status, mitochondrial integrity and mitophagy in the liver of rainbow trout (*Oncorhynchus mykiss*). *Scientific Reports*, *8*(1), 1–14. <https://doi.org/10.1038/s41598-018-28559-8>
- Selye, H. (1950). Stress and the general adaptation syndrome. *British Medical Journal*, *1*(4667), 1383–1392. <https://doi.org/10.1136/bmj.1.4667.1383>
- Serna-Duque, J. A., Espinosa Ruiz, C., Martínez Lopez, S., Sánchez-Ferrer, Á., & Esteban, M. Á. (2022). Immunometabolic involvement of hepcidin genes in iron homeostasis, storage, and regulation in gilthead seabream (*Sparus aurata*). *Frontiers in Marine Science*, *9*(December), 1–13. <https://doi.org/10.3389/fmars.2022.1073060>
- Shafik, M., Ibrahim, H., Elyazeid, I. A., Abass, O., & Saad, H. M. (2014). The stress of phenylalanine on rats to study the phenylketonuria at biochemical and molecular level. *Journal of Applied Pharmaceutical Science*, *4*(4), 24–29. <https://doi.org/10.7324/JAPS.2014.40405>
- Shannon, P., Markiel, A., Ozier, O., Baliga, N. S., Wang, J. T., Ramage, D., Amin, N., Schwikowski, B., & Ideker, T. (2003). Cytoscape: A Software Environment for Integrated Models of Biomolecular Interaction Networks. *Genome Research*, *13*(11), 2498–2504. <https://doi.org/10.1101/GR.1239303>
- Shephard, K. L. (1994). Functions for fish mucus. *Reviews in Fish Biology and Fisheries*, *4*, 401–429.
- Shi, X., Zhou, H., Wei, J., Mo, W., Li, Q., & Lv, X. (2022). The signaling pathways and therapeutic potential of itaconate to alleviate inflammation and oxidative stress in inflammatory diseases. *Redox Biology*, *58*(October), 102553. <https://doi.org/10.1016/j.redox.2022.102553>
- Silva, T. (2013). Using proteomic technologies to understand the impact of stress and nutritional factors on fish metabolism, welfare and quality. In *Doutoramento em Ciências da Vida, do Mar, da Terra e do Ambiente. Ramo de Ciências Biológicas: Vol. PhD*.
- Silva, T. S., da Costa, A. M. R., Conceição, L. E. C., Dias, J. P., Rodrigues, P. M. L., & Richard, N. (2014). Metabolic fingerprinting of gilthead seabream (*Sparus aurata*) liver to track interactions between dietary factors and seasonal temperature variations. *PeerJ*, *2*, e527. <https://doi.org/10.7717/peerj.527>
- Silva, T. S., Matos, E., Cordeiro, O. D., Colen, R., Wulff, T., Sampaio, E., Sousa, V., Valente, L. M. P., Gonçalves, A., Silva, J. M. G., Bandarra, N., Nunes, M. L., Dinis, M. T., Dias, J., Jessen, F., & Rodrigues, P. M. (2012). Dietary tools to modulate glycogen storage in gilthead seabream muscle: Glycerol supplementation. *Journal of Agricultural and Food Chemistry*, *60*(42), 10613–10624. <https://doi.org/10.1021/jf3023244>
- Silver, N., Best, S., Jiang, J., & Thein, S. L. (2006). Selection of housekeeping genes for gene expression studies in human reticulocytes using real-time PCR. *BMC Molecular Biology*, *7*, 1–9. <https://doi.org/10.1186/1471-2199-7-33>
- Simpson, K. L., Whetton, A. D., & Dive, C. (2009). Quantitative mass spectrometry-based techniques for clinical use: Biomarker identification and quantification. *Journal of Chromatography B*, *877*(13), 1240–1249. <https://doi.org/10.1016/J.JCHROMB.2008.11.023>

- Simsek, D., & Barna, M. (2017). An emerging role for the ribosome as a nexus for post-translational modifications. *Current Opinion in Cell Biology*, 45, 92–101. <https://doi.org/10.1016/j.ceb.2017.02.010>
- Skrzynska, A. K., Martos-Sitcha, J. A., Martínez-Rodríguez, G., & Mancera, J. M. (2018). Unraveling vasotocinergic, isotocinergic and stress pathways after food deprivation and high stocking density in the gilthead sea bream. *Comparative Biochemistry and Physiology -Part A: Molecular and Integrative Physiology*, 215(August 2017), 35–44. <https://doi.org/10.1016/j.cbpa.2017.10.012>
- Smith, B. C. (2011). *Fundamentals of Fourier Transform Infrared Spectroscopy* (B. C. Smith, Ed.; Second Edi). CRC Press.
- Smith, C. A., Want, E. J., O'Maille, G., Abagyan, R., & Siuzdak, G. (2006). XCMS: Processing mass spectrometry data for metabolite profiling using nonlinear peak alignment, matching, and identification. *Analytical Chemistry*, 78(3), 779–787. https://doi.org/10.1021/AC051437Y/SUPPL_FILE/AC051437YSI20050810_093207.PDF
- Smith, R. W., Cash, P., Ellefsen, S., & Nilsson, G. E. (2009). Proteomic changes in the crucian carp brain during exposure to anoxia. *Proteomics*, 9(8), 2217–2229. <https://doi.org/10.1002/pmic.200800662>
- Sneddon, L. U. (2004). Evolution of nociception in vertebrates: comparative analysis of lower vertebrates. *Brain Research Reviews*, 46, 123–130.
- Sneddon, L. U. (2007). Fish behaviour and welfare. *Applied Animal Behaviour Science*, 104, 173–175. <http://www.sciencedirect.com/science/article/B6T48-4KYY3HG-2/2/9519101ee8956f2519d17dbbb2fab8db>
- Sneddon, L. U. (2009). Pain perception in fish: indicators and endpoints. *Institute for Laboratory Animal Research Journal*, 50(4), 338–342.
- Sneddon, L. U. (2015). Pain in aquatic animals. *Journal of Experimental Biology*, 218(7), 967–976. <https://doi.org/10.1242/jeb.088823>
- Soares, R., Franco, C., Pires, E., Ventosa, M., Palhinhas, R., Koci, K., Martinho de Almeida, A., & Varela Coelho, A. (2012). Mass spectrometry and animal science: Protein identification strategies and particularities of farm animal species. *Journal of Proteomics*, 75(14), 4190–4206. <https://doi.org/10.1016/j.jprot.2012.04.009>
- Somboonwivat, K., Chaikereratsak, V., Wang, H.-C., Fang Lo, C., & Tassanakajon, A. (2010). Proteomic analysis of differentially expressed proteins in *Penaeus monodon* hemocytes after *Vibrio harveyi* infection. *Proteome Science*, 8(1), 39. <https://doi.org/10.1186/1477-5956-8-39>
- Somero, G. N. (2020). The cellular stress response and temperature: Function, regulation, and evolution. *Journal of Experimental Zoology Part A: Ecological and Integrative Physiology*, 333(6), 379–397. <https://doi.org/10.1002/JEZ.2344>
- Song, J., & McDowell, J. R. (2021). Comparative transcriptomics of spotted seatrout (*Cynoscion nebulosus*) populations to cold and heat stress. *Ecology and Evolution*, 11(3), 1352–1367. <https://doi.org/10.1002/ECE3.7138>
- Song, M., Zhao, J., Wen, H. S., Li, Y., Li, J. F., Li, L. M., & Tao, Y. X. (2019). The impact of acute thermal stress on the metabolome of the black rockfish (*Sebastes schlegelii*). *PLoS ONE*, 14(5), 1–23. <https://doi.org/10.1371/journal.pone.0217133>
- Southam, A. D., Easton, J. M., Stentiford, G. D., Ludwig, C., Arvanitis, T. N., & Viant, M. R. (2008). Metabolic changes in flatfish hepatic tumours revealed by NMR-based metabolomics and metabolic correlation networks. *Journal of Proteome Research*, 7(12), 5277–5285. <https://doi.org/10.1021/pr800353t>
- Stehfest, K., Toepel, J., & Wilhelm, C. (2005). The application of micro-FTIR spectroscopy to analyze nutrient stress-related changes in biomass composition of phytoplankton algae. *Plant Physiology and Biochemistry*, 43(7), 717–726. <https://doi.org/10.1016/j.plaphy.2005.07.001>
- Stentiford, G. D., Viant, M. R., Ward, D. G., Johnson, P. J., Martin, A., Wenbin, W., Cooper, H. J., Lyons, B. P., & Feist, S. W. (2005). Liver Tumors in Wild Flatfish: A Histopathological,

- Proteomic, and Metabolomic Study. *OMICS: A Journal of Integrative Biology*, 9(3), 281–299. <https://doi.org/10.1089/omi.2005.9.281>
- Sterling, P. (2012). Allostasis: a model of predictive regulation. *Physiol Behav.*, 106, 5–15.
- Stevens, A., & Ramirez-Lopez, L. (2013). An introduction to the prospectr package. *R Package Version 0.1.3*. <https://cran.r-project.org/web/packages/prospectr/citation.html>
- Stien, L. H., Bracke, M., Noble, C., & Kristiansen, T. S. (2020). *Assessing Fish Welfare in Aquaculture*. 303–321. https://doi.org/10.1007/978-3-030-41675-1_13
- Storey, K. B. (1996). Oxidative stress: Animal adaptations in nature. *Brazilian Journal of Medical and Biological Research*, 29(12), 1715–1733.
- Subramanian, A., Tamayo, P., Mootha, V. K., Mukherjee, S., Ebert, B. L., Gillette, M. A., Paulovich, A., Pomeroy, S. L., Golub, T. R., Lander, E. S., & Mesirov, J. P. (2005). Gene set enrichment analysis: A knowledge-based approach for interpreting genome-wide expression profiles. *Proceedings of the National Academy of Sciences of the United States of America*, 102(43), 15545–15550. <https://doi.org/10.1073/pnas.0506580102>
- Subramanian, S., MacKinnon, S. L., & Ross, N. W. (2007). A comparative study on innate immune parameters in the epidermal mucus of various fish species. *Comparative Biochemistry and Physiology Part B: Biochemistry and Molecular Biology*, 148(3), 256–263. <https://doi.org/10.1016/J.CBPB.2007.06.003>
- Sumner, L. W., Alexander, A. E., Ae, A., Ae, D. B., Ae, M. H. B., Beger, R., Daykin, C. A., Teresa, A. E., Fan, W.-M., Oliver, A. E., Ae, F., Goodacre, R., Julian, A. E., Griffin, L., Thomas, A. E., Ae, H., Hardy, N., James, A. E., Ae, H., ... Goodacre, R. (2007). Proposed minimum reporting standards for chemical analysis. *Metabolomics 2007 3:3*, 3(3), 211–221. <https://doi.org/10.1007/S11306-007-0082-2>
- Sun, Y. C., Wu, S., Du, N. N., Song, Y., & Xu, W. (2018). High-throughput metabolomics enables metabolite biomarkers and metabolic mechanism discovery of fish in response to alkalinity stress. *RSC Advances*, 8(27), 14983–14990. <https://doi.org/10.1039/c8ra01317a>
- Sun, Y. J., Li, A. W., Zhang, Y. C., Dai, J. H., & Zhu, X. (2021). Evaluation of Urine NDRG1 as Noninvasive Biomarker for Bladder Cancer Diagnosis. *Clinical Laboratory*, 67(3), 667–673. <https://doi.org/10.7754/CLIN.LAB.2020.191020>
- Sun, Y., Li, W., Shen, S., Yang, X., Lu, B., Zhang, X., Lu, P., Shen, Y., & Ji, J. (2019). Loss of alanine-glyoxylate and serine-pyruvate aminotransferase expression accelerated the progression of hepatocellular carcinoma and predicted poor prognosis. *Journal of Translational Medicine*, 17(1), 1–16. <https://doi.org/10.1186/s12967-019-02138-5>
- Sundaray, J. K., Dixit, S., Rather, A., Rasal, K. D., & Sahoo, L. (2022). Aquaculture omics: An update on the current status of research and data analysis. *Marine Genomics*, 64(June 2021), 100967. <https://doi.org/10.1016/j.margen.2022.100967>
- Sunyer, J. O., Tort, L., & Lambris, J. D. (1997). Structural C3 diversity in fish: characterization of five forms of C3 in the diploid fish *Sparus aurata*. *Journal of Immunology (Baltimore, Md. : 1950)*, 158(6), 2813–2821. <http://www.ncbi.nlm.nih.gov/pubmed/9058817>
- Suppers, A., van Gool, A. J., & Wessels, H. J. C. T. (2018). Integrated chemometrics and statistics to drive successful proteomics biomarker discovery. *Proteomes*, 6(2). <https://doi.org/10.3390/PROTEOMES6020020>
- Szklarczyk, D., Gable, A. L., Lyon, D., Junge, A., Wyder, S., Huerta-Cepas, J., Simonovic, M., Doncheva, N. T., Morris, J. H., Bork, P., Jensen, L. J., & Von Mering, C. (2019). STRING v11: Protein-protein association networks with increased coverage, supporting functional discovery in genome-wide experimental datasets. *Nucleic Acids Research*, 47(D1), D607–D613. <https://doi.org/10.1093/nar/gky1131>
- Szklarczyk, D., Gable, A. L., Nastou, K. C., Lyon, D., Kirsch, R., Pyysalo, S., Doncheva, N. T., Legeay, M., Fang, T., Bork, P., Jensen, L. J., & von Mering, C. (2021). The STRING database in 2021: customizable protein-protein networks, and functional characterization of user-uploaded gene/measurement sets. *Nucleic Acids Research*, 49(D1), D605–D612. <https://doi.org/10.1093/NAR/GKAA1074>
- Talari, A. C. S., Martinez, M. A. G., Movasaghi, Z., Rehman, S., & Rehman, I. U. (2017). Advances in Fourier transform infrared (FTIR) spectroscopy of biological tissues. *Applied*

- Tyanova, S., Temu, T., Sinitcyn, P., Carlson, A., Hein, M. Y., Geiger, T., Mann, M., & Cox, J. (2016). The Perseus computational platform for comprehensive analysis of (prote)omics data. *Nature Methods* 2016 13:9, 13(9), 731–740. <https://doi.org/10.1038/nmeth.3901>
- Union, E. (2007). Treaty of Lisbon amending the treaty on European Union and the treaty establishing the European Community. *Official Journal of the European Union*.
- Uren Webster, T. M., Williams, T. D., Katsiadaki, I., Lange, A., Lewis, C., Shears, J. A., Tyler, C. R., & Santos, E. M. (2017). Hepatic transcriptional responses to copper in the three-spined stickleback are affected by their pollution exposure history. *Aquatic Toxicology*, 184, 26–36. <https://doi.org/10.1016/j.aquatox.2016.12.023>
- Valenti, W. C., Kimpara, J. M., de Preto, B. L., & Moraes-Valenti, P. (2018). Indicators of sustainability to assess aquaculture systems. *Ecological Indicators*, 88, 402–413. <https://doi.org/10.1016/j.ecolind.2017.12.068>
- Valenzuela, C. A., Ponce, C., Zuloaga, R., González, P., Avendaño-Herrera, R., Valdés, J. A., & Molina, A. (2020). Effects of crowding on the three main proteolytic mechanisms of skeletal muscle in rainbow trout (*Oncorhynchus mykiss*). *BMC Veterinary Research*, 16(1), 1–11. <https://doi.org/10.1186/S12917-020-02518-W/TABLES/4>
- Valenzuela, C. A., Zuloaga, R., Mercado, L., Einarsdottir, I. E., Björnsson, B. T., Valdés, J. A., & Molina, A. (2018). Chronic stress inhibits growth and induces proteolytic mechanisms through two different nonoverlapping pathways in the skeletal muscle of a teleost fish. *Am J Physiol Regul Integr Comp Physiol*, 314, R102–R113. <https://doi.org/10.1152/ajpregu.00009.2017>
- Valero, Y., Martínez-Morcillo, F. J., Esteban, M. Á., Chaves-Pozo, E., & Cuesta, A. (2015). Fish peroxiredoxins and their role in immunity. *Biology*, 4(4), 860–880. <https://doi.org/10.3390/biology4040860>
- Van Der Marel, M., Caspari, N., Neuhaus, H., Meyer, W., Enss, M.-L., & Steinhagen, D. (2010). Changes in skin mucus of common carp, *Cyprinus carpio* L., after exposure to water with a high bacterial load. *Journal of Fish Diseases*, 33(5), 431–439. <https://doi.org/https://doi.org/10.1111/j.1365-2761.2010.01140.x>
- van Riggelen, J., Yetil, A., & Felsher, D. W. (2010). MYC as a regulator of ribosome biogenesis and protein synthesis. *Nature Reviews Cancer* 2010 10:4, 10(4), 301–309. <https://doi.org/10.1038/nrc2819>
- Vandesompele, J., De Preter, K., Pattyn, F., Poppe, B., Van Roy, N., De Paepe, A., & Speleman, F. (2002). Accurate normalization of real-time quantitative RT-PCR data by geometric averaging of multiple internal control genes. *Genome Biology*, 3(7), research0034.1–0034.11.
- Vecchi, C., Montosi, G., Zhang, K., Lamberti, I., Duncan, S. A., Kaufman, R. J., & Pietrangelo, A. (2009). ER Stress Controls Iron Metabolism Through Induction of Hcpidin. *Science*, 325(5942), 977–880.
- Veiseth-Kent, E., Grove, H., Færgestad, E. M., & Fjæra, S. O. (2010). Changes in muscle and blood plasma proteomes of Atlantic salmon (*Salmo salar*) induced by crowding. *Aquaculture*, 309(1–4), 272–279. <https://doi.org/10.1016/j.aquaculture.2010.09.028>
- Vélez, E. J., Lutfi, E., Jiménez-Amilburu, V., Riera-Codina, M., Capilla, E., Navarro, I., & Gutiérrez, J. (2014). IGF-I and amino acids effects through TOR signaling on proliferation and differentiation of gilthead sea bream cultured myocytes. *General and Comparative Endocrinology*, 205, 296–304. <https://doi.org/10.1016/J.YGCEN.2014.05.024>
- Velmurugan, B., Senthilkumaar, P., & Karthikeyan, S. (2018). Toxicity impact of fenvalerate on the gill tissue of *Oreochromis mossambicus* with respect to biochemical changes utilizing FTIR and principal component analysis. *Journal of Biological Physics*, 44(3), 301–315. <https://doi.org/10.1007/s10867-018-9484-9>
- Vettese, T., Franks, B., & Jacquet, J. (2020). The Great Fish Pain Debate. *Issues in Science and Technology*, 36(4), 49–53. <https://www.jstor.org/stable/26949166>
- Vijayan, M. M., Aluru, N., & Leatherland, J. F. (2010). Stress response and the role of cortisol. In J. F. Leatherland & P. Woo (Eds.), *Fish diseases and disorders, Vol 2: Non-infectious disorders* (pp. 182–201). CAB International. <http://www.cabi.org/cabebooks/ebook/20103120625>

- Walter, P., & Ron, D. (2011). The Unfolded Protein Response: From Stress Pathway to Homeostatic Regulation. *Science*, 334(6059), 1081–1086.
- Wang, Y. Da, Huang, S. J., Chou, H. N., Liao, W. L., Gong, H. Y., & Chen, J. Y. (2014). Transcriptome analysis of the effect of *Vibrio alginolyticus* infection on the innate immunity-related complement pathway in *Epinephelus coioides*. *BMC Genomics*, 15(1), 1–15. <https://doi.org/10.1186/1471-2164-15-1102>
- Wang, Y., Li, C., Pan, C., Liu, E., Zhao, X., & Ling, Q. (2019). Alterations to transcriptomic profile, histopathology, and oxidative stress in liver of pikeperch (*Sander lucioperca*) under heat stress. *Fish and Shellfish Immunology*, 95(November), 659–669. <https://doi.org/10.1016/j.fsi.2019.11.014>
- Wang, Z., Gerstein, M., & Snyder, M. (2009). RNA-Seq: a revolutionary tool for transcriptomics. *Nature Reviews Genetics*, 10(1), 57–63. <https://doi.org/10.1038/nrg2484>
- Warnes, G. R., Bolker, B., Bonebakker, L., Gentleman, R., Huber, W., Liaw, A., Lumley, T., Maechler, M., Magnusson, A., Moeller, S., Schwartz, M., & Venables, B. (2020). gplots: Various R Programming Tools for Plotting Data. *R Package Version 3.1.1*. <https://cran.r-project.org/package=gplots>
- Weber, J.-M., Choi, K., Gonzalez, A., & Omlin, T. (2016). Metabolic fuel kinetics in fish: swimming, hypoxia and muscle membranes. *Journal of Experimental Biology*, 219, 250–258. <https://doi.org/10.1242/jeb.125294>
- Wei, T., & Simko, V. (2017). corrplot: Visualization of a Correlation Matrix. *R Package Version 0.84*. <https://github.com/taiyun/corrplot> <https://github.com/taiyun/corrplot/issues>
- Wei, Y., Li, B., Xu, H., & Liang, M. (2021). Liver Metabolome and Proteome Response of Turbot (*Scophthalmus maximus*) to Lysine and Leucine in Free and Dipeptide Forms. *Frontiers in Marine Science*, 8, 743. <https://doi.org/10.3389/FMARS.2021.691404/BIBTEX>
- Wen, X., Hu, Y., Zhang, X., Wei, X., Wang, T., & Yin, S. (2019). Integrated application of multi-omics provides insights into cold stress responses in pufferfish *Takifugu fasciatus*. *BMC Genomics*, 20(1), 1–15. <https://doi.org/10.1186/S12864-019-5915-7/FIGURES/5>
- Wendelaar Bonga, S. E. (1997). The stress response in fish. *Physiological Reviews*, 77(3), 591–625. <https://doi.org/10.1152/physrev.1997.77.3.591>
- Wenne, R., Boudry, P., Hemmer-Hansen, J., Lubieniecki, K. P., Was, A., & Kause, A. (2007). What role for genomics in fisheries management and aquaculture? *Aquatic Living Resources*, 20(3), 241–255. <https://doi.org/10.1051/alr:2007037>
- Westermeier, Reiner., & Naven, Tom. (2002). *Proteomics in practice : a laboratory manual of proteome analysis*. Wiley-VCH. <https://www.wiley.com/en-us/Proteomics+in+Practice%3A+A+Laboratory+Manual+of+Proteome+Analysis-p-9783527600175>
- Wheeler, T. J., & Eddy, S. R. (2013). Nhmmer: DNA homology search with profile HMMs. *Bioinformatics*, 29(19), 2487–2489. <https://doi.org/10.1093/bioinformatics/btt403>
- Wickham, H. (2016). *ggplot2: Elegant Graphics for Data Analysis*. Springer-Verlag.
- Wilkinson, R. J., Paton, N., & Porter, M. J. R. (2008). The effects of pre-harvest stress and harvest method on the stress response, rigor onset, muscle pH and drip loss in barramundi (*Lates calcarifer*). *Aquaculture*, 282(1–4), 26–32. <https://doi.org/10.1016/J.AQUACULTURE.2008.05.032>
- Williams, K. J., Cassidy, A. A., Verhille, C. E., Lamarre, S. G., & MacCormack, T. J. (2019). Diel cycling hypoxia enhances hypoxia tolerance in rainbow trout (*Oncorhynchus mykiss*): Evidence of physiological and metabolic plasticity. *Journal of Experimental Biology*, 222(14). <https://doi.org/10.1242/JEB.206045/258922/AM/DIEL-CYCLING-HYPOXIA-ENHANCES-HYPOXIA-TOLERANCE-IN>
- Wiseman, S., Osachoff, H., Bassett, E., Malhotra, J., Bruno, J., VanAggelen, G., Mommsen, T. P., & Vijayan, M. M. (2007). Gene expression pattern in the liver during recovery from an acute stressor in rainbow trout. *Comparative Biochemistry and Physiology - Part D: Genomics and Proteomics*, 2(3), 234–244. <https://doi.org/10.1016/j.cbd.2007.04.005>
- Wood, A. W., Duan, C., & Bern, H. A. (2005). Insulin-Like Growth Factor Signaling in Fish. *International Review of Cytology*, 243, 215–285. [https://doi.org/10.1016/S0074-7696\(05\)43004-1](https://doi.org/10.1016/S0074-7696(05)43004-1)

- Wood, C. M., Turner, J. D., & Graham, M. S. (1983). Why do fish die after severe exercise? *Journal of Fish Biology*, *22*, 189–201.
- Word Federation for Animals. (2022). *Animal Welfare: a must in the climate negotiations*.
- Wright, K. A., Woods, C. M. C., Gray, B. E., & Lokman, P. M. (2007). Recovery from acute, chronic and transport stress in the pot-bellied seahorse *Hippocampus abdominalis*. *Journal of Fish Biology*, *70*(5), 1447–1457. <https://doi.org/https://doi.org/10.1111/j.1095-8649.2007.01422.x>
- Wu, L., Liu, Y., & Kong, D. C. (2014). Mechanism of chromosomal DNA replication initiation and replication fork stabilization in eukaryotes. *Science China Life Sciences*, *57*(5), 482–487. <https://doi.org/10.1007/s11427-014-4631-4>
- Wu, T., Hu, E., Xu, S., Chen, M., Guo, P., Dai, Z., Feng, T., Zhou, L., Tang, W., Zhan, L., Fu, X., Liu, S., Bo, X., & Yu, G. (2021). clusterProfiler 4.0: A universal enrichment tool for interpreting omics data. *The Innovation*, *2*(3), 100141. <https://doi.org/10.1016/j.xinn.2021.100141>
- Wulff, T., Jessen, F., Roepstorff, P., & Hoffmann, E. K. (2008). Long term anoxia in rainbow trout investigated by 2-DE and MS/MS. *Proteomics*, *8*(5), 1009–1018. <https://doi.org/10.1002/pmic.200700460>
- Xiao, T., Shoeb, M., Siddiqui, M. S., Zhang, M., Ramana, K. V., Srivastava, S. K., Vasiliou, V., & Ansari, N. H. (2009). Molecular cloning and oxidative modification of human lens ALDH1A1: Implication in impaired detoxification of lipid aldehydes. *Journal of Toxicology and Environmental Health - Part A: Current Issues*, *72*(9), 577–584. <https://doi.org/10.1080/15287390802706371>
- Xie, F., Xiao, P., Chen, D., Xu, L., & Zhang, B. (2012). miRDeepFinder: A miRNA analysis tool for deep sequencing of plant small RNAs. *Plant Molecular Biology*, *80*(1), 75–84. <https://doi.org/10.1007/s11103-012-9885-2>
- Xiong, X.-P., Dong, C.-F., Xu, X., Weng, S.-P., Liu, Z.-Y., & He, J.-G. (2011). Proteomic analysis of zebrafish (*Danio rerio*) infected with infectious spleen and kidney necrosis virus. *Developmental & Comparative Immunology*, *35*(4), 431–440. <https://doi.org/10.1016/J.DCI.2010.11.006>
- Xiong, Y., Dan, C., Ren, F., Su, Z. H., Zhang, Y., & Mei, J. (2020). Proteomic profiling of yellow catfish (*Pelteobagrus fulvidraco*) skin mucus identifies differentially-expressed proteins in response to *Edwardsiella ictaluri* infection. *Fish & Shellfish Immunology*, *100*, 98–108. <https://doi.org/10.1016/J.FSI.2020.02.059>
- Xu, D., Song, L., Wang, H., Xu, X., Wang, T., & Lu, L. (2015). Proteomic analysis of cellular protein expression profiles in response to grass carp reovirus infection. *Fish & Shellfish Immunology*, *44*(2), 515–524. <https://doi.org/10.1016/j.fsi.2015.03.010>
- Xu, Z., Gan, L., Li, T., Xu, C., Chen, K., Wang, X., Qin, J. G., Chen, L., & Li, E. (2015). Transcriptome profiling and molecular pathway analysis of genes in association with salinity adaptation in Nile tilapia *Oreochromis niloticus*. *PLoS ONE*, *10*(8), 1–25. <https://doi.org/10.1371/journal.pone.0136506>
- Yada, T., & Tort, L. (2016). Stress and Disease Resistance: Immune System and Immunoendocrine Interactions. *Fish Physiology*, *35*, 365–403. <https://doi.org/10.1016/B978-0-12-802728-8.00010-2>
- Yang, B., Wang, C., Tu, Y., Hu, H., Han, D., Zhu, X., Jin, J., Yang, Y., & Xie, S. (2015). Effects of repeated handling and air exposure on the immune response and the disease resistance of gibel carp (*Carassius auratus gibelio*) over winter. *Fish & Shellfish Immunology*, *47*(2), 933–941. <https://doi.org/10.1016/j.fsi.2015.10.013>
- Yang, E. jun, Amenyogbe, E., Zhang, J. dong, Wang, W. zheng, Huang, J. sheng, & Chen, G. (2022). Integrated transcriptomics and metabolomics analysis of the intestine of cobia (*Rachycentron canadum*) under hypoxia stress. *Aquaculture Reports*, *25*(February), 101261. <https://doi.org/10.1016/j.aqrep.2022.101261>
- Ye, H., Lin, Q., & Luo, H. (2018). Applications of transcriptomics and proteomics in understanding fish immunity. *Fish and Shellfish Immunology*, *77*(April), 319–327. <https://doi.org/10.1016/j.fsi.2018.03.046>

- Yeh, C.-H., Chen, Y.-S., Wu, M.-S., Chen, C.-W., Yuan, C.-H., Pan, K.-W., Chang, Y.-N., Chuang, N.-N., & Chang, C.-Y. (2008). Differential display of grouper iridovirus-infected grouper cells by immunostaining. *Biochemical and Biophysical Research Communications*, 372(4), 674–680. <https://doi.org/10.1016/J.BBRC.2008.05.126>
- Yi, Z., Deng, M., Scott, M. J., Fu, G., Loughran, P. A., Lei, Z., Li, S., Sun, P., Yang, C., Li, W., Xu, H., Huang, F., & Billiar, T. R. (2020). Immune-Responsive Gene 1/Itaconate Activates Nuclear Factor Erythroid 2–Related Factor 2 in Hepatocytes to Protect Against Liver Ischemia–Reperfusion Injury. *Hepatology*, 72(4), 1394–1411. <https://doi.org/10.1002/HEP.31147>
- Yildiz, H. Y. (2009). Reference biochemical values for three cultured Sparid fish: Striped sea bream, *Lithognathus mormyrus*; common dentex, *Dentex dentex*; and gilthead sea bream, *Sparus aurata*. *Comparative Clinical Pathology*, 18(1), 23–27. <https://doi.org/10.1007/s00580-008-0743-1>
- Yoo, H.-C. ;, Han, J.-M., Yoo, H.-C., & Han, J.-M. (2022). Amino Acid Metabolism in Cancer Drug Resistance. *Cells* 2022, Vol. 11, Page 140, 11(1), 140. <https://doi.org/10.3390/CELLS11010140>
- Young, T., & Alfaro, A. C. (2018). Metabolomic strategies for aquaculture research: a primer. *Reviews in Aquaculture*, 10(1), 26–56. <https://doi.org/10.1111/raq.12146>
- Yu, G. (2022a). enrichplot: Visualization of Functional Enrichment Result. *R Package Version 1.16.0*. <https://yulab-smu.top/biomedical-knowledge-mining-book/>
- Yu, G. (2022b). enrichplot: Visualization of Functional Enrichment Result. *R Package Version 1.18.3*.
- Yu, G., & He, Q.-Y. (2016). ReactomePA: an R/Bioconductor package for reactome pathway analysis and visualization. *Molecular BioSystems*, 12, 477–479.
- Yuan, Z., Liu, S., Yao, J., Zeng, Q., Tan, S., & Liu, Z. (2016). Expression of Bcl-2 genes in channel catfish after bacterial infection and hypoxia stress. *Developmental and Comparative Immunology*, 65, 79–90. <https://doi.org/10.1016/j.dci.2016.06.018>
- Yue, G. H., & Wang, L. (2017). Current status of genome sequencing and its applications in aquaculture. *Aquaculture*, 468, 337–347. <https://doi.org/10.1016/j.aquaculture.2016.10.036>
- Zahedi, S., Akbarzadeh, A., Mehrzad, J., Noori, A., & Harsij, M. (2019). Effect of stocking density on growth performance, plasma biochemistry and muscle gene expression in rainbow trout (*Oncorhynchus mykiss*). *Aquaculture*, 498, 271–278. <https://doi.org/10.1016/J.AQUACULTURE.2018.07.044>
- Zeifman, L., Hertog, S., Kantorova, V., & Wilmoth, J. (2022). *A World of 8 Billion* (Issue Policy Brief n°140).
- Zhang, G., Zhang, J., Wen, X., Zhao, C., Zhang, H., Li, X., & Yin, S. (2017). Comparative iTRAQ-Based Quantitative Proteomic Analysis of *Pelteobagrus vachelli* Liver under Acute Hypoxia: Implications in Metabolic Responses. *Proteomics*, 17(17–18), 170–140. <https://doi.org/10.1002/pmic.201700140>
- Zhang, L., Song, Z., Zhong, S., Gan, J., Liang, H., Yu, Y., Wu, G., & He, L. (2022). Acute hypoxia and reoxygenation induces oxidative stress, glycometabolism, and oxygen transport change in red swamp crayfish (*Procambarus clarkii*): Application of transcriptome profiling in assessment of hypoxia. *Aquaculture Reports*, 23(January). <https://doi.org/10.1016/j.aqrep.2022.101029>
- Zhang, X., Wen, H., Wang, H., Ren, Y., Zhao, J., & Li, Y. (2017). RNA-Seq analysis of salinity stress-responsive transcriptome in the liver of spotted sea bass (*Lateolabrax maculatus*). *PLoS ONE*, 12(3), 1–18. <https://doi.org/10.1371/journal.pone.0173238>
- Zhang, Y., Liu, C., Liu, J., Liu, X., Tu, Z., Zheng, Y., Xu, J., Fan, H., Wang, Y., & Hu, M. (2022). Multi-omics reveals response mechanism of liver metabolism of hybrid sturgeon under ship noise stress. *Science of the Total Environment*, 851(July), 158348. <https://doi.org/10.1016/j.scitotenv.2022.158348>
- Zhang, Z., Cao, Y., Zhai, Y., Ma, X., An, X., Zhang, S., & Li, Z. (2018). MicroRNA-29b regulates DNA methylation by targeting Dnmt3a/3b and Tet1/2/3 in porcine early embryo

- development. *Development Growth and Differentiation*, 60(4), 197–204. <https://doi.org/10.1111/dgd.12537>
- Zhao, H., Kassama, Y., Young, M., Kell, D. B., & Goodacre, R. (2004). Differentiation of *Micromonospora* isolates from a coastal sediment in Wales on the basis of fourier transform infrared spectroscopy, 16S rRNA sequence analysis, and the amplified fragment length polymorphism technique. *Applied and Environmental Microbiology*, 70(11), 6619–6627. <https://doi.org/10.1128/AEM.70.11.6619-6627.2004>
- Zhao, X., Li, L., Li, C., Liu, E., Zhu, H., & Ling, Q. (2022). Heat stress-induced endoplasmic reticulum stress promotes liver apoptosis in largemouth bass (*Micropterus salmoides*). *Aquaculture*, 546, 737401. <https://doi.org/10.1016/J.AQUACULTURE.2021.737401>
- Zhao, Y., Wang, J., Thammaratsuntorn, J., Wu, J. W., Wei, J. H., Wang, Y., Xu, J. W., & Zhao, J. L. (2015). Comparative transcriptome analysis of Nile tilapia (*Oreochromis niloticus*) in response to alkalinity stress. *Genetics and Molecular Research*, 14(4), 17916–17926. <https://doi.org/10.4238/2015.December.22.16>
- Zhou, T., Gui, L., Liu, M., Li, W., Hu, P., Duarte, D. F. C., Niu, H., & Chen, L. (2019). Transcriptomic responses to low temperature stress in the Nile tilapia, *Oreochromis niloticus*. *Fish and Shellfish Immunology*, 84(November 2018), 1145–1156. <https://doi.org/10.1016/j.fsi.2018.10.023>
- Zhou, X., Ding, Y., & Wang, Y. (2012). Proteomics: Present and future in fish, shellfish and seafood. *Reviews in Aquaculture*, 4(1), 11–20. <https://doi.org/10.1111/j.1753-5131.2012.01058.x>
- Zhou, X., Liao, W., Liao, J., Liao, P., & Lu, H. (2015). Ribosomal proteins : functions beyond the ribosome. *Journal of Molecular Cell Biology*, 7(2), 92–104.
- Zhou, Z., He, Y., Wang, S., Wang, Y., Shan, P., & Li, P. (2022). Autophagy regulation in teleost fish: A double-edged sword. *Aquaculture*, 558(April), 738369. <https://doi.org/10.1016/j.aquaculture.2022.738369>
- Zhu, A., Ibrahim, J. G., Love, M. I., & Stegle, O. (2019). Heavy-tailed prior distributions for sequence count data: removing the noise and preserving large differences. *Bioinformatics*, 35(12), 2084–2092. <https://doi.org/10.1093/bioinformatics/bty895>
- Zhu, Z. X., Jiang, D. L., Li, B. J., Qin, H., Meng, Z. N., Lin, H. R., & Xia, J. H. (2019). Differential Transcriptomic and Metabolomic Responses in the Liver of Nile Tilapia (*Oreochromis niloticus*) Exposed to Acute Ammonia. *Marine Biotechnology*, 21(4), 488–502. <https://doi.org/10.1007/S10126-019-09897-8>
- Ziarrusta, H., Mijangos, L., Picart-Armada, S., Irazola, M., Perera-Lluna, A., Usobiaga, A., Prieto, A., Etxebarria, N., Olivares, M., & Zuloaga, O. (2018). Non-targeted metabolomics reveals alterations in liver and plasma of gilt-head bream exposed to oxybenzone. *Chemosphere*, 211, 624–631. <https://doi.org/10.1016/J.CHEMOSPHERE.2018.08.013>

APPENDIX

Supplementary material from Chapter 3.1

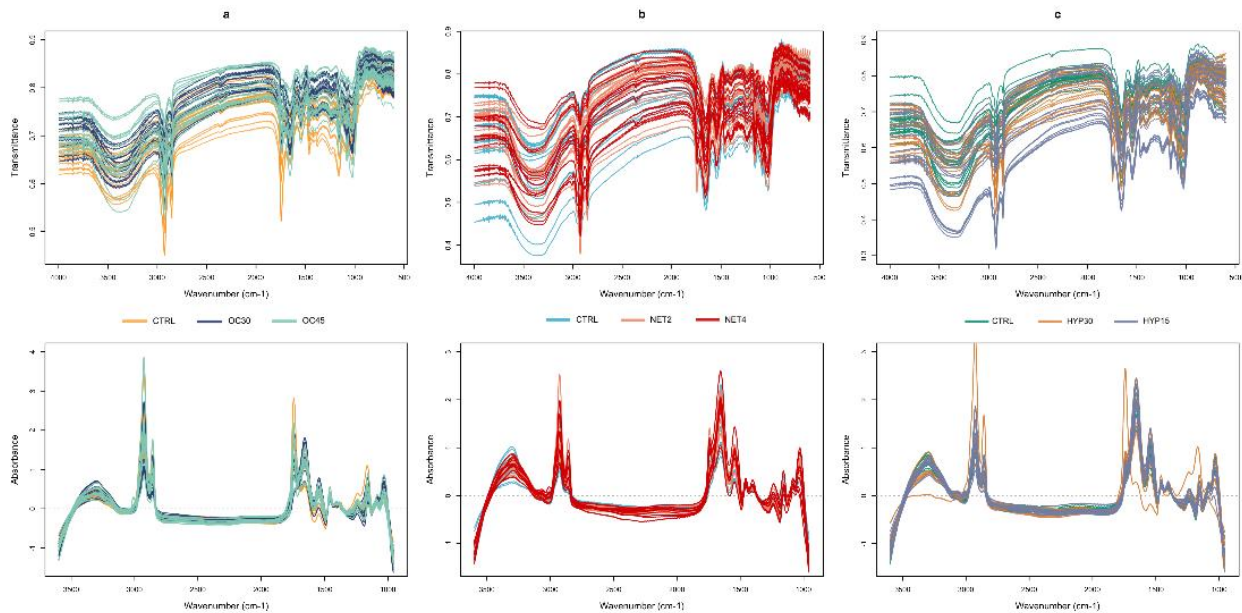


Figure S3.1.1. FTIR spectra ($n = 18$ per experimental condition) of gilthead seabream (*Sparus aurata*) liver submitted to three different stressful rearing conditions ((a) – OC trial, (b) – NET trial, (c) – HYP trial). Raw transmittance spectra are represented in the first row, while processed absorbance spectra, used for multivariate and univariate analyses, are displayed in the second row.

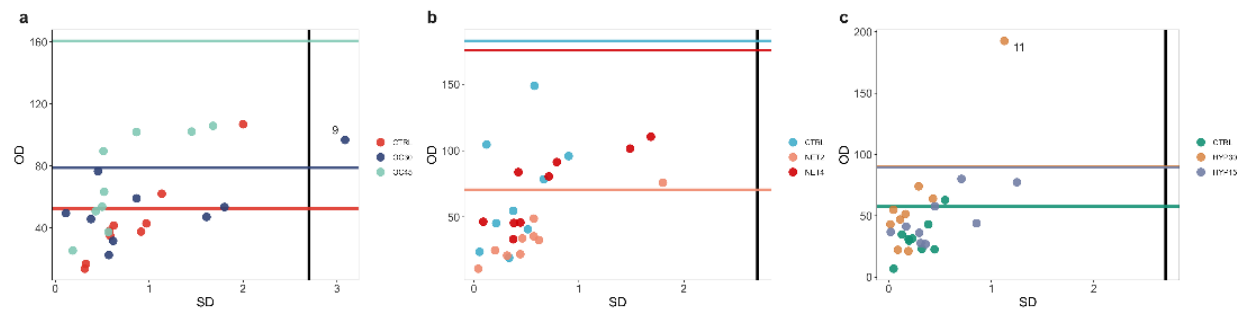
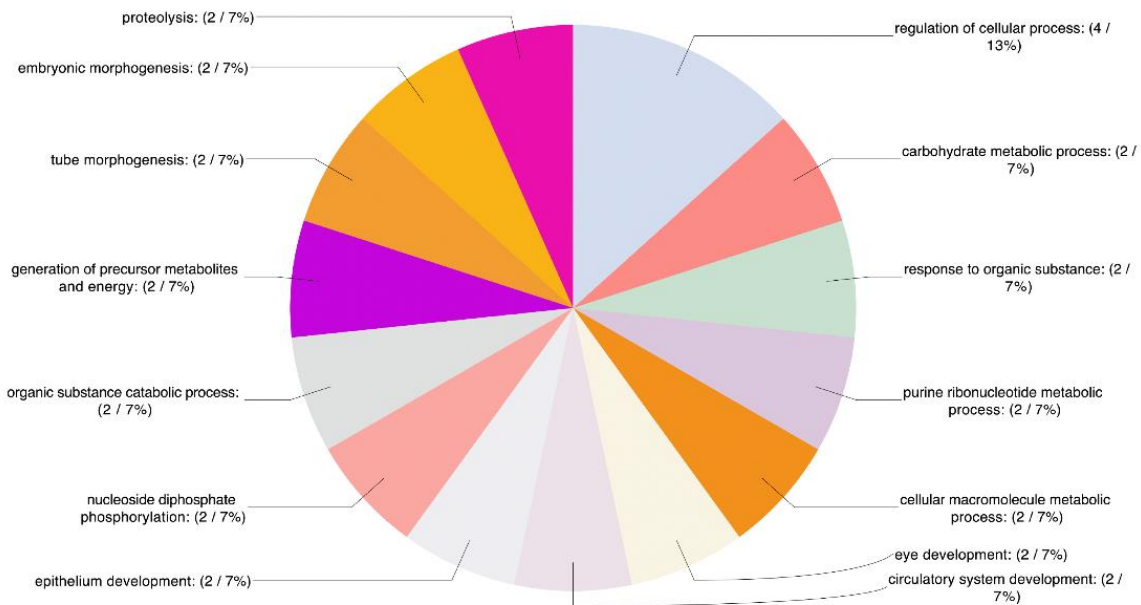


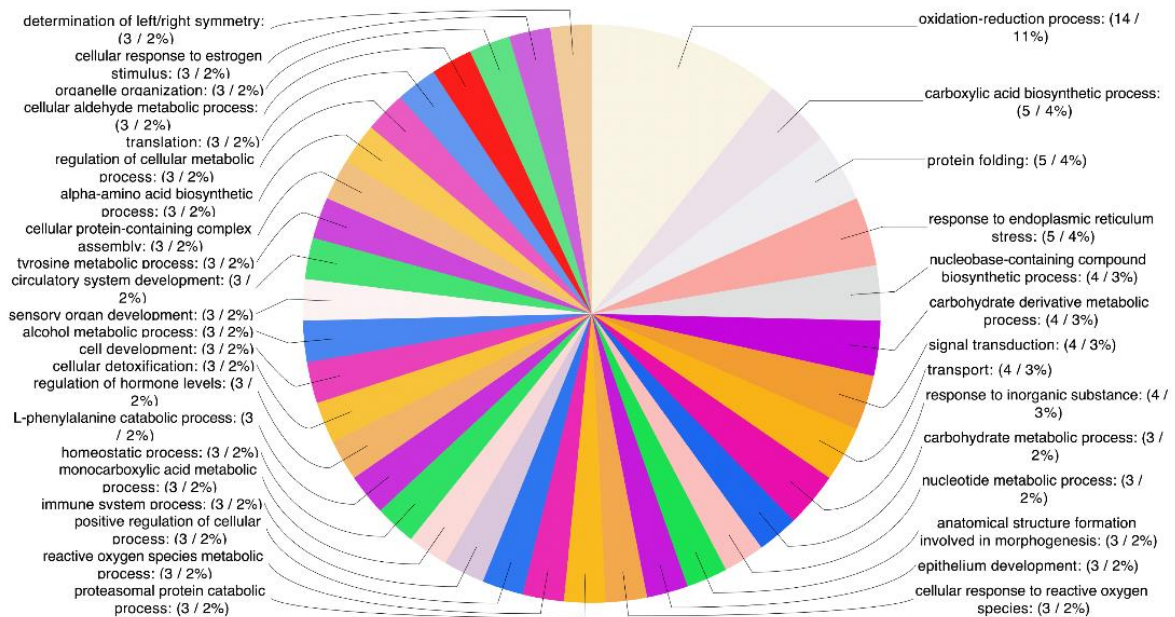
Figure S3.1.2. Multivariate outlier detection on the FTIR spectra of gilthead seabream (*Sparus aurata*) liver submitted to three different stressful rearing conditions ((a) – OC trial, (b) – NET trial, (c) – HYP trial). A robust principal component analysis was performed through the projection pursuit method using the GRID algorithm. Bad leverage points and orthogonal outliers which proved to be some kind of measurement error were eliminated from the datasets, here represented by the corresponding sample number.

Supplementary material from Chapter 3.2

Overcrowding trial - Gene ontology (GO) annotation, Biological process, multi-level



Net handling trial - Gene ontology (GO) annotation, Biological process, multi-level



Hypoxia trial - Gene ontology (GO) annotation, Biological process, multi-level

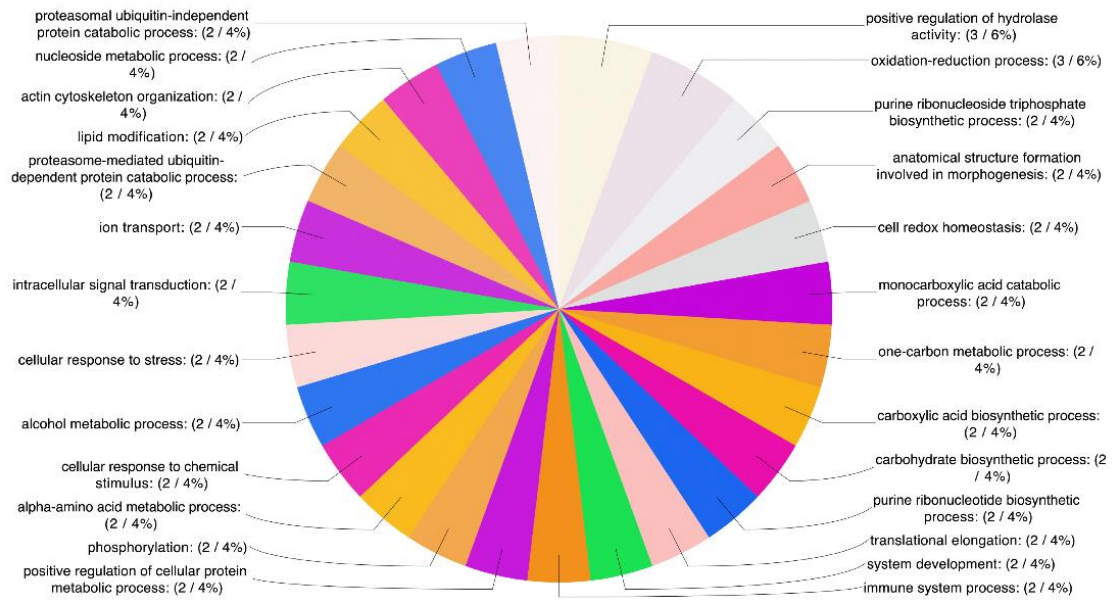
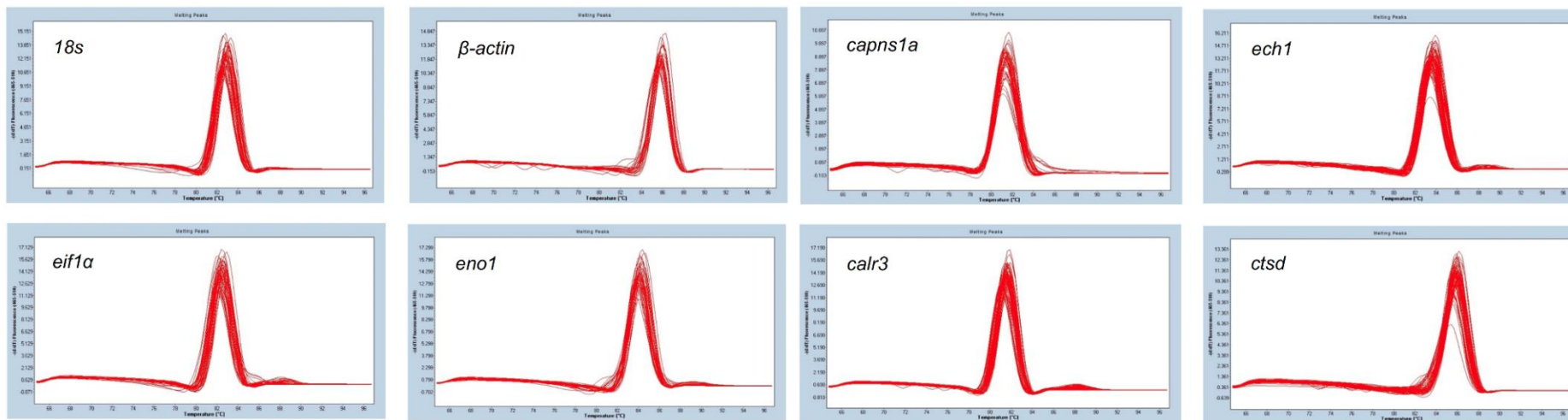
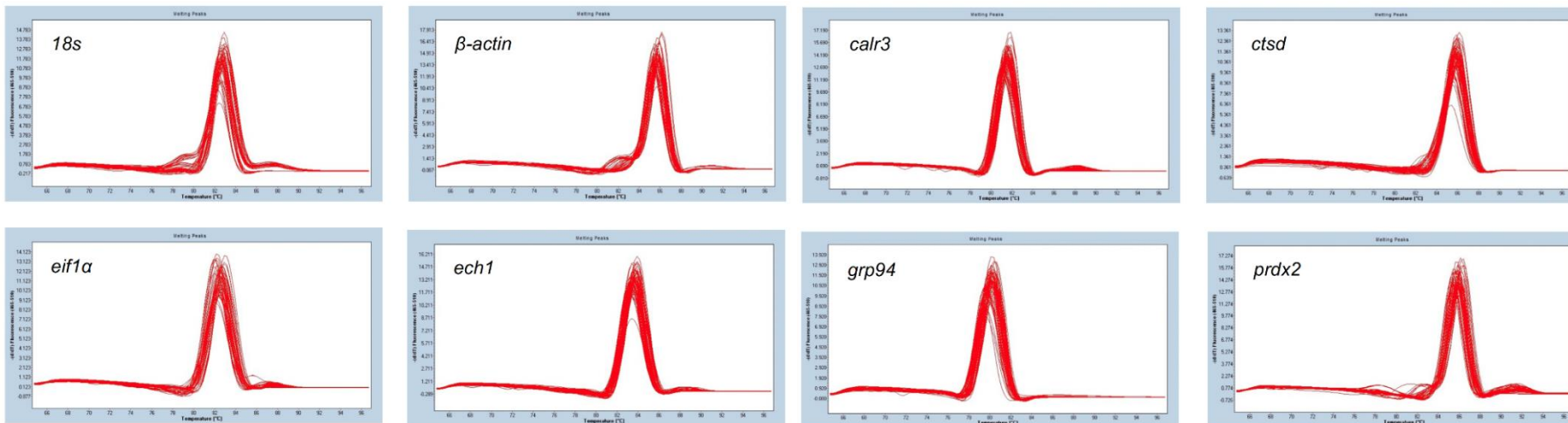
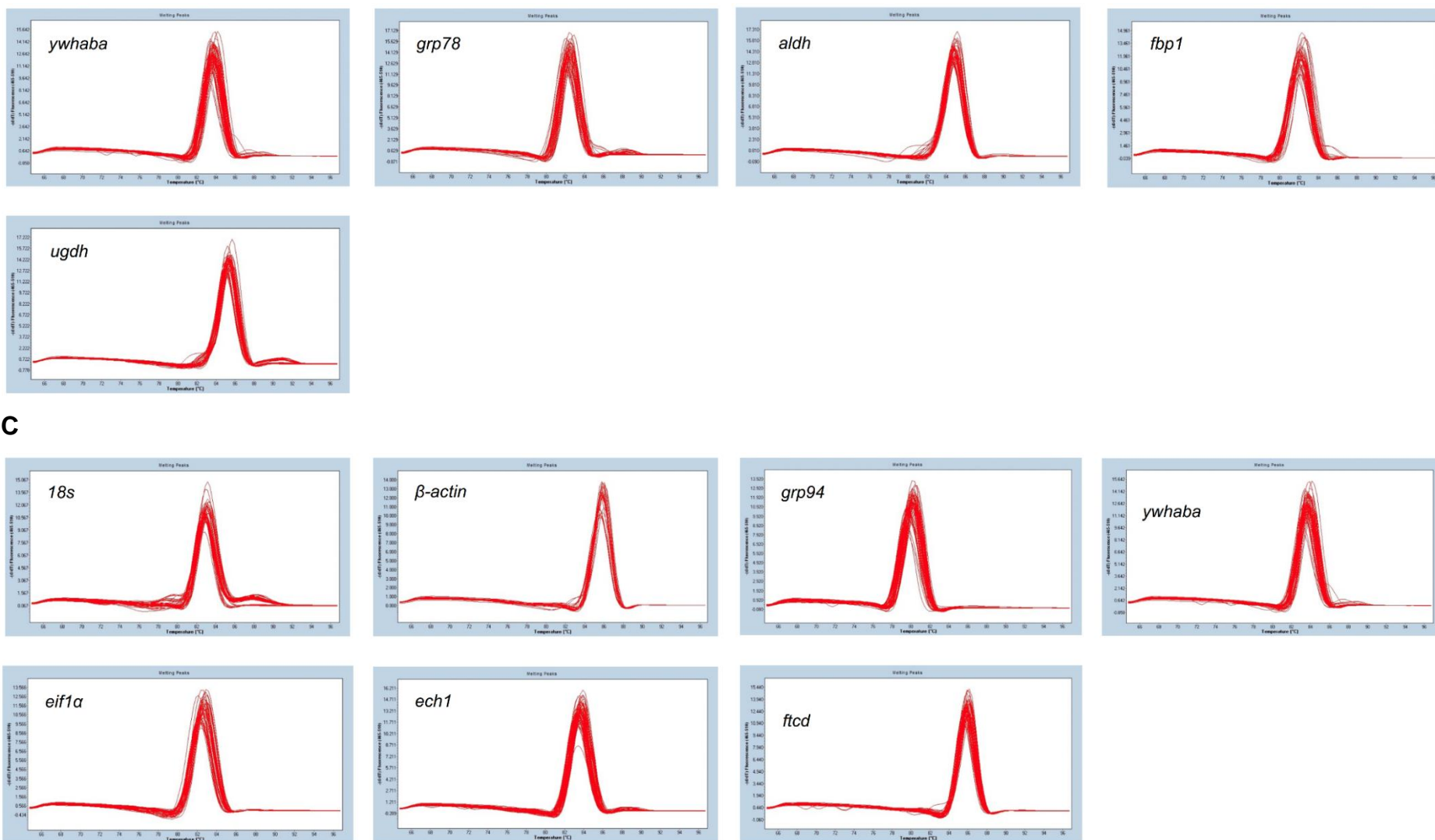


Figure S3.2.1. Multi-level pie charts of GO functional annotation, on the basis of biological process, of the differential proteins identified in the liver of gilthead seabream exposed to different stressors (overcrowding, net handling and hypoxia).

A**B**



C

Figure S3.2.2. Melting peaks, to evaluate PCR specificity, obtained from the melting curve analysis of the RT-qPCR performed with the liver samples of gilthead seabream subjected to A - overcrowding (OC), B - net handling (NET) and C - hypoxia challenges (HYP).

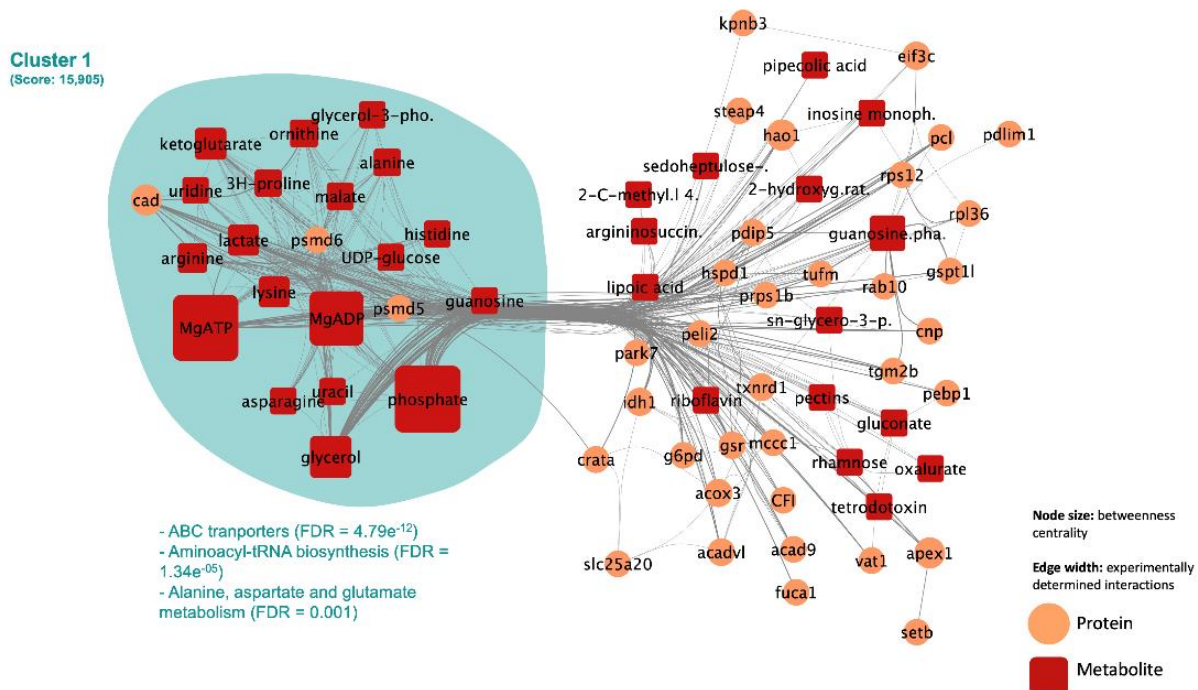


Figure S3.3.2. Metabolic reaction network generated with the differential abundant proteins and metabolites identified in the liver of gilthead seabream submitted to a hypoxia challenge. Node shape and color represent the type of biomolecule, according to the legend. Edges represent functional linkages between them. The highlighted cluster, depicted with MCODE plugin within Cytoscape software, represent the most interconnected region, with the corresponding overrepresented KEGG terms (FDR < 0.05).

Supplementary material from Chapter 4

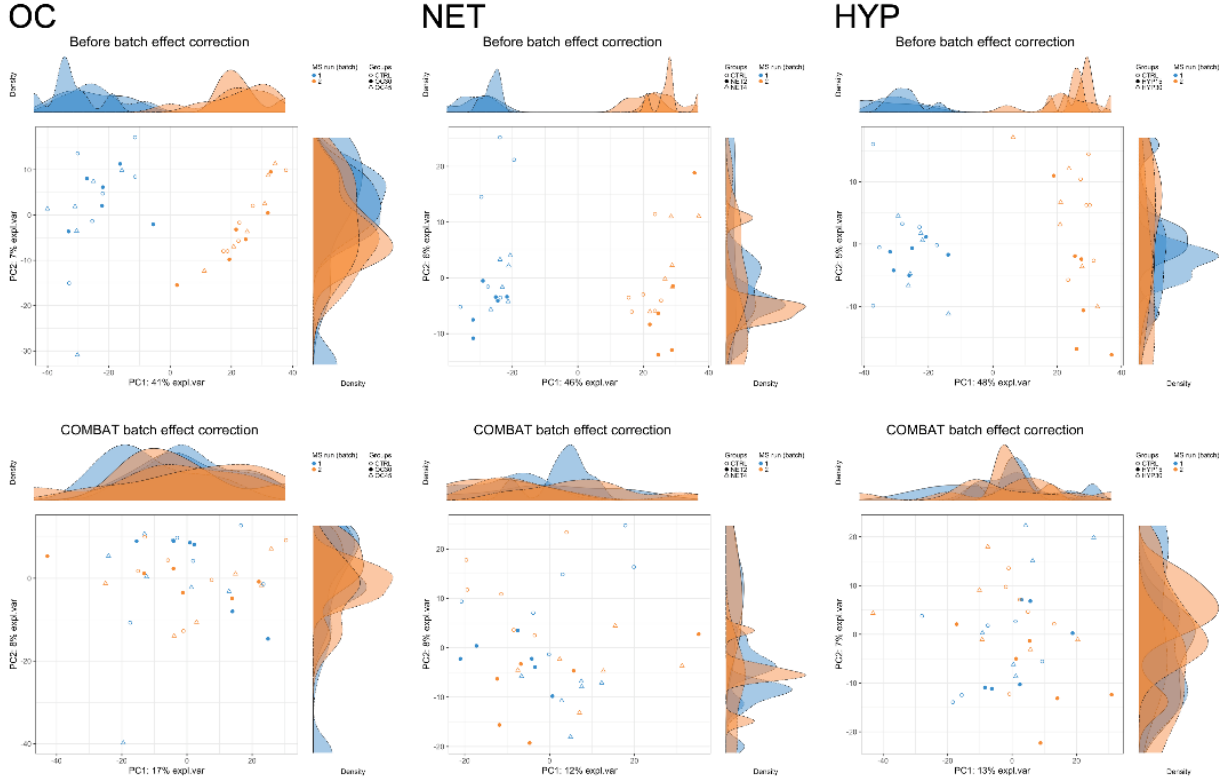


Figure S4.1. Score scatter plots, with density plots, of the PCA performed with the proteins identified in the gilthead seabream skin mucus from the different experimental trials (OC, NET and HYP). Top plots show the PCA performed with the datasets prior to batch effect correction, and the bottom plots show the same datasets after batch correction.

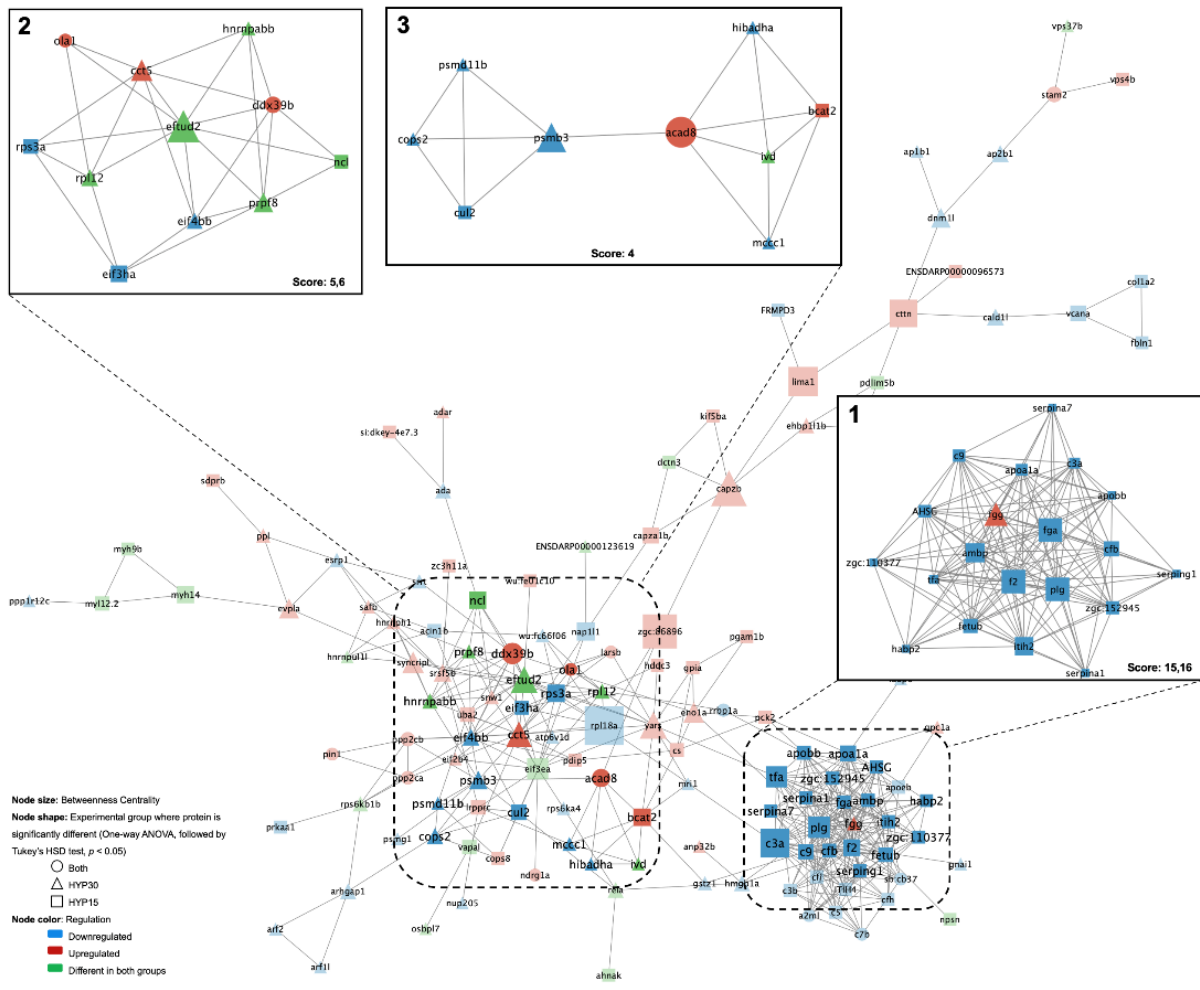


Figure S4.2. PPI network of the DAPs identified in the skin mucus of gilthead seabream, submitted to control and hypoxia in two intensities, namely “HYP30” and “HYP15” challenging conditions (Table S4 - [online](#)). Nodes represent proteins, and edges, the interactions between them. Betweenness centrality is represented by the size of the nodes, while node color and shape indicate protein regulation and significant differences, respectively, according to the figure legend. Three densely interconnected regions/clusters are highlighted in the squared boxes.

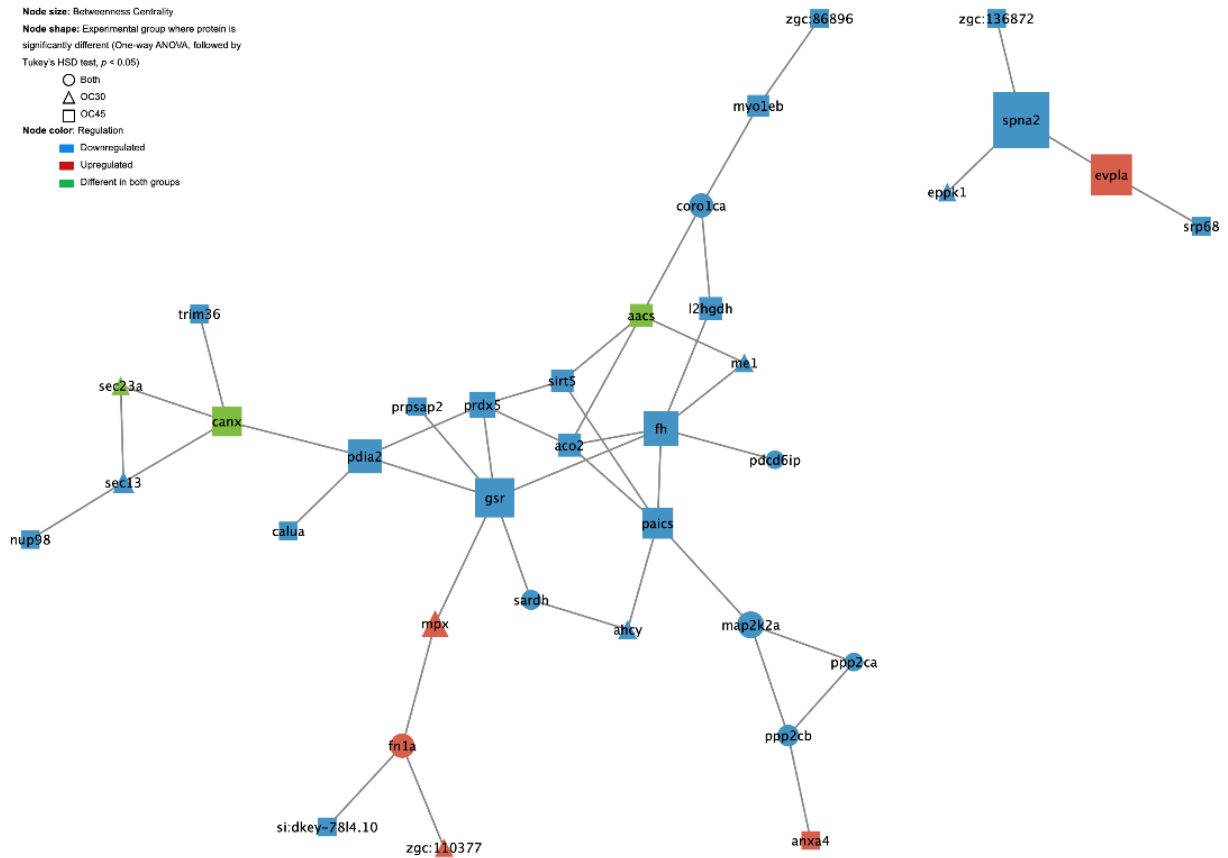


Figure S4.3. PPI network of the DAPs identified in the skin mucus of gilthead seabream, submitted to control and overcrowding in two intensities, namely “OC30” and “OC45” challenging conditions (Table S4 - [online](#)). Nodes represent proteins, and edges, the interactions between them. Betweenness centrality is represented by the size of the nodes, while node color and shape indicate protein regulation and significant differences, respectively, according to the figure legend.

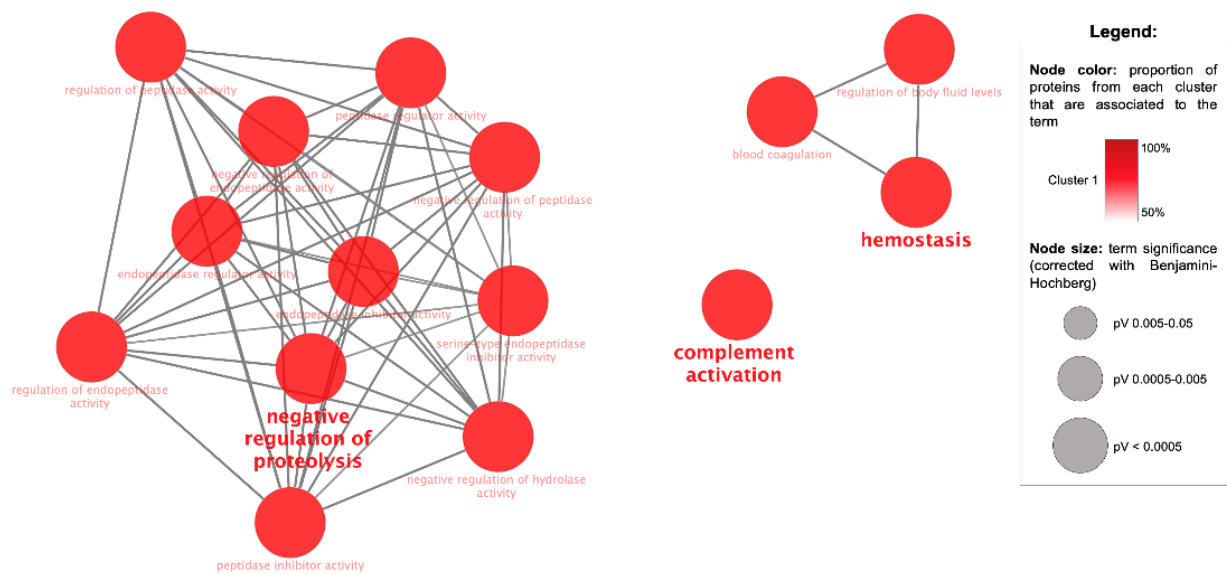


Figure S4.4. Networks of enriched GO terms (hypergeometric Benjamini & Hochberg FDR < 0.05) in the main clusters depicted in the HYP PPI network (Figure S4.2). GO enrichment analysis was performed based on the biological process category.

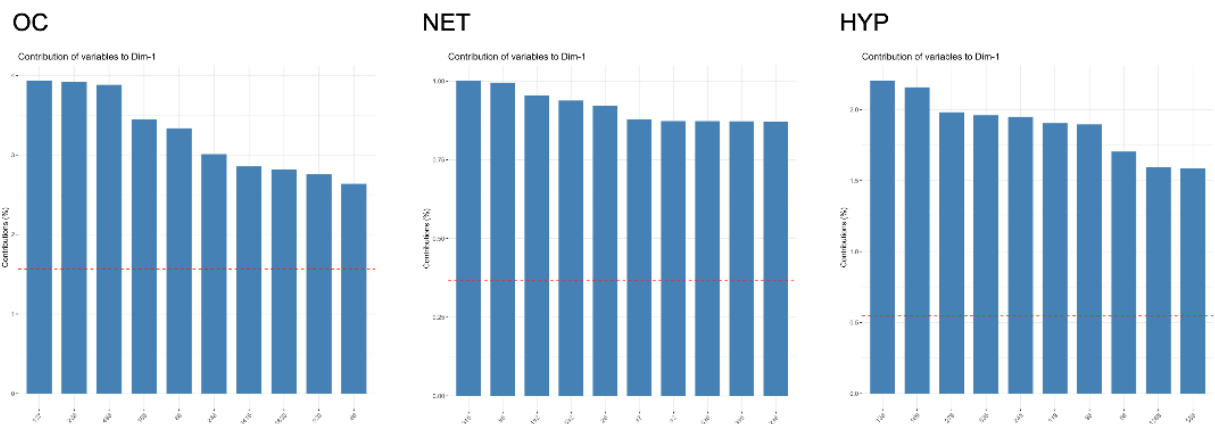


Figure S4.5. Bar plots of the loadings extracted from the first component of the PCAs performed with the DAPs identified in the skin mucus of the gilthead seabream from all experimental trials (OC – overcrowding, NET – net handling, HYP – hypoxia). Protein IDs indicated in x-axis are listed in Table S4 – [online](#).